

12-18-2018

## Singularity Resolution in Anisotropic and Black Hole Spacetimes in Loop Quantum Cosmology

Sahil Saini

*Louisiana State University and Agricultural and Mechanical College*

Follow this and additional works at: [https://digitalcommons.lsu.edu/gradschool\\_dissertations](https://digitalcommons.lsu.edu/gradschool_dissertations)



Part of the [Elementary Particles and Fields and String Theory Commons](#), and the [Quantum Physics Commons](#)

---

### Recommended Citation

Saini, Sahil, "Singularity Resolution in Anisotropic and Black Hole Spacetimes in Loop Quantum Cosmology" (2018). *LSU Doctoral Dissertations*. 4775.

[https://digitalcommons.lsu.edu/gradschool\\_dissertations/4775](https://digitalcommons.lsu.edu/gradschool_dissertations/4775)

This Dissertation is brought to you for free and open access by the Graduate School at LSU Digital Commons. It has been accepted for inclusion in LSU Doctoral Dissertations by an authorized graduate school editor of LSU Digital Commons. For more information, please contact [gradetd@lsu.edu](mailto:gradetd@lsu.edu).

# SINGULARITY RESOLUTION IN ANISOTROPIC AND BLACK HOLE SPACETIMES IN LOOP QUANTUM COSMOLOGY

A Dissertation

Submitted to the Graduate Faculty of the  
Louisiana State University and  
Agricultural and Mechanical College  
in partial fulfillment of the  
requirements for the degree of  
Doctor of Philosophy

in

The Department of Physics and Astronomy

by

Sahil Saini

M.S., Indian Institute of Technology, Delhi, 2010

May 2019

*I dedicate this dissertation to my parents -  
Surya Kanta Saini and Jai Prakash Saini,  
who sowed the seeds of curiosity in me.*

# Acknowledgments

First of all, I would like to thank my advisor Parampreet Singh for his continuous support, guidance and encouragement through out my PhD. I feel deeply indebted to him for showing me how to do research. He has shown immense patience in guiding me through various research problems, helping me along the way and showing me how to pen down and present my ideas. He has also been kind enough to help me navigate my life outside of work. I feel very fortunate to have worked with him and will forever be indebted for his support and guidance.

I would specially like to thank Jorge Pullin for devoting his valuable time and patience in helping me prepare this dissertation. It has been my privilege to know him, and I am very grateful for his guidance and support, and the warm and welcoming environment he has extended to all the members at the quantum gravity group at LSU. I have specially enjoyed many of the courses delivered by him. His clarity of thought and grasp of fundamental ideas will always be an inspiration for me.

I have immensely benefited from numerous discussions with Ivan Agullo. His incisive lectures on a wide range of topics, openness to discuss new ideas and endless enthusiasm have been a constant source of inspiration. I hope some of his enthusiasm and vibrancy has rubbed off on me as well.

I would specially like to thank Javier Olmedo for his collaboration. His support and discussions have also been crucial in the completion of this dissertation. I am grateful to him for many stimulating discussions, and for patiently explaining various intricacies of quantum cosmology to me.

I would like to thank Juhan Frank, A. Ravi P. Rau and Tryfon T. Charalampopoulos for agreeing to be a part of my PhD committee, and for their valuable feedback. I specially thank A. Ravi P. Rau for stimulating courses, discussions and informal lunch seminars which have enriched me in numerous ways.

My sincere thanks to all my colleagues and friends at LSU, especially, Alison Dreyfuss, Anthony Brady, David Kekejian, David Alspaugh, Eklavya Thareja, Emily Safron, Eneet Kaur,

Grigor Sargsyan, Karunya Shirali, Kelsie Kرافton, Kevin Valsen Jacob, Kunal Sharma, Samuel Cupp, Sergio Lopez Caceres, Siddhartha Das, Siddharth Soni, Sudarsan Balakrishnan, Sumeet Khatri, Tyler Ellis and Vishal Katariya. I thank all of them for making my time memorable here.

I would also like to thank the administrative staff members at the Department of Physics and Astronomy especially Arnell Nelson, Carol Duran, Claire Bullock, Stephanie Jones, Laurie Rea, Shanan Schatzle and Shemeka Law for their continuous help and support.

Finally, I would like to thank my relatives and friends in India who have been a constant pillar of support. I would specially like to thank my cousins Ajay and Kamal for constant support, emotional and otherwise. I would also like to thank my friends Lucky, Nandu and Yogi for their warmth and support.

# Table of Contents

ACKNOWLEDGMENTS .....	iv
ILLUSTRATIONS .....	vii
ABSTRACT .....	ix
CHAPTER	
1 INTRODUCTION .....	1
1.1 The canonical approach to quantum gravity .....	6
1.2 Loop quantum gravity .....	10
1.3 Loop quantum cosmology .....	14
1.4 Motivation .....	23
1.5 Overview of the dissertation .....	26
2 A REVIEW OF CLASSICAL AND QUANTUM GRAVITY .....	31
2.1 Strong and weak singularities in GR .....	31
2.2 Hamiltonian formulation of GR .....	37
2.3 Loop quantum cosmology .....	44
2.4 Effective dynamics of loop quantized spatially flat FLRW model .....	51
2.5 Anisotropic models .....	53
3 SINGULARITY AVOIDANCE IN EFFECTIVE LOOP QUANTIZED BIANCHI-II SPACETIME .....	57
3.1 Introduction .....	57
3.2 Classical dynamics of diagonal Bianchi-II spacetime .....	64
3.3 Effective dynamics: ‘A’ quantization .....	68
3.4 Effective dynamics: ‘K’ quantization .....	79
3.5 Potential divergences in curvature invariants and $\dot{\theta}$ .....	82
3.6 Geodesic completeness .....	84
3.7 Lack of strong singularities .....	86
3.8 Conclusions .....	88
4 SINGULARITY AVOIDANCE IN EFFECTIVE LOOP QUANTIZED BIANCHI-IX SPACETIME .....	92
4.1 Introduction .....	92
4.2 Classical aspects of Bianchi-IX spacetime in connection-triad variables .....	94
4.3 Effective loop quantum cosmological dynamics: ‘A’ quantization .....	97
4.4 Effective loop quantum cosmological dynamics: ‘K’ quantization .....	110
4.5 Possible divergences in curvature invariants .....	112
4.6 Geodesic completeness .....	115
4.7 Lack of strong singularities .....	117
4.8 Conclusion .....	119

5	SINGULARITY AVOIDANCE IN EFFECTIVE LOOP QUANTIZED KANTOWSKI–SACHS COSMOLOGY .....	122
5.1	Introduction .....	122
5.2	Classical dynamics of Kantowski–Sachs spacetime .....	125
5.3	Effective dynamics of the Kantowski–Sachs spacetime .....	128
5.4	Geodesics .....	132
5.5	Lack of strong singularities .....	134
5.6	Conclusions .....	136
6	SYMMETRIC BOUNCE IN EFFECTIVE LOOP QUANTIZED BLACK HOLE SPACETIMES .....	139
6.1	Introduction .....	139
6.2	Classical setting .....	145
6.3	Effective loop quantum cosmology .....	151
6.4	Dynamical prescriptions for symmetric bounces .....	156
6.5	Conclusions .....	176
7	CONCLUSIONS .....	180
APPENDIX		
A	PERMISSIONS FROM IOP PUBLISHING LTD. ....	190
VITA .....		203

# Illustrations

## Table

4.1	Different possible fates for the triad variables upon evolution. ....	104
-----	---	-----

## List of Figures

2.1	$3 + 1$ split of spacetime. ....	38
6.1	Choice 1: the evolution of the spatial volume as a function of the normalized time $T/ T_b $ . The curves ranging from thickest to the thinnest correspond to $M = 0.1, 0.3, 1, 10, 1000$ (in Planck units), respectively. ....	159
6.2	Choice 1: the volume at the bounce as a function of the mass. ....	159
6.3	Choice 1: the value of the Kretschmann scalar at the bounce as a function of mass. ....	161
6.4	Choice 2: we plot the LHS and RHS of Eq. (6.43) as a function of $\alpha$ for different values of the mass $M$ . The horizontal lines correspond to the RHS of (6.43). The curves ranging from the thickest to the thinnest correspond to $M = 0.1, 0.3, 1, 10, 1000$ in Planck units, respectively. ....	162
6.5	Choice 2: $\alpha$ as a function of $M$ . ....	163
6.6	Choice 2: the logarithmic of $p_b$ as a function of the logarithm of $p_c$ for different values of the mass $M$ . The curves ranging from the thickest to the thinnest correspond to $M = 0.05, 0.1, 0.3, 1, 10, 1000$ in Planck units respectively. ....	164
6.7	Choice 2: the evolution of the spatial volume as a function of the normalized time $T/ T_b $ . The curves ranging from the thickest to the thinnest correspond to $M = 0.05, 0.1, 0.3, 1, 10, 1000$ in Planck units respectively. ....	164
6.8	Choice 2: volume at the bounce as a function of mass. ....	165
6.9	Choice 2: the value of the Kretschmann scalar at the bounce as a function of mass. ....	166
6.10	Choice 3 : the parameter $\beta$ is plotted as a function of the mass $M$ . ....	167



6.11	Choice 3: the logarithmic of $p_b$ as a function of the logarithm of $p_c$ for different values of the mass $M$ . The curves ranging from the thickest to the thinnest correspond to $M = 0.05, 0.1, 0.3, 1, 10, 1000$ , in Planck units, respectively.....	167
6.12	Choice 3: the evolution of the spatial volume as a function of the normalized time $T/ T_b $ . The curves ranging from the thickest to the thinnest correspond to $M = 0.05, 0.1, 0.3, 1, 10, 1000$ , in Planck units, respectively.....	168
6.13	Choice 3: bounce volume as a function of mass. ....	168
6.14	Choice 3: the value of the Kretschmann scalar at the bounce as a function of mass. ....	169
6.15	Choice 4: we plot the left and right hand side of Eq. (6.52) as a function of $\alpha$ for several values of the mass $M$ . The curves ranging from thickest to the thinnest correspond to $M = 0.05, 0.1, 0.3, 1, 10, 1000$ (in Planck units), respectively. The curves converging on the left of the graph are of the left hand side of Eq. (6.52), and vice-versa. ....	171
6.16	Choice 4: $\alpha$ as a function of $M$ . ....	171
6.17	Choice 4: we plot the logarithmic of $p_b$ as a function of the logarithm of $p_c$ for different values of the mass $M$ . The curves ranging from the thickest to the thinnest correspond to $M = 0.05, 0.1, 0.3, 1, 10, 1000$ , in Planck units, respectively.....	172
6.18	Choice 4: the evolution of the spatial volume as a function of the normalized time $T/ T_b $ . The curves ranging from the thickest to the thinnest correspond to $M = 0.05, 0.1, 0.3, 1, 10, 1000$ , in Planck units, respectively.....	172
6.19	Choice 4: bounce volume as a function of mass. ....	173
6.20	Choice 4: the value of the Kretschmann scalar at the bounce as a function of mass. ....	173
6.21	Penrose diagram for the interior of Schwarzschild spacetime undergoing symmetric bounce to white hole solution is shown. ....	175

# Abstract

Loop quantum cosmology (LQC) has in recent years led to successful resolution of singularities in cosmological models while agreeing with general relativity in low curvature limit. Existence of a bounce and the possibility of an effective continuum description closely approximating the quantum evolution have been notable features of this singularity resolution. The effective spacetimes of loop quantized isotropic and Bianchi-I models have been shown to be geodesically complete and free from strong singularities. In this dissertation, we extend these results to effective loop quantized Bianchi-II, Bianchi-IX and Kantowski–Sachs models with arbitrary minimally coupled matter, and also explore the possibility of symmetric bounces in loop quantized black hole interiors. These are anisotropic spacetimes with spatial curvature. For models with both anisotropy and spatial curvature, earlier techniques to loop quantize the isotropic and Bianchi-I models do not work. Using holonomies along open edges, two quantizations of these models are available in literature - the Ashtekar connection based ‘A’ quantization and the extrinsic curvature based ‘K’ quantization. Considering the effective dynamics of both these quantizations in the Bianchi-II model, we show that the scale factors and the volume remains non-zero and finite for all finite time evolution. Though the energy density, the expansion and shear scalars are bounded, some curvature invariants may potentially diverge. However, geodesic evolution remains regular at such potential divergences and no strong singularities are present. In comparison to the ‘K’ quantization, the ‘A’ quantization in Bianchi-II requires to either impose weak energy conditions (WEC) or include inverse triad corrections to obtain these results. We then show singularity resolution in Bianchi-IX model in both these quantizations. However, now inverse triad corrections must be included in the ‘A’ quantization as WEC are insufficient for singularity resolution. We prove singularity resolution in effective Kantowski–Sachs model with matter without needing inverse triad corrections, where ‘A’ and ‘K’ quantizations are equivalent due to special symmetries. Finally, using an analysis based on Dirac observables of the vacuum effective Kantowski–Sachs spacetime as a model for the Schwarzschild interior, we obtain a symmetric bounce condition, and analyze implications of different dynamical prescriptions giving symmetric bounces.

# Chapter 1

## Introduction

Over the last hundred years since its publication in 1916, Einstein's theory of general relativity (GR) has emerged as the rightful successor to Newton's theory of gravity and led to numerous advances in our understanding of gravity, cosmology and most importantly in our conception of spacetime itself. GR has led to the radical realization that spacetime, instead of being an inert stage on which everything else happens, actively participates in the dynamics of the universe. The far reaching consequences of this radical revision in our conception of spacetime are being validated by precise experimental observations carried out in recent decades and continuing today. Perhaps the most evident example of the dynamic nature of the spacetime is the existence of gravitational waves predicted by GR, which are nothing but ripples in the fabric of the spacetime caused by motion of massive objects interacting with the spacetime. The reality of their existence was recently confirmed with the direct observation of gravitational waves coming from the merger of two massive black holes by the Laser Interferometer Gravitational-Wave Observatory (LIGO) [1], leading to the birth of gravitational wave astronomy. GR also provides a precise description of the large scale universe and cosmology which nicely explains the observational data such as the Hubble's law of recession of galaxies, the accelerated expansion of the universe, the existence of cosmic microwave background (CMB) radiation from early universe and the relative abundances of elements in the universe. We are currently in the era of precision measurements in cosmology with experiments such as the Cosmic Background Explorer (COBE) [2], followed by Wilkinson Microwave Anisotropy Probe (WMAP) [3, 4] and Planck Mission [5, 6] to observe the CMB to an ever increasing precision, and DEEP2 Redshift Survey [7], the 2dF Galaxy Redshift Survey [8, 9], the Sloan Digital Sky Survey (SDSS) [10] for precision measurements of the large scale structure of the universe, and various others. The remarkable thing is that GR provides a framework to build a cosmological model which fits most of this precision data.

Despite its successes, the shortcomings of the theory have been known to us from the time of its inception. Singularities were discovered in a spherically symmetric solution by Schwarzschild [11] and later by Droste [12] barely a year after the theory was published, which was also one of the first exact solutions discovered of the Einstein field equations. The Schwarzschild metric, which is a unique solution of the Einstein's field equations in vacuum under spherical symmetry, described a static solution which was singular both at the center (in terms of the radial coordinate: at  $r = 0$ ) and at a spherical surface situated at the “Schwarzschild radius” (at  $r = R_s$ ). It took several decades of work by various scholars (see e.g. Eddington [13], Lemaitre [14], Einstein and Rosen [15], Synge [16] Finkelstein [17], Fronsdal [18], Kruskal [19], Szekeres [20], Novikov [21], Penrose [22] ) in understanding the properties of the Schwarzschild spacetime to establish that there is a real singularity at the center where the curvature of spacetime diverges, while the  $r = R_s$  surface is instead an event horizon, and the singular nature of the Schwarzschild metric at this surface is merely a coordinate singularity which disappears after a change of coordinates. This picture of a singularity with an event horizon as a surface of no escape was later termed “black hole”. Further, the solutions of Einstein's equations corresponding to a charged black hole (called Reissner–Nordstrom black hole [23, 24, 25, 26]), a rotating black hole (the Kerr metric [27]), and a charged rotating black hole (the Kerr–Newmann metric [28]) were also discovered by the 1960s. Meanwhile, studies of compact, relativistic gravitational objects also led us to the idea of singularity. Starting with the work of Chandrasekhar on white dwarfs [29] and the works of Landau [30], and Oppenheimer and Volkoff [31] and others on neutron stars, and of Oppenheimer and Snyder on the collapse of a massive star [32] which showed that stars with only a few times the mass of the sun would be unstable against a gravitational collapse in their final stages, it became clear that such objects may actually exist in nature which become compact enough to become black hole candidates. On the other hand, the applications of GR to cosmology were also mired by singularities. Our universe is very closely described at the large scales by an expanding, spatially flat, isotropic and homogeneous cosmological model, called the spatially flat Friedmann–Lemaître–Robertson–Walker (FLRW) model which is a solution of GR. Lemaitre was the first one to point out that

an expanding universe described by GR must have been in a highly dense and hot state in the past [33, 34]. This is called the hot big-bang model of the universe, which was further elaborated by Gamow [35], Alpher and Herman [36], and others, and was supported by the observations of the expansion of the universe by Hubble [37] and of the CMB radiation starting with Penzias and Wilson in the 1960s [38]. It turns out that the large scale universe is described by the spatially flat, expanding FLRW model extremely well. However, GR predicts that the spatially flat FLRW model must have a singularity in its past evolution.

At these singularities, both of the cosmological type and the black hole singularities, certain physical quantities such as the energy density and the curvature diverge, and there is no unique extension of the spacetime geometry past the singularity. The geodesic evolution of light rays and particles also breaks down and the past evolution of the spacetime is incomplete. Thus the singularity appears to be an edge of the spacetime where we lose the ability to probe the universe further. However, it was hoped that these singularities were an artifact of the special symmetries of all these idealized models considered, which may not hold exactly in any realistic situation. This hope was crashed by the work of Raychaudhuri, Geroch, Hawking, Penrose and others, summarized in the monograph [39], which established that singularities can be shown to exist in general relativistic spacetimes without assuming any special symmetries provided some reasonable energy conditions are satisfied by the matter content (such as the weak energy conditions, which intuitively imply the positivity of the energy density). This established singularities as a generic feature of general relativistic spacetimes, and a real limitation on our ability to probe the universe further if we continue using GR as a description of gravity.

Thus, it has become clear that GR cannot be the final word on gravity and cosmology. As described above, there are various regimes where GR fails to provide satisfactory answers, such as the very early universe and the end states of massive stars. In both of these scenarios, the spacetime curvature diverges and a singularity is encountered in GR in a finite time, and the evolution is incomplete. Since the curvature is so high and the matter is compressed to microscopically small scales, we expect both gravitational and quantum effects to be important in these scenarios. In the case of cosmology, the whole universe itself is expected to be of

microscopic size in the very early phase warranting a quantum description. A reliable description of the early universe is also needed to explain some of the puzzling features of our current universe, such as the high degree of isotropy and homogeneity observed at large scales in our universe. The theory of cosmic inflation does explain some of these features but fails to help the issue of the big bang singularity at the beginning [40]. Past evolution is still incomplete and leaves the questions of the origin of inflation and the conditions required for its emergence unanswered. The resolution of the problem of singularities is one of the primary motivations for the search for a theory of quantum gravity. We also expect it to provide a general framework to formulate a reliable description of the early universe. And most importantly, quantum gravity may lead to a revision in our conception of spacetime. Every time our conception of spacetime has been revised, it has led to a renaissance in whole of physics. GR replaced the Newtonian idea of gravity as a force with the idea of gravity as the dynamics of spacetime, which changed our conception of spacetime from being a fixed and inert background on which everything else evolves, to a dynamical one which takes part in the drama that unfolds in it. This brought a paradigm shift in cosmology and led to the current big-bang model of cosmology which explains numerous features of our observed universe (but fails to reliably describe the early universe and has a singularity as discussed above). If history is any indication, perhaps the most revolutionary outcome that quantum gravity might lead to is yet another radical revision in our conception of spacetime.

The regimes in which quantum nature of gravity is expected to play a prominent role, currently seem out of our reach to probe directly. Due to lack of substantial experimental cues to rely upon, theoretical explorations beyond GR, based primarily on physical principles and mathematical consistency, have led to a diversity of approaches to quantum gravity. Depending on which principles are considered to be fundamental, and which ones are relaxed or diluted, we have different approaches to quantum gravity. Some major ones are string theory [41, 42, 43], loop quantum gravity (LQG) [44, 45, 46, 47, 48], causal dynamical triangulations [49, 50, 51], causal sets theory [52, 53, 54, 55] and twistor theory [56, 57]. Some approaches preserve the background independence of GR and aim to construct a background independent theory of

quantum gravity, for example, LQG. LQG is a non-perturbative canonical quantization of GR based on a reformulation of GR in terms of Ashtekar variables. Some of the approaches assume a discrete or quantum substratum beneath the continuum spacetime of GR at the Planck scales as their starting point. Examples of this approach include causal dynamical triangulation and causal set theory. These approaches are also background independent. String theory, on the other hand, takes inspiration from particle physics theories and assumes in its initial formulation a background spacetime similarly to the quantum field theories of particle physics. Apart from quantizing gravity, string theory also aims to provide a unified theory of all four interactions of nature. However, attempts to formulate string theory in a completely background independent way have so far been inconclusive.

As of now, attempts are being made to make contact with experimental observations, however, obtaining direct measurements of quantum gravity effects has been hard. Due to lack of guidance from direct observational evidence, classical singularities of GR provide us with an important setting to test the various emerging approaches to quantum gravity as singularities prove to be the essential roadblocks where our explorations in GR fail. A reliable resolution of the problem of singularities is thus crucial. Apart from the end states of massive stars, singularities in GR are also encountered in various cosmological models. This is pertinent, considering that early universe cosmology seems to be the most promising avenue today for observing signatures of quantum gravity. Thus solving the problem of singularities will also have important ramifications for the physics of the early universe which could possibly be observed in precision experiments. In this dissertation, our focus will be the application of ideas and techniques from LQG to cosmological spacetimes of interest, and investigating the question of resolution of singularities. LQG, as mentioned, is a canonical quantization of GR. Even though it is presently a matter of taste (due to lack of experimental evidence) as to which approach to quantum gravity one chooses, we provide some of our motivations for our interest in canonical quantization of gravity in the following. First of all, various singularities of interest are regions of strong gravitational field with highly non-linear behavior. So non-perturbative effects of quantum gravity are likely to be very important in this regime. Secondly, GR admits solution-spacetimes with

various different topologies, and the solutions are not guaranteed to be asymptotically Euclidean in general. This seems to suggest the appropriateness of a background independent approach to quantum gravity. The following intuitive, but heuristic reasoning can be given as to why background independence is desirable: even though the gravitational field in GR couples to matter through the Newton's gravitational constant, the interaction of the gravitational field with itself is completely described by the geometry itself and is not dictated by a coupling constant. Thus, dividing the gravitational field into a non-interacting background spacetime and a dynamic geometric part which is interacting seems unnatural. The canonical approach addresses the above mentioned concerns as it is background independent and non-perturbative. Moreover, unlike some other non-perturbative and background independent approaches to quantum gravity which assume a discrete structure as the basis of quantum spacetime as their starting point, the canonical approach (specifically LQG) has the nice feature that the programme of quantization itself leads us to a kinematical framework for the quantum theory which results into discrete spectra for various geometrical quantities. In the end, all these are motivating factors at best and the choice of theory is still largely a matter of taste at the moment as mentioned above. We begin with a discussion of the canonical quantization program in the next section.

## 1.1 The canonical approach to quantum gravity

The canonical approach to quantizing gravity, as the name suggests, attempts the canonical quantization of GR by taking its Hamiltonian formulation as the starting point. In the Hamiltonian formulation of GR, which is also crucial in its initial value formulation, the four dimensional spacetime is foliated into a stack of three dimensional spacelike hypersurfaces which are sequenced by a time parameter. This allows the spacetime of GR to be viewed as the time development of the metric of a three dimensional spacelike hypersurface [58]. Recasting GR in this Hamiltonian form paves the way for its canonical quantization. However, we encounter one of the conceptual tensions between GR and the quantum theory here. In the quantum theory, the system is described by a wave function (or a state in the Hilbert space) whose time evolution is dictated by the Schroedinger's equation. Time is an external parameter in the quantum theory. Whereas time is just a coordinate in GR and is treated on an equal footing to space. The



action of GR is invariant under four-dimensional diffeomorphisms of the spacetime manifold. Thus there is no absolute time parameter in GR in contrast to ordinary quantum mechanics. The consequence is that the flow generated by the total Hamiltonian of GR in the phase space turns out to be a gauge transformation (this is related to the fact that the total Hamiltonian in GR is a sum of constraints, which we discuss below in more detail). And since any physical observable must be gauge invariant, its Poisson bracket with the Hamiltonian must vanish. Thus it seems that the dynamics is ‘frozen’ in GR in this sense. This contradiction between GR and the quantum theory poses a fundamental question about the nature of time and is known as the *problem of time* in quantum gravity. Thus quantization of GR necessarily entails dealing with this question which has several consequences for the theory. Due to split into space and time in the Hamiltonian formalism, the four-dimensional covariance of GR is not explicitly manifest. Although classically it can be shown that, though hidden, the four-dimensional covariance is encoded in the canonical formulation. But in the quantum theory it leads to anomalies in the constraint algebra in LQG which turns out to be a difficult problem to handle.

We mentioned in previous paragraph that the total Hamiltonian of GR is a sum of constraints. In order to understand the significance of this, we first note that a constraint means a relation between the variables which is preserved by the dynamics of the system. In physics, constraints appear whenever we describe a system or theory with more variables than the actual number of degrees of freedom. For example, describing a simple pendulum using Cartesian coordinates has a constraint ensuring the length of the pendulum is constant during the motion. In some cases, we begin constructing a theory using the natural variables available to us, and only later discover that there are constraints, e.g. electromagnetism. Electric and magnetic fields seem to be natural quantities in terms of which to formulate our theory, however, we then discover that the electric field is constrained by the Gauss law (or the Gauss constraint). The Yang–Mills theories which are a generalization of the electromagnetism also have an analogous Gauss constraint. The constraints, like any other function on the phase space, generate a flow in the phase space. But since the constraints are preserved by the dynamics, the flows generated by the constraints are gauge transformations which do not affect the Hamiltonian. However,

GR falls into a special class of constrained systems called totally constrained systems. In such systems, the total Hamiltonian is itself a constraint, such that there is no true dynamics in the system. The flow generated by the Hamiltonian is also a gauge transformation. This is what we noted in the above paragraph. GR is invariant under different choices of the time variable. The whole universe is a spacetime manifold. Everything is contained in it and it doesn't evolve with respect to any external time parameter. Thus the spacetime manifold is frozen. It is only when we split the spacetime into spatial slices that we can view the spacetime as the time evolution of the spatial slices. Since the manifold is diffeomorphism invariant, there are many ways to split it into spatial slices corresponding to different choices of time parameter. However the whole spacetime has no dynamics and this is reflected in the fact that the total Hamiltonian is always a sum of constraints.

The quantization of the fully constrained Hamiltonian of GR is handled following Dirac's approach to the quantization of constrained Hamiltonian systems, the groundwork for which was laid by the pioneering contributions of Dirac [59, 60, 61, 62, 63], and later Bergmann and Komar [64, 65, 66, 67]. The work by Arnowitt, Deser and Misner led to a precise Hamiltonian formulation of GR in metric variables [68] called the ADM formulation. Wheeler and DeWitt then developed a canonical quantization of GR in the ADM formulation based on the methods developed by Dirac et al. for constrained systems [69, 70, 71, 72]. In the Wheeler–DeWitt canonical quantization of gravity, the 3-metric  $q_{ij}$  of the hypersurfaces is treated as the configuration variable of the theory. The conjugate variable turns out to be the extrinsic curvature of the spatial slices in this case. In the quantum theory, the kinematical states are considered to be functionals of the metric  $q_{ij}$  represented as  $\Psi[q_{ij}]$ . Following Dirac, the constraints are then implemented in the quantum theory as conditions on the states defined in a suitable Hilbert space. This space is called the kinematical Hilbert space which is analogous to the unrestricted phase space in the classical picture on which the constraints are defined. Classically the imposition of constraints leads us to the constraint-surface in the unrestricted phase space which is called the reduced phase space. By requiring that their corresponding operators must annihilate the physical states, we pick out the physical states from the kinematical Hilbert space. Just

like the plane wave solutions of basic quantum mechanics, the physical states may turn out to be non-normalizable combinations of the kinematical states, in which case a suitable physical inner product is defined on the physical states to define the physical Hilbert space. Following this route in the Wheeler–DeWitt theory, the physical states are then the solutions of the Wheeler–DeWitt equation  $\hat{H}\Psi[q_{ij}] = 0$ , which is the requirement that the operator corresponding to the Hamiltonian constraint must annihilate the physical states. The absence of a time derivative in the Wheeler–DeWitt equation, unlike the time-dependent Schrödinger’s equation, is representative of the problem of time discussed above in this approach.

However, the Wheeler–DeWitt equation is a functional differential equation which turns out to be intractable. In particular, the constraints have a complicated non-polynomial dependence on the metric variables and it is not clear how to rigorously define the corresponding operator. Similar problems exist in defining the corresponding Hilbert space on which this operator acts, and obtaining the solutions. Thus the quantization of general theory remains elusive even at the kinematical level. This remains a major roadblock in the Wheeler–DeWitt theory. Thus, except for some symmetry reduced situations, a rigorous formulation of a general kinematical quantum Hilbert space representation for general geometries is lacking. The approach in the Wheeler–DeWitt theory has been to solve the the Wheeler–DeWitt equation in some symmetry reduced situations (such as cosmology). However, the boundary conditions that need to be imposed on the solution wave functions remain a topic of debate. The symmetries and the requirements of mathematical consistency are not sufficient to select the boundary conditions as was initially hoped, and various proposals for the boundary conditions exist [70, 73, 74, 75], most importantly the no-boundary proposal [73] and the tunneling boundary proposal [74]. Further, addressing the issue of singularity resolution has remained a challenge in these symmetry reduced models. In Wheeler–DeWitt cosmology, singularity resolution has been variously characterized by the highly non-classical nature of the wave function near the singularity or by the vanishing of the wave function at the classical singularity [76, 77]. Using these as the criteria, it can be shown that the singularity is resolved for some cases [78], however counter examples also exist. For example, it can be shown that the no-boundary proposal for the isotropic and homogeneous

spacetimes with closed topology with a massive scalar field and a cosmological constant may be singular [79]. Even in cases where it works, these vague indications such as vanishing of the wave function at classical singularity cannot be taken to signal singularity resolution unless the behavior of the expectation values of the physical observables is analyzed using a physical inner product on a physical Hilbert space, and it is shown that the observables which diverge in the classical theory at the singularity remain finite in the quantum evolution. Moreover, there exist models for which the physical sector along with the full set of physical observables for the Wheeler–DeWitt quantization can be constructed and it can be shown in a precise sense that the singularity is not resolved. Thus is the spatially flat isotropic spacetime with massless scalar field [80]. By obtaining the backward numerical evolution of semi-classical states peaked at the classical GR trajectory at late times, it has been demonstrated in this case that the classical big-bang singularity is not avoided by the Wheeler–DeWitt quantization [80]. The states remain peaked on the classical singularity right up to the singularity. The values of the physical observables representing the spatial volume also vanishes as it does in the classical evolution [81]. Moreover, using the generalized consistent histories approach in this case, it can be shown that for arbitrary choice of states in the physical Hilbert space, the probability for this Wheeler–DeWitt quantum universe to encounter a singularity is unity [82]. Thus, without guidance from a complete theory, the results in the Wheeler–DeWitt theory on the question of singularity resolution have been mixed. This is where the programme of LQG becomes relevant, where it has been possible to obtain a unique and rigorously defined kinematical framework. This has been possible due to a different choice of operator algebra inspired from the connection formulation of GR which leads to a starkly different quantum theory than Wheeler–DeWitt theory and the availability of a complete kinematical description has allowed progress where it was stalled in Wheeler–DeWitt theory.

## 1.2 Loop quantum gravity

The canonical quantization program was reinvigorated by Ashtekar’s observation that the constraints of GR can be expressed in a simpler form if we reformulate GR in terms of the so called connection and triad conjugate variables [83]. This was based on earlier work by Sen

in this direction [84, 85]. This led to rapid progress in the field of canonical quantization of GR and eventually morphed into what is today called LQG. It has been well known that GR can be equivalently described in terms of triad fields instead of the spacetime metric approach (this formulation also allows to couple fermions to the gravitational field). The triads are three dimensional vector fields related to the spatial metric that carry all the information contained in the metric, but have additional internal degrees of freedom. The Hamiltonian formulation can be written in terms of the densitized<sup>1</sup> triads and the extrinsic curvature as canonically conjugate variables, with three extra constraints for the extra internal degrees of freedom introduced with the triads. A canonical transformation then yields a formulation of GR akin to Yang–Mills theories in terms of the densitized triads and the Ashtekar connection as conjugate variables, and the three extra constraints take the form of Gauss constraint of Yang–Mills theories [83, 46]. This raised the hope that techniques from Yang–Mills theories could be used to quantize gravity. Initially, this formulation was obtained using the complex-valued Ashtekar connections introduced by Ashtekar, which required extra reality conditions to be imposed. However, much simplification has been obtained by the introduction of real-valued Ashtekar variables by Barbero [86]. The Yang–Mills theories are naturally described in terms of the gauge invariant Wilson loops [87, 88, 89, 90] (analogous to the situation in magnetism where the information of the field is contained in the circulation of the vector potential around closed loops). Thus, the key departure from the Wheeler–DeWitt quantization occurs in the choice of basic quantization variables. The Gauss constraint, when elevated to an operator, requires the states to be gauge invariant. The basic variables for quantization are the holonomies of the connection and the fluxes of the triads instead of the connection and the triad themselves. Holonomy is the generalization of the idea of circulation of vector potential in magnetism to connections in curved spacetimes. It is the circulation of the connection around a closed path in the manifold using parallel transport. The holonomies contain all the gauge invariant information of the connection (as per the Giles theorem [90]) and the corresponding conjugate variables are the fluxes of the densitized triad

---

<sup>1</sup>Densitized quantities are obtained from the corresponding tensor quantities upon dividing by the square root of the determinant of the metric.

across two dimensional surfaces dual to the holonomy paths [46]. The kinematical Hilbert space consists of functions of the holonomies of the connection around closed loops, and spin networks serve as convenient basis states of the kinematical Hilbert space. The algebra of basic observables is obtained by treating holonomies of connection and the fluxes of the triads as the basic objects [91]. It is this choice of holonomy-flux algebra which induces a unique diffeomorphism invariant measure on the kinematical Hilbert space, called the Ashtekar–Lewandowski measure [92], which leads to the novel features of LQG. In particular the holonomy operators no longer have a continuous representation on the Hilbert space due to the Ashtekar–Lewandowski measure, consequently the connection and triad are no longer well-defined operators on the Hilbert space. Thus the quantization suggested by the holonomy-flux variables lead to a radically different theory compared to the Wheeler–DeWitt theory.

One of the highlights of the results of LQG is that it may lead to a fundamental revision in our conception of spacetime. It is possible to define various operators representing geometrical quantities such as length, area and volume of curves, surfaces and regions of the spatial hypersurfaces on the kinematical Hilbert space which turn out to possess Planck scale discreteness in their spectra [93, 92, 94]. Thus LQG seems to suggest a picture of geometry which is fundamentally discrete at the Planck scale. Unlike some other approaches to quantum gravity where a discrete geometry is assumed as a postulate, a discrete geometry seems to naturally emerge out of canonical quantization of GR in LQG. This fundamental discreteness ensures the theory is free from UV divergences. Applications of LQG to black hole physics have led to precise calculations of the black hole entropy [95, 96, 97, 98, 99, 100]. Most importantly, LQG has been successful in developing a mathematically rigorous, manifestly background independent and non-perturbative framework for quantum gravity following the canonical quantization program which allows the formulation and investigation of various pertinent questions in quantum gravity.

However, there are various open issues in LQG and the picture is far from complete. We hinted in the previous section on the potential issues caused by the problem of time in the canonical framework. Splitting the spacetime into space and time in the canonical framework

leads to a different treatment of spatial diffeomorphisms and time diffeomorphisms. While this seems to still be consistent with the spacetime covariance at the classical level, at the quantum level it leads to anomalies in the constraint algebra of the quantum constraint operators. Moreover, the fact that the spacetime can be foliated in infinitely many equivalent ways leads to the problem of the definition of a unique Hamiltonian constraint operator in the quantum theory. Another issue is of the classical limit of the theory. Starting with the choice of gauge invariant variables, the choice of inner product to obtain a background independent Hilbert space, we take many complicated steps to reach the quantum theory including sophisticated methods to regularize the operators at various stages. So it remains a non-trivial task to show that LQG contains GR as its classical limit, and the programme of semiclassical analysis of the theory is still in a nascent stage. Many proposals have been suggested in the literature to deal with these and other problems, such as the master constraint program of Thiemann [101] to address the problem of defining the Hamiltonian constraint, the partial observable approach developed by Rovelli [102, 103], Page and Wootters [104], Kuchař [105, 106], Pons, Salisbury and Sundermeyer [107, 108], Dittrich [109, 110, 111], Thiemann, Giesel and others [112, 113, 114, 115, 116, 117], Gambini et al. [118, 119, 120, 121, 122] to address the issue of finding physical observables as well as addressing the problem of time in both GR and LQG. While progress is being made on multiple fronts, yet we are far from a conclusive resolution of the outstanding issues.

Nevertheless, it has been possible to make progress in certain special circumstances and approximations, most prominently in the area of quantum cosmology. Due to the symmetries of cosmological spacetimes, various technical issues become simplified and allow us to make predictions. More importantly, cosmology allows us to tackle one of the most important outstanding problems of quantum gravity - the problem of singularities. The applications of LQG techniques to symmetry reduced cosmological models is known as loop quantum cosmology (LQC) where it has been shown that the classical big bang singularity is resolved in the quantum evolution [123, 124, 80] in the FLRW spacetime, and also in various other cosmological spacetimes. We discuss the symmetry reduced quantization of LQC in the next section and note some of the important results obtained in this area.

### 1.3 Loop quantum cosmology

As we noted in the beginning of this chapter, most of the cosmological models of interest have singularities in classical GR. We also discussed how the question of cosmological singularity is intimately tied with the several other questions regarding the state of the early universe and the origin of various features of our current universe. One of the goals of quantum gravity is to resolve the problem of singularities and provide a consistent framework to formulate the physics of the early universe, possibly answering questions regarding the origin of cosmic inflation or providing an alternative to it. Cosmology also offers the most promising avenue today to look for the signatures of quantum gravity effects and discriminate between various candidate theories of quantum gravity. This is so because of two reasons. First, on the observational side, we seem to be getting closer to discovering unexpected and new features in the cosmological data due to the advancements in observational cosmology over the past few decades. Second, on the theory side, the presence of large scale symmetries in cosmological models lead to simplifications in various technical issues faced in the full theory (such as the issues mentioned in LQG in the previous section) which makes it possible to complete the quantization procedure and obtain physically relevant predictions, possibly by calculating quantum gravity imprints in the CMB and other observational data. Thus cosmology seems to be the sweet spot where experiment and theory could meet for the first time in case of quantum gravity.

Moreover, cosmology provides a convenient setting to explore various other conceptual issues discussed above, such as the problem of time, the construction of the physical Hilbert space and corresponding physical observables etc. Most importantly, quantum cosmology can give us insights into Planck scale behavior of gravity and spacetime as we explore the dynamics close to classical singularities. We can explore whether quantum gravity puts an upper bound on physical quantities such as the energy density and the curvature invariants. And how does the resolution of singularity affect the physics of the early universe. It is often the case in physics that application of new ideas on simple models leads to novel insights, some of which turn out to be general features of the theory that transcend the simple model at hand. It is very likely that the



application of quantum gravity to exactly solvable cosmological models might lead to lessons for the quantum gravity in general. This expectation is also supported by the Belinski–Khalatnikov–Lifshitz (BKL) conjecture [125] with regards to generic cosmological singularities in GR. The BKL conjecture states that close to a generic singularity in GR, the dynamics is dominated by the time derivatives in the Einstein’s equations and the spatial derivatives can be ignored. Thus, the dynamics of different spatial points decouples from each other and the evolution resembles that of spatially homogeneous spacetimes and is well approximated using certain homogeneous and anisotropic cosmological models called Bianchi models. The spatially homogeneous solutions of Einstein’s equations can be classified using their symmetry groups. This classification was first obtained by Bianchi [126], who classified all but one of the homogeneous and anisotropic models into classes called Bianchi models from I through IX, which we describe in the next chapter. The simplest of these, the Bianchi-I model, is a generalization of the FLRW model, in which different spatial directions expand as different powers of the time coordinate, and the exponents are called Kasner exponents. In the BKL scenario, the dynamics towards the singularity at each point can be described by a sequence of epochs described by Bianchi I model (also called Kasner phases as the Bianchi-I model is described using the exponents of the metric co-efficients called Kasner exponents) which are mediated by Bianchi-II transitions. Similar chaotic oscillations from one Kasner phase to another are also seen in the Bianchi-IX spacetime in the approach to singularity where this behavior has been termed as the Mixmaster dynamics [127]. If the conjecture extends to quantum gravity as well, we can indeed gain insights into the main features of quantum dynamics in the approach to a generic cosmological singularity by studying the singularity resolution in the quantum dynamics of these homogeneous and anisotropic models. All of the above mentioned reasons provide a strong motivation for studying quantum cosmology.

LQC is the application of the quantization scheme of LQG to symmetry reduced cosmological models. The approach is to first simplify the dynamical description using the symmetries of the cosmological models and then apply the techniques of quantization of LQG to this simple system. Due to the high symmetry of the cosmological models, symmetry reduction at the

classical level reduces the system to a finite number of degrees of freedom which simplifies many technicalities faced in the full theory. The hope is that this will allow us to surpass some of the problems in dealing with the Hamiltonian constraint encountered in the full theory. Indeed, this strategy worked as expected and loop quantization of various cosmological models has been performed beginning with the isotropic and homogeneous FLRW model, which has led to a series of promising results regarding singularity resolution and has provided an arena to calculate the effects of quantum gravity in cosmological data. It must be kept in mind that LQC is not obtained as the cosmological sector of the full theory LQG, rather it is a quantization of the cosmological sector of GR on the lines of LQG. Thus there are concerns whether LQC corresponds precisely to the cosmological sector of LQG. One way to establish such a connection could be to first obtain the cosmological sector of LQG and find an embedding from the physical states of LQC to this sector. However, different proposals exist on identifying the states of the full theory that correspond to the cosmological sector. Attempts in this direction, some of which are [128, 129, 130, 131, 132, 133], have so far been only partially successful and the connection of LQC to LQG remains an open question. Nevertheless, there are important lessons to be learned by adopting the methods of LQC in quantizing symmetry reduced models to obtain insights.

The first steps in this direction were taken by Bojowald in [134] which provided the initial indication of potential singularity resolution in the LQC of the isotropic and homogeneous models. This was followed by a series of papers [135, 136, 137, 138, 139, 140, 141, 142] discussing various implications of LQC in homogeneous cosmological models. However it was soon noticed that the loop quantization of these early works differed from the older Wheeler–DeWitt cosmology due to an implicit assumption ensuring periodicity of the extrinsic curvature which was unjustified on physical grounds. Eventually, the concepts of LQC were put on a concrete mathematical foundation by Ashtekar, Bojowald and Lewandowski in [143] which showed that the results obtained in LQC could be obtained without any assumption on the extrinsic curvature if the quantization techniques of LQG are more closely followed. However, due to a lack of a detailed description including a physical Hilbert space and a set of physical observables, doubts remained on the precise sense in which the singularity is resolved in LQC [144]. A

detailed study of the spatially flat isotropic model with a massless scalar field, including construction of the physical Hilbert space, physical observables and semi-classical states was then carried out in [123, 124] based on the Hamiltonian constraint suggested in [143] and it was shown numerically by backward evolution of certain states which are semi-classical at late times that the big bang singularity is replaced by a quantum bounce for these states. So a precise description of singularity resolution was obtained, but it was noticed at this stage that this quantization predicts large quantum gravity effects even at low curvatures where GR provides a good description of the universe. A careful review of the quantization of the Hamiltonian constraint led to the “improved” quantization of [80] which not only provided the full physical Hilbert space and set of physical observables for a detailed and precise characterization of the quantum bounce in the high curvature regime yielding singularity resolution, but was also free from various shortcomings of previous loop quantizations of the spatially flat isotropic model such as departures from classical GR even at low curvatures. It was seen in numerical simulations of certain semi-classical states, which closely approximated classical GR evolution at large volumes and low curvatures, that the evolution was symmetric about the bounce and the pre-bounce branch was also semi-classical at large volumes. A mild simplification of this model based on well motivated approximations yielded an exactly solvable model for LQC of spatially flat isotropic model (referred to as “sLQC”), which was studied in [81] to put this detailed picture of singularity resolution obtained in the numerical simulations of some specific semi-classical states on a more concrete basis. It was shown analytically that in sLQC that the quantum bounce is generic and the matter density has an absolute upper bound. Further, it was shown using the consistent histories approach, it was shown for generic states in sLQC that the probability of occurrence of a singularity is zero, while that of a bounce is unity [145]. This is a very encouraging result considering that we were hoping to resolve the problem of singularities in GR using quantum gravity. However, it was still doubtful whether the other features of the bounce obtained in numerical simulations of some specific states mentioned above, namely the symmetricity of the bounce and the semi-classical nature of the pre-bounce branch, were stable under quantum fluctuations. This was addressed in [146] where using the exactly solvable model

it was shown that for all states that are semi-classical at late times, there are very stringent bounds on the fluctuations on the other side of the bounce, implying semi-classicality for the pre-bounce branch. Further results on bounds on fluctuations in more general situations were obtained in [147, 148, 149]. Thus it became established that in LQC in the improved quantization of [80], a semi-classical spatially flat and isotropic, expanding universe emerges from an identical, semi-classical and contracting universe in the past via a symmetric quantum bounce. Further, it has been shown by analysis of various quantization ambiguities coming from different proposals [150, 151], that physical requirements such as agreement with GR at low curvatures and invariance of physical predictions under rescaling of fiducial structures (fiducial structures are introduced in intermediate steps to suitably define Poisson brackets on non-compact spatial slices) lead to a unique quantization prescription for the spatially flat isotropic model, namely the improved quantization of [80]. Following this, various other conceptual and mathematical issues such as the problem of time, the self-adjointness of the Hamiltonian constraint in this quantization have been addressed [152, 153, 154, 155]. Further, extensive studies of numerical evolution of various semi-classical states peaked at the classical trajectory at late times further establish the robustness of the existence of the quantum bounce in these spacetimes [156, 157]. Recently, the robustness of the bounce has been checked using non-Gaussian states as well [158].

The results in the spatially flat FLRW model have since been generalized to the spatially curved FLRW model [159]. The loop quantization of the isotropic models in a variety of contexts has been studied including the open and closed topologies with non-zero spatial curvature [160, 161, 162, 163, 164] and with various matter models [165, 166, 167, 168, 169]. Further, loop quantization of the various anisotropic spacetimes has also been obtained such as the Bianchi-I [170, 171, 172, 173], Bianchi-II [174], Bianchi-IX [175, 176, 177] which are relevant to the analysis of generic singularities due to the BKL conjecture discussed above. Further, loop quantization of Kantowski–Sachs cosmological models has also been performed which are a good example of models with both spatial curvature and anisotropies [178, 179, 180, 181, 182, 183], and are also relevant in the analysis of the black hole singularity as we will discuss below. Further, inhomogeneous cosmological models have also been considered in LQC. The simplest of inhomogeneous

models is the Gowdy model in which inhomogeneities can be viewed as propagating gravitational waves on a homogeneous Bianchi-I background. The loop quantization of the inhomogeneous Gowdy models was first obtained using a hybrid model where the homogeneous Bianchi-I background was loop quantized while the inhomogeneities were Fock quantized [184, 185, 186, 187]. Progress on full loop quantization of inhomogeneous model was made recently in case of local rotationally symmetric Gowdy models [188]. On the other hand, symmetry reduced quantizations of the gravitational collapse leading to black hole spacetimes have also been obtained in order to study the black hole singularity [189, 190, 191, 192, 193, 194, 195, 196, 197, 198]. The black hole singularity is also studied as a special case of the Kantowski–Sachs cosmological spacetime as the interior of a Schwarzschild black hole is isomorphic to the vacuum Kantowski–Sachs model. The loop quantization of the Kantowski–Sachs model from this perspective have also been studied to analyze the resolution of black hole singularity [183]. It should be noted from the references above that a couple of different quantizations may exist in the literature for a given cosmological spacetime. Symmetry reduction allows various different routes to the quantization of these models, thus making it important to ask, what effect these quantization ambiguities have on the predictions of these models. We will, in part, be exploring the effects of quantization ambiguities in the context of singularity resolution in this manuscript, using the effective spacetime descriptions of these models which we discuss below.

An important aspect of these loop quantizations of symmetry reduced models, which we have not touched upon yet, is the approximate effective continuum description of the dynamics which was discovered early on in the isotropic FLRW models. The LQC quantization of cosmological models described above replaces the classical Hamiltonian description based on differential equations with a description based on quantum difference equations. Just like in the full theory discussed in the previous section, the geometrical operators such as area and volume have discrete spectra in LQC. This endows the loop quantized model with a discrete quantum geometry, the dynamics of which is described by the difference equation of LQC. However, using the geometrical formulation of quantum mechanics [199], a way of mapping the trajectories of expectation values of the quantum observables into a classical symplectic phase space like

manifold has been found [199, 200]. Classically, the state of a system is described by a point in the phase space which is a symplectic manifold. The observables are real-valued functions on the phase space, and the time evolution is described by the flow associated with a specific function called the Hamiltonian [201]. However in quantum mechanics, the symplectic manifold of classical mechanics is replaced by the Hilbert space of states where the observables are given by linear self-adjoint operators on the Hilbert space. Thus, the geometrical structure of the two theories seem to be quite different. However, note that the physical states of a system in quantum mechanics correspond to the equivalence classes of states, called rays, in the Hilbert space. The correct space of physical states to consider is thus the space of rays in the Hilbert space, the so called projective Hilbert space, which has the structure of a Kahlerian manifold [202, 203, 204]. The inner-product on the Hilbert space corresponds to the symplectic structure on this manifold. Moreover, if we take the expectation values of any quantum observable to define a real-valued function on the projective Hilbert space manifold, the flow associated with this function corresponds exactly to the unitary flow generated by the corresponding operator [205, 206, 207, 208, 209, 199]. In particular, the Hamiltonian flow generated on the projective Hilbert space manifold by the real-valued function based on expectation values of the Hamiltonian corresponds to the Schroedinger evolution. Thus, the geometry of classical and quantum mechanics are not as dramatically different as they initially appear. We can then find a way to suitably map the trajectories in the projective Hilbert space manifold onto the classical phase space in order to compare the quantum dynamics with the classical dynamics of a system. This can be done in two different ways. One way is called the truncation method, where the idea is to capture the leading order quantum corrections to the classical evolution by truncating the evolution equations of the Hamiltonian flow on the projective Hilbert space [210, 211]. On the other hand, it is possible in some cases to find an embedding of the classical phase space into projective Hilbert space which suitably captures the quantum dynamics [212, 200]. The effective continuum description in a classical phase space, thus obtained by any of the above two methods, is called the effective dynamics of the loop quantized cosmological model and provides a useful avenue for comparison with the classical dynamics and for various phenomenological

issues. Due to its convenience, the effective dynamics is widely employed in phenomenological investigations in the physics of pre-inflationary dynamics of the early universe.

The effective dynamics for the loop quantized FLRW model has been obtained in [80, 200] and has been shown to incorporate the essential features of the full quantum dynamics obtained from difference equations. The effective dynamics incorporates the effects of quantum geometry via two types of modifications over the classical equations. These are called the holonomy corrections and the inverse triad corrections. The holonomy corrections refer to the fact that by considering holonomies of the connection as a basic variable in our quantization (instead of the connection itself), we are led to a polymerized version of the classical expression in the effective spacetime picture with the connection variables only appearing inside certain trigonometric functions. Various factors containing the connection variable get replaced by bounded trigonometric functions of the connection, leading to bounded expressions for various physical quantities. On the other hand, the inverse triad corrections result from the fact that the operators corresponding to the inverse of the triad or the volume have a bounded spectrum in the kinematical Hilbert space. The numerical studies cited above on the robustness of the bounce [156, 157, 158] verify the validity of the effective dynamics in closely approximating the full evolution of the solutions for states which are sharply peaked on the classical trajectory at late times and bounce at volumes much larger than Planck volume. Even though departures of the effective dynamics from the quantum dynamics have been found in states probing deep Planck regimes in these works, interestingly, the departures are such that the effective dynamics overestimates the curvature at the bounce. Thus the results on singularity resolution established using effective dynamics are likely to be robust in these cases as well. Recently, numerical studies of the bounce using a wide variety of states has also been studied for anisotropic Bianchi-I cosmological models [213] where similar results regarding the validity of effective dynamics have been found.

Using the effective dynamics approach, a number of important results relevant to singularity resolution in LQC have been obtained. The effective description of the loop quantized FLRW model has been used to analytically show that the effective spacetime is geodesically complete

and free from all singularities [214]. Moreover, it has been shown that the expansion and shear scalars are universally bounded in various cases [151, 215, 216, 217, 164, 176, 218, 183], and possible effects of spatial curvature, anisotropies and inhomogeneities on singularity resolution is analyzed [215, 219, 220]. The result on the generic resolution of strong singularities have been extended to Bianchi-I models as well [217] (it is to be noted that the results on generic resolution of singularities in both isotropic [214] and Bianchi-I models [217] have been obtained by just incorporating the holonomy corrections in the effective Hamiltonian. The inverse triad corrections, as we discussed above, could be ignored as they had a negligible effect on singularity resolution these models). In the light of the BKL conjecture mentioned above, it is important to extend the results on generic resolution of singularities in LQC to various other homogeneous cosmological models in order to pave the way for generic singularity resolution in quantum cosmology. It is our goal in this manuscript is to extend the results on generic resolution of singularities to Bianchi-II, Bianchi-IX and Kantowski–Sachs cosmology. These results will strengthen the case for generic singularity resolution in LQC. Moreover, as we discussed above, the dynamics of the homogeneous models capture the main features of the dynamics in the approach to singularity in a generic spacetime as per the BKL conjecture. Thus, analysis of singularity resolution in these models will provide us detailed insights into the role of various quantum geometry corrections (such as the holonomy corrections and the inverse triad corrections) and of quantization ambiguities in singularity resolution.

Apart from cosmological singularities such as the big-bang at the beginning of a classical FLRW model of our universe, the other prominent singularity in GR is the black hole singularity formed by the collapse of massive stars. In GR the end state of such stars is a black hole singularity, which in the simplest spherically-symmetric case is described by the Schwarzschild spacetime. As we discussed above, while efforts towards a complete description of this singularity by studying dynamical black holes formed by gravitational collapse are under way [190, 191, 196, 197], the first step can be to exploit the fact that the Schwarzschild black hole interior is isomorphic to the vacuum Kantowski–Sachs model. Thus, by studying the singularity resolution in the vacuum Kantowski–Sachs model, we can gain initial insights into the resolution of black



hole singularity in LQC. Various loop quantizations of the Kantowski–Sachs model have been performed and analyzed at the effective level [178, 179, 180, 181, 182, 221, 195, 218, 222, 183]. However, most of the early attempts suffered from fiducial structure dependence in predictions, and large quantum effects at the horizon which might be at low curvatures for large mass black holes. It was in [183] for the first time, that a quantization of the vacuum Kantowski–Sachs model overcoming these drawbacks was obtained. It was demonstrated in reference [183] that the black hole singularity is replaced by a quantum bounce and a semi-classical universe obeying Einstein’s field equations is obtained on the other side, which is called a “white hole”. The bounce is found to be asymmetric in the mass: the mass of the white hole on the other side is proportional to the fourth power of the parent black hole. In this manuscript, we will explore whether a symmetric bounce can be obtained in this case, and if so, under what conditions.

## 1.4 Motivation

As we have detailed above, LQC has led to substantial progress towards the resolution of singularities by incorporating quantum effects of gravity into dynamics, but there is still a long way to go. Although the preliminary analysis in many cosmological models indicates the replacement of the singularity by a bounce, the existence and robustness of the bounce in the quantum evolution is only sufficiently established in a handful of cases using a combination of analytical and numerical investigations involving a variety of different types of initial states. In some cases, the isotropic and Bianchi-I cosmologies, results on generic resolution of singularities have been established using the effective dynamics as well. However, this is still far from the generality of the singularity theorems of GR [39], which show the existence of singularities in GR in quite general situations without assuming any specific symmetries usually associated with cosmological spacetimes studied above in LQC. Thus, there is a long way to go before we can establish the resolution of singularities in a generic context. However, we are helped in this regard by the BKL conjecture as discussed above. The conjecture states that the dynamics in the approach to a singularity in generic spacetimes is well approximated by homogeneous cosmologies because the spatial derivatives in Einstein’s equations become negligible in this limit. The Bianchi-I, Bianchi-II and Bianchi-IX models are specifically important in this context

as we have discussed earlier. Thus, extending the results on generic singularity resolution to homogeneous and anisotropic cosmologies can yield insights into the resolution of singularities in generic spacetimes. Moreover, these models are also relevant as potential initial states for our own universe since the universe may not have been isotropic and homogeneous in the very early phase. While efforts are continuing to extensively probe the bounce in these models at the level of quantum evolution, using numerical and analytical tools, we focus here on the effective dynamics of these models. Specifically, our aim is to establish generic resolution of singularities, such as the one obtained in the effective dynamics of isotropic and Bianchi-I models, to effective dynamics of models of further complexity - namely, Bianchi-II, Bianchi-IX and Kantowski–Sachs models.

In this context, we note that there are various viable quantizations of these models available in the literature. Using the criteria of independence of predictions from fiducial structures and appropriate low curvature limit, it is possible to rule out some of the quantizations, still there may be more than one quantizations which satisfy these criteria in these models. For example, there are two available quantizations of the Bianchi-II and Bianchi-IX models which survive - they are called the ‘A’ and the ‘K’ quantizations (see e.g. [176] for details). We note here that, these two quantizations emerge by considering different canonical variables for quantization. We will discuss the details in their respective chapters on these models. Our aim is to explore whether all the viable quantizations lead to singularity resolution in LQC, and what are the differences in them with regards to singularity resolution.

In addition, we also investigate the case of the black hole singularity from the perspective of vacuum Kantowski–Sachs spacetime. As we discussed in the previous section, a unique quantization of this model in the context of black hole spacetimes has been obtained [183], however, the bounce is found to be asymmetric in the mass of the daughter white hole versus the mass of the parent black hole. We will reconsider this quantization to check if a symmetric bounce can be obtained in this quantization, and what are the conditions that need to be satisfied for the bounce to be symmetric.

Thus we aim to ask and answer the following questions in this work:

- Using the effective spacetime description, generic singularity resolution has been shown in the isotropic and Bianchi-I models. Can these results be extended to more complex cosmological models? If so, what lessons can we draw for singularity resolution in generic spacetimes which do not have any of the symmetries of the cosmological models considered?
- We know that energy conditions (such as the weak energy conditions) play an important role in the singularity theorems of GR proving the generic occurrence of singularities in GR [39]. What is the role of these energy conditions in the context of singularity resolution in LQC? Are energy conditions important in establishing a generic non-occurrence of singularities in LQC?
- The effects of quantum geometry enter the dynamics of LQC in two important ways - through the holonomy corrections and the inverse triad corrections in the Hamiltonian constraint. So far, in the analysis of singularities in isotropic models and in Bianchi-I models, it was found that singularity resolution could be obtained just by including holonomy corrections, and the inverse triad corrections could be ignored. Does this still hold when we go to more complex cosmological models? What can we say about the importance of inverse triad corrections in general singularity resolution in LQC?
- What, if any, is the effect of quantization ambiguities on singularity resolution? Do all the different viable quantizations lead to singularity resolution in the considered models? Do some of the quantizations lend themselves better to singularity resolution as compared to others?
- Finally, in the case of the black hole interior spacetime studied using the loop quantized vacuum Kantowski–Sachs model in [183], is it possible to obtain a symmetric bounce where the white hole mass is equal to the parent black hole mass? If so, what are conditions required for a symmetric bounce?

We give an overview of the manuscript on the following section and detail how the above questions are addressed in various chapters.

## 1.5 Overview of the dissertation

Our primary goal in this thesis is to extend the results on generic singularity resolution obtained in the effective spacetimes of loop quantized isotropic and Bianchi-I models to more complicated models. In particular, we will be considering the Bianchi-II, Bianchi-IX and Kantowski–Sachs models and will also explore the role of quantization ambiguities, inverse triad modifications and energy conditions in singularity resolution. We will also consider the vacuum Kantowski–Sachs cosmology in the context of the black hole singularity to obtain a symmetric bounce from the black hole to a white hole of the same mass. The overview of the thesis is as follows:

In chapter 2, we aim to provide a brief review of LQC by mainly focusing on the FLRW cosmological model as our test case. We start with a discussion of the characterization of singularities in GR, leading to the discussion of the so called weak and strong type singularities in GR. We then study the classical dynamics of the FLRW model and show that it has an initial singularity and that the singularity is of strong curvature type. We then briefly summarize the LQG program to quantize GR and provide the basic results. We describe LQC as a application of techniques and ideas of LQG to symmetry reduced models and study the standard LQC quantization of FLRW model. We also describe here the holonomy corrections and the inverse triad corrections as they appear in the difference equations of LQC. We then discuss and apply the important technique of von-Neumann stability analysis to LQC difference equations to check for the correct semi-classical behavior of the difference equations. We proceed to the effective spacetime description obtained for FLRW model from standard LQC and show that all strong singularities including the big bang are removed. We then discuss the need for considering more general spacetimes such as anisotropic cosmological models that are relevant to general spacetime singularities due to the BKL conjecture and could be relevant to the initial conditions of our own universe. We finally end the chapter by a discussion of various quantization ambiguities in LQC.

In chapter 3, we aim to generalize the results on generic singularity resolution in isotropic and Bianchi-I effective dynamics to the effective spacetime of Bianchi-II models with minimally coupled arbitrary matter content in LQC. This has not been achieved so far. We consider the effective dynamics of the Bianchi-II model in two different quantization one by one - the ‘A’ and the ‘K’ quantizations as discussed above. Previously, it has been shown in the effective dynamics of the ‘A’ quantization, that the energy density, the expansion and shear scalars can be bounded if the weak energy conditions are applied on the energy density [215]. However, a general resolution of singularities on the lines of isotropic and Bianchi-I models could not be obtained. Moreover, the ‘K’ quantization, which has been proposed for the closed FLRW models and Bianchi-IX models, has not been obtained and analyzed for the Bianchi-II model. In chapter 3, we will derive the effective dynamics for the ‘K’ quantization for our considerations of singularity resolution. As a first step towards singularity resolution, we obtain the result that the triad variables remain non-zero and finite in all finite time evolution in the effective spacetime in both the quantizations. It turns out that in contrast to the isotropic and Bianchi-I models, additional conditions are needed for obtaining the desired behavior of triad variables for proving singularity resolution in the ‘A’ quantization in the Bianchi-II model if the inverse triad corrections coming from quantum geometry are ignored. Inverse triad correction were thought to be of negligible importance compared to holonomy corrections in effective dynamics based on the analysis of isotropic and Bianchi-I models. However we find that inverse triad corrections cannot always be ignored, specially when we want to show singularity resolution in more general spacetimes. In Bianchi-II model in ‘A’ quantization, we need to impose weak energy conditions on the matter content if we want to ignore the inverse triad corrections and still want to prove singularity resolution. In sharp contrast to this, we find that the extrinsic curvature based ‘K’ quantization readily yields these results without requiring inverse triad corrections or weak energy conditions. We then go on to state the boundedness of energy density, the expansion and shear scalars as a consequence of the bounded behavior of the triads in both quantizations. However, we show that not all curvature invariants are bounded, specifically, the Ricci scalar can diverge at certain events from pressure singularities coming from the second derivatives of

the triads. We then go on to show that these divergences do not affect the geodesic evolution and show that no strong singularities are possible in the loop quantized effective Bianchi-II spacetime in both ‘A’ and ‘K’ quantizations. We note the relative ease in obtaining singularity resolution in the ‘K’ quantization as compared to ‘A’ quantization where either inverse triad corrections or weak energy conditions are needed for the same.

In chapter 4, we consider the effective loop quantized Bianchi-IX model with minimally coupled arbitrary matter content in both ‘A’ and ‘K’ quantizations which also exist for the Bianchi-IX case. It is an anisotropic, spatially homogeneous and spatially curved model. Unlike the previous models considered so far, both spatial curvature and anisotropy are present in this case. It has been established that the weak energy conditions are not sufficient to bound the energy density in the case of ‘A’ quantization if inverse triad corrections are ignored [215]. Previous attempts using inverse triad corrections also were not able to obtain bounds on the energy density in this case in the ‘A’ quantization [176]. However, bounds on the energy density, the expansion and shear scalars had been obtained in the ‘K’ quantization [176]. In chapter 4, we demonstrate that the bounds on the triad variables, and the energy density, the expansion and shear scalars can be obtained in the effective dynamics of the ‘A’ quantization if the inverse triad corrections are included, even though this is not possible by just imposing weak energy conditions unlike the Bianchi-II case of chapter 3. These results can be obtained in the ‘K’ quantization without the need for the energy conditions or the inverse triad corrections [176]. We then show that some curvature invariants may still diverge due to pressure divergences in both quantizations, however, the geodesics remain well-defined at such events indicating they are harmless. Finally, we show that no strong singularities are possible in the effective Bianchi-IX spacetime for both the quantizations. The contrast between the ‘A’ and ‘K’ quantizations becomes sharper in this case. If one uses the ‘A’ quantization, inverse triad corrections are absolutely necessary and energy conditions are not sufficient for singularity resolution. In the light of the BKL conjecture, this means that in a generic spacetime in a quantization similar to the ‘A’ quantization, the inverse triad corrections are absolutely indispensable, and contrary to the scenario in GR, energy conditions are unlikely to play any role. On the other hand,

singularity resolution is obtained in the ‘K’ quantization without involving either the energy conditions or the inverse triad corrections.

In chapter 5, we further generalize the results on singularity resolution to Kantowski–Sachs cosmology with minimally coupled arbitrary matter. While the vacuum Kantowski–Sachs model is isomorphic to Schwarzschild interior spacetime, the Kantowski–Sachs cosmology with matter provides an anisotropic cosmological spacetime with spatial curvature. This is interesting because we found in the spatially curved and anisotropic Bianchi-IX model considered in chapter 4 that inverse triad corrections play an important part in singularity resolution. Interestingly, due to special symmetries of the Kantowski–Sachs model, the ‘A’ and ‘K’ quantization turn out to be equivalent in this case [178]. The Kantowski–Sachs cosmology with arbitrary matter content has been shown to have a unique quantization in which the predictions are free from fiducial structures and leads to generic bounds on the expansion and shear scalars [182, 218]. This is called the Boehmer–Vandersloot quantization. In chapter 5, using the effective dynamics of the Boehmer–Vandersloot quantization, we begin by establishing that the triad variables remain non-zero and finite for any finite time evolution. We then show that the energy density remains bounded for all finite time. The expansion and shear scalars were already shown to be generically bounded in [218]. We then explore the possible divergences in the curvature invariants due to pressure singularities as the above two cases. It is then shown that the geodesic equations remain well-defined at these divergences and that no strong singularities can occur in the effective spacetime. Surprisingly, we do not need either the energy condition or the inverse triad corrections to prove singularity resolution in this case.

In chapter 6, we focus on the vacuum Kantowski–Sachs spacetime which is isomorphic to the Schwarzschild interior spacetime. The Boehmer–Vandersloot quantization of the Kantowski–Sachs model of previous chapter is not viable for this case as it leads to large scale quantum corrections at the coordinate singularity at the black hole horizon (this happens because in presence of matter it becomes a real singularity where the energy density and curvature diverge, and the Boehmer–Vandersloot quantization is tuned to that case). Quantizations of the vacuum Kantowski–Sachs model suited to the black hole case have been obtained in [183] and [223] where

a bounce from black hole to white hole geometry has been obtained. However, the bounce turns out to be asymmetric in general, specially in Corichi–Singh quantization [183] with a large mass difference between the parent black hole and the child white hole. Moreover, the Corichi–Singh quantization [183] can lead to bounces at low curvatures in large mass limit, while the Ashtekar–Olmedo–Singh (AOS) quantization [223] provides universal bounds for curvature at bounce and the bounce always occurs in Planck regime. In this chapter we explore the possibility of a symmetric bounce by modifying the Corichi–Singh quantization of [183] and analyze some of the phenomenological effects. Using the setting of Dirac observables and geometric clocks we obtain a symmetric bounce condition which can be satisfied by a slight modification in the construction of loops over which holonomies are considered in the quantization procedure. These modifications can be viewed as quantization ambiguities, and can be constructed in three different ways which all lead to a symmetric bounce. We find that two of our choices overcome the drawback of low curvature bounces for large masses in Corichi–Singh quantization, however, they do not lead to universal bounds on the curvature (unlike AOS quantization) which grows with the mass of the black hole in large mass limit. Our results provide a method of obtaining a symmetric bounce in the Schwarzschild interior which can be further explored to investigate the viability of an exactly symmetric bounce for the black hole singularity in LQC. Further, these results are potentially helpful in motivating and constructing symmetric bounce scenarios in other spacetimes.



## Chapter 2

# A Review of Classical and Quantum Gravity

### 2.1 Strong and weak singularities in GR

One of the most troubling features of the general theory of relativity is the existence of spacetime singularities in its solutions, which are events where we reach the boundaries of the spacetime. These events are characterized by an unusual behavior in a number of physical quantities of interest (such as divergences in energy density or curvature, or the vanishing of spatial volume etc), which suggests that the theory has reached the limits of its validity. The most generic indication of a singularity is considered to be geodesic incompleteness, which means that some geodesics in the spacetime have a finite proper length, and the evolution of particles (or photons in case of null geodesics) following those geodesics comes to an abrupt end as they reach the singularity in a finite time. The geodesic incompleteness in GR solutions may or may not be associated with curvature pathologies such as divergences in curvature or energy density, etc. [224, 225]. On the other hand, there exist scenarios where divergences occur in some curvature invariants but geodesic curves are complete [226]. It remains a topic of debate as to which of these scenarios correspond to situations that are physically relevant to our universe. However most would agree that there is a genuine singularity if both curvature pathology and geodesic incompleteness are present.

Unlike the Newton's theory of gravity, where singularities may exist in some solutions when certain symmetries hold exactly (see e.g. [227] for singularities in Newtonian gravity, and [39], page 262 for a discussion on role of symmetries), singularities in GR can be shown to occur without assuming any symmetries if the matter content satisfies certain physically reasonable energy conditions (such as the weak energy condition) [39]. The work of Raychaudhuri, Komar, Penrose, Geroch and Hawking among others, summarized in the monograph [39], established that singularities occur in quite generic situations in solutions of GR. This is the reason why singularities are a fundamental issue in GR, because we cannot rule them out as outcomes of idealistic assumptions of perfect symmetries. This means that, if GR predicts spacetime

singularities in a physically relevant model, that cannot be avoided by relaxing some symmetry conditions or taking small perturbations away from the exact solution, i.e. we are forced to either accept singularities as part of physical reality or conclude that GR fails to describe physical reality in the vicinity of such extreme events. The search for a quantum theory of gravity is in part motivated from the problem of singularities. However, most of the singularities of physical interest to our real world are of the type which are associated with curvature pathology along with geodesic incompleteness, such as the big bang singularity in cosmology and the black hole singularity in astrophysical settings. Henceforth we will refer to these singularities broadly as curvature singularities to distinguish them from singularities in GR where geodesic incompleteness is present without any pathological symptoms in curvature invariants, energy density or Hubble rates etc (such singularities do exist in some solutions of GR, however their physical relevance is not clear). The question of extendability of the spacetime beyond curvature singularities has been explored in GR and has led to the notion of strong curvature singularities beyond which the spacetime cannot be extended [228]. A strong curvature singularity is defined to be one where any in-falling object is crushed to zero volume in a finite time regardless of the properties of the object [224, 229, 230]. The studies in LQC of the black hole spacetimes and various cosmological spacetimes have revealed that loop quantization resolves precisely these strong curvature singularities. Hence, we proceed to discuss the precise formulation of the strong curvature singularity in the following.

Consider an extended object falling into a singularity. It can be thought of as a system of particles following adjacent radial geodesics. The object will get squeezed as the geodesics get focused towards the singularity. The notion of a strong singularity then implies that the tidal gravitational forces squeezing the congruence of geodesics are strong enough that the object is crushed down to zero volume as it approaches the singularity, regardless of the material properties of the object. This can be made precise using the so called Jacobi fields along geodesics running into the singularity.

A Jacobi field is a vector field used to describe the focusing properties of a congruence of geodesics. It is a solution of the geodesic deviation equation (also known as Jacobi equation):

$$u^a \nabla_a (u^b \nabla_b \eta^c) \equiv \frac{D^2 \eta^c}{d\tau^2} = -R_{abd}{}^c u^a u^d \eta^b, \quad (2.1)$$

where  $R_{abd}{}^c$  represents the Riemann curvature tensor.  $u^a$  is the tangent vector along a timelike (or null) geodesic,  $\eta^a$  represents a Jacobi field and  $\tau$  is the affine parameter along the geodesic. The geodesic deviation equation describes the relative acceleration of nearby geodesics as they approach or recede away from each other. The Jacobi fields at any point on the geodesics form a vector field and lie in the tangent space at that point. Any three linearly independent Jacobi fields which are normal to the tangent vector of a timelike geodesic define a spacelike volume element along the geodesic through their exterior product (in case of null geodesics we have to consider the spatial area defined by normal Jacobi fields). Given a congruence of initially parallel geodesics, the above definition of strong curvature singularity then implies that the volume defined by three normal Jacobi fields along the geodesic must vanish as  $\tau$  approaches the singularity [229]. This requirement has been reformulated in terms of the Riemann curvature tensor in references [229, 230], where necessary and sufficient conditions for the singularity to be a strong curvature singularity are derived. It was found in these works that it is not just the Riemann curvature tensor, but also certain integrals of the Riemann tensor which should diverge at the singularity if it is a strong singularity. We will here focus on the necessary and sufficient conditions provided in [230]. The necessary conditions are given as the following:

If a given singularity, located at  $\tau_o$  along a non-spacelike geodesic running into the singularity, is a strong curvature singularity then for some component  $R_{0j0}^i$  of the Riemann tensor evaluated in a parallel-propagated frame, the following integral evaluated along the geodesic

$$K_j^i = \int_0^\tau d\tau' |R_{0j0}^i(\tau')| \quad (2.2)$$

does not converge as  $\tau \rightarrow \tau_o$ . If the singularity does not satisfy these necessary conditions, then it is called a weak singularity. We will discuss the spatially flat FLRW model in classical GR

in the next section where these conditions are satisfied. The spatially flat FLRW model of a homogeneous and isotropic universe has an initial singularity called the big bang singularity. We will also discuss the sufficient conditions in the next section to show that the big bang singularity is a strong singularity.

### 2.1.1 Example: Classical FLRW spacetime

The simplest cosmological model is the spatially flat FLRW model in which an isotropic and homogeneous space expands or contracts with time. The spacetime manifold has the product topology  $\mathbb{R} \times \Sigma$  where  $\Sigma$  represents a three-dimensional non-compact spatial section. The spatial sections are isotropic and homogeneous. The metric can be locally described as follows,

$$ds^2 = -N(t)^2 dt^2 + a(t)^2 (dr^2 + r^2 (d\theta^2 + \sin^2 \theta d\phi^2)), \quad (2.3)$$

where  $a(t)$  is the scale factor and  $N(t)$  is the lapse function. We will work with lapse  $N = 1$  in this chapter. We consider a relativistic fluid as the matter content in this model. If  $u^\alpha$  is the velocity vector field of the matter world lines of the fluid, then the energy-momentum tensor can be written generally as,

$$T^{\mu\nu} = (\rho + P)u^\mu u^\nu + Pg^{\mu\nu} + \Pi^{\mu\nu} + (q^\mu u^\nu + q^\nu u^\mu) \quad (2.4)$$

where  $\rho$  is called the energy density of the fluid,  $P$  is the isotropic pressure,  $\Pi^{\mu\nu}$  is the anisotropic stress and  $q^\mu$  is the momentum density or the heat flux vector. There are various special cases, such as the perfect fluid where the anisotropic stress and the heat flux vector are zero, and the dust where the pressure is zero as well. We shall restrict ourselves to the case of perfect fluid in this section. Einstein's equations then lead to the following evolution equations for the scale factor  $a(t)$ :

$$H^2 = \frac{\kappa\rho}{3}, \quad (2.5)$$

$$\frac{\ddot{a}}{a} = H^2 + \dot{H} = -\frac{\kappa}{6}(\rho + 3P), \quad (2.6)$$

where  $\kappa = 8\pi G$  and  $H(t) \equiv \dot{a}/a$  is called the Hubble rate.  $\rho(t)$  is the energy density of the matter content and  $P(t)$  is its pressure. The above two equations can be combined to yield,

$$\dot{\rho} = -3H(\rho + P), \quad (2.7)$$

which is equivalent to the conservation of the energy-momentum tensor, namely  $\nabla_\mu T^{\mu\nu} = 0$ . Since the energy density and pressure are related to each other through the matter equation of state, only two of the above three equations are independent. For a perfect fluid equation of state  $P = w\rho$ , the above equations can be integrated to give,

$$\rho \propto a^{-3(1+w)}, \quad (2.8)$$

$$a \propto t^{\frac{2}{3(1+w)}}. \quad (2.9)$$

If we evolve backwards from a finite initial value of the scale factor, we can see that the scale factor vanishes in a finite amount of time when  $t$  approaches zero, i.e the volume of the universe vanishes. Simultaneously the energy density, and hence the Hubble rate from equation (2.5) diverge at this event. This is the so called big bang singularity. From the expressions of the Ricci scalar,

$$R = 6\left(H^2 + \frac{\ddot{a}}{a}\right) = \kappa(\rho - 3P), \quad (2.10)$$

it is clear that the curvature also diverges at the big bang singularity. The matter particles follow the geodesics of the spacetime, which also can be shown to break down at the singularity. The geodesic equations for the FLRW spacetime in Cartesian coordinates are as follows:

$$x'' = -\frac{a'}{a}x', \quad y'' = -\frac{a'}{a}y', \quad z'' = -\frac{a'}{a}z', \quad (2.11)$$

$$t'' = -\frac{aa'}{t'}(x'^2 + y'^2 + z'^2), \quad (2.12)$$

where prime denotes derivative with respect to the affine parameter. The above set of equations give us the accelerations along the geodesics. These can be integrated to find the velocities along the geodesics as follows:

$$x' = C_x/a^2, \quad y' = C_y/a^2, \quad z' = C_z/a^2, \quad (2.13)$$

$$t'^2 = \epsilon + \frac{C_x^2 + C_y^2 + C_z^2}{a^2}. \quad (2.14)$$

$C_x, C_y$  and  $C_z$  are integration constants. Here  $\epsilon$  is 1 for timelike geodesics and 0 for null geodesics. We note from the above set of equations that the accelerations and velocities along the geodesics will diverge at points where either the scale factor vanishes or the Hubble rate diverges. For example at the big bang singularity. Further, we can see that the big bang singularity is a strong singularity as defined above. In the previous section, we defined the strong curvature singularities and gave the necessary conditions for a singularity to be a strong singularity. However, in order to show that a singularity is a strong singularity, we need a sufficient condition for a strong singularity. A sufficient condition for a singularity to be a strong curvature singularity is [230]:

For a non-spacelike geodesic, if the integral

$$I = \int_0^\tau |R_{00}(\tau')| d\tau' \quad (2.15)$$

diverges, then the singularity is a strong singularity. Here  $\tau$  represents the affine parameter along the geodesic. Now consider the above integral for the timelike geodesics followed by homogeneous and isotropic matter in the FLRW spacetime, for which the affine parameter is just the coordinate  $t$  for comoving observers. For FLRW spacetime, we have  $R_{00} = -3\ddot{a}/a$ . Then using (2.6), the integral becomes,

$$I = 3H(t) + 3 \int_0^t dt' H^2(t'). \quad (2.16)$$

We noted above that the Hubble rate diverges as the big bang singularity is approached. Hence the integral  $I$  diverges. This shows that the big bang singularity is a strong singularity

as per the definitions given above. We will see that loop quantization leads to the resolution of this singularity in the FLRW spacetime. Moreover, the effective loop quantized spacetime can be shown to be free from all strong singularities. We start with a brief introduction of canonical formulation of GR in the next section, and then discuss the basic ideas of LQC which we will employ for loop quantizing the FLRW spacetime to obtain the quantum evolution equation which is a difference equation. We will then move on to show the absence of strong singularities using the effective description of the loop quantized spatially flat FLRW spacetime.

## 2.2 Hamiltonian formulation of GR

GR is a generally covariant theory in which the spacetime is represented as a four dimensional Lorentzian manifold satisfying the Einstein's equations. In the conventional approach, we solve for the geometry of the manifold for a given matter content using the Einstein's equations, which in their usual four dimensional covariant form do not look like an initial value problem, i.e. there is no time evolution in the covariant picture. Given a specific type of matter content, we get the whole four dimensional manifold with a given geometry as the solution. Space and time are treated on equal footing in the covariant approach. The canonical approach to quantum gravity is based on the Hamiltonian formulation of GR, which requires the four dimensional spacetime to be foliated into a sequence of three dimensional spacelike hypersurfaces, so that the four dimensional spacetime can be thought of as the time development of a three dimensional spacelike hypersurface. Hence a specific choice of the time parameter is needed and the manifest covariance of the covariant approach is hidden. However, the coordinate invariance of GR implies that the choice of time parameter is not unique, so a given spacetime can be split into three dimensional hypersurfaces in many different ways.

Given a specific foliation of the spacetime manifold, let  $\Sigma_t$  denote the spacelike hypersurfaces parameterized by a global time function  $t$ . Let  $n^a$  represent the unit normal vector field to these hypersurfaces. Then the spacetime metric  $g_{ab}$  induces a three dimensional metric on each of the hypersurfaces given by,

$$q_{ab} = g_{ab} + n_a n_b. \quad (2.17)$$

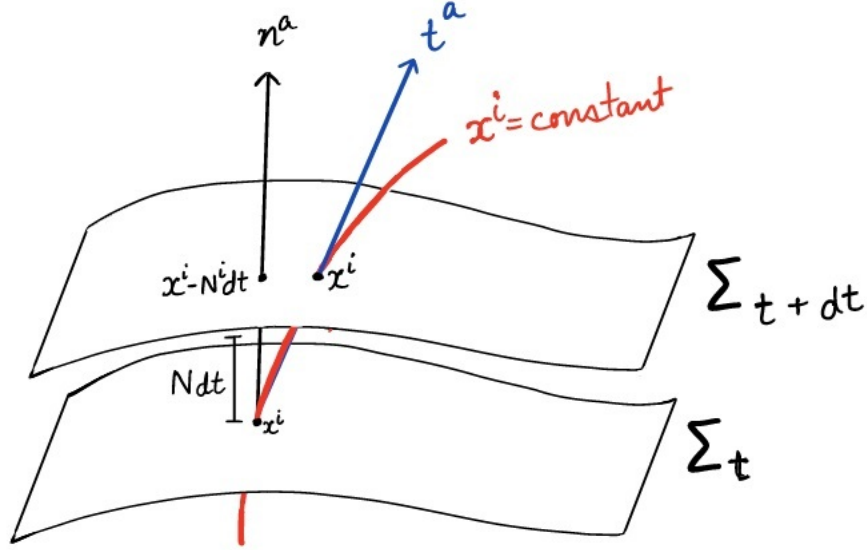


Figure 2.1: 3 + 1 split of spacetime.

Given two nearby hypersurfaces  $\Sigma_t$  and  $\Sigma_{t+dt}$ , we define the function  $N(t, x^i)$ , called the lapse function which determines the rate of flow of time along the normal  $n^a$ . That is, the proper time  $d\tau$  elapsed between  $\Sigma_t$  and  $\Sigma_{t+dt}$  for observers moving along the normal  $n^a$  is given by (see the figure above),

$$d\tau = N(t, x^i)dt. \quad (2.18)$$

Here  $x^i$  are the coordinates on the hypersurfaces. Then the timelike tangent vector field  $t^a$  to lines of constant spatial coordinates is given in general by,

$$t^a = Nn^a + N^a \quad (2.19)$$

where  $N^a(t, x^i)$  is called the shift vector and represents the fact that in general  $t^a$  may not be normal to the hypersurfaces. the shift vector is tangent to the hypersurfaces at any given point. Lapse and shift are arbitrary functions that determine a given foliation. The diffeomorphism invariance of GR is reflected in the fact that a given spacetime can be foliated in a number of



different ways, which can be obtained by choosing specific values for the arbitrary functions,  $N(t, x^i)$  and  $N^a(t, x^i)$ . Using these functions, the spacetime metric can be represented as follows:

$$ds^2 = (-N^2 + N^a N_a) dt^2 + 2N_a dt dx^a + q_{ab} dx^a dx^b. \quad (2.20)$$

The conventional Hamiltonian formulation of GR is obtained by treating the three dimensional spatial metric  $q_{ab}$  as the configuration variable. The action functional for GR is given by

$$S = \frac{1}{2\kappa} \int d^4x \sqrt{-g} R = \frac{1}{2\kappa} \int d^4x \mathcal{L}_G, \quad (2.21)$$

where  $R$  is the Ricci scalar of the spacetime and  $g$  is the determinant of the spacetime metric. The constant  $\kappa = 8\pi G$  represents the gravitational constant. The conjugate momentum to the metric  $q_{ab}$  is then given by

$$\pi^{ab} = \frac{\partial \mathcal{L}_g}{\partial \dot{q}_{ab}} = \sqrt{q} (K^{ab} - K q^{ab}), \quad (2.22)$$

where  $q$  is the determinant of  $q^{ab}$  and  $K^{ab} = (1/2) \mathcal{L}_n q^{ab}$  is the extrinsic curvature which is given by the Lie derivative of the spatial metric along the normal vector field. And  $K = K^a_a$  is the trace of  $K^{ab}$ . The non-vanishing Poisson bracket between the phase space variables is given by,

$$\{\pi^{ab}(x), q_{cd}(y)\} = 2\kappa \delta_c^a \delta_d^b \delta(x - y). \quad (2.23)$$

Then the action can be rewritten in terms of the conjugate pair  $(q_{ab}, \pi^{ab})$  as follows:

$$\begin{aligned} S = & \frac{1}{2\kappa} \int dt \int d^3x \left\{ \pi^{ab} \dot{q}_{ab} + 2N_b \nabla_a^{(3)} \left( \frac{\pi^{ab}}{\sqrt{q}} \right) \right. \\ & \left. + N \sqrt{q} \left[ R^{(3)} - \frac{\pi^{ab} \pi_{ab}}{q} + \frac{\pi^2}{2q} \right] \right\}, \end{aligned} \quad (2.24)$$

where  $\pi = \pi^a_a$  and  $\nabla_a^{(3)}$  is the covariant derivative on the spatial slices compatible with the metric  $q_{ab}$ . And  $R^{(3)}$  is the Ricci scalar of the metric  $q_{ab}$ .

Variations of the above action (2.24) with respect to the shift lead to the three *diffeomorphism* or *vector* constraints:

$$\mathcal{V}^b = -\nabla_a^{(3)} \left( \frac{\pi^{ab}}{\sqrt{q}} \right). \quad (2.25)$$

They are called diffeomorphism constraints because they are the generators of spatial diffeomorphisms of the 3-metric on the spatial hypersurfaces. Variations of the above action with respect to the lapse leads to the *Hamiltonian* or *scalar* constraint:

$$\mathcal{H} = -\sqrt{q} \left[ R^{(3)} - \frac{\pi^{ab}\pi_{ab}}{q} + \frac{\pi^2}{2q} \right], \quad (2.26)$$

which is the generator of the time translations with respect to the time parameter chosen for the foliation. The total Hamiltonian of GR, which is a sum of constraints, is then given by,

$$\mathcal{C} = \int dx^3 (N\mathcal{H} + N_a\mathcal{V}^a). \quad (2.27)$$

The Wheeler–DeWitt quantization is based on the above form of the total Hamiltonian constraint in terms of the metric variables. The wave functions are considered to be functionals of the configuration variable  $q_{ab}$  and the operator forms of the scalar and the vector constraints are required to annihilate the physical states. Due to the non-polynomial dependence of the constraints on the metric variables, it becomes very difficult to implement in the quantum theory and obtain solutions. As detailed in the previous chapter, these technical issues have stalled progress in the Wheeler–DeWitt theory. It is possible to implement these constraints in metric variables and obtain solutions in some symmetry reduced cosmological spacetimes in the Wheeler–DeWitt theory, however the resulting solutions in some cases turn out to contain the same singularities as the classical model. The search for a simple form of the constraints led to the connection-triad variables discussed in the next subsection, which eventually led the way to a quantization very different from the Wheeler–DeWitt quantization.

### 2.2.1 Ashtekar's reformulation of GR

Ashtekar's observation that the constraints of GR can be expressed in a polynomial form if a canonical transformation is made in the gravitational phase space provided new hope to the programme of non-perturbative canonical quantization of GR. The transformation from metric variables to the so called Ashtekar variables opened the doors to move beyond the difficulties faced in the Wheeler–DeWitt theory. GR, when expressed as a theory of connections in terms of these new variables, assumes a form similar to Yang–Mills theories. The original set of variables introduced by Ashtekar were complex-valued, which required further reality conditions to be imposed. Later, real-valued Ashtekar variables were introduced by Barbero [86] which led to further simplifications.

In this section, we introduce the real Ashtekar variables and sketch the basics of LQG. We start with the co-triads as they are directly related to the metric. Co-triads are a set of three 1-forms which provide an orthonormal frame at each point of the spatial hypersurface  $\Sigma$ . The spatial metric  $q_{ab}$  can be expressed in terms of these co-triads as follows,

$$q_{ab} = e_a^i e_b^j \delta_{ij}. \quad (2.28)$$

The co-triads contain the information about the local metric of the spatial hypersurface. The set of co-triads are the inverses of the triads such that  $e_i^a e_a^j = \delta_i^j$ . The densitized triads are then expressed in terms of the triads,

$$E_i^a := \sqrt{q} e_i^a, \quad (2.29)$$

where  $q$  is the determinant of the metric  $q_{ab}$ . We further define the curvature one-form as follows,

$$K_a^i := K_{ab} e^{bi}. \quad (2.30)$$

Then the symmetry property of the extrinsic curvature  $K_{[ab]}$  can be shown to lead to the condition,

$$\mathcal{G}_i := \epsilon_{ijk} K_a^j E_k^a = 0. \quad (2.31)$$

We demand that the metric compatible covariant derivative  $D_a$  annihilates the triad, i.e.

$$D_a e_b^i = \partial_a e_b^i - \Gamma_{ab}^c e_c^i + \Gamma_{ak}^i e_b^k = 0. \quad (2.32)$$

Since  $D_a \delta_j^i = D_a e_b^i e_j^b = 0$ , this implies that  $D_a e_i^a = 0$  and hence  $D_a E_i^a = 0$ . Since  $E_i^a$  is a vector density of weight one, we have

$$D_a E_i^a = \partial_a E_i^a + \Gamma_{ai}^j E_j^a = \partial_a E_i^a + \epsilon_{ij}^k \Gamma_a^j E_k^a = 0. \quad (2.33)$$

Using this we can recast the constraint (2.31) in the form of a Gauss constraint of an SU(2) gauge theory as follows:

$$\mathcal{G}_i = 0 + \gamma \epsilon_{ijk} K_a^j E_k^a = \partial_a E_i^a + \epsilon_{ijk} (\Gamma_a^j + \gamma K_a^j) E_k^a =: \partial_a E_i^a + \epsilon_{ijk} A_a^j E_k^a = \mathcal{D}_a E_i^a, \quad (2.34)$$

defining a new connection  $A_a^j = \Gamma_a^j + \gamma K_a^j$ , and the corresponding derivative operator  $\mathcal{D}_a$ , where  $\gamma$  is a non-zero constant parameter called the Barbero–Immirzi parameter. The advantage of introducing this new connection is that it is conjugate to the densitized triad  $E_i^a$ . They satisfy the Poisson brackets,

$$\{E_i^a(x), A_b^j(y)\} = \kappa \gamma \delta_b^a \delta_j^i. \quad \{E_i^a(x), E_j^b(y)\} = \{A_a^i(x), A_b^j(y)\} = 0. \quad (2.35)$$

These are our new canonical variables called Ashtekar variables, or simply connection variables. As mentioned above, the advantage of expressing the action of classical gravity in terms of these

variables simplifies the expressions of constraints which paves the way for their quantization. It can be shown that the action in terms of these new variables becomes,

$$S = \frac{1}{2\kappa} \int dt \int_{\Sigma} dx^3 \left( 2E_i^a \dot{A}_a^i - [\Lambda^i \mathcal{G}_i + N^a \mathcal{H}_a + N \mathcal{H}] \right), \quad (2.36)$$

where the constraints are now given by:

$$\mathcal{G}_i = D_a E_i^a, \quad (2.37)$$

$$\mathcal{H}_b = E_i^a F_{ab}^i, \quad (2.38)$$

$$\mathcal{H} = \frac{E_j^a E_k^b}{\sqrt{q}} [\epsilon_{ijk} F_{ab}^i - 2(1 + \gamma^2) K_{[a}^j K_{b]}^k], \quad (2.39)$$

where  $F_{ab}$  is the curvature of the connection  $A_a$ . This allows us to formulate GR as a theory of real-valued  $SU(2)$  connections similar to Yang–Mills theories, except we now have four more constraints apart from the Gauss constraint  $\mathcal{G}_i$ . Another peculiar property of GR is that the total Hamiltonian is just a sum of constraints. So GR is a fully constrained theory. Due to these differences, the dynamics of GR is likely to be very different from Yang–Mills theories, nevertheless the similarity allows us to borrow techniques from the well-developed field of Yang–Mills theories. Just like Yang–Mills theories, the Gauss constraint is the generator of gauge transformations in the classical description. The vector constraint  $\mathcal{H}_b$  combined with the Gauss constraint generates spatial diffeomorphisms. And the scalar constraint generates time translations with respect to the time parameter of the chosen foliation of the manifold.

As we discussed in the previous chapter, the way these constraints are imposed in the quantum theory is that the operators corresponding to the constraints are required to annihilate the physical states. This translates into the requirement that the physical states be invariant under the corresponding transformations. This leads us to holonomies of the connection as in Yang–Mills theories which encode gauge-invariant information of the connection. It turns out that working with linear combinations of the holonomies over all possible loops as our space of basis states, we can automatically satisfy the Gauss and the vector constraints. And we are

left with only the scalar constraint. This is why the scalar constraint is also sometimes referred to as the Hamiltonian constraint itself. In order to calculate physically observable quantities, a suitable scalar product is defined on the space of physical states, which can be done by defining a measure on this space. Luckily, the diffeomorphism invariance leads to the choice of a unique measure to be defined on the space of states, the Ashtekar–Lewandowski measure [143]. However, this scalar product has the consequence that the connection and the densitized triads no longer correspond to well-defined operators. The holonomies of the connection and surface integrals of the triads are the simplest well-defined operators.

### 2.3 Loop quantum cosmology

Loop quantum cosmology is the application of techniques of LQG to symmetry reduced cosmological models. It happens quite often in physics that simplified models with high levels of symmetry are considered to gain insights into the possible predictions of a theory when the full theory seems too difficult to solve directly at first sight. Indeed, many valuable and novel insights have been gained by applying LQG techniques to symmetry reduced models. We consider here the simplest of them all, the spatially flat isotropic and homogeneous cosmological model to illustrate the ideas and main insights.

The spatially flat FLRW model has the topology  $\mathbb{R} \times \Sigma$  where  $\Sigma$  represents a three-dimensional non-compact manifold. The local spacetime metric can be written as,

$$ds^2 = -N(t)^2 dt^2 + a(t)^2 (dr^2 + r^2 (d\theta^2 + \sin^2 \theta d\phi^2)), \quad (2.40)$$

The canonical quantization approach requires us to first obtain a Hamiltonian formulation of GR. The four-dimensional spacetime in GR can be viewed as the time evolution of a three-dimensional spacetime with respect to the coordinate time  $t$  which is governed by a Hamiltonian function. However in LQG, the Hamiltonian is first expressed in terms of Ashtekar variables

via a canonical transformation. In case of spatially flat FLRW model, these variables take the following simple form due to symmetry reduction,

$$A_a^i = cV_o^{1/3} {}^o\omega_a^i \quad \text{and} \quad E_i^a = pV_o^{-2/3} \sqrt{{}^oq} {}^oe_i^a. \quad (2.41)$$

Here  $\{{}^oe_i^a\}$  are a set of orthonormal triads and  $\{{}^o\omega_a^i\}$  are the corresponding set of co-triads.  $V_o$  represents the volume of an elementary fiducial cell. Since the spatial slices are homogeneous and non-compact, the integrals in the Poisson brackets diverge. A well defined symplectic structure can be placed on the spatial slices by introducing a finite fiducial cell by restricting the integrations in the Poisson brackets to the cell. The reduced phase space variables in this case satisfy the following Poisson bracket,

$$\{c, p\} = \frac{\kappa\gamma}{3}, \quad (2.42)$$

where  $\kappa = 8\pi G$  and  $\gamma$  is the Barbero–Immirzi parameter. We separate the expression for the gravitational part of general Hamiltonian constraint given in (2.39) into two parts here which we evaluate separately,

$$\mathcal{H}_{\text{grav}} = \int_V d^3x \frac{E^{aj} E^{bk}}{2\kappa \sqrt{\det(q)}} [\epsilon_{ijk} F_{ab}^i - 2(1 + \gamma^2) K_{[a}^j K_{b]}^k] \equiv \mathcal{H}^E - 2(1 + \gamma^2) \mathcal{T}. \quad (2.43)$$

$\mathcal{H}^E$  and  $\mathcal{T}$  are called the Euclidean and the Lorentzian term respectively in the literature. After symmetry reduction, they turn out to be proportional to each other in case of spatially flat FLRW spacetime,

$$\mathcal{H}^E = \int_V d^3x \frac{E^{aj} E^{bk}}{2\kappa \sqrt{\det(q)}} \epsilon_{ijk} F_{ab}^i = \frac{3}{\kappa} c^2 \sqrt{|p|}, \quad (2.44)$$

$$\mathcal{T} = \int_V d^3x \frac{E^{aj} E^{bk}}{2\kappa \sqrt{\det(q)}} K_{[a}^j K_{b]}^k = \frac{3}{2\kappa\gamma^2} c^2 \sqrt{|p|}. \quad (2.45)$$

In standard LQC treatment [123, 124, 80], the symmetry reduced expressions for the two terms are combined at the classical level to give the symmetry reduced Hamiltonian constraint as,

$$\mathcal{H}_{\text{grav}} = -3c^2 \sqrt{|p|} / \kappa \gamma^2 = -\frac{1}{\gamma^2} \mathcal{H}^E. \quad (2.46)$$

As we noted above, since there is no operator in LQG corresponding to the connection variables, all the expressions involving them are first expressed in terms of holonomies of the connection around closed loops. The Euclidean term contains the curvature  $F_{ab}^i$  and a factor involving the densitized triads. We first consider the terms involving triads. It can be shown that the following identity holds,

$$\epsilon_{ijk} \frac{E^{aj} E^{bk}}{\sqrt{\det(q)}} = \frac{2}{\kappa \gamma} \epsilon^{abc} \{A_c^i, V\}. \quad (2.47)$$

We will need to find an expression for the Poisson bracket on RHS in terms of holonomies. Let us consider the field strength before we come to that. The field strength  $F_{ab}^i$  is the curvature of the connection and can be represented using the holonomy  $h_{\square_{ij}}^{(\mu)}$  around a square loop  $\square_{ij}$  in the  $i - j$  plane parallel to one of the faces of the elementary cell. The loop has edges of length  $\mu V_o^{1/3}$  each with respect to the fiducial metric.  $F_{ab}^i$  is then given by [80]:

$$F_{ab}^k = -2 \lim_{Ar_{\square} \rightarrow 0} \text{Tr} \left( \frac{h_{\square_{ij}}^{(\mu)} - 1}{\mu^2 V_o^{2/3}} \right) \tau^k \circ \omega_a^i \circ \omega_b^j \quad (2.48)$$

where  $Ar_{\square}$  is the area of the square loop. The holonomy  $h_{\square_{ij}}^{(\mu)}$  around the square is given by the product of the holonomies along its four edges:

$$h_{\square_{ij}}^{(\mu)} = h_i^{(\mu)} h_j^{(\mu)} (h_i^{(\mu)})^{-1} (h_j^{(\mu)})^{-1}, \quad (2.49)$$

where the holonomies  $h_i^{(\mu)}$  are given by,

$$h_i^{(\mu)} = \cos \left( \frac{\mu c}{2} \right) \mathbb{I} + 2 \sin \left( \frac{\mu c}{2} \right) \tau_i, \quad (2.50)$$



along edges of length  $\mu$  parallel to the triads  ${}^oe_i^a$ . Here  $\tau_i = -i\sigma_i/2$  are the  $SU(2)$  generators where  $\sigma_i$  Pauli spin matrices and  $\mathbb{I}$  is the 2-dimensional identity matrix. However, the limit  $Ar_{\square_{ij}} \rightarrow 0$  in (2.48) for the field strength, does not exist in the quantum theory. The underlying geometry in LQG is discrete and there is a minimum non-zero eigenvalue for the area operator given by  $\Delta = 4\sqrt{3}\pi\gamma l_{\text{Pl}}^2$ , where  $l_{\text{Pl}}$  is the Planck length. The area of the loop can be shrunk to the value  $\Delta$ , but not to zero. The corresponding quantity obtained in this way is taken to be the quantum analog of the term  $F_{ab}^k$ . This is related to the fact that in LQG, there are no operators corresponding to the connection and its curvature.

In case of isotropic and homogeneous model, the connection  $A_a^i$  takes a simple form and the Poisson brackets above reduce to Poisson brackets of  $c\tau_i$  with  $V$ , which can be expressed in terms of the holonomies as follows,

$$\{c\tau_i, V\} = -\frac{1}{\mu} h_i^{(\mu)} \{ (h_i^{(\mu)})^{-1}, V \}. \quad (2.51)$$

Now it is possible to recast the Hamiltonian constraint of standard LQC given in equation (2.46) in terms of the holonomies and the volume  $V = |p|^{3/2}$ . This is the first step towards quantization. The expression can be written as follows:

$$\mathcal{H}_{\text{grav}} = -\frac{2\text{sgn}(p)}{\kappa^2\gamma^3\lambda^3} \epsilon^{ijk} \text{Tr} \left( h_i^{(\mu)} h_j^{(\mu)} h_i^{(\mu)-1} h_j^{(\mu)-1} h_k^{(\mu)} \left\{ h_k^{(\mu)-1}, V \right\} \right). \quad (2.52)$$

We also encounter one of the quantization ambiguities here itself. The quantization depends on how the loops are chosen for evaluating the holonomies. Consider the  $\mu_o$  scheme, in which the area of the square loop  $\square_{ij}$  is taken to be  $\Delta$  with respect to the fiducial metric. The length  $\mu$  of the edges of the square are constant in this case. This constant value is denoted  $\mu_o$  in the literature, hence the name  $\mu_o$  scheme. In the  $\mu_o$  scheme, it is convenient to consider  $\hat{p}$  and

$\exp(\widehat{i\mu_o c}/2)$  as the fundamental operators as they have a simple action on the eigen states of the triad operator [143]:

$$\exp(\widehat{i\mu_o c}/2)|n\rangle = |n + \mu_o\rangle, \quad (2.53)$$

$$\hat{p}|n\rangle = \left(\frac{8\pi\gamma l_{\text{Pl}}^2}{6}\right)n|n\rangle, \quad (2.54)$$

These two operators allow us to evaluate the action of the Hamiltonian operator on these states. Since the Hamiltonian constraint operator must annihilate the physical states, we can get a difference equation for the basis states as follows,

$$\mathcal{H}_{\text{grav}}|n\rangle + \mathcal{H}_{\text{m}}|n\rangle = 0, \quad (2.55)$$

where  $\mathcal{H}_{\text{m}}$  corresponds to quantized matter Hamiltonian. For simplicity, the matter field is usually taken to be the scalar field and is Fock quantized in LQC. Since there is no external time parameter in GR, we can use the scalar field as our reference variable and interpret the above equation as giving the evolution of the states with respect to the scalar field. We will return to the discussion of this difference equation, but let us first also familiarize with the  $\bar{\mu}$  scheme and how it is different.

It was soon realized in standard LQC [80] that the  $\mu_o$  scheme leads to a dynamics where the strength of quantum gravity effects depends on fiducial parameters such as edge lengths of the cell around which the holonomies are evaluated. It was realized that the minimum area  $\Delta$  to which the square  $\square_{ij}$  is shrunk should correspond to the physical area of the square, hence it should refer to the area of the loop with respect to the physical metric  $q_{ab}$ . This implies that the the edge lengths of the square are no longer constant, i.e.  $\mu$  is now a function  $\bar{\mu}(p)$  of the triad given by,

$$\bar{\mu}^2|p| = \Delta. \quad (2.56)$$

The major difference from  $\mu_o$  scheme is that the operator  $\exp(\widehat{i\bar{\mu}c}/2)$  no longer has a simple action on the basis states  $|p\rangle$  due to dependence of  $\bar{\mu}$  on the triad itself. It was found [80] that

it is more convenient to use basis states adapted to the volume operator in this case as it turns out that  $\widehat{\exp(i\bar{\mu}c/2)}$  acts as a simple difference operator on this basis:

$$\widehat{\exp(i\bar{\mu}c/2)}|v\rangle = |v+1\rangle, \quad (2.57)$$

$$\hat{V}|v\rangle = \left(\frac{8\pi\gamma l_{\text{Pl}}^2}{6}\right)^{3/2} \frac{|v|}{L}|v\rangle, \quad (2.58)$$

where  $\hat{V}$  is the volume operator and

$$L = \frac{4}{3} \sqrt{\frac{\pi\gamma l_{\text{Pl}}^2}{3\Delta}}. \quad (2.59)$$

As in the  $\mu_o$  scheme, we obtain a difference equation for the states  $\{|v\rangle\}$ . As an example, we show here the difference equation obtained in the  $\bar{\mu}$  scheme. In the  $\bar{\mu}$  scheme, the gravitational Hamiltonian constraint of standard LQC given in equation (2.52) reduces to the operator expression (we omit the hats on the operators here),

$$\begin{aligned} \mathcal{H}_{\text{grav}} = & \frac{12i}{\kappa^2 \hbar \gamma^3} \sin(\bar{\mu}c) \frac{\text{sgn}(v)}{\bar{\mu}^3} \left( \sin\left(\frac{\bar{\mu}c}{2}\right) V \cos\left(\frac{\bar{\mu}c}{2}\right) \right. \\ & \left. - \cos\left(\frac{\bar{\mu}c}{2}\right) V \sin\left(\frac{\bar{\mu}c}{2}\right) \right) \sin(\bar{\mu}c). \end{aligned} \quad (2.60)$$

where a certain choice of factor-ordering has been used. Note that  $1/\bar{\mu}^3$  acts as an operator, which is proportional to the volume operator. This leads to the following action on the basis states  $\{|v\rangle\}$ ,

$$\mathcal{H}_{\text{grav}}|v\rangle = C_+(v)|v+4\rangle + C_o(v)|v\rangle + C_-(v)|v-4\rangle, \quad (2.61)$$

where the coefficients are given by,

$$C_+(v) = R_1(v+2)(|v+3| - |v+1|), \quad (2.62)$$

$$C_-(v) = C_+(v-4), \quad (2.63)$$

$$C_o(v) = -C_+(v) - C_-(v), \quad (2.64)$$

and  $R_1$  is a constant given by,

$$R_1 = \frac{27}{32\kappa} \sqrt{\frac{8\pi}{6}} \frac{Ll_{\text{Pl}}}{\gamma^{\frac{3}{2}}}. \quad (2.65)$$

In order to impose the complete Hamiltonian constraint on the basis states, we need to evaluate the matter part of the Hamiltonian as well. Consider a massless scalar field as the matter content. The classical matter Hamiltonian is then given by  $\mathcal{H}_m = p_\phi^2/2V$ . The non-trivial part is the volume in the denominator. In order to evaluate the action of the corresponding operator  $\hat{V}^{-1} = \hat{p}^{-3/2}$  on the basis states, we need to define the action of the inverse triad operators  $\hat{p}^{-r}$  on the basis states. One might be tempted to take the eigenvalues of this to be inverse of the eigenvalues of the triad operator  $\hat{p}^r$ , however that fails to be a densely defined self-adjoint operator because  $\hat{p}$  has a normalized eigenstate  $|v=0\rangle$  with zero eigenvalue [143]. This issue is dealt on the lines of the full theory following Thiemann's ideas [231, 232] by noting that the classically the triad  $|p|^{-1/2}$  can be rewritten as the Poisson bracket  $\{c, V^{1/3}\}$ . This can be expressed in terms of holonomies as follows [143, 80]:

$$|p|^{-1/2} = \text{sgn}(p) \frac{4}{\kappa\gamma\bar{\mu}} \text{Tr} \left( \Sigma_i \tau^i h_i^{(\bar{\mu})} \{ (h_i^{(\bar{\mu})})^{-1}, V^{1/3} \} \right). \quad (2.66)$$

Using this the Hamiltonian constraint  $\mathcal{H}_{\text{grav}}|n\rangle + \mathcal{H}_m|n\rangle = 0$  leads to the following difference equation:

$$\frac{R_2}{2} |v| \left| |v+1|^{1/3} - |v-1|^{1/3} \right|^3 \partial_\phi^2 |v\rangle = C_+(v)|v+4\rangle + C_o(v)|v\rangle + C_-(v)|v-4\rangle, \quad (2.67)$$

where

$$R_2 = \left( \frac{3}{2} \right)^3 \left( \frac{6}{\kappa\hbar\gamma} \right)^{3/2} L. \quad (2.68)$$

However, unlike usual quantum mechanics, the above difference equation does not seem to describe the evolution of the quantum states with respect a time parameter. This is due to the fact that the time coordinate in GR is not an external parameter, but merely a part of the coordinatization of the spacetime manifold and holds no physical information by itself. The diffeomorphism invariance of GR means that we are allowed to make arbitrary coordinate

transformations and the physics remains independent of such changes. The only physically meaningful statements correspond to the relational dynamics of the physical variables with respect to each other as these correlations are coordinate independent. This is reflected in the above difference equation by the absence of any external time parameter. One can, if required, view the above difference equation as describing the evolution of the states with respect to the scalar field which can be treated as a time parameter. In the next section, we discuss the effective description obtained from the loop quantized spatially flat FLRW model of this section.

## 2.4 Effective dynamics of loop quantized spatially flat FLRW model

As we discussed in the introductory chapter, a remarkable and useful feature of LQC dynamics is that the most important features of the quantum dynamics can be described by an effective continuous description, called effective dynamics. This helps in interpreting the quantum dynamics and also provides an arena to explore various phenomenological questions with ease. As detailed in the previous chapter, effective dynamics can be obtained by using the geometrical formulation of quantum mechanics [199] to map the flow (on the projective Hilbert space manifold) corresponding to the expectation value of the Hamiltonian operator of the quantum theory to the classical phase space in a way that captures leading order quantum corrections [212, 200, 210, 211]. For the case of loop quantized spatially flat FLRW model of the previous section, the effective Hamiltonian turns out to be [80]:

$$\mathcal{H}_{\text{eff}} = -\frac{3}{\kappa\gamma^2}\sqrt{p}\frac{\sin^2(\bar{\mu}c)}{\bar{\mu}^2} + \mathcal{H}_{\text{m}}. \quad (2.69)$$

Then the equations of motion for the triad can be calculated as follows:

$$\dot{p} = \{p, \mathcal{H}_{\text{eff}}\} = \frac{p}{\gamma\sqrt{\Delta}} \sin(2\bar{\mu}c). \quad (2.70)$$

This shows that the Hubble rate  $H \equiv \dot{a}/a = \dot{p}/2p$  is given by,

$$H = \frac{\sin(2\bar{\mu}c)}{2\gamma\sqrt{\Delta}}, \quad (2.71)$$

which is generically bounded in contrast to classical dynamics. The vanishing of the effective Hamiltonian constraint gives the energy density,

$$\rho = \frac{3}{\kappa\gamma^2\Delta} \sin^2(\bar{\mu}c), \quad (2.72)$$

which is also generically bounded. Here  $\rho = \mathcal{H}_m/V$ . The dynamics of the effective spacetime can be equivalently described using the modified Friedmann and Raychaudhuri equations, which can be derived from the equations of motion in terms of the energy density and isotropic pressure as follows,

$$H^2 = \frac{\kappa}{3}\rho\left(1 - \frac{\rho}{\rho_c}\right), \quad (2.73)$$

$$\frac{\ddot{a}}{a} = -\frac{\kappa}{6}\rho\left(1 - 4\frac{\rho}{\rho_c}\right) - \frac{\kappa}{2}P\left(1 - 2\frac{\rho}{\rho_c}\right), \quad (2.74)$$

where  $\rho_c = 3/\kappa\gamma^2\Delta \approx 0.41\rho_{\text{Pl}}$  is called the critical density at which the bounce occurs. From the expression for the Hubble rate, we see that  $\dot{a}$  vanishes at  $\rho = \rho_c$ , and the universe bounces.

Since the Hubble rate and the scale factor are bounded as the big bang singularity is approached (which is now replaced by a bounce), the geodesic equations remain well-defined. Note that divergences may still occur in the Raychaudhuri equation if the isotropic pressure diverges at finite values of the energy density, the Hubble rate and the scale factor. Moreover, the Ricci scalar  $R = 6(H^2 + \ddot{a}/a)$  also diverges at such pressure divergences. However such divergences do not amount to a strong singularity. The first hint is that the Hubble rate, the scale factor and the energy density are all finite at such events; and the geodesics given in equations (2.11), (2.12), (2.13) and (2.14) are well-defined. The components of the Riemann tensor are given by:

$$R_{110}^0 = R_{220}^0 = R_{330}^0 = -a\ddot{a}, \quad (2.75)$$

$$R_{010}^1 = R_{020}^2 = R_{030}^3 = -\ddot{a}/a = -H^2 - \dot{H}, \quad (2.76)$$

$$R_{221}^1 = R_{331}^1 = R_{332}^2 = -R_{121}^2 = -R_{131}^3 = -R_{232}^3 = -\dot{a}^2. \quad (2.77)$$

Although some components of the Riemann tensor may diverge at the pressure divergences due to the  $\ddot{a}$  term, we can see that the necessary condition (2.2) is not satisfied. For a timelike geodesic for comoving observers, the integral in (2.2) remains bounded as after the integration, all the terms containing  $\ddot{a}$  are removed and we are left with an expression that depend on the Hubble rate and the scale factor itself. Since the Hubble rate and the scale factor are bounded in the effective dynamics, the integral (2.2) does not diverge for any curvature singularity which is reached in finite time along a geodesic. So the effective spacetime is free from all strong singularities.

## 2.5 Anisotropic models

One of the central questions in cosmology has been the origin of the isotropy and homogeneity of our universe at large scales. Assuming isotropy and homogeneity as part of the initial conditions is hardly an explanation. Given that it is unlikely that the universe started out in a very special fine-tuned initial state, there exist many proposals in the literature which provide various mechanisms which would result into isotropization and homogenization at late times starting from quite general conditions, the most popular being the theory of cosmic inflation. Being able to generate isotropy and homogeneity from general initial conditions is naturally considered superior to fine tuning the initial conditions to include isotropy and homogeneity to begin with. In light of this, it is quite possible that our universe may not have started in a very isotropic and homogeneous state. Hence it is important to explore if the result on the replacement of the big bang with a bounce in LQC is general enough, by exploring the fate of the initial singularity in LQC in more general spacetimes than the isotropic and homogeneous model only. The class of homogeneous but anisotropic spacetimes provide an important test bed to generalize the results of isotropic LQC. Fortunately, it is possible to classify all the homogeneous and anisotropic cosmological solutions of GR into a finite number of types. This classification, utilizing concepts from group theory, was first obtained by Bianchi [126], thus these models are called Bianchi models. There is only one homogeneous and anisotropic model, called Kantowski–Sachs model, which lies outside the Bianchi classification. We discuss this classification later in this section. Classically, these models exhibit a wide variety of cosmological singularities.

As we emphasized in the previous chapter, these anisotropic models are also important in the analysis of general spacetime singularity as per BKL (Belinski–Khalatnikov–Lifshitz) conjecture, which states that in the asymptotic vicinity of a generic singularity in GR, the spatial derivatives in Einstein’s equations become negligible compared to the time derivatives, and the dynamics at each point effectively becomes decoupled from other points in the spatial manifold [125]. This situation is similar to the case of homogeneous cosmologies where due to spatial homogeneity, only the time derivatives survive and Einstein’s equations reduce to a system of ordinary differential equations with respect to time. Infact, if the BKL conjecture is true, then close to the generic singularity, the evolution at each point goes through an infinite series of chaotic oscillations (called Mixmaster behavior), which can be well approximated by the homogeneous and anisotropic cosmologies [125]. In particular, as the singularity is approached, the spacetime at each spatial point goes through an infinite sequence of Kasner epochs, where each Kasner epoch is a particular Bianchi-I spacetime, and the transitions between these Kasner epochs are well approximated by Bianchi-II spacetimes. This closely resembles the Mixmaster dynamics observed in Bianchi-IX spacetimes [127]. The BKL conjecture has been a subject of various numerical and analytical investigations which have substantiated its validity near a generic spacetime singularity [233, 234, 235, 236, 237, 238, 239]. Thus, it becomes important from this perspective to analyze the dynamics of these anisotropic and homogeneous models in the context of LQC.

By definition, any homogeneous spacetime can be foliated into a one parameter family of hypersurfaces  $\Sigma_t$  in such a way that the spatial slices are homogeneous, i.e. given any two points on the spatial hypersurface, there exists a symmetry of the metric which carry them to one another. In other words, homogeneous spacetimes possess a group of isometries whose orbits are the spatial hypersurfaces that foliate the spacetime manifold. This implies that the group of isometries acts transitively on the spatial hypersurfaces.



An  $n$ -dimensional manifold can have at most  $n(n+1)/2$  Killing vector fields<sup>1</sup>, i.e. the three dimensional hypersurfaces  $\Sigma_t$  can at most possess 6 Killing vector fields. The case with 6 Killing vector fields corresponds to the homogeneous and isotropic FLRW spacetime itself. The rest of the homogeneous but anisotropic models can be neatly classified using techniques from group theory. As we mentioned, the group of isometries acts transitively on the spatial hypersurfaces of a homogeneous spacetime. If we restrict ourselves to the case where the group acts simply transitively, we are led to a class of homogeneous cosmologies called the Bianchi cosmologies. When the group action is simply transitive, the spatial slices can be put into one to one correspondence with the group manifold itself, and the Killing vector fields correspond to the right invariant vector fields of the group which form a Lie algebra. Different choices of the three dimensional Lie group then lead to different homogeneous spacetimes and we can thus obtain all the homogeneous cosmologies with simply transitive action [240, 58]. All the distinct three-dimensional Lie groups have been obtained and classified by Bianchi in [126], which leads to the Bianchi classification of homogeneous and anisotropic cosmologies [240]. It turns out that there is only one case where the group does not act simply transitively, which is the group  $SO(3) \times \mathbb{R}$  acting on the manifold  $S^2 \times \mathbb{R}$ , which leads to the spatially homogeneous Kantowski–Sachs model [240]. Thus the Bianchi cosmologies and the Kantowski–Sachs model exhaust all the homogeneous but anisotropic cosmologies. The Bianchi-I model is also important in the analysis of inhomogeneous Gowdy model, where the inhomogeneities can be modeled as propagating gravitational waves on a homogeneous Bianchi-I background. The Kantowski–Sachs is also relevant in the case of astrophysical black hole singularity as the interior of a Schwarzschild black hole is isomorphic to the vacuum Kantowski–Sachs spacetime.

A lot has been achieved in the case of anisotropic spacetimes in LQC over the past few years. Rigorous quantizations of the Bianchi-I, Bianchi-II and Bianchi-IX and Kantowski–Sachs spacetimes have been performed and the respective effective dynamics have been obtained [173, 174, 175, 176, 185, 182]. The results on the absence of strong singularities in the effective

---

<sup>1</sup>Killing vector fields are the generators of symmetries of the metric, i.e, the metric is preserved along the integral curves of these vector fields.

spacetime were first extended to anisotropic spacetimes in [217] in case of Bianchi-I spacetimes. Numerical studies of the difference equations in this case establish the robustness of the bounce and the validity of the effective dynamics in this case [241]. Further, in the case of effective Kantowski–Sachs spacetime, it has been shown that the energy density, the Hubble rates and the expansion scalars are generically bounded and the properties of the bounce have been numerically studied [218, 222]. We will extend the results on singularity avoidance in the effective dynamics to Bianchi-II, Bianchi-IX and Kantowski–Sachs spacetimes in the present work, and also consider the symmetric bounce in the vacuum Kantowski–Sachs model in the context of the black hole singularity.

# Chapter 3

## Singularity Avoidance in Effective Loop Quantized Bianchi-II Spacetime

### 3.1 Introduction

In this chapter, we take an important step towards generalizing the results on generic resolution of strong singularities obtained in the effective dynamics of isotropic and homogeneous FLRW model and Bianchi-I model to other homogeneous and anisotropic models. Specifically, we consider here the singularity resolution in effective loop quantized Bianchi-II spacetimes. The relevance of this exploration is highlighted in chapter 2, where we discussed the importance of anisotropic spacetimes to our own universe as a possible initial state, and as an approximation to the dynamics near a generic singularity as per the BKL conjecture. In the context of anisotropic and homogeneous solutions, we note that the results on resolution of singularities have already been extended to the Bianchi-I models [217]. Recall our discussion on the enumeration and classification of all the possible homogeneous and anisotropic models in chapter 2, the simplest of which is the Bianchi-I model. The Bianchi-I model generalizes the FLRW model by allowing the three space directions to have different scale factors associated to each of them. This model has been loop quantized in references [173, 243], and extensive numerical investigations with a wide variety of states have been carried out in [213] which establish the robustness of the bounce and the validity of the effective dynamics. The question of singularities has been further addressed in the effective theory for Bianchi-I in [217] where it has been found that all the strong singularities are removed just like the isotropic case [214]. Various other phenomenological studies on the nature of singularities, the role of anisotropies and various other aspects have been performed in the effective theory of Bianchi-I [170, 244, 245, 219, 246, 247, 248]. Loop quantized Bianchi-I spacetimes have also been utilized in the hybrid quantization of inhomogeneous Gowdy models, and the singularity avoidance in the consequent effective model has also been

---

This chapter is adapted from the contents of S. Saini and P. Singh, *Classical and Quantum Gravity*, 34(23), (2017), 235006 [242] with the permission of IOP Publishing Ltd. See Appendix A for the copyright permission from the publishers.

studied [186, 185, 249]. Hence we focus our attention in this chapter on the Bianchi-II spacetime in this chapter.

The Bianchi-II spacetime is of special importance due to the BKL conjecture. Recall from chapter 2, the BKL conjecture states that the dynamics near a generic singularity is such that the time derivatives in the Einstein's equations dominate over spatial derivatives, which can thus be ignored in the asymptotic vicinity of the singularity [125]. The evolution at each spatial point in that approximation is described by chaotic oscillations between various phases described by Bianchi-I type cosmology with Bianchi-II mimicking transitions between these phases. Thus it is important to study the LQC of Bianchi-I and II cosmologies in the context of generic spacetime singularities. We have mentioned above all the investigations carried out in the loop quantization of Bianchi-I cosmologies, where it has been found that the initial singularity is resolved. Naturally the next step is to study the Bianchi-II cosmology. In particular, we will consider the question of singularity avoidance in effective loop quantized Bianchi-II spacetime. As mentioned above, the validity of the effective dynamics has recently been also tested for anisotropic Bianchi-I spacetimes [213]. In this chapter, we will assume the validity of the effective dynamics in Bianchi-II spacetimes.

However, the generalization of results of the loop quantization of Bianchi-I spacetime to Bianchi-II spacetime is not straightforward and the presence of both spatial curvature and anisotropy complicate matters. Unlike Bianchi-I model, the Killing vector fields of the spatial slices no longer commute with each other, thus a closed loop cannot be formed by integral curves along these vector fields. This creates an obstacle in obtaining the operator for the Hamiltonian constraint, specifically for the terms containing the curvature of the connection. As we mentioned in previous chapters, taking inspiration from LQG, the connection terms in the classical expressions are first re-expressed in terms of holonomies of the connection, which are then promoted to operators on the kinematical Hilbert space. The holonomies are made of almost periodic functions of the connection which constitute the basic operators on the kinematical Hilbert space [143]. The curvature term is then represented by taking the holonomy of the connection around a closed loop, which classically is exactly equal to the curvature under

the limit of vanishing area of the loop considered. As mentioned above, one cannot get a closed loop by using integral curves of the Killing vector fields (which correspond to the right invariant vector fields on the group manifold) of the Bianchi-II hypersurfaces. Using any general loop does not work as the holonomies around them are not almost periodic functions of the connection components. Thus the strategies used in quantizing Bianchi-I model do not work in Bianchi-II model. A similar problem was encountered in going from spatially flat isotropic FLRW model considered in [123, 124, 80] to spatially curved isotropic FLRW model, where the fiducial triads do not commute in the presence of spatial curvature and do not form a closed loop. There, the problem was resolved by forming loops by alternatively following left and right invariant vector fields which do commute with each other [162, 159]. It was found that the holonomies of the isotropic connection around such loops turned out to be almost periodic functions of the connection and could be used to express the curvature term. It is possible to form closed loops in a similar way in the Bianchi-II model. However, the anisotropy of Bianchi-II model implies that the Ashtekar connection now has three independent components, due to which the holonomy around such closed loops fails to be an almost periodic function of the connection components for one of the curvature components [174] and thus fails to be a well-defined operator on the kinematical Hilbert space. Thus the strategy to re-express the field strength (or curvature) in the Hamiltonian constraint using holonomies over closed loops does not work. These problems also occur in other homogeneous models such as loop quantized Bianchi-IX model.

One solution to the above issue is suggested in [231, 232, 174], where an operator for the connection is obtained from holonomies over open edges which allows the constraint to be expressed as an operator using almost periodic functions. The quantization involves using homogeneity and careful geometrical considerations to establish correspondence between LQG and LQC to obtain a  $\bar{\mu}$ -like quantization (of the isotropic model discussed in chapter 2) of the Bianchi-II model where physical results are free from fiducial structures. This is carried out in such a way that it is consistent with the usual loop quantization in other spacetimes where the usual quantization can be carried out such as the Bianchi-I and isotropic spacetimes. This is called the Ashtekar–Barbero connection based ‘A’ quantization. Though the resulting

quantization leads to that of Bianchi-I spacetime in the limit when spatial curvature vanishes, the physics of this loop quantized spacetime is quite unexpected. It has been pointed out in reference [215] that showing boundedness of energy density, the expansion and shear scalars in the corresponding effective dynamics turns out to be rather non-trivial compared to isotropic and Bianchi-I models. It turns out that the holonomy corrections to the effective Hamiltonian constraint are not sufficient, and one has to further impose weak energy conditions to achieve this. It gets worse in the case of Bianchi-IX model where even imposing weak energy conditions does not yield these results [215].

These difficulties with the ‘A’ quantization have led to a revisiting of the so called ‘K’ quantization in LQC [176] which was earlier used in the context of isotropic models with spatial curvature when the above mentioned difficulties in obtaining suitable loops to evaluate the holonomies of the Ashtekar connection to yield almost periodic functions of the connection were first encountered [139, 250, 160, 251], and had also been suggested in spherically symmetric models [252], Schwarzschild interior spacetimes [178] and inhomogeneous cosmological models [253]. This is based on the fact that the symmetry reduction in LQC involves a complete gauge fixing of the internal  $SU(2)$  degrees of freedom in our variables, which allows us to treat the extrinsic curvature  $K_a^i$  as a connection [178, 160]. This connection variable can then be used to construct holonomies along open loops to obtain the expression of Hamiltonian constraint operator in terms of almost periodic functions defined on the kinematical Hilbert space. In contrast to the ‘A’ quantization, this quantization has been shown to yield generic bounds on expansion and shear scalars and Hubble rates in Bianchi-IX model without any extra conditions such as the weak energy conditions [176]. However, there are important caveats to using the extrinsic curvature based ‘K’ quantization. Since the extrinsic curvature is not a connection in the full theory, its holonomies are not defined. Thus, ‘K’ quantization deviates slightly from the ideas of LQG and may not adequately capture the physics of the corresponding cosmological sector of the fully quantum theory. In the case of spatially closed isotropic models, where both ‘A’ and ‘K’ quantizations can be performed in addition to the standard LQC quantization using holonomies around closed loops, their predictions are found to differ from each other and

from the standard quantization [139, 159, 254]. Thus, any results obtained by considering the extrinsic curvature as a connection in symmetry reduced settings must be interpreted with care.

We will consider both of these quantizations for the Bianchi-II model in this chapter. We show that for the effective dynamics of the ‘A’ quantization, if one only takes into account holonomy modifications arising from regularization of the Hamiltonian constraint, then the strong singularities are not resolved. The effective spacetime is geodesically incomplete. This is unlike the situation in loop quantization of isotropic and Bianchi-I and the cause of this lies in potential singularities arising due to one of the triads vanishing in a finite time evolution, and unboundedness of associated directional Hubble rate. Though the energy density has a global maxima, it is unbounded from below and may diverge which is tied to the unbounded behavior of one of the triads as mentioned above. To remedy this situation there are two avenues. First, since the energy density is unbounded from below, we may try to remedy the situation by restricting the energy density from below. In GR, this is achieved by imposing various types of energy conditions on the energy-momentum tensor requiring positive-definiteness. Energy conditions also play an important role in the singularity theorems of GR. As in GR, it has been shown in [215] that imposing energy conditions results in a lower bound on the energy density in the effective dynamics which translates to remedying the troubling behavior of one of the triads and directional Hubble rates getting cured. We will use the weak energy conditions (WEC) in this chapter as these are satisfied by most types of matter content. Building on these results, we show in this chapter that if WEC is imposed on the energy density, then it can be shown that the effective spacetime is geodesically complete and all strong singularities are avoided.

However, energy conditions have been not played any role in singularity resolution in LQC up to this point. Thus one might search if there are other avenues to rescue the ‘A’ quantization which do not involve any external input such as the energy conditions. A possible avenue could be the inverse triad corrections in the effective Hamiltonian constraint. Recall that the effective Hamiltonian incorporates the effects of quantum geometry in two important ways - the holonomy corrections entering through the terms containing the field strength of the connection, and the inverse triad modifications entering through the terms containing inverse powers of the

triads. We discussed how the inverse triad operators are evaluated in chapter 2 while quantizing the matter Hamiltonian in standard LQC. The significance of inverse triad modifications in singularity resolution in LQC has been negligible so far compared to the holonomy corrections in spatially flat isotropic and Bianchi-I models [80, 214, 217]. In these models, a bounce can be obtained without including inverse triad corrections. In fact, it is shown that the effect of inverse triad corrections turn out to vanish in the spatially non-compact models such as the spatially flat FLRW model and the Bianchi-I model [80]. This is so because the inverse triad corrections as defined currently in the literature depend on the fiducial cell volume introduced in non-compact cases to regulate the integrals, and vanish as the regulator is removed by taking the limit of the fiducial cell volume to infinity. Nevertheless, inverse triad corrections are likely to play an important role in spatially compact spacetimes in singularity resolution [164, 177], as well as spacetimes with spatial curvature [215]. Studies of the closed isotropic FLRW model [255] and Lemaitre–Tolman–Bondi spacetimes [256] including only inverse triad modifications show that they cause these models to bounce. However, when holonomy corrections are also present, they only play an important role when the volume of the universe is Planckian, and have negligible role if the bounce occurs at volume much larger than Planck volume [257]. In this chapter, we will be analyzing singularity resolution in the spatially curved Bianchi-II model in a non-compact topology. As mentioned above, the effect of the inverse triads vanish in non-compact models. On the other hand, their potential role in singularity resolution in spatially curved models such as the Bianchi-II model has been emphasized in [215]. In this regard, we note that in [258], it has been suggested that the vanishing of the inverse triad corrections in spatially non-compact models indicates that they have not been appropriately adapted from the full theory to LQC, and an attempt at obtaining non-vanishing inverse triad operators is made. Since a satisfactory formulation of a non-vanishing inverse triad operator is still lacking in non-compact cases, we will include the inverse triad corrections in this chapter in a heuristic semi-classical way in the effective Hamiltonian for the non-compact Bianchi-II model. We shall replace the inverse powers of the triads in the effective Hamiltonian by the eigenvalues of the inverse triad operators and assume that this heuristic picture adequately captures the effects of inverse triad corrections.



We will show in this chapter that one can indeed obtain singularity resolution by including the inverse triad corrections in this way in the effective Bianchi-II spacetime.

The main result from the ‘A’ quantization of the Bianchi-II spacetime is that all strong singularities are resolved and the effective spacetime is geodesically complete if inverse triad modifications are included. If these are excluded, then the weak energy condition is necessary to be imposed in order to resolve singularities. Curvature invariants can still diverge if either of these routes are taken, but such divergences turn out to be weak singularities. Thus the ‘A’ quantization hints that the holonomy corrections may not be sufficient to resolve a general singularity, and inverse triad corrections might play an important role in generic singularity resolution in LQC, or some additional physical conditions will be needed to be imposed if one wants to ignore the inverse triad corrections.

In contrast to the ‘A’ quantization, the ‘K’ quantization readily yields generic resolution of singularities without the need to impose any energy conditions or to include inverse triad corrections. We show that the triads remain non-zero and finite in any finite time evolution. The Hubble rates, the expansion and shear scalars are generically bounded. The energy density remains bounded for all finite time evolution. There can be divergences in some curvature invariants and the time derivative of expansion scalar, but such divergences are weak singularities. The geodesics are unaffected at such divergences and the effective spacetime is free from any strong singularities. Unlike the ‘A’ quantization, we can obtain these results in the ‘K’ quantization without including inverse triad corrections or imposing weak energy conditions. This contrast in the two quantization becomes more striking in the case of Bianchi-IX model as we will show in the next chapter. However, the main result of this chapter is that generic resolution of strong singularities can be obtained in the loop quantized effective Bianchi-II spacetime.

We begin with a brief overview of the Hamiltonian formulation in terms of Ashtekar variables of the classical Bianchi-II spacetime in the next section, where we will also obtain expressions for the expansion and shear scalars, and curvature invariants. We will then consider the effective dynamics of the ‘A’ quantization with and without inverse triad corrections in the next section, which will be followed by a section on the effective dynamics of ‘K’ quantization. We will then

follow with sections on general considerations of the potential divergences in curvature invariants in both the quantizations, the behavior of geodesics, and the strength of singularities. Let us begin with the classical dynamics of Bianchi-II model.

### 3.2 Classical dynamics of diagonal Bianchi-II spacetime

In this section, we provide the classical Hamiltonian description of the Bianchi-II spacetime and obtain expressions for important quantities needed for the analysis of this chapter. Bianchi-II is a spatially homogeneous and anisotropic spacetime. This implies that the four dimensional spacetime can be split in such a way that the spatial slices are homogeneous. In this case, the spatial slices each have a set of three independent Killing vector fields ( $\zeta_1, \zeta_2$  and  $\zeta_3$ , say), satisfying the algebra  $[\zeta_i, \zeta_j] = C_{ij}^k \zeta_k$  with the only non-zero structure constants being  $C_{23}^1 = -C_{32}^1 \in \mathbb{R}^+$ . We work with the spatial topology  $\mathbb{R}^3$  of the spatial slices, which then requires us to introduce a fiducial cell to define the symplectic structure due to the non-compactness of the spatial slices. Let us denote  $V_o$  as the fiducial volume of a cuboid fiducial cell with fiducial lengths  $L_i$  ( $i = 1..3$ ) with fiducial metric  $\overset{\circ}{q}_{ab}$  on the hypersurfaces. The metric of the Bianchi-II spacetime can then be written as follows [174]:

$$ds^2 = -dt^2 + a_1^2(dx - \frac{L_1}{L_2 L_3} \alpha z dy)^2 + a_2^2 dy^2 + a_3^2 dz^2 \quad (3.1)$$

where  $\alpha = C_{23}^1$  is the only non-zero structure constant. And the symmetry reduced Ashtekar variables are as follows [174]:

$$E_i^a = \tilde{p}_i \sqrt{|\overset{\circ}{q}|} \overset{\circ}{e}_i^a \quad \text{and} \quad A_a^i = \tilde{c}^i \overset{\circ}{\omega}_a^i \quad (3.2)$$

where  $\overset{\circ}{\omega}_a^i$  represent the fiducial co-triads and the symmetry reduced variables satisfy:

$$\{\tilde{c}^i, \tilde{p}_j\} = \frac{8\pi G \gamma}{V_o} \delta_j^i. \quad (3.3)$$

We can absorb the dependence on fiducial volume by redefining the symmetry reduced variables,

$$p_i = \frac{V_o \tilde{p}_i}{L_i} \quad \text{and} \quad c^i = L_i \tilde{c}^i. \quad (3.4)$$

Consequently the Poisson brackets are free from fiducial structure:

$$\{c^i, p_j\} = 8\pi G \gamma \delta_j^i. \quad (3.5)$$

Physically, the triad variables are related to the directional scale factors:

$$a_i = \frac{\sqrt{|p_1 p_2 p_3|}}{L_i p_i}. \quad (3.6)$$

while the connection variables correspond to the time derivatives of these scale factors. Now we state the classical Hamiltonian in terms of our symmetry reduced variables, which has the following form [174]:

$$\begin{aligned} \mathcal{H}_{cl} = & -\frac{1}{8\pi G \gamma^2 \sqrt{|p_1 p_2 p_3|}} \left[ p_1 p_2 c_1 c_2 + p_2 p_3 c_2 c_3 + p_3 p_1 c_3 c_1 + \alpha \epsilon p_2 p_3 c_1 \right. \\ & \left. - (1 + \gamma^2) \left( \frac{\alpha p_2 p_3}{2p_1} \right)^2 \right] + \rho \sqrt{|p_1 p_2 p_3|}. \end{aligned} \quad (3.7)$$

In the above, the energy density  $\rho$  of a minimally coupled matter field can be written as  $\rho = \mathcal{H}_m/V$  where  $\mathcal{H}_m$  denotes matter Hamiltonian and  $V = V_o |a_1 a_2 a_3|$  denotes the physical volume of the fiducial cell. The constant  $\epsilon = \text{sgn}(p_1) \text{sgn}(p_2) \text{sgn}(p_3)$  is either  $+1$  or  $-1$  depending on whether the triads are right-handed or left-handed respectively. Interestingly, changing the orientation of any of the triads also changes the sign of the corresponding connection variable, and hence leave the above Hamiltonian invariant such a transformation. Due to which, the energy density obtained from the vanishing of the Hamiltonian constraint  $\mathcal{C}_{cl} = 8\pi G \mathcal{H}_{cl} \approx 0$  depends only the magnitude of the triad and connection variables. We give here the expression

for energy density in the positive octant (i.e. when  $\text{sgn}(p_i) = +1$  for all three triads):

$$\rho = \frac{1}{8\pi G\gamma^2} \left[ \frac{c_3 c_1}{p_2} + \frac{c_1 c_2}{p_3} + \frac{c_2 c_3 + \alpha c_1}{p_1} - (1 + \gamma^2) \alpha^2 \frac{p_2 p_3}{4p_1^3} \right]. \quad (3.8)$$

From the above expression, we can see that the energy density may diverge if one or more of the connection components diverge, or the triad components vanish. The scale factors, the Hubble rates and other invariants depend on the triad variables and their time derivatives. We can find out the time evolution of the triad variables from Hamilton's equations,

$$\dot{p}_1 = -8\pi G\gamma \frac{\partial \mathcal{H}_{cl}}{\partial c_1} = \frac{p_1}{\gamma \sqrt{|p_1 p_2 p_3|}} \left( p_2 c_2 + p_3 c_3 + \frac{\alpha \epsilon p_2 p_3}{p_1} \right), \quad (3.9)$$

$$\dot{p}_2 = -8\pi G\gamma \frac{\partial \mathcal{H}_{cl}}{\partial c_2} = \frac{p_2}{\gamma \sqrt{|p_1 p_2 p_3|}} \left( p_3 c_3 + p_1 c_1 \right), \quad (3.10)$$

and

$$\dot{p}_3 = -8\pi G\gamma \frac{\partial \mathcal{H}_{cl}}{\partial c_3} = \frac{p_3}{\gamma \sqrt{|p_1 p_2 p_3|}} \left( p_1 c_1 + p_2 c_2 \right). \quad (3.11)$$

Note that the above equations do not ensure that the triad variables or their time derivatives remain non-zero and finite. They may diverge for example if the connection variables diverge due to time evolution. Such events may lead to divergences in the Hubble rates, the energy density and other curvature invariants. For example, the Hubble rates are given by,

$$H_i = \frac{\dot{a}_i}{a_i} = \frac{1}{2} \left( \frac{\dot{p}_j}{p_j} + \frac{\dot{p}_k}{p_k} - \frac{\dot{p}_i}{p_i} \right) \quad \text{where } i \neq j \neq k; \quad i, j, k \in \{1, 2, 3\}, \quad (3.12)$$

which diverge whenever the quantities  $\dot{p}_i/p_i$  diverge. Divergences in Hubble rates can lead to divergences in other curvature invariants. Consider the expansion scalar, its time derivative and shear scalar. They describe the effects of the spacetime on an extended object as it travels along a geodesic, and are crucial in the analysis of singularities as they capture the Raychaudhuri equation. For co-moving observers the expansion scalar ( $\theta$ ), its time derivative and shear scalar

$(\sigma^2)$  are given by,

$$\theta = \frac{\dot{V}}{V} = H_1 + H_2 + H_3 = \frac{1}{2} \sum_{i=1}^3 \frac{\dot{p}_i}{p_i} \quad (3.13)$$

$$\dot{\theta} = \frac{1}{2} \sum_{i=1}^3 \left( \frac{\ddot{p}_i}{p_i} - \left( \frac{\dot{p}_i}{p_i} \right)^2 \right) \quad (3.14)$$

$$\sigma^2 = \sum_{i=1}^3 (H_i - \theta)^2 = \frac{1}{3} \left( (H_1 - H_2)^2 + (H_2 - H_3)^2 + (H_3 - H_1)^2 \right). \quad (3.15)$$

Note that the expansion and shear scalar only depend on the first time derivatives of the triads, or more precisely on the ratios  $\dot{p}_i/p_i$ . Whereas the time derivative of the expansion scalar also involves the accelerations  $\ddot{p}_i$ . This fact will play an important role in LQC in the boundedness of  $\theta$  and  $\sigma^2$  and potential divergences in  $\dot{\theta}$ .

Finally we consider the curvature invariants such as the Ricci and Kretschmann scalar. On general grounds, we can say that these can at most depend on the second time derivatives of the triads as these are obtained from the second derivatives of the metric with respect to the coordinates. As a demonstration, we give the expressions for the Ricci and Kretschmann scalars. The Ricci scalar in this case is,

$$R = \frac{\ddot{p}_1}{p_1} + \frac{\ddot{p}_2}{p_2} + \frac{\ddot{p}_3}{p_3} - \alpha^2 \frac{p_2 p_3}{2p_1^3}, \quad (3.16)$$

while the Kretschmann scalar comes out to be,

$$\begin{aligned}
K = & \frac{1}{4p_1^6 p_2^4 p_3^4} \left[ 11\alpha^4 p_2^6 p_3^6 + 14p_1^6 p_3^4 \dot{p}_2^4 - 2\alpha^2 p_1 p_2^5 p_3^3 \left( 29p_3^2 \dot{p}_1^2 - 26p_1 p_3 \dot{p}_1 \dot{p}_3 + 5p_1^2 \dot{p}_3^2 \right) \right. \\
& - 4p_1^5 p_2 p_3^2 \dot{p}_2^2 \left( 4\dot{p}_2 (p_3 \dot{p}_1 + p_1 \dot{p}_3) + 5p_1 p_3 \ddot{p}_2 \right) + 4p_1^4 p_2^2 p_3^2 \left( p_1^2 \dot{p}_2^2 \dot{p}_3^2 \right. \\
& + p_3^2 \{ \dot{p}_2^2 [\dot{p}_1^2 + 3p_1 \ddot{p}_1] + 2p_1 \dot{p}_1 \dot{p}_2 \ddot{p}_2 + 3p_1^2 \ddot{p}_2^2 \} + p_1 p_3 \dot{p}_2 \{ 2\dot{p}_3 [2\dot{p}_1 \dot{p}_2 + p_1 \ddot{p}_2] + 3p_1 \dot{p}_2 \ddot{p}_3 \} \\
& + 2p_1^3 p_2^3 p_3 \left( -5\alpha^2 p_3^4 \dot{p}_2^2 - 8p_1^3 \dot{p}_2 \dot{p}_3^3 + p_3^3 \{ 4\dot{p}_1 \dot{p}_2 [-2\dot{p}_1^2 + p_1 \ddot{p}_1] + 2p_1 [3\dot{p}_1^2 - 2p_1 \ddot{p}_1] \ddot{p}_2 \} \right. \\
& + 2p_1^2 p_3 \dot{p}_3 \{ \dot{p}_3 [4\dot{p}_1 \dot{p}_2 + 3p_1 \ddot{p}_2] + 2p_1 \dot{p}_2 \ddot{p}_3 \} + 4p_1 p_3^2 \{ \dot{p}_3 [\dot{p}_2 (2\dot{p}_1^2 - 3p_1 \ddot{p}_1) - 3p_1 \dot{p}_1 \ddot{p}_2] \\
& - p_1 [3\dot{p}_1 \dot{p}_2 + p_1 \ddot{p}_2] \ddot{p}_3 \} \left. \right) + 2p_1^2 p_2^4 \left( 26\alpha^2 p_3^5 \dot{p}_1 \dot{p}_2 + 7p_1^4 \dot{p}_3^4 + p_3^4 [7\dot{p}_1^4 - 14\alpha^2 p_1 \dot{p}_2 \dot{p}_3 - 10p_1 \dot{p}_1^2 \ddot{p}_1 \right. \\
& + 6p_1^2 \ddot{p}_1^2] - 2p_1^3 p_3 \dot{p}_3^2 [4\dot{p}_1 \dot{p}_3 + 5p_1 \ddot{p}_3] + 2p_1 p_3^3 [2\dot{p}_1 \dot{p}_3 (-2\dot{p}_1^2 + p_1 \ddot{p}_1) \\
& \left. \left. p_1 (3\dot{p}_1^2 - 2p_1 \ddot{p}_1) \ddot{p}_3] + 2p_1^2 p_3^2 [\dot{p}_3^2 (\dot{p}_1^2 + 3p_1 \ddot{p}_1) + 2p_1 \dot{p}_1 \dot{p}_3 \ddot{p}_3 + 3p_1^2 \ddot{p}_3^2] \right) \right] . \quad (3.17)
\end{aligned}$$

As mentioned above, they depend at most on the second time derivatives of the triads. The same applies to all the Riemann tensor components, or any other tensor obtained from second derivatives of the metric such as the Weyl tensor. We will see that we do not need to consider higher order curvature invariants for our purposes in this chapter. Having obtained the classical dynamics and the expressions for important quantities, we proceed in the next section to study the loop quantized Bianchi-II model in the ‘A’ quantization.

### 3.3 Effective dynamics: ‘A’ quantization

We describe the connection operator based ‘A, quantization in this section which was first obtained for the Bianchi-II model in [174]. It should be noted that in this quantization, unlike the isotropic and Bianchi-I case where the curvature operator in the Hamiltonian constraint is expressed using holonomies of the connection around closed loops, here define an operator corresponding to the connection itself using holonomies of the connection along straight edges and construct the curvature operator using these connection operators. The reason and motivation for such a strategy is explained in detail in [174]. The difficulty arises due to the presence of both spatial curvature and anisotropy. Briefly, unlike the spatially flat isotropic and Bianchi-I

cases, the Killing vector fields (which are the right invariant vector fields on the group manifold) representing the symmetries of the spatial hypersurfaces do not commute here, so forming a closed loop by following the integral curves of the Killing vector fields is not possible. A similar difficulty in the case of  $k = 1$  curved isotropic models was overcome by using the fact that the right invariant vector fields commute with the left invariant vector fields. A closed loop could then be obtained by alternatively following the integral curves of the right and left invariant vector fields [162, 159]. Unfortunately, this strategy also fails in Bianchi-II model because the holonomies obtained by this procedure fail to be almost periodic functions of the connection and are not supported by the kinematical Hilbert space. A quantization based on the connection operator in terms of holonomies along open edges is thus obtained in [174] in such a way that it is consistent with the usual quantization based on closed loops in models where the usual procedure can be carried out (such as Bianchi-I) to write the curvature operator in terms of holonomies around closed loops. This quantization was also studied in [186, 185] with a different factor ordering which results in decoupling of the singularity at the vanishing of the triads. It was pointed out in [174] that the same strategy works in all class A Bianchi models including Bianchi-IX which we will be considering in the next chapter.

Here we recall that modifications in the quantum Hamiltonian not only come from rewriting operators using holonomies, but also comes from including inverse triad corrections to correctly write operators corresponding to inverse powers of the triad. Inverse triad corrections, as discussed in chapter 2 in the context of the isotropic model, ensure that the eigenvalues of the inverse triad operators remain finite even when the triad operators have zero eigenvalue. It has been pointed out in [215] that the inverse triad corrections are likely to be important in singularity resolution in curved anisotropic models. We show in this section that this intuition turns out to be correct. In subsection 3.3.1, we consider the effective dynamics of the ‘A’ quantization of the Bianchi-II model which ignores the inverse triad corrections. We find out that this leads to possible singularities where one of the triads can vanish in a finite time evolution. We show that imposing weak energy conditions on the energy density is necessary in this case to ensure bounded behavior of the triads. However, we show in subsection 3.3.2 that the same results

can be obtained without imposition of weak energy conditions if inverse triad corrections are included.

For simplicity, we will restrict ourselves in the triad space to only the positive octant. This can be justified in the quantization of [174] by choosing to work with reflection symmetric quantum states. Or it can also be justified by a different factor ordering in the Hamiltonian constraint, as performed in [186] for Bianchi-I spacetime, which leads to decoupling of various octants and any one can be studied separately. Both of these approaches lead to the same effective Hamiltonian in the positive octant. The analysis in any other octant can be analogously performed without changing much in the expressions in this section. We will again comment on this choice in remarks 1 and 2 below. Further in remark 3 we address a subtle point regarding the decoupling of zero volume states in the quantization [186] and the effective dynamics.

### 3.3.1 ‘A’ quantization without inverse triad corrections

Before we restrict to the positive octant, let us begin with the formulation of reference [174] where the effective Hamiltonian obtained for lapse  $N = 1$  for any orientations of the triads is given by,

$$\begin{aligned} \mathcal{H} = & -\frac{\sqrt{|p_1 p_2 p_3|}}{8\pi G \gamma^2 \Delta l_{pl}^2} \left[ \text{sgn}(p_1) \text{sgn}(p_2) \sin(\bar{\mu}_1 c_1) \sin(\bar{\mu}_2 c_2) + \text{cyclic} \right] \\ & -\frac{1}{8\pi G \gamma^2} \left[ \text{sgn}(p_1) \frac{\alpha |p_2 p_3|}{(\sqrt{\Delta} l_{pl}) |p_1|} \sin(\bar{\mu}_1 c_1) - (1 + \gamma^2) \frac{\alpha^2 |p_2 p_3|^{3/2}}{4 |p_1|^{5/2}} \right] + \rho \sqrt{|p_1 p_2 p_3|} . \end{aligned} \quad (3.18)$$

Here  $\rho$  represents minimally coupled matter field and  $\bar{\mu}_i$  represent the lengths of the edges used in expressing the connection operator in terms of holonomies. These are obtained by geometric considerations of correspondence between LQG and LQC as detailed in references [173, 174].

They are given as

$$\bar{\mu}_1 = \lambda \sqrt{\frac{|p_1|}{|p_2 p_3|}} \quad \bar{\mu}_2 = \lambda \sqrt{\frac{|p_2|}{|p_1 p_3|}} \quad \bar{\mu}_3 = \lambda \sqrt{\frac{|p_3|}{|p_1 p_2|}} \quad (3.19)$$



where  $\lambda^2 = \Delta l_{pl}^2 = 4\sqrt{3}\pi\gamma l_{Pl}^2$  is the minimum non-zero eigenvalue of the area operator in LQG.

The effective equations of motion are as follows:

$$\frac{\dot{p}_1}{p_1} = -\frac{8\pi G\gamma}{p_1} \frac{\partial \mathcal{H}}{\partial c_1} = \frac{1}{\gamma\lambda} (\text{sgn}(p_2) \sin(\bar{\mu}_2 c_2) + \text{sgn}(p_3) \sin(\bar{\mu}_3 c_3) + \lambda\xi) \cos(\bar{\mu}_1 c_1), \quad (3.20)$$

$$\frac{\dot{p}_2}{p_2} = -\frac{8\pi G\gamma}{p_2} \frac{\partial \mathcal{H}}{\partial c_2} = \frac{1}{\gamma\lambda} (\text{sgn}(p_3) \sin(\bar{\mu}_3 c_3) + \text{sgn}(p_1) \sin(\bar{\mu}_1 c_1)) \cos(\bar{\mu}_2 c_2), \quad (3.21)$$

and

$$\frac{\dot{p}_3}{p_3} = -\frac{8\pi G\gamma}{p_3} \frac{\partial \mathcal{H}}{\partial c_3} = \frac{1}{\gamma\lambda} (\text{sgn}(p_1) \sin(\bar{\mu}_1 c_1) + \text{sgn}(p_2) \sin(\bar{\mu}_2 c_2)) \cos(\bar{\mu}_3 c_3). \quad (3.22)$$

$$(3.23)$$

where

$$\xi = \alpha \sqrt{\frac{|p_2 p_3|}{|p_1|^3}} \quad (3.24)$$

To analyze the evolution of the triads, let us assume that the triads have some initial finite values  $p_1^0, p_2^0, p_3^0$  at some initial time  $t_0$  in the present. Then from (3.21) we have

$$\int_{p_2^0}^{p_2(t)} \frac{dp_2}{p_2} = \int_{t_0}^t \frac{1}{\gamma\lambda} (\text{sgn}(p_3) \sin(\bar{\mu}_3 c_3) + \text{sgn}(p_1) \sin(\bar{\mu}_1 c_1)) dt. \quad (3.25)$$

Upon formal integration, we get

$$p_2(t) = p_2^0 \exp \left\{ \frac{1}{\gamma\lambda} \int_{t_0}^t \left( (\text{sgn}(p_3) \sin(\bar{\mu}_3 c_3) + \text{sgn}(p_1) \sin(\bar{\mu}_1 c_1)) \cos(\bar{\mu}_2 c_2) \right) dt \right\}. \quad (3.26)$$

Note that (3.26) ensures that the sign of  $p_2(t)$  remains the same as the sign of the initial value  $p_2^0$  as long as the equation is well defined, i.e. does not break down at a singularity etc. Similar arguments apply to the evolution of  $p_1(t)$  and  $p_3(t)$  regarding the sign as long as the evolution is non-singular.

Note that the effective Hamiltonian and the equations of motion have  $\text{sgn}(p_i)$  factors in various terms. We can clean up further calculations if we could restrict the  $p_i$ 's to a particular

octant in the triad space. This can be justified from two different approaches, both of which lead to the same effective Hamiltonian. We can either follow the approach in [173] and [174] where at the quantum level, the basis states for the kinematical Hilbert space are chosen to be symmetric under reflections in the triad space. The effective Hamiltonian then can be obtained by restriction to a positive octant [173, 174]. Following this, at the effective level we can choose our initial conditions such that the triads start out in the positive octant in our analysis. From the discussion in the previous paragraph, we then find that the triads remain in the same octant where their initial conditions were specified during a non-singular time evolution. Different octants are related to each other via parity operations and the qualitative behavior of the Hamiltonian constraint does not change from one octant to another.

Alternatively, one can achieve this without even restricting to symmetric states if one adopts a different factor ordering in the Hamiltonian constraint on the lines of Ref. [185] where this is done for Bianchi-I model in order to decouple different octants. In this factor ordering, the action of the Hamiltonian constraint leaves the different octants invariant so that the octants, and specifically the zero volume states, decouple. This is done in [185] to resolve the singularity at the kinematical level by decoupling the zero volume states. Thus a quantization of the Bianchi-II model on these lines will lead to decoupling of the different octants which are then related by parity operations, and we can restrict our analysis to the positive octant without any loss of generality.

Henceforth, we restrict ourselves to the positive octant assuming one of the above choices has been made. So that we can drop all the sign factors and remove the modulus signs from the triads. To be consistent, we must also assume that the initial values  $p_i^o$  are positive definite. Now returning to equation (3.26), we see that the integration on RHS remains finite for finite time evolution since  $|(\sin(\bar{\mu}_3 c_3) + \sin(\bar{\mu}_1 c_1)) \cos(\bar{\mu}_2 c_2)| \leq 2$  is bounded. Thus for any finite past or future evolution, we have:

$$0 < p_2(t) < \infty. \quad (3.27)$$

Similarly we can show that  $0 < p_3(t) < \infty$  from (3.22). But the equation (3.20) for  $p_1$  is non-trivial as it contains another term which has  $\xi$  in it. Upon formal integration, we get

$$p_1(t) = p_1^0 \exp \left\{ \frac{1}{\gamma \lambda} \int_{t_0}^t \left( (\sin(\bar{\mu}_2 c_2) + \sin(\bar{\mu}_3 c_3)) \cos(\bar{\mu}_1 c_1) \right) dt \right\} \exp \left\{ \frac{\alpha}{\gamma} \int_{t_0}^t \sqrt{\frac{p_2 p_3}{p_1^3}} \cos(\bar{\mu}_1 c_1) dt \right\} \quad (3.28)$$

The first exponential on RHS remains finite and non-zero for all finite times since  $|(\sin(\bar{\mu}_2 c_2) + \sin(\bar{\mu}_3 c_3)) \cos(\bar{\mu}_1 c_1)| \leq 2$ . However, we cannot conclude the same for the second exponential term. We note that the second exponential ensures that  $p_1$  cannot diverge in a finite time evolution starting from a finite non-zero value. This can be seen by comparing the LHS with the RHS of (3.28) as  $p_1$  diverges. LHS is  $p_1$  itself, and diverges if  $p_1$  diverges. However, since  $p_2$  and  $p_3$  are finite for finite times, the integral in the second exponential of (3.28) stays finite when  $p_1$  becomes large as it is in the denominator. Thus equation (3.28) ensures that  $p_1$  cannot diverge in a finite time evolution. However the equation is consistent with  $p_1$  vanishing in a finite time evolution if the factor  $\cos(\bar{\mu}_1 c_1)$  in the second exponential happens to be negative in the region when  $p_1$  is approaching zero. This can lead to a potential cigar type singularity. To see this, let us consider the behavior of the directional scale factors. From the relations of the triads with the scale factors and the conclusions obtained from the equations of motion above, we have the following situation:

$$\begin{aligned} p_1 &\propto |a_2 a_3|, & p_1 &< \infty, \\ p_2 &\propto |a_3 a_1|, & 0 &< p_2 < \infty \end{aligned}$$

and

$$p_3 \propto |a_1 a_2|, \quad 0 < p_3 < \infty.$$

Under these conditions,  $p_1$  can vanish if  $a_1$  diverges and  $a_2, a_3$  approach zero at the same rate. This is called a cigar singularity where the spatial volume vanishes in such a way that one

of the scale factor diverges while the other two are vanishing. The expansion and shear scalars also diverge as they contain the quantity  $\dot{p}_1/p_1$  which diverges when  $p_1$  goes to zero.

Recall that the above effective dynamics can be obtained from either the quantizations of Ref. [174], or from a quantization along the lines of Ref. [185]. As we mentioned above, the zero volume states are decoupled from rest of the octants in the approach of Ref. [185], and the singularity is avoided at the kinematical level itself. If the effective dynamics is assumed to be obtained from a quantization similar to Ref. [185], then this result points to a limitation of the effective dynamics in capturing the correct behavior of this quantization when the volume becomes extremely small, as the above mentioned singularity is absent in the quantum dynamics based on the approach of [185]. This is expected as the effective dynamics is obtained in LQC under the assumption of large volume to keep only the leading order corrections to the classical dynamics [200]. This is substantiated by numerical simulations which show that the effective dynamics becomes less reliable for states which probe deep Planck volumes [213].

Nevertheless, we can remedy the above situation in effective dynamics by imposing energy conditions on the energy density. The expression for energy density can be obtained by the vanishing of the Hamiltonian constraint (3.18),

$$\rho = \frac{1}{8\pi G\gamma^2\lambda^2} \left[ (\sin(\bar{\mu}_1 c_1) \sin(\bar{\mu}_2 c_2) + \text{cyclic terms}) \right] + \frac{1}{8\pi G\gamma^2} \left[ \frac{\xi}{\lambda} \sin(\bar{\mu}_1 c_1) - (1 - \gamma^2) \frac{\xi^2}{4} \right]. \quad (3.29)$$

It is shown in [174] that the above expression for energy density has a global maxima at  $\xi = \frac{2}{\lambda(1+\gamma^2)} = \xi_0$  and  $\sin(\bar{\mu}_1 c_1) = 1$ . However, there is no lower bound on the energy density and it diverges in the negative when the above mentioned cigar singularities occur. We will discuss in section 3.7 that these singularities turn out to be strong singularities. Since these singularities are associated with lack of a lower bound on the energy density, a remedy suggests itself. Namely, imposing an energy condition on the energy density to put a lower bound on it. As mentioned in the introduction, energy conditions have been used in GR as physically reasonable conditions on the energy-momentum tensor. They are also instrumental in the singularity theorems of GR. Most of the singularity theorems in GR use weak energy condition (WEC), which is satisfied by

most of the known types of matter. Thus we impose WEC on the energy density here. WEC demands that the energy density remains non-negative. We can then use the expression for energy density to restrict  $p_1$  to non-zero values as we show in the following.

Dynamically, the energy density  $\rho$  is an inverse parabola as a function of  $\xi$  as per equation (3.29). Restricting  $\rho$  to positive values using WEC restricts the range of  $\xi$  to a finite interval.  $\xi$  contains  $p_1$  in the denominator. Since  $\xi$  cannot diverge and  $p_2$  and  $p_3$  are finite, we see that  $p_1$  must remain non-zero. Thus, when WEC is imposed on the energy density, we can say that for all the triads,

$$0 < p_i < \infty \quad \text{and} \quad 0 < \frac{\dot{p}_i}{p_i} < \infty. \quad (3.30)$$

This ensures that the volume, the scale factors, the Hubble rates, the expansion and shear scalars remain finite and non-zero for any finite time evolution. We will see in section 3.5 that the Ricci scalar, the Kretschmann scalar and components of the Riemann tensor may still diverge, but this does not pose serious problems as the geodesics remain well defined and all the strong singularities are resolved which we will show in sections 3.6 and 3.7 respectively.

In conclusion, resolution of strong singularities is not necessarily ensured in the effective dynamics of ‘A’ quantization if inverse triad corrections are ignored, unless we impose WEC on the energy density. In the next subsection, we include the inverse triad corrections in the effective dynamics of ‘A’ quantization and show that no energy conditions are required to obtain the desired results on singularities.

### 3.3.2 ‘A’ quantization with inverse triad corrections

We note that the classical Hamiltonian (3.7) contains terms with inverse powers of the triad  $p_1$ . A proper loop quantization will thus include the effects of inverse triad corrections. However, in isotropic and Bianchi-I models it was observed that singularity resolution could be obtained just by including the holonomy corrections to the effective Hamiltonian. However, as we saw above, this does not hold in Bianchi-II model in the ‘A’ quantization and extra conditions such as WEC are needed to be imposed if inverse triad corrections are ignored. In this subsection, we consider the ‘A’ quantization including the inverse triad corrections. We discussed how the

inverse triad operators are obtained in LQG in chapter 2 using Thiemann's trick. Here, we consider the action of the operator  $\widehat{|p_1|^{-1/4}}$  as obtained in reference [174] based on Thiemann's approach. The action of  $\widehat{|p_1|^{-1/4}}$  is given by

$$\widehat{|p_1|^{-1/4}}|p_1 p_2 p_3\rangle \propto \frac{(p_2 p_3)^{1/4}}{(\sqrt{|v+1|} - \sqrt{|v-1|})} |p_1 p_2 p_3\rangle \quad (3.31)$$

where

$$g(p_1) = \frac{(p_2 p_3)^{1/4}}{\sqrt{2\pi\gamma\sqrt{\Delta}l_{pl}^3}} (\sqrt{|v+1|} - \sqrt{|v-1|}); \quad v = \frac{\sqrt{p_1 p_2 p_3}}{2\pi\gamma\sqrt{\Delta}l_{pl}^3}. \quad (3.32)$$

As we discussed above, the inverse triad corrections for non-compact models in LQC depend on the fiducial structure introduced to regulate the integrals and vanish when the regulator is removed. Attempts at defining non-vanishing inverse triad operators for non-compact models have so far been inconclusive. Thus we include the inverse triad corrections in the effective Hamiltonian in a heuristic manner by replacing the inverse powers of the triads in the Hamiltonian constraint with the eigen values of the inverse triad operators given above. We assume that the resultant effective Hamiltonian captures the essential features of the dynamics of loop quantized Bianchi-II model with inverse triad corrections. Note that the functions  $g(p_i)$  are not differentiable at  $v = \pm 1$ . However, we will only need the evolution equations for the triad equations which do not involve the derivatives of these functions as shown below. Thus we use these functions in the effective Hamiltonian to reflect the inverse triad corrections in the evolution of triad variables. The effective Hamiltonian with inverse triad corrections for the lapse  $N = 1$  then becomes,

$$\begin{aligned} \mathcal{H} = & -\frac{\sqrt{p_1 p_2 p_3}}{8\pi G \gamma^2 \Delta l_{pl}^2} \left[ (\sin(\bar{\mu}_1 c_1) \sin(\bar{\mu}_2 c_2) + \sin(\bar{\mu}_2 c_2) \sin(\bar{\mu}_3 c_3) + \sin(\bar{\mu}_3 c_3) \sin(\bar{\mu}_1 c_1)) \right] \\ & -\frac{1}{8\pi G \gamma^2} \left[ \frac{\alpha p_2 p_3}{(\sqrt{\Delta} l_{pl})} g(p_1)^4 \sin(\bar{\mu}_1 c_1) - (1 - \gamma^2) \frac{\alpha^2 (p_2 p_3)^{3/2}}{4} g(p_1)^{10} \right] + \rho \sqrt{p_1 p_2 p_3} \end{aligned} \quad (3.33)$$

In comparison to the effective Hamiltonian (3.18), the above Hamiltonian does not contain any inverse powers of the triads. The Hamilton's equations for triads then become:

$$\frac{\dot{p}_1}{p_1} = -\frac{8\pi G\gamma}{p_1} \frac{\partial \mathcal{H}}{\partial c_1} = \frac{1}{\gamma\lambda} \left( \sin(\bar{\mu}_2 c_2) + \sin(\bar{\mu}_3 c_3) + \lambda\alpha\sqrt{p_2 p_3} \frac{g(p_1)^4}{\sqrt{p_1}} \right) \cos(\bar{\mu}_1 c_1), \quad (3.34)$$

$$\frac{\dot{p}_2}{p_2} = -\frac{8\pi G\gamma}{p_2} \frac{\partial \mathcal{H}}{\partial c_2} = \frac{1}{\gamma\lambda} (\sin(\bar{\mu}_3 c_3) + \sin(\bar{\mu}_1 c_1)) \cos(\bar{\mu}_2 c_2), \quad (3.35)$$

and

$$\frac{\dot{p}_3}{p_3} = -\frac{8\pi G\gamma}{p_3} \frac{\partial \mathcal{H}}{\partial c_3} = \frac{1}{\gamma\lambda} (\sin(\bar{\mu}_1 c_1) + \sin(\bar{\mu}_2 c_2)) \cos(\bar{\mu}_3 c_3). \quad (3.36)$$

Since the equations for  $p_2$  and  $p_3$  are unchanged compared to previous subsection, the conclusion that they remain non-zero and finite remains valid here as well. The problem was with the triad  $p_1$  that it could possibly vanish in a finite time evolution. As we see above, inverse triad corrections modify precisely the equation of motion for  $p_1$  and thus the evolution of  $p_1$  will now be different. If we start from non-zero and finite initial value  $p_1^o$ , then a formal integration of equation (3.34) gives:

$$p_1(t) = p_1^o \exp \left\{ \frac{1}{\gamma\lambda} \int_{t_0}^t \left( (\sin(\bar{\mu}_2 c_2) + \sin(\bar{\mu}_3 c_3)) \cos(\bar{\mu}_1 c_1) \right) dt \right\} \exp \left\{ \frac{\alpha}{\gamma} \int_{t_0}^t \sqrt{p_2 p_3} \frac{g(p_1)^4}{\sqrt{p_1}} \cos(\bar{\mu}_1 c_1) dt \right\} \quad (3.37)$$

The first exponential on RHS above remains finite and non-zero in a finite time evolution as the integral inside the exponential is over a bounded integrand. The integrand in the second exponential contains the term  $g(p_1)^4/\sqrt{p_1}$  which could possibly cause trouble. However, the function  $g(p_1)$  obtained from inverse triad operator corresponding to  $p_1$  has such a form that the factor  $g(p_1)^4/\sqrt{p_1}$  tends to zero in the limit of very small or very large  $p_1$ . This, along with the finiteness of  $p_2$  and  $p_3$  ensures that the second exponential term in the expression for  $p_1$  also remains finite and non-zero. Hence we conclude that  $p_1$ , like  $p_2$  and  $p_3$ , also remains positive

definite and finite for all times. Consequently the following holds for all the triads over a finite time evolution when the inverse triad corrections are included:

$$0 < p_i < \infty \quad \text{and} \quad 0 < \frac{\dot{p}_i}{p_i} < \infty. \quad (3.38)$$

Thus the volume, the scale factors, the Hubble rates, the expansion and shear scalars are also well-behaved for all finite time evolution. Compared to the previous subsection, we do not need to invoke WEC here to obtain these results. Instead the inclusion of inverse triad corrections here automatically ensures that the energy density remains finite and non-zero. The energy density can be obtained by the vanishing of the effective Hamiltonian constraint:

$$\begin{aligned} \rho = & \frac{1}{8\pi G \gamma^2 \Delta l_{pl}^2} \left[ (\sin(\bar{\mu}_1 c_1) \sin(\bar{\mu}_2 c_2) + \sin(\bar{\mu}_2 c_2) \sin(\bar{\mu}_3 c_3) + \sin(\bar{\mu}_3 c_3) \sin(\bar{\mu}_1 c_1)) \right] \\ & + \frac{1}{8\pi G \gamma^2 \sqrt{p_1 p_2 p_3}} \left[ \frac{\alpha p_2 p_3}{(\sqrt{\Delta} l_{pl})} g(p_1)^4 \sin(\bar{\mu}_1 c_1) - (1 - \gamma^2) \frac{\alpha^2 (p_2 p_3)^{3/2}}{4} g(p_1)^{10} \right]. \end{aligned} \quad (3.39)$$

Due to the result (3.38), all the terms in the expression for energy density are well behaved for all finite times. Hence the energy density remain finite for all finite times.

We conclude this section by summarizing that to obtain the desired behavior of the triad variables for singularity resolution in the ‘A’ quantization, we either have to include the inverse triad corrections, or must impose the weak energy condition on the energy density. Note that we have included the inverse triad corrections here in a heuristic manner by directly replacing the inverse powers of the triads in the effective Hamiltonian by the eigen values of the inverse triad operators, to include their contribution to the evolution of the triad variables only. We have assumed that the essential effects of inverse triad corrections on singularity resolution are captured in this heuristic approach. We demonstrate in the next section that in the extrinsic curvature based ‘K’ quantization, we can obtain the desired evolution without including inverse triad corrections or imposing weak energy condition.



### 3.4 Effective dynamics: ‘K’ quantization

We discussed in the previous section how ‘A’ quantization was proposed in the case of Bianchi-II model due to difficulties posed by the fact that the holonomies over closed loop do not form almost periodic functions. These difficulties occur in various other spacetimes as well. Another route to overcome those difficulties was proposed in [139, 250, 251] by considering the holonomies of the extrinsic curvature over open edges where the extrinsic curvature was considered as a connection by guage fixing the Gauss constraint. The resulting quantization is known as ‘K’ quantization which has recently been obtained for the Bianchi-IX model [176] and was shown to be promising. As we have noted in the beginning of this chapter, since it is not possible to consider the extrinsic curvature as a connection in the full theory, the ‘K’ quantization may differ in predictions from the cosmological sector of the full theory. With this caveat in mind, we obtain in this section the ‘K’ quantization for the Bianchi-II model and analyze the evolution of triads obtained from its effective dynamics. We will restrict ourselves to the positive octant in the triad space as per our discussion in the previous section. The first step is to obtain the classical Hamiltonian constraint in terms of the triads and the extrinsic curvature components. In Bianchi-II spacetime, the extrinsic curvature is given by:

$$K_a^i = \gamma^{-1}(A_a^i - \Gamma_a^i), \quad \text{where} \quad K_a^i = \frac{k^i}{L_i}({}^o\omega_a^i) \quad (3.40)$$

where  $\Gamma_a^i$  is the spin connection. We need to obtain the relation between  $k_i$ ’s and  $c_i$ ’s in order to substitute for the  $c_i$ ’s. An easy way to obtain these relations is to use the Hamilton’s equations (3.7) and make use of the fact that,

$$k_i = L_i \dot{a}_i . \quad (3.41)$$

The expressions for the connection components in the classical theory turn out to be:

$$c_1 = \gamma k_1 + \frac{\alpha \epsilon}{2} \frac{p_2 p_3}{p_1^2}, \quad (3.42)$$

$$c_2 = \gamma k_2 - \frac{\alpha \epsilon}{2} \frac{p_3}{p_1}, \quad (3.43)$$

and

$$c_3 = \gamma k_3 - \frac{\alpha \epsilon p_2}{2 p_1}. \quad (3.44)$$

The  $k_i$  and  $p_i$  satisfy the following Poisson bracket:

$$\{k_i, p_j\} = 8\pi G \delta_{ij}. \quad (3.45)$$

The classical Hamiltonian (3.7) then becomes

$$\begin{aligned} \mathcal{H}_{cl} = & -\frac{1}{8\pi G \gamma^2 \sqrt{p_1 p_2 p_3}} \left[ \gamma^2 p_1 p_2 k_1 k_2 + \gamma^2 p_2 p_3 k_2 k_3 + \gamma^2 p_3 p_1 k_3 k_1 \right. \\ & \left. - \frac{\alpha^2 \gamma^2}{4} \left( \frac{p_2 p_3}{p_1} \right)^2 \right] + \rho \sqrt{p_1 p_2 p_3}. \end{aligned} \quad (3.46)$$

A quantization of this Hamiltonian constraint, analogous to the quantization of the Bianchi-IX model in [176] without inverse triad corrections, results in the following effective Hamiltonian:

$$\begin{aligned} \mathcal{H} = & -\frac{\sqrt{p_1 p_2 p_3}}{8\pi G \gamma^2 \lambda^2} \left[ \sin(\bar{\mu}_1 \gamma k_1) \sin(\bar{\mu}_2 \gamma k_2) + \sin(\bar{\mu}_2 \gamma k_2) \sin(\bar{\mu}_3 \gamma k_3) + \sin(\bar{\mu}_3 \gamma k_3) \sin(\bar{\mu}_1 \gamma k_1) \right. \\ & \left. - \frac{\alpha^2 \lambda^2 \gamma^2}{4} \frac{p_2 p_3}{p_1^3} \right] + \rho \sqrt{p_1 p_2 p_3}, \end{aligned} \quad (3.47)$$

From which the Hamilton's equations for the triads can be obtained as:

$$\frac{\dot{p}_1}{p_1} = \gamma \lambda \left( \sin(\bar{\mu}_2 \gamma k_2) + \sin(\bar{\mu}_3 \gamma k_3) \right) \cos(\bar{\mu}_1 \gamma k_1), \quad (3.48)$$

$$\frac{\dot{p}_2}{p_2} = \gamma \lambda \left( \sin(\bar{\mu}_3 \gamma k_3) + \sin(\bar{\mu}_1 \gamma k_1) \right) \cos(\bar{\mu}_2 \gamma k_2), \quad (3.49)$$

and

$$\frac{\dot{p}_3}{p_3} = \gamma \lambda \left( \sin(\bar{\mu}_1 \gamma k_1) + \sin(\bar{\mu}_2 \gamma k_2) \right) \cos(\bar{\mu}_3 \gamma k_3). \quad (3.50)$$

The beauty of the ‘K’ quantization is that the quantities  $\dot{p}_i/p_i$  are now generically bounded for all time. This immediately implies that the Hubble rates (3.12), the expansion scalar (3.13) and the shear scalar (3.15) are bounded for all times. Compare it to the ‘A’ quantization of the previous section where we had to do substantial work to obtain these results by either imposing the WEC or including the inverse triad corrections. It is now straight forward to show that the triads  $p_i$  remain finite and non-zero for all finite time evolution. For example, given some finite and non-zero initial value  $p_1^o$ , the integration of the equation of motion for  $p_1$  gives:

$$p_1(t) = p_1^o \exp \left\{ \frac{1}{\gamma\lambda} \int_{t_0}^t \left( (\sin(\bar{\mu}_2\gamma k_2) + \sin(\bar{\mu}_3\gamma k_3)) \cos(\bar{\mu}_1\gamma k_1) \right) dt \right\} \quad (3.51)$$

Since the integrand in the above equation is generically bounded, the integral over a finite time is finite. Thus  $p_1$  remains finite and non-zero for all finite time evolution, i.e.  $0 < p_1 < \infty$ . Similar conclusions analogously follow for both  $p_2$  and  $p_3$ . This in turn ensures that the energy density remains well behaved. the energy density can be obtained from the vanishing of the Hamiltonian constraint:

$$\rho = \frac{1}{8\pi G\gamma^2\lambda^2} \left[ \sin(\bar{\mu}_1\gamma k_1) \sin(\bar{\mu}_2\gamma k_2) + \sin(\bar{\mu}_2\gamma k_2) \sin(\bar{\mu}_3\gamma k_3) + \sin(\bar{\mu}_3\gamma k_3) \sin(\bar{\mu}_1\gamma k_1) - \frac{\alpha^2\lambda^2\gamma^2}{4} \frac{p_2 p_3}{p_1^3} \right]. \quad (3.52)$$

Since triads remain finite and bounded for all finite times, the energy density never diverges in a finite time evolution. We will note in the next section that some curvature invariants which depend on  $\ddot{p}_i$  and higher derivatives may still diverge, but we will see in the chapter that these divergences are not harmful.

Thus, in contrast to the ‘A’ quantization, the results on the boundedness of the triads, the energy density, the Hubble rates, the expansion and shear scalars and the finiteness of the volume are easily obtained in ‘K’ quantization without including inverse triad corrections or imposing WEC. In the next section we proceed to show the divergences that may still be present in some of the curvature invariants.

### 3.5 Potential divergences in curvature invariants and $\dot{\theta}$

In this section, we demonstrate that some of the curvature invariants such as the Ricci scalar, the Kretschmann scalar and the components of the Riemann tensor may still diverge in the effective LQC dynamics of the two different quantizations studied above even if the energy density, the Hubble rates, the expansion and shear scalars are all finite and the volume is non-zero. We also consider the behavior of the time derivative of the expansion scalar, which according to the Raychaudhuri equation describes the focusing behavior of geodesics, and plays a key role in the formulation of singularity theorems in GR. We will find that this can also diverge in the effective dynamics.

Let us first note, as already pointed out above, that the accelerations  $\ddot{p}_i$  will be present in the Ricci scalar, the Kretschmann scalar, the time derivative of the expansion scalar and in general in the components of any tensor derived from the second derivatives of the metric such as the Riemann tensor. We demonstrated in the previous sections that the triads will remain finite and non-zero and the ratios  $\dot{p}_i/p_i$  involving first derivatives will be bounded for all finite time evolution in the effective dynamics of ‘A’ quantization if WEC is imposed or inverse triad corrections are included, and in the effective dynamics of the ‘K’ quantization even without requiring WEC or inverse triad corrections. However, if we take the time derivatives of equations (3.20) or (3.34) (for ‘A’ quantization), and (3.48) (for ‘K’ quantization), we immediately see that the second derivatives  $\ddot{p}_i$  are going to contain first time derivatives  $\dot{c}_i$  of the connection variables. These are obtained from Hamilton’s equations,

$$\dot{c}_i = 8\pi G\gamma \frac{\partial \mathcal{H}}{\partial p_i} \quad (3.53)$$

and contain the derivatives of the energy density with respect to the triad variables  $\partial\rho/\partial p_i$ . Thus, whenever for some specific choices of the matter content, the derivatives  $\partial\rho/\partial p_i$  diverge at finite values of volume, energy density, and expansion and shear scalar, then we are sure to have divergences in  $\ddot{p}_i$  and consequently in some of the curvature invariants.

As an illustration, we consider the case of ‘A’ quantization without the inverse triad corrections. We obtain the second time derivatives of the triads from equations (3.20), (3.21) and (3.22) as follows:

$$\begin{aligned} \frac{\ddot{p}_1}{p_1} &= \left( \frac{\dot{p}_1}{p_1} \right)^2 + \frac{1}{\gamma\lambda} \left[ (\dot{\bar{\mu}}_2 c_2 + \bar{\mu}_2 \dot{c}_2) \cos(\bar{\mu}_2 c_2) + (\dot{\bar{\mu}}_3 c_3 + \bar{\mu}_3 \dot{c}_3) \cos(\bar{\mu}_3 c_3) \right] \cos(\bar{\mu}_1 c_1) \\ &\quad - \frac{1}{\gamma\lambda} \left[ \sin(\bar{\mu}_2 c_2) + \sin(\bar{\mu}_3 c_3) + \lambda\xi \right] (\dot{\bar{\mu}}_1 c_1 + \bar{\mu}_1 \dot{c}_1) \sin(\bar{\mu}_1 c_1) + \frac{\dot{\xi}}{\gamma} \cos(\bar{\mu}_1 c_1) \end{aligned} \quad (3.54)$$

$$\begin{aligned} \frac{\ddot{p}_2}{p_2} &= \left( \frac{\dot{p}_2}{p_2} \right)^2 + \frac{1}{\gamma\lambda} \left[ (\dot{\bar{\mu}}_1 c_1 + \bar{\mu}_1 \dot{c}_1) \cos(\bar{\mu}_1 c_1) + (\dot{\bar{\mu}}_3 c_3 + \bar{\mu}_3 \dot{c}_3) \cos(\bar{\mu}_3 c_3) \right] \cos(\bar{\mu}_2 c_2) \\ &\quad - \frac{1}{\gamma\lambda} \left[ \sin(\bar{\mu}_1 c_1) + \sin(\bar{\mu}_3 c_3) \right] (\dot{\bar{\mu}}_2 c_2 + \bar{\mu}_2 \dot{c}_2) \sin(\bar{\mu}_2 c_2) \end{aligned} \quad (3.55)$$

$$\begin{aligned} \frac{\ddot{p}_3}{p_3} &= \left( \frac{\dot{p}_3}{p_3} \right)^2 + \frac{1}{\gamma\lambda} \left[ (\dot{\bar{\mu}}_1 c_1 + \bar{\mu}_1 \dot{c}_1) \cos(\bar{\mu}_1 c_1) + (\dot{\bar{\mu}}_2 c_2 + \bar{\mu}_2 \dot{c}_2) \cos(\bar{\mu}_2 c_2) \right] \cos(\bar{\mu}_3 c_3) \\ &\quad - \frac{1}{\gamma\lambda} \left[ \sin(\bar{\mu}_1 c_1) + \sin(\bar{\mu}_2 c_2) \right] (\dot{\bar{\mu}}_3 c_3 + \bar{\mu}_3 \dot{c}_3) \sin(\bar{\mu}_3 c_3) \end{aligned} \quad (3.56)$$

Note that  $\ddot{p}_1$  also contains  $\xi$  and  $\dot{\xi}$  ( $\xi$  is given by (3.24)).  $\xi$  and  $\dot{\xi}$  are both bounded due to bounds on the triads given in equation (3.30), which hold in case of ‘A’-quantization provided either WEC is assumed or inverse triad corrections are included. Hence the divergence properties of  $\ddot{p}_i/p_i$  depends only on quantities of type  $(\dot{\bar{\mu}}_i c_i + \bar{\mu}_i \dot{c}_i)$ . Let us consider  $(\dot{\bar{\mu}}_1 c_1 + \bar{\mu}_1 \dot{c}_1)$  as an example:

$$\begin{aligned} \dot{\bar{\mu}}_1 c_1 + \bar{\mu}_1 \dot{c}_1 &= \frac{1}{2\gamma\lambda} \left[ -(\sin(\bar{\mu}_1 c_1) \sin(\bar{\mu}_2 c_2) + \text{cyclic terms}) + 2\lambda\xi \sin(\bar{\mu}_1 c_1) - \frac{5\lambda^2(1-\gamma^2)}{4} \xi^2 \right. \\ &\quad + 8\pi G\gamma^2 \lambda^2 \rho + (\bar{\mu}_2 c_2 - \bar{\mu}_1 c_1)(\sin(\bar{\mu}_3 c_3) + \sin(\bar{\mu}_1 c_1)) \cos(\bar{\mu}_2 c_2) \\ &\quad \left. + (\bar{\mu}_3 c_3 - \bar{\mu}_1 c_1)(\sin(\bar{\mu}_1 c_1) + \sin(\bar{\mu}_2 c_2)) \cos(\bar{\mu}_3 c_3) \right] + \lambda p_1 \frac{\partial \rho}{\partial p_1}. \end{aligned} \quad (3.57)$$

In the above equation, except for  $\partial\rho/\partial p_1$  and factors of type  $(\bar{\mu}_2 c_2 - \bar{\mu}_1 c_1)$  and  $(\bar{\mu}_3 c_3 - \bar{\mu}_1 c_1)$ , rest of the factors are again bounded. We can further analyze the behavior of the factors of type  $(\bar{\mu}_2 c_2 - \bar{\mu}_1 c_1)$ . Using (4.21) we have,

$$\bar{\mu}_2 c_2 - \bar{\mu}_1 c_1 = \frac{\lambda}{V} (c_2 p_2 - c_1 p_1). \quad (3.58)$$

Since  $V$  is bounded in the above expression, we consider  $(c_2 p_2 - c_1 p_1)$ . Its time derivative can be written as follows,

$$\frac{d}{dt}(c_2 p_2 - c_1 p_1) = V \left( p_2 \frac{\partial \rho}{\partial p_2} - p_1 \frac{\partial \rho}{\partial p_1} \right) + \text{other bounded terms} . \quad (3.59)$$

which again depends on the derivatives of the energy density  $\partial \rho / \partial p_i$ . Thus we see that the fate of the second derivatives  $\ddot{p}_i$  of the triads ultimately depends on the behavior of  $\partial \rho / \partial p_i$  as we had pointed out above. This can be shown to be true similarly for ‘A’ quantization with inverse triad corrections and for ‘K’ quantization as well. We call these divergences emerging from  $\partial \rho / \partial p_i$  as “pressure divergences” as  $\partial \rho / \partial p_i$  are related to the pressure when we have the simple case of matter with vanishing anisotropic stress.

Thus we find that not all quantities of interest are ensured to be bounded in the effective dynamics of the quantizations considered above. However, these divergences occur at finite values of the Hubble rates, the energy density, the expansion and shear scalars and finite and non-zero volume. This is a strong indication that these divergences may not lead to a strong singularity. Indeed we will show in the following sections that these divergences are harmless as geodesics are unaffected at such events. And then we will show explicitly that there are no strong singularities in the effective spacetime.

### 3.6 Geodesic completeness

We first find out the geodesic equations for the Bianchi-II spacetime by using the geodesic equation for a general metric as follows,

$$(x^i)'' = \Gamma_{jk}^i (x^j)' (x^k)', \quad (3.60)$$

where the prime denotes differentiation with respect to the affine parameter. The Christoffel symbols for Bianchi-II can be calculated using the metric (3.1). Plugging them into the above

equation and integrating, we get

$$x' = C_x \left( \frac{1}{a_1^2} + \alpha^2 z^2 \frac{1}{a_2^2} \right) + C_y \alpha z, \quad (3.61)$$

$$y' = C_x \alpha z \frac{1}{a_2^2} + C_y, \quad (3.62)$$

$$z' = -C_x \alpha y \frac{1}{a_3^2} + C_z \quad (3.63)$$

and

$$(t')^2 = \varepsilon + \frac{C_x^2}{a_1^2} + a_2^2 \left( C_y + C_x \alpha z \frac{1}{a_2^2} \right)^2 + a_3^2 \left( C_z - C_x \alpha y \frac{1}{a_3^2} \right)^2. \quad (3.64)$$

Here  $C_x, C_y$  and  $C_z$  are constants of integration. The constant  $\varepsilon$  is unity for timelike geodesics and is zero for null geodesics. This set of equations represents the velocity vector along the geodesic. The equation for the geodesic can be obtained in parametric form by integrating the above set of equations. First of all we note that for co-moving observers, the proper time is equal to the coordinate time  $t$  itself.

It is clear from the above set of equations that the velocity vector will diverge whenever any of the scale factors vanishes. This is the case with the classical cosmological singularity in Bianchi-II spacetime. However, we showed above that the triad variables (and hence the scale factors) remain finite and non-zero for all finite time evolution in the coordinate time  $t$  in both ‘K’ quantization, and ‘A’ quantization with WEC or with inverse triad modifications. Thus the scale factors remain finite and non-zero for all finite time evolution. Even though there can be potential divergences in curvature invariants in a finite time evolution in LQC as noted in the previous section, since the scale factors do not vanish at such events, the geodesic equations do not break down. Recall that the inverse triad corrections in the ‘A’ quantization are included in a heuristic manner to include their effect on the evolution of the triad variables and hence on the geodesics which only depend on the triad variables.

Further note that the geodesic equations for the coordinates  $y$  and  $z$  are coupled to each other but are independent of the geodesic equation for coordinate  $x$ . These two equations (3.62)

and (3.63) together form a linear system of first-order ordinary differential equations and hence have a unique global solution if initial positions are specified at a given initial time [259]. Since the RHS of these equations is well defined for all finite times  $t$ , the unique global solution is maximally extendable. Given that  $y$  and  $z$  can be maximally extended as functions of proper time, which really is  $t$  for co-moving observers, then equation (3.61) also has a maximally extendable solution because the RHS is of zeroth order in  $x$  and only contains functions that are all finite for all finite time  $t$ . For the geodesic equation in time  $t$ , for comoving time the LHS turns out to be unity and the equation becomes a constraint between quantities on the RHS of (3.64), which are all finite in finite time  $t$ . This implies that the geodesics in case of Bianchi-II are maximally extendable in effective dynamics.

### 3.7 Lack of strong singularities

The fact that geodesics do not break down at the points where potential divergences in curvature invariants occur hints that such divergences may be harmless. We strengthen this intuition by showing in this section that the effective Bianchi-II spacetime is free from strong singularities, and the above mentioned potential divergences may only amount to a weak singularity. Recall that a strong curvature singularity is characterized by the property that it crushes any in-falling object to zero volume regardless of what they are made of [224, 229, 230]. We discussed them in chapter 2 and provided the necessary conditions for their occurrence, namely, for a timelike or null geodesic running into the singularity, we require the integral (2.2) to diverge. The integral is

$$K_j^i = \int_0^\tau d\tilde{\tau} |R^i_{0j0}(\tilde{\tau})|. \quad (3.65)$$

If these necessary conditions are not satisfied by a potential singularity, then it is a weak or soft singularity and the geodesics can be extended past them. This has been shown in classical GR in cases of weak singularities in both isotropic [260, 261, 262, 263] and anisotropic spacetimes [264, 265]. Since these weak singularity events are harmless, we do not expect these to be modified by quantum gravity effects. Thus weak singularities may still exist in the effective spacetime. In this section, we use the above necessary condition to show that no strong singularities exist



in the effective loop quantized Bianchi-II spacetime in both the ‘A’ quantization (along with WEC or inverse triad corrections) and the ‘K’ quantization.

First of all note that for co-moving observers, the coordinate time  $t$  is the affine parameter itself. Hence, to check whether these conditions are satisfied by the spacetime under consideration, we must look at the evolution of the Riemann tensor components as a function of the coordinate time  $t$ .

As mentioned in the section on curvature invariants, the Riemann curvature tensor is obtained from the second derivative of the metric. The metric is a function of time through the triad variables, and also depends on the coordinate  $z$ . Hence any term obtained via the second derivative of the metric will necessarily be one of the following three types, i.e. the following three possibilities exhaust the types of terms that can appear in the Riemann tensor components:

T-I. Terms of type  $f(p_1, p_2, p_3, z)$ .

T-II. Terms of type  $\left(\frac{\dot{p}_1}{p_1}\right)^m \left(\frac{\dot{p}_2}{p_2}\right)^n \left(\frac{\dot{p}_3}{p_3}\right)^q f(p_1, p_2, p_3, z)$  where  $m, n, q$  are positive integers and  $m + n + q = 2$ .

T-III. Terms of type  $\left(\frac{\ddot{p}_i}{p_i}\right) f(p_1, p_2, p_3, z)$ , where  $i$  can be 1, 2 or 3.

The components of the curvature tensors are made of sums or differences of these three types of terms. Using the fact that,

$$\int_a^b |f_1 + f_2 + \dots + f_n| dt \leq \int_a^b |f_1| dt + \int_a^b |f_2| dt + \dots + \int_a^b |f_n| dt \quad (3.66)$$

we only need to consider divergence properties of the three types of terms individually to conclude about the divergence of the integral in (5.39).

We have shown in section 3.3 that in the ‘A’ quantization, both  $p_i$  and  $\dot{p}_i/p_i$  will be finite for all finite times if weak energy condition is imposed or inverse triad corrections are incorporated. In the ‘K’ quantization this is the case without including either weak energy condition or the inverse triad corrections. Hence the terms of type T-I and T-II will remain finite for any finite time  $t$ . Consequently their integral over a finite range of  $t$  will also be finite. Hence, we conclude

that the terms of type T-I and T-II in the above integral do not diverge. The same can not be said about the terms of the type T-III because they contain second derivatives of triads. As noted in section 3.5 these can potentially diverge for events where pressure or its derivatives become infinite at finite energy density. Thus, only terms of type T-III could possibly lead to divergence of the above integral. In fact, these are the very scenarios which make the curvature invariants and  $\dot{\theta}$  diverge. However as we show below, these problematic second derivatives of the triad variables are removed by integration. Let us consider such a term for the above integral. Then it can be expressed as

$$\int_0^{t_o} \frac{\ddot{p}_i}{p_i} f(p_1, p_2, p_3) dt = \frac{\dot{p}_i}{p_i} f(p_1, p_2, p_3) \Big|_0^{t_o} - \int_0^{t_o} \dot{p}_i \left( \frac{d}{dt} f_1(p_1, p_2, p_3) \right) dt . \quad (3.67)$$

We note that both the terms on the RHS are finite. Hence, the terms of type T-III do not lead to divergence of the integral (3.65). Consequently the integral (3.65) does not diverge in the effective dynamics of LQC in Bianchi-II spacetime. So we have proved that the necessary conditions for existence of strong singularities are not satisfied by the effective dynamics of the ‘K’ quantization or ‘A’ quantization with weak energy condition or inverse triad corrections. In summary, the effective spacetime in ‘A’ (with either weak energy condition or inverse triad modifications included) and ‘K’ quantizations is free of strong singularities. Notably the events where potential divergences in curvature invariants or  $\dot{\theta}$  occur correspond to weak curvature singularities.

Note that in the case of ‘A’ quantization when neither WEC nor inverse triad modifications are included,  $p_1$  can vanish in finite time and  $\dot{p}_1/p_1$  is not bounded. In this case, all the terms: T-I, T-II and T-III result in divergences in eq.(3.65). The cigar singularity in this quantization thus turns out to be a strong curvature singularity. It is straightforward to see from our arguments in the previous section that the geodesics also break down in this case.

### 3.8 Conclusions

In this chapter, we have generalized the results on the generic resolution of strong singularities in the effective isotropic [214, 266] and Bianchi-I [217] spacetimes to effective Bianchi-II

spacetime. This is important due to the BKL conjecture according to which the Bianchi-I, Bianchi-II and Bianchi-IX models play an important part in the analysis of generic spacetime singularities in GR. However, there are important differences to be noted in the results obtained in Bianchi-II model here as compared to the results in isotropic and Bianchi-I models. First, due to presence of both spatial curvature and anisotropy, the techniques used in quantizing isotropic and Bianchi-I models failed in Bianchi-II case [174], and the search for alternatives has led to two different quantizations for the Bianchi-II model - the Ashtekar connection based ‘A’ quantization and the extrinsic curvature based ‘K’ quantization. Unlike the standard quantization procedure of LQC, holonomies of the Ashtekar connection around closed loops does not lead to almost periodic functions of the connection in Bianchi-II model. Thus an operator corresponding to the Ashtekar connection itself is defined in the ‘A’ quantization by taking holonomies of the connection along straight edges. Alternatively, the gauge fixing due to symmetry reduction allows to treat the extrinsic curvature as a connection in the ‘K’ quantization, which is then used to evaluate the holonomies. The results we have obtained in this chapter are using the effective dynamics of these quantizations of Bianchi-II model. In this regard, we note here that ‘A’ and ‘K’ quantizations can also be obtained for isotropic and Bianchi-I models. For the spatially flat FLRW model and the Bianchi-I model, they turn out to be equivalent to each other and to the standard LQC quantizations of these models. However, for spatially curved FLRW models, these quantizations differ from each other and from the standard LQC quantization as well [176]. In case of anisotropic models with spatial curvature such as Bianchi-II model, only ‘A’ and ‘K’ quantizations are possible, and they lead to qualitatively different theories as we have discussed in this chapter. Moreover the triad variables in the effective dynamics of the isotropic and Bianchi-I model were generically bounded for all time, thus the energy density, the Hubble rates, the expansion and shear scalars were also generically bounded and the volume remained non-zero for all time. Comparatively, the results obtained in this chapter in the effective dynamics of Bianchi-II model make a slightly weaker statement of boundedness of all these quantities for all finite time evolution. Nevertheless this suffices to prove singularity resolution.

Even though certain pressure divergences may occur in some curvature invariants within a finite time evolution, we show that the geodesics remain unaffected by these divergences and the effective spacetime is free from all strong singularities. However, we observed a contrast in the two quantizations in the obtaining these results. We found that in the ‘A’ quantization, the holonomy corrections in the Hamiltonian constraint are not sufficient to obtain these results by themselves. We had to impose WEC on the energy density to obtain these results. This is the first time that energy conditions seem to play a role in singularity resolution in LQC, at least in the ‘A’ quantization. However, energy conditions can still be bypassed if inverse triad corrections are included in the effective dynamics. In absence of a non-vanishing inverse triad operator for spatially non-compact models in the literature, we here introduced the inverse triad corrections heuristically and found that strong singularities could be removed without including WEC in the ‘A’ quantization. This is another point of departure from the results in isotropic and Bianchi-I models which can also be quantized using ‘A’ quantization. This is the first time that energy conditions or inverse triad corrections are needed in an essential way to resolve the singularities in the effective dynamics. In contrast, in the effective dynamics of ‘K’ quantization, these results are obtained with comparative ease without including inverse triad corrections or imposing WEC. This sharp contrast between ‘A’ and ‘K’ quantizations is interesting specially considering that the ‘K’ quantization is farther removed from the full theory LQG in terms of techniques as compared to the ‘A’ quantization. As we have mentioned, unlike the symmetry reduced cosmological models, the extrinsic curvature cannot be considered as a connection in the full theory, thus it is not possible to quantize classical expressions using holonomies of the extrinsic curvature. However, we noted in chapter 2 that it is possible to consider the extrinsic curvature as the conjugate variable to the densitized triad. The results of this chapter seems to suggest the advantage of using an extrinsic curvature based quantization in singularity resolution. If this contrast in the ‘A’ and ‘K’ quantization continues in more complex cosmological models, it might be worthwhile to explore a quantization of GR based on densitized triads and the extrinsic curvature 1-form as phase space variables.

Both these quantizations also exist in case of the Bianchi-IX spacetime which is the subject of our next chapter, where the standard quantization techniques of LQC fail for the same reasons as in Bianchi-II model. We will explore the singularity resolution of Bianchi-IX models and also see how the contrast between the two quantizations plays out in that case. Our results in the Bianchi-II model indicate that the inverse triad corrections are likely to play an important role in the ‘A’ quantization in the more complex Bianchi-IX model. Since energy conditions play an important role in the singularity theorems of GR, it will be interesting to explore whether energy conditions become an essential ingredient in singularity resolution in LQC as we go on to more complex models.

## Chapter 4

# Singularity Avoidance in Effective Loop Quantized Bianchi-IX Spacetime

### 4.1 Introduction

As indicated in the previous chapter, quite like the Bianchi-II model, the standard holonomy quantization of LQC fails to yield an algebra of almost periodic functions in the case of Bianchi-IX models due to presence of both spatial curvature and anisotropy. And an approach similar to the one adopted in the Bianchi-II case of the previous chapter leads to the ‘A’ and ‘K’ quantizations of the Bianchi-IX model [175, 176]. The results of the previous chapter brought out a sharp contrast between the ‘A’ and the ‘K’ quantization in the ease of obtaining singularity resolution. Namely, that in the effective description of the ‘A’ quantization of Bianchi-II model, just including holonomy corrections in the effective Hamiltonian constraint is not enough to obtain singularity resolution, and one has to further impose WEC or instead include inverse triad modifications. In contrast, it was possible to obtain singularity resolution in the ‘K’ quantization without the need of WEC or introducing inverse triad corrections. In this chapter, we aim to extend the results on the generic singularity resolution to the effective description of loop quantized Bianchi-IX model and further explore the contrast in the ‘A’ and ‘K’ quantization. Our results of this chapter will show that the contrast between the ‘A’ and ‘K’ quantizations further sharpens in the loop quantized Bianchi-IX model.

As has been said earlier, Bianchi-IX spacetimes are of special importance in the study of generic approach to singularities due to the BKL conjecture [125] along with the Bianchi-I and Bianchi-II models. The chaotic and oscillatory approach to a generic singularity in the BKL scenario resembles the Mixmaster dynamics observed in the approach to the singularity in the Bianchi-IX model [127]. Thus the Bianchi-IX spacetime approximately models the dynamics of a generic spacetime near a singularity. A good understanding of the Planck scale dynamics and

---

This chapter is adapted from the contents of S. Saini and P. Singh, *Classical and Quantum Gravity*, 35(6), (2018), 065014 [267] with the permission of IOP Publishing Ltd. See Appendix A for the copyright permission from the publishers.

singularity resolution in loop quantized Bianchi-IX model will give valuable insights into the quantum dynamics in the vicinity of a singularity encountered in a general spacetime. Together with the results on singularity resolution in loop quantized Bianchi-I model [217] and the loop quantized Bianchi-II model of the previous chapter, the results of this chapter will provide important lessons for the resolution of a generic singularity in LQC.

We give a brief summary of the classical Hamiltonian description of Bianchi-IX spacetime in terms of Ashtekar variables in section 4.2. This section also provides the expressions for some key quantities such as expansion and shear scalars, the directional Hubble rates and the time derivative of the expansion scalar. Section 4.3 covers the effective dynamics of the ‘A’ quantization of Bianchi-IX spacetime. This is divided into two parts: section 4.3.1 deals with the ‘A’ quantization without inverse triad corrections, and section 4.3.2 includes the effects of inverse triad corrections in the effective dynamics. We show in section 4.3.1, that vanishing of triads in finite time evolution can not be avoided if inverse triad corrections are not included, and that imposing weak energy condition, in addition, on the energy density is not sufficient to prevent such a phenomena either. Section 4.3.2 shows that none of the triads vanish or diverge in a finite time evolution in the ‘A’ quantization when inverse triad corrections are included. In section 4.4, we describe the effective dynamics of the ‘K’ quantization for Bianchi-IX model, and we find that the triads, the energy density, and the expansion and shear scalars are bounded without requiring any energy condition or inverse triad modifications. However, we find in section 4.5, that the curvature invariants, the components of Riemann tensor and the time derivative of the expansion scalar can potentially still diverge both in ‘A’ and ‘K’ quantizations. This may indicate potential singularities in the effective spacetime. However, the divergences in the curvature invariants at certain events may not always indicate a breakdown of the spacetime fabric. As studies in classical GR have shown that sometimes these divergences indicate the so called weak or soft singularities which do not affect the geodesic evolution [260, 261, 262, 263, 264, 265]. Since these weak singularities are harmless, they are unaffected by quantum gravity effects which is why they may appear in the effective spacetime. Indeed, we show in section 4.6 that for the ‘A’ quantization with inverse triad correction and the ‘K’ quantization even without the

inverse triad modifications, the geodesics are well behaved when such divergences in curvature invariants occur. In section 4.7, we show that in finite time evolution no strong singularities exist in the effective dynamics of the ‘K’ quantization or the ‘A’ quantization with inverse triad corrections. The events where curvature invariants may potentially diverge thus only amount to weak singularities. We conclude in the final section with a summary of the results.

We remind the reader of the caveats to our approach in this chapter. In an approach similar to the previous chapter, the inverse triad corrections are included in the effective dynamics of the ‘A’ quantization in a heuristic manner by replacing the inverse powers of the triads in the effective Hamiltonian by the eigen values of the inverse triad operators. We assume that this heuristic approach will capture the essential effects of inverse triad corrections on the effective dynamics. Further, we remind the reader that the extrinsic curvature based ‘K’ quantization is unavailable in LQG as the extrinsic curvature cannot be treated as a connection in the full theory. This may lead to results that depart from the expectations based on symmetry reduction of LQG to cosmological models. Thus the results obtained using the ‘K’ quantization should be interpreted with care. With these caveats in mind, we proceed to section .

## 4.2 Classical aspects of Bianchi-IX spacetime in connection-triad variables

Since it is a homogeneous and anisotropic model, Bianchi-IX spacetime can be split in such a way that the spatial hypersurfaces turn out to be homogeneous. In Bianchi-IX, the spatial hypersurfaces are of topology  $\mathcal{S}^3$  with the symmetries corresponding to the three spatial rotations on  $\mathcal{S}^3$ . The metric of the spacetime can be written as [175]:

$$ds^2 = -dt^2 + q_{ab}dx^a dx^b . \quad (4.1)$$

where  $q_{ab}$  is the physical metric of the spatial hypersurface. It can be given as  $q_{ab} = \omega_a^i \omega_b^j \delta_{ij}$ , where the physical co-triads are related to the fiducial ones by  $\omega_a^i = a^i(t)^o \omega_a^i$ , and the fiducial



co-triads are [175],

$${}^o\omega_a^1 = \sin \beta \sin \eta (d\alpha)_a + \cos \eta (d\beta)_a, \quad (4.2)$$

$${}^o\omega_a^2 = -\sin \beta \cos \eta (d\alpha)_a + \sin \eta (d\beta)_a, \quad (4.3)$$

$${}^o\omega_a^3 = \cos \beta (d\alpha)_a + (d\eta)_a. \quad (4.4)$$

Here  $\alpha$ ,  $\beta$  and  $\eta$  represent angular coordinates on a fiducial 3-sphere of radius  $r_o = 2$  and volume  $V_0 = 2\pi^2 r_o^3$ . We define a fiducial length  $l_o \equiv V^{1/3}$ . After symmetry reduction, the Ashtekar variables are related to the fiducial triads  $\hat{e}_i^a$  and co-triads  $\hat{\omega}_a^i$  as [175]:

$$E_i^a = \frac{p_i}{l_o^2} \sqrt{|\hat{q}|} \hat{e}_i^a \quad \text{and} \quad A_a^i = \frac{c^i}{l_o} \hat{\omega}_a^i \quad (4.5)$$

where  $\hat{q}$  is the determinant of the fiducial 3-metric. The symmetry reduced variables then satisfy the following Poisson brackets,

$$\{c^i, p_j\} = 8\pi G \gamma \delta_j^i. \quad (4.6)$$

Here, the directional scale factors are related to the triad variables as follows

$$p_1 = \text{sgn}(a_1) |a_2 a_3| l_o^2, \quad (4.7)$$

(and similarly for  $p_2$  and  $p_3$ ). And the classical Hamilton's equations show that the connection variables are related to the time derivatives of the metric components. The classical Hamiltonian for lapse  $N = 1$  is given as [175],

$$\begin{aligned} \mathcal{H}_{\text{cl}} = & -\frac{1}{8\pi G \gamma^2 \sqrt{|p_1 p_2 p_3|}} \left[ p_1 p_2 c_1 c_2 + p_2 p_3 c_2 c_3 + p_3 p_1 c_3 c_1 + l_o \epsilon (p_1 p_2 c_3 + p_2 p_3 c_1 + p_3 p_1 c_2) \right. \\ & \left. + \frac{l_o^2 (1 + \gamma^2)}{4} \left( 2p_1^2 + 2p_2^2 + 2p_3^2 - \frac{p_1^2 p_2^2}{p_3^2} - \frac{p_2^2 p_3^2}{p_1^2} - \frac{p_3^2 p_1^2}{p_2^2} \right) \right] + \rho \sqrt{|p_1 p_2 p_3|}, \end{aligned} \quad (4.8)$$

where  $\rho$  represents the energy density of matter which is minimally coupled. Similar to Bianchi-II case, the constant  $\epsilon = \text{sgn}(p_1) \text{sgn}(p_2) \text{sgn}(p_3)$  is either  $+1$  or  $-1$  depending on whether the

triads are right-handed or left-handed respectively. Note that the Hamiltonian is invariant under change of the orientation of any given physical triad. In other words, the Hamiltonian (as well as the energy density) depend only on the magnitude of the triad and connection variables. The energy density can be dynamically obtained from the vanishing of the Hamiltonian constraint  $\mathcal{C}_{\text{cl}} = 8\pi G\mathcal{H}_{\text{cl}} \approx 0$ . Since it only depends on the magnitudes of the triads, we give here the expression only in the positive octant:

$$\rho = \frac{1}{8\pi G\gamma^2 p_1 p_2 p_3} \left[ p_1 p_2 c_1 c_2 + p_2 p_3 c_2 c_3 + p_3 p_1 c_3 c_1 + l_o(p_1 p_2 c_3 + p_2 p_3 c_1 + p_3 p_1 c_2) + \frac{l_o^2(1+\gamma^2)}{4} \left( 2p_1^2 + 2p_2^2 + 2p_3^2 - \frac{p_1^2 p_2^2}{p_3^2} - \frac{p_2^2 p_3^2}{p_1^2} - \frac{p_3^2 p_1^2}{p_2^2} \right) \right]. \quad (4.9)$$

We can use the classical Hamiltonian (4.8) to obtain the equations of motion for the triads, which in turn give the time evolution for various other quantities of interest that depend on the triads:

$$\dot{p}_1 = \frac{p_1}{\gamma \sqrt{|p_1 p_2 p_3|}} \left( p_2 c_2 + p_3 c_3 + l_o \epsilon \frac{p_2 p_3}{p_1} \right), \quad (4.10)$$

$$\dot{p}_2 = \frac{p_2}{\gamma \sqrt{|p_1 p_2 p_3|}} \left( p_3 c_3 + p_1 c_1 + l_o \epsilon \frac{p_3 p_1}{p_2} \right), \quad (4.11)$$

$$\dot{p}_3 = \frac{p_3}{\gamma \sqrt{|p_1 p_2 p_3|}} \left( p_1 c_1 + p_2 c_2 + l_o \epsilon \frac{p_1 p_2}{p_3} \right). \quad (4.12)$$

Similar to Bianchi-II model, we can use relations (4.7) to obtain the directional Hubble rates, the expansion scalar and its time derivative, and the shear scalars in terms of the triads as follows:

$$H_i = \frac{\dot{a}_i}{a_i} = \frac{1}{2} \left( \frac{\dot{p}_j}{p_j} + \frac{\dot{p}_k}{p_k} - \frac{\dot{p}_i}{p_i} \right) \quad \text{where } i, j, k \in \{1, 2, 3\}; i \neq j \neq k, \quad (4.13)$$

$$\theta = H_1 + H_2 + H_3, \quad (4.14)$$

$$\dot{\theta} = \frac{1}{2} \sum_{i=1}^3 \left( \frac{\ddot{p}_i}{p_i} - \left( \frac{\dot{p}_i}{p_i} \right)^2 \right), \quad \text{and} \quad (4.15)$$

$$\sigma^2 = \frac{1}{3} \left( (H_1 - H_2)^2 + (H_2 - H_3)^2 + (H_3 - H_1)^2 \right). \quad (4.16)$$

We see that all these quantities except the time derivative of the expansion scalar depend on the triads and their first time derivatives. The time derivative of the expansion scalar in addition also depends on the accelerations  $\ddot{p}_i$ . Similarly the Ricci scalar, Kretschmann scalar and other curvature invariants obtained from the Riemann tensor can be obtained from the second derivatives of the metric turn out to depend on the accelerations  $\ddot{p}_i$ . We demonstrated this fact in the case of Bianchi-II by giving explicit expressions for the Ricci and Kretschmann scalars in the previous chapter. We omit their expressions here for the sake of brevity as we will not use them in the analysis.

The classical time evolution leads some of the triads variables to vanish in a finite time evolution while others may diverge, which implies divergences in the Hubble rates, the energy density, the expansion and shear scalars, and the above mentioned curvature invariants leading to a cosmological singularity. The dynamics leading to the cosmological singularity in this case shows the Mixmaster dynamics akin to the chaotic oscillatory approach to a generic singularity in the BKL conjecture, which makes it relevant for generic singularity resolution. We proceed in the next two sections to quantize the Bianchi-IX model as a first step towards showing generic singularity resolution in this model.

### 4.3 Effective loop quantum cosmological dynamics: ‘A’ quantization

This section discusses the effective dynamics of the ‘A’ quantization of the Bianchi-IX model. We discussed in the Bianchi-II model in the previous chapter the difficulties in defining operators which are based on holonomies over closed loops. Unlike the isotropic and Bianchi-I models, Bianchi-II model has both spatial curvature and anisotropy, due to which the holonomies of the connection over closed loops cannot be represented as almost periodic functions of the connection, leading to difficulties in representing them as operators on the kinematical Hilbert space of LQC. Thus the standard holonomy quantization of earlier models in LQC does not work in case of Bianchi-II model. We face the same issue in case of Bianchi-IX model as both spatial curvature and anisotropy are present in this model as well. These difficulties were overcome in the Bianchi-II case by defining the connection operator based ‘A’ quantization using holonomies of the connection over open edges. Using that same approach, the ‘A’ quantization

for the Bianchi-IX model can be obtained and was first studied in [175]. Our results of the previous chapter emphasize the necessity of inverse triad corrections in singularity resolution in the ‘A’ quantization in spatially curved models with anisotropy. However, in the loop quantized Bianchi-II model of the previous chapter, it was possible to still ignore inverse triad corrections and obtain singularity resolution in the ‘A’ quantization if weak energy condition (WEC) is imposed on the energy density. However, as we will show in subsection 4.3.1 that unlike the Bianchi-II case, WEC is not sufficient to ensure the boundedness of the triads in the Bianchi-IX model in the ‘A’ quantization if the inverse triad corrections are ignored [215]. We proceed in subsection 4.3.2 to include the inverse triad corrections, and show that if inverse triad corrections are included, then triads remain non-zero and finite in a finite time evolution, signaling resolution of singularities. In short, the inverse triad corrections are essential for singularity resolution in the loop quantized Bianchi-IX model in the ‘A’ quantization.

In order to simplify the analysis, we will restrict the triads to the positive octant. Analogously to the case of loop quantized Bianchi-II model in the previous chapter, this can be obtained without any loss of generality by choosing to work with reflection symmetric quantum states in a way similar to [174]. Alternatively, a different factor ordering in the quantum Hamiltonian constraint on the lines of [185, 186] results in decoupling of the various octants and we can choose to work in one of them. As we explained in the previous chapter, dynamics in different octants is related by parity operators following either of the above two approaches. The qualitative behavior of the effective Hamiltonian is unaffected by these parity operations and thus there is no loss of generality in focusing on just one octant. The effective Hamiltonian obtained from both these approaches is the same in the positive octant. We will point out these subtleties at appropriate places as we go along.

### 4.3.1 ‘A’ quantization without inverse triad corrections

The effective Hamiltonian obtained in the reference [175] for the ‘A’ quantization of Bianchi-IX model for general triad orientations is given by (lapse  $N = 1$ ):

$$\begin{aligned} \mathcal{H} = & -\frac{\sqrt{|p_1 p_2 p_3|}}{8\pi G \gamma^2 \lambda^2} \left[ (\text{sgn}(p_1) \text{sgn}(p_2) \sin(\bar{\mu}_1 c_1) \sin(\bar{\mu}_2 c_2) + \text{cyclic}) + l_o \lambda \left( \text{sgn}(p_3) \sqrt{\frac{|p_1 p_2|}{|p_3|^3}} \sin(\bar{\mu}_3 c_3) \right. \right. \\ & \left. \left. + \text{cyclic} \right) + \frac{l_o^2 \lambda^2 (1 + \gamma^2)}{4|p_1 p_2 p_3|} \left( 2p_1^2 + 2p_2^2 + 2p_3^2 - \frac{p_1^2 p_2^2}{p_3^2} - \frac{p_2^2 p_3^2}{p_1^2} - \frac{p_3^2 p_1^2}{p_2^2} \right) \right] + \rho \sqrt{|p_1 p_2 p_3|}. \quad (4.17) \end{aligned}$$

The equations of motion for triads are:

$$\dot{p}_1 = \frac{p_1}{\gamma \lambda} \left( \text{sgn}(p_2) \sin(\bar{\mu}_2 c_2) + \text{sgn}(p_3) \sin(\bar{\mu}_3 c_3) + l_o \lambda \frac{\sqrt{|p_2 p_3|}}{|p_1|^{3/2}} \right) \cos(\bar{\mu}_1 c_1), \quad (4.18)$$

$$\dot{p}_2 = \frac{p_2}{\gamma \lambda} \left( \text{sgn}(p_3) \sin(\bar{\mu}_3 c_3) + \text{sgn}(p_1) \sin(\bar{\mu}_1 c_1) + l_o \lambda \frac{\sqrt{|p_3 p_1|}}{|p_2|^{3/2}} \right) \cos(\bar{\mu}_2 c_2), \quad (4.19)$$

$$\dot{p}_3 = \frac{p_3}{\gamma \lambda} \left( \text{sgn}(p_1) \sin(\bar{\mu}_1 c_1) + \text{sgn}(p_2) \sin(\bar{\mu}_2 c_2) + l_o \lambda \frac{\sqrt{|p_1 p_2|}}{|p_3|^{3/2}} \right) \cos(\bar{\mu}_3 c_3). \quad (4.20)$$

Here  $\lambda^2 = \Delta = 4\sqrt{3}\pi\gamma l_{\text{pl}}^2$ , as we have used in previous chapters, denotes minimum area eigenvalue from the underlying quantum geometry, and

$$\bar{\mu}_1 = \lambda \sqrt{\frac{|p_1|}{|p_2 p_3|}}, \quad \bar{\mu}_2 = \lambda \sqrt{\frac{|p_2|}{|p_1 p_3|}}, \quad \bar{\mu}_3 = \lambda \sqrt{\frac{|p_3|}{|p_1 p_2|}}. \quad (4.21)$$

Let us consider the eq. (4.18), which we can formally integrate as:

$$\int_{p_1^0}^{p_1(t)} \frac{dp_1}{p_1} = \int_{t_0}^t \frac{1}{\gamma \lambda} \left( \text{sgn}(p_2) \sin(\bar{\mu}_2 c_2) + \text{sgn}(p_3) \sin(\bar{\mu}_3 c_3) + l_o \lambda \frac{\sqrt{|p_2 p_3|}}{|p_1|^{3/2}} \right) \cos(\bar{\mu}_1 c_1) dt. \quad (4.22)$$

It yields,

$$p_1(t) = p_1^0 \exp \left\{ \int_{t_0}^t \frac{1}{\gamma \lambda} \left( \text{sgn}(p_2) \sin(\bar{\mu}_2 c_2) + \text{sgn}(p_3) \sin(\bar{\mu}_3 c_3) + l_o \lambda \frac{\sqrt{|p_2 p_3|}}{|p_1|^{3/2}} \right) \cos(\bar{\mu}_1 c_1) dt \right\}. \quad (4.23)$$

Similarly, we can obtain the expressions for  $p_2$  and  $p_3$  as:

$$p_2(t) = p_2^0 \exp \left\{ \int_{t_0}^t \frac{dt}{\gamma\lambda} \left( \text{sgn}(p_3) \sin(\bar{\mu}_3 c_3) + \text{sgn}(p_1) \sin(\bar{\mu}_1 c_1) + l_o \lambda \frac{\sqrt{|p_3 p_1|}}{|p_2|^{3/2}} \right) \cos(\bar{\mu}_2 c_2) \right\}, \quad (4.24)$$

$$p_3(t) = p_3^0 \exp \left\{ \int_{t_0}^t \frac{dt}{\gamma\lambda} \left( \text{sgn}(p_1) \sin(\bar{\mu}_1 c_1) + \text{sgn}(p_2) \sin(\bar{\mu}_2 c_2) + l_o \lambda \frac{\sqrt{|p_1 p_2|}}{|p_3|^{3/2}} \right) \cos(\bar{\mu}_3 c_3) \right\}. \quad (4.25)$$

It can be seen that singularities are not necessarily avoided by these dynamical equations. For example, the above equations seem to allow a situation when one of the triads, say  $p_1$ , approaches zero while  $p_2$  and  $p_3$  remain finite. Or, the scenario where all three of the triads vanish simultaneously. Analytically it is not obvious that above scenarios for singularities can be excluded dynamically by the equations of motion.

The expressions for the Hubble rates, the expansion and shear scalars, and the time derivative of the expansion scalar remain the same in the effective dynamics as in the classical case. They are given by eqs. (4.13), (4.14), (4.16) and (4.15) respectively. We note that all these quantities can diverge in the ‘A’ quantization without inverse triad corrections as one or more of the triad variables can vanish in a finite time evolution.

In the following analysis, it is convenient to restrict to the positive octant in a similar way as we did in Bianchi-II case above. The first way to work with the positive octant is to take the approach in Refs. [173] and [174] where one chooses the basis states of the kinematical Hilbert space to be reflection-symmetric in the triad space. Since the states are symmetric at the quantum level, we can thus restrict ourselves to the positive octant while obtaining the effective Hamiltonian [173, 174]. Moreover, we can choose our initial conditions such that the triads start out in the positive octant in our analysis at the effective level. The equations (4.23), (4.24) and (4.25) indicate that the triads will remain in the same octant where they started out initially until a singularity is reached and one of the triads vanishes, where the equations of motion break down.

Alternatively, the restriction to an octant can be justified merely on the basis of factor ordering while quantizing the Hamiltonian constraint, without requiring the quantum states to be symmetric. In this regard, one can take the path followed in Ref. [185, 186] where a different factor ordering of the quantum Hamiltonian constraint is employed so that the different octants are decoupled. This allows us to restrict the triads in the positive octant in our analysis and gives the same effective Hamiltonian in the positive octant. However, in this approach, the state corresponding to vanishing volume is also decoupled from all the octants. Note that we found above from the behavior of triads at the effective level, that it is possible for one or more triads to vanish in a finite-time evolution starting from the positive octant. This behavior of effective dynamics indicates a limitation of the effective dynamics. The effective Hamiltonian is indifferent to different factor orderings at the quantum level and hence does not know about the effect of decoupling of zero volume state. This limitation is tied to the derivation of the effective Hamiltonian which assumes that volumes are greater than the Planck volume [200].

In the rest of this chapter, we assume that one of the above two choices is applied so that we can focus ourselves on the positive octant in the triad space. Further, let us consider that the initial values of the triads  $p_i^o$  are positive definite. Then the expression of the energy density from the vanishing of the effective Hamiltonian constraint is given by:

$$\begin{aligned} \rho = & \frac{1}{8\pi G\gamma^2\lambda^2} \left[ \sin(\bar{\mu}_1 c_1) \sin(\bar{\mu}_2 c_2) + \text{cyclic} \right] + l_o \lambda \left( \sqrt{\frac{p_1 p_2}{p_3^3}} \sin(\bar{\mu}_3 c_3) + \text{cyclic terms} \right) \\ & + \frac{l_o^2 \lambda^2 (1 + \gamma^2)}{4p_1 p_2 p_3} \left( 2p_1^2 + 2p_2^2 + 2p_3^2 - \frac{p_1^2 p_2^2}{p_3^2} - \frac{p_2^2 p_3^2}{p_1^2} - \frac{p_3^2 p_1^2}{p_2^2} \right). \end{aligned} \quad (4.26)$$

It has been shown in Ref. [215] that the above energy density is not bounded above. Moreover, unlike the Bianchi-II case, imposing the weak energy condition on the energy density does not prevent any of the triads from vanishing in a finite time evolution. Thus, in contrast to the Bianchi-II case, there is no way the above energy density can be bounded in a generic evolution.

The expression for the Hubble rates can be evaluated using equations (4.13). The directional Hubble rate  $H_1$  is given by,

$$H_1 = \frac{1}{2\gamma\lambda}(\sin(\bar{\mu}_1 c_1 - \bar{\mu}_2 c_2) + \sin(\bar{\mu}_1 c_1 - \bar{\mu}_3 c_3) + \sin(\bar{\mu}_2 c_2 + \bar{\mu}_3 c_3)) \\ + \frac{l_o}{2\gamma} \left( \frac{\sqrt{p_1 p_2}}{p_3^{3/2}} \cos(\bar{\mu}_3 c_3) + \frac{\sqrt{p_3 p_1}}{p_2^{3/2}} \cos(\bar{\mu}_2 c_2) - \frac{\sqrt{p_2 p_3}}{p_1^{3/2}} \cos(\bar{\mu}_1 c_1) \right). \quad (4.27)$$

Similarly, the directional Hubble rates  $H_2$  and  $H_3$  can be obtained by cyclic permutations of the above equation. We note that the directional Hubble rates can diverge if any of the triad variables diverges or vanishes. This, through equations (4.14) and (4.16), produces divergences in expansion and shear scalars as well.

In a similar way, the expressions for the curvature scalars such as the Ricci scalar, the Kretschmann scalar and the square of the Weyl tensor can be shown to diverge as one or more triads vanish or diverge. Hence, we find that the ‘A’ quantization without inverse triad corrections is inadequate for the resolution of singularities. Unlike the case of ‘A’ quantization in Bianchi-II spacetime, even imposing WEC is not sufficient to prevent the singularities. This implies that it is essential to at least include inverse triad corrections if one hopes to resolve the classical singularities. Indeed, as we will see in the next subsection that including inverse triad corrections helps us obtain the crucial result that none of the triads vanish or diverge in a finite time evolution. This result is crucial to prove generic resolution of singularities.

### 4.3.2 ‘A’ quantization with inverse triad corrections

The effective Hamiltonian (4.17) in previous subsection includes the holonomy corrections but ignores the inverse-triad corrections. The inverse triad corrections in the case of lapse  $N = V$  have been obtained in [215]. We use the same procedure as in Ref. [215] to obtain the inverse triad corrections for the case of lapse  $N = 1$ , which is similar to what we did in Bianchi-II case, except that here we will need to include the inverse triad corrections for all three triads as all



of them appear in the denominator in the Hamiltonian. Let us note that the eigenvalues of the inverse triad operator  $\widehat{|p_1|^{-1/4}}$  are given as follows (see discussion in chapter 2):

$$\widehat{|p_1|^{-1/4}}|p_1 p_2 p_3\rangle = g_1(p_1)|p_1 p_2 p_3\rangle, \quad (4.28)$$

where

$$g_1(p_1) = \frac{(p_2 p_3)^{1/4}}{\sqrt{2\pi\gamma\lambda l_{\text{pl}}^2}} (\sqrt{|v+1|} - \sqrt{|v-1|}); \quad v = \frac{\sqrt{p_1 p_2 p_3}}{2\pi\gamma\lambda l_{\text{pl}}^2}. \quad (4.29)$$

Similarly, we can obtain inverse triad corrections for the inverse powers of  $p_2$  and  $p_3$  which will involve the corresponding functions  $g_2$  and  $g_3$ . Using these expressions, the effective Hamiltonian with inverse triad corrections for the  $N = 1$  case is obtained as follows:

$$\begin{aligned} \mathcal{H} = & -\frac{\sqrt{p_1 p_2 p_3}}{8\pi G \gamma^2 \lambda^2} \left[ (\sin(\bar{\mu}_1 c_1) \sin(\bar{\mu}_2 c_2) + \text{cyclic}) + l_o \lambda \left( \sqrt{\frac{p_1 p_2}{p_3}} g_3^4 \sin(\bar{\mu}_3 c_3) + \text{cyclic} \right) \right. \\ & \left. + \frac{l_o^2 \lambda^2 (1 + \gamma^2) (g_1 g_2 g_3)^2}{4\sqrt{p_1 p_2 p_3}} \left( 2p_1^2 - p_1^2 p_2^2 g_3^8 + \text{cyclic} \right) \right] + \rho \sqrt{p_1 p_2 p_3}. \end{aligned} \quad (4.30)$$

The resulting equations of motion for triads are:

$$\dot{p}_1 = \frac{p_1}{\gamma\lambda} \left( \sin(\bar{\mu}_2 c_2) + \sin(\bar{\mu}_3 c_3) + l_o \lambda \sqrt{\frac{p_2 p_3}{p_1}} g_1^4 \right) \cos(\bar{\mu}_1 c_1), \quad (4.31)$$

$$\dot{p}_2 = \frac{p_2}{\gamma\lambda} \left( \sin(\bar{\mu}_3 c_3) + \sin(\bar{\mu}_1 c_1) + l_o \lambda \sqrt{\frac{p_3 p_1}{p_2}} g_2^4 \right) \cos(\bar{\mu}_2 c_2), \quad \text{and}, \quad (4.32)$$

$$\dot{p}_3 = \frac{p_3}{\gamma\lambda} \left( \sin(\bar{\mu}_1 c_1) + \sin(\bar{\mu}_2 c_2) + l_o \lambda \sqrt{\frac{p_1 p_2}{p_3}} g_3^4 \right) \cos(\bar{\mu}_3 c_3). \quad (4.33)$$

We can formally integrate these equations to understand the form of the solution. For example, let  $p_1$  starts with some positive-definite value  $p_1^o$  at some initial time  $t_o$ . Then from (4.31) we can write,

$$\begin{aligned} p_1(t) = & p_1^o \exp \left\{ \frac{1}{\gamma\lambda} \int_{t_o}^t (\sin(\bar{\mu}_2 c_2) + \sin(\bar{\mu}_3 c_3)) \cos(\bar{\mu}_1 c_1) dt \right\} \\ & \times \exp \left\{ \int_{t_o}^t \left( \frac{l_o}{\gamma} \sqrt{\frac{p_2 p_3}{p_1}} g_1^4 \right) \cos(\bar{\mu}_1 c_1) dt \right\}. \end{aligned} \quad (4.34)$$

The corresponding equations for  $p_2$  and  $p_3$  are obtained by cyclic permutations. The directional scale factors are related kinematically to the triad variables through equations of the form (4.7). We are interested to see whether the time evolution of the triads leads them to either vanish or diverge in a finite time evolution. In Table 4.1 we list all the different possibilities for the evolution of the triad variables for all finite values of time  $t$  and label the different possibilities from A1 to A10.

	Finite & non-zero	Vanishing	Diverging	Remarks
A1	3	0	0	All the triads remain finite and non-zero
A2	0	3	0	All the triads vanish
A3	0	0	3	All the triads diverge
A4	1	1	1	One triad vanishes while one of them diverges
A5	2	1	0	Two triads are finite and non-zero while the third vanishes
A6	2	0	1	Two triads are finite and non-zero while the third diverges
A7	1	2	0	Two triads vanish while the third remains finite and non-zero
A8	0	2	1	Two triads vanish while the third diverges
A9	1	0	2	Two triads diverge while the third remains finite and non-zero
A10	0	1	2	Two triads diverge while the third vanishes

Table 4.1: Different possible fates for the triad variables upon evolution.

We will show now in the rest of this subsection that the properties of the functions  $g_1, g_2$  and  $g_3$  defined through (4.29) are such that the triads  $p_i$  remain non-zero, positive and finite for all finite time evolution. That is, except the possibility A1, no other case is possible. We will break down the analysis into three different limits:

(i) *The limit of vanishing volume:* In this case,  $v$  tends to zero and the case A1, A3, A6 and A9 are automatically ruled out. We now show that no other cases are possible either. In this

limit, it can be seen from (4.29) that the functions  $g_i$  take the form:

$$g_1 = \sqrt{\beta}(p_2 p_3)^{1/4} \left( v - \frac{v^3}{8} + \dots \right), \quad (4.35)$$

$$g_2 = \sqrt{\beta}(p_3 p_1)^{1/4} \left( v - \frac{v^3}{8} + \dots \right), \quad (4.36)$$

$$g_3 = \sqrt{\beta}(p_1 p_2)^{1/4} \left( v - \frac{v^3}{8} + \dots \right). \quad (4.37)$$

$$(4.38)$$

where we have defined for convenience,  $\beta = 1/(2\pi\gamma\lambda l_{\text{pl}}^2)$ . Since  $v$  is vanishing, the terms in the parentheses in RHS of the above equations are all tending to zero. Then equations of motion for triads become,

$$\begin{aligned} p_1(t) &= p_1^0 \exp \left\{ \frac{1}{\gamma\lambda} \int_{t_0}^t (\sin(\bar{\mu}_2 c_2) + \sin(\bar{\mu}_3 c_3)) \cos(\bar{\mu}_1 c_1) dt \right\} \\ &\quad \times \exp \left\{ \frac{l_o \beta^6}{\gamma} \int_{t_0}^t p_1^{3/2} (p_2 p_3)^{7/2} \left( 1 - \frac{v^2}{8} + \dots \right)^4 \cos(\bar{\mu}_1 c_1) dt \right\}, \end{aligned} \quad (4.39)$$

$$\begin{aligned} p_2(t) &= p_2^0 \exp \left\{ \frac{1}{\gamma\lambda} \int_{t_0}^t (\sin(\bar{\mu}_3 c_3) + \sin(\bar{\mu}_1 c_1)) \cos(\bar{\mu}_2 c_2) dt \right\} \\ &\quad \times \exp \left\{ \frac{l_o \beta^6}{\gamma} \int_{t_0}^t p_2^{3/2} (p_3 p_1)^{7/2} \left( 1 - \frac{v^2}{8} + \dots \right)^4 \cos(\bar{\mu}_2 c_2) dt \right\}, \text{ and} \end{aligned} \quad (4.40)$$

$$\begin{aligned} p_3(t) &= p_3^0 \exp \left\{ \frac{1}{\gamma\lambda} \int_{t_0}^t (\sin(\bar{\mu}_1 c_1) + \sin(\bar{\mu}_2 c_2)) \cos(\bar{\mu}_3 c_3) dt \right\} \\ &\quad \times \exp \left\{ \frac{l_o \beta^6}{\gamma} \int_{t_0}^t p_3^{3/2} (p_1 p_2)^{7/2} \left( 1 - \frac{v^2}{8} + \dots \right)^4 \cos(\bar{\mu}_3 c_3) dt \right\}. \end{aligned} \quad (4.41)$$

Let us note that in eq. (4.39), the terms in the first line on RHS are bounded for all finite time because the integrand in the exponential is a bounded function. In the limit of vanishing  $v$ , all the terms in the integrand in the second exponential are bounded except for the factor  $p_1^{3/2}(p_2 p_3)^{7/2}$ . We thus find that in order for  $p_1$  to either vanish or diverge in a finite time, the factor  $p_1^{3/2}(p_2 p_3)^{7/2}$  in the exponential must diverge. Similarly for  $p_2$  and  $p_3$  to either vanish or diverge, the corresponding factors in their expressions, given respectively by  $p_2^{3/2}(p_3 p_1)^{7/2}$  and  $p_3^{3/2}(p_1 p_2)^{7/2}$  must diverge. Using this we can easily see that none of the remaining possibilities

from Table 4.1 are consistent with the equations of motion of triads in the case of vanishing volume. For example, the case A2 corresponds to all vanishing triads. But from the argument in the above paragraph, for  $p_1$  to vanish in finite time,  $p_1^{3/2}(p_2p_3)^{7/2}$  must diverge in finite time. Similarly, for  $p_2$  and  $p_3$  to vanish,  $p_2^{3/2}(p_3p_1)^{7/2}$  and  $p_3^{3/2}(p_1p_2)^{7/2}$  must diverge respectively. We thus reach an inconsistency, and the case A2 is not physically possible. Similarly, A4, A5, A7 and A8 choices in Table I are also ruled out. Thus, none of the cases in Table I allow a vanishing volume consistent with the equations of motion.

(ii) *The diverging volume limit:* In this case,  $v$  tends to infinity and the cases A1, A2, A5 and A7 in Table I are automatically ruled out. In this limit, the expressions for  $g_i$  become:

$$g_1 = \frac{1}{p_1^{1/4}} \left( 1 - \frac{1}{8v^2} + \dots \right), \quad (4.42)$$

$$g_2 = \frac{1}{p_2^{1/4}} \left( 1 - \frac{1}{8v^2} + \dots \right), \quad \text{and} \quad (4.43)$$

$$g_3 = \frac{1}{p_3^{1/4}} \left( 1 - \frac{1}{8v^2} + \dots \right). \quad (4.44)$$

In the above equations, the terms in the parentheses on the RHS do not pose any problem as they remain finite in this limit. The expressions for the equations of motion for triads become:

$$p_1(t) = p_1^0 \exp \left\{ \frac{1}{\gamma\lambda} \int_{t_0}^t (\sin(\bar{\mu}_2 c_2) + \sin(\bar{\mu}_3 c_3)) \cos(\bar{\mu}_1 c_1) dt \right\} \\ \times \exp \left\{ \int_{t_0}^t \left( \frac{l_o}{\gamma} \sqrt{\frac{p_2 p_3}{p_1^3}} \left( 1 - \frac{1}{8v^2} + \dots \right)^4 \right) \cos(\bar{\mu}_1 c_1) dt \right\}, \quad (4.45)$$

$$p_2(t) = p_1^0 \exp \left\{ \frac{1}{\gamma\lambda} \int_{t_0}^t (\sin(\bar{\mu}_3 c_3) + \sin(\bar{\mu}_1 c_1)) \cos(\bar{\mu}_2 c_2) dt \right\} \\ \times \exp \left\{ \int_{t_0}^t \left( \frac{l_o}{\gamma} \sqrt{\frac{p_3 p_1}{p_2^3}} \left( 1 - \frac{1}{8v^2} + \dots \right)^4 \right) \cos(\bar{\mu}_2 c_2) dt \right\}, \quad \text{and} \quad (4.46)$$

$$p_3(t) = p_1^0 \exp \left\{ \frac{1}{\gamma\lambda} \int_{t_0}^t (\sin(\bar{\mu}_1 c_1) + \sin(\bar{\mu}_2 c_2)) \cos(\bar{\mu}_3 c_3) dt \right\} \\ \times \exp \left\{ \int_{t_0}^t \left( \frac{l_o}{\gamma} \sqrt{\frac{p_1 p_2}{p_3^3}} \left( 1 - \frac{1}{8v^2} + \dots \right)^4 \right) \cos(\bar{\mu}_3 c_3) dt \right\}. \quad (4.47)$$

Note that in eq. (4.45), the factor  $p_2 p_3 / p_1^3$  needs to diverge in order for  $p_1$  to either vanish or diverge. In case of  $p_2$  and  $p_3$  we need the corresponding factors, given respectively by  $p_3 p_1 / p_2^3$  and  $p_1 p_2 / p_3^3$ , to diverge for them to either vanish or diverge. In case of options A4, A6 and A8, one of the triads is diverging (say  $p_1$ ) while the other two remain finite. Since the other two are finite, then the factor  $p_2 p_3 / p_1^3$  can not be diverging. Hence,  $p_1$  cannot be diverging according to eq. (4.45). Similar arguments hold for  $p_2$  and  $p_3$ . Thus, cases A4, A6 and A8 are also inconsistent in this limit. In case A3, all three of the triads diverge. For that to happen according to the above equations of motion we need the factors  $p_2 p_3 / p_1^3$ ,  $p_3 p_1 / p_2^3$  and  $p_1 p_2 / p_3^3$  to diverge simultaneously which is self contradictory. Similarly, we can show that A9 and A10 are also inconsistent with the equations of motion in this limit. We are thus left with no viable case in Table I which allows a diverging volume.

(iii) *Volume remains finite and non-zero*: In this case, options A2, A3, A5, A6, A7 and A9 in Table I are inconsistent. In this case, directly from (4.29) we get:

$$g_1(p_1) = \beta^{1/2} (p_2 p_3)^{1/4} (\sqrt{|v+1|} - \sqrt{|v-1|}), \quad (4.48)$$

and similarly for  $g_2$  and  $g_3$ , where the terms in parentheses in RHS remain finite since  $v$  is finite.

Then, the Hamilton's equations for triads become:

$$p_1(t) = p_1^0 \exp \left\{ \frac{1}{\gamma \lambda} \int_{t_0}^t (\sin(\bar{\mu}_2 c_2) + \sin(\bar{\mu}_3 c_3)) \cos(\bar{\mu}_1 c_1) dt \right\} \\ \times \exp \left\{ \int_{t_0}^t \left( \frac{l_o \beta^2}{\gamma} \sqrt{\frac{(p_2 p_3)^3}{p_1}} (\sqrt{|v+1|} - \sqrt{|v-1|})^4 \right) \cos(\bar{\mu}_1 c_1) dt \right\}, \quad (4.49)$$

$$p_2(t) = p_2^0 \exp \left\{ \frac{1}{\gamma \lambda} \int_{t_0}^t (\sin(\bar{\mu}_3 c_3) + \sin(\bar{\mu}_1 c_1)) \cos(\bar{\mu}_2 c_2) dt \right\} \\ \times \exp \left\{ \int_{t_0}^t \left( \frac{l_o \beta^2}{\gamma} \sqrt{\frac{(p_3 p_1)^3}{p_2}} (\sqrt{|v+1|} - \sqrt{|v-1|})^4 \right) \cos(\bar{\mu}_2 c_2) dt \right\}, \quad (4.50)$$

$$p_3(t) = p_3^0 \exp \left\{ \frac{1}{\gamma \lambda} \int_{t_0}^t (\sin(\bar{\mu}_1 c_1) + \sin(\bar{\mu}_2 c_2)) \cos(\bar{\mu}_3 c_3) dt \right\} \quad \text{and} \quad , \\ \times \exp \left\{ \int_{t_0}^t \left( \frac{l_o \beta^2}{\gamma} \sqrt{\frac{(p_1 p_2)^3}{p_3}} (\sqrt{|v+1|} - \sqrt{|v-1|})^4 \right) \cos(\bar{\mu}_3 c_3) dt \right\}. \quad (4.51)$$

Let us consider the remaining options in Table I. In options A4 and A8, only one of the triads diverges (say  $p_1$ ). For this to happen, we must have the product  $p_2 p_3$  diverging according to eq. (4.49). But this is inconsistent with respect to eqs.(4.50) and (4.51). Hence, A4 and A8 are ruled out as well. In option A10, one of the triad is vanishing (say  $p_1$ ) while the other two are diverging simultaneously. Since the volume is supposed to be finite and non-zero, that means  $p_1 p_2 p_3$  is finite and non-zero. Since  $p_2$  and  $p_3$  are diverging, this means that the products  $p_1 p_2$  and  $p_1 p_3$  are vanishing. But for  $p_2$  and  $p_3$  to diverge according to above equations, we need the products  $p_1 p_2$  and  $p_1 p_3$  to diverge. Hence, A10 is also ruled out. Therefore, we are left with only option A1, which means all the three triads remain finite and non-zero for all finite time.

In summary, we find that out of all possible choices the only physically consistent case is when all the triads remain finite and non-zero for all finite time evolution. Note that this is tied to the inclusion of the inverse triad corrections for the 'A' quantization, and this result does not arise without the inverse triad corrections.

Let us now consider the energy density in this case. Using the vanishing of the Hamiltonian constraint, it turns out to be

$$\begin{aligned} \rho = & \frac{1}{8\pi G\gamma^2\lambda^2} \left[ (\sin(\bar{\mu}_1 c_1) \sin(\bar{\mu}_2 c_2) + \text{cyclic}) + l_o \lambda \left( \sqrt{\frac{p_1 p_2}{p_3}} g_3^2 \sin(\bar{\mu}_3 c_3) + \text{cyclic} \right) \right. \\ & \left. + \frac{l_o^2 \lambda^2 (1 + \gamma^2) (g_1 g_2 g_3)^2}{4\sqrt{p_1 p_2 p_3}} \left( 2p_1^2 - p_1^2 p_2^2 g_3^8 + \text{cyclic} \right) \right]. \end{aligned} \quad (4.52)$$

Since the triads are non-zero and finite in a finite time evolution, consequently the energy density also remains finite.

The Hubble rates can be evaluated using equations (4.13). The directional Hubble rate  $H_1$  is given by,

$$\begin{aligned} H_1 = & \frac{1}{2\gamma\lambda} (\sin(\bar{\mu}_1 c_1 - \bar{\mu}_2 c_2) + \sin(\bar{\mu}_1 c_1 - \bar{\mu}_3 c_3) + \sin(\bar{\mu}_2 c_2 + \bar{\mu}_3 c_3)) \\ & + \frac{l_o}{2\gamma} \left( \sqrt{\frac{p_1 p_2}{p_3}} g_3^4 \cos(\bar{\mu}_3 c_3) + \sqrt{\frac{p_3 p_1}{p_2}} g_2^4 \cos(\bar{\mu}_2 c_2) - \sqrt{\frac{p_2 p_3}{p_1}} g_1^4 \cos(\bar{\mu}_1 c_1) \right). \end{aligned} \quad (4.53)$$

We can obtain  $H_2$  and  $H_3$  by cyclic permutations of the above equation. We note that the Hubble rates are also bounded and finite as the triads remain bounded and finite for all finite time evolution. This implies that the expansion and shear scalars, given by equations (4.14) and (4.16), will also be bounded and finite by virtue of directional Hubble rates being finite for all finite time evolution.

We would also like to mention that the above exercise can be repeated for lapse  $N = V$  including inverse triad corrections and the results on boundedness of the triad variables, the energy density and the Hubble rates in any finite time evolution can be obtained. The effective Hamiltonian including inverse triad corrections for  $N = V$  case has been obtained in [215] and is given by:

$$\begin{aligned} \mathcal{H} = & -\frac{p_1 p_2 p_3}{8\pi G\gamma^2\lambda^2} \left[ (\sin(\bar{\mu}_1 c_1) \sin(\bar{\mu}_2 c_2) + \text{cyclic}) + l_o \lambda \left( \frac{\sqrt{p_1 p_2}}{p_3} g_3^2 \sin(\bar{\mu}_3 c_3) + \text{cyclic} \right) \right. \\ & \left. + \frac{l_o^2 \lambda^2 (1 + \gamma^2)}{4p_1 p_2 p_3} \left( 2p_1^2 - p_1^2 p_2^2 g_3^8 + \text{cyclic} \right) \right] + \rho \sqrt{p_1 p_2 p_3}. \end{aligned} \quad (4.54)$$

This effective Hamiltonian leads to the following evolution equations for the triad variables in terms of proper time along matter world lines:

$$\frac{dp_1}{d\tau} \equiv \dot{p}_1 = \frac{p_1}{\gamma\lambda} \left( \sin(\bar{\mu}_2 c_2) + \sin(\bar{\mu}_3 c_3) + l_o \lambda \frac{\sqrt{p_2 p_3}}{p_1} g_1^2 \right) \cos(\bar{\mu}_1 c_1). \quad (4.55)$$

The equations for  $\dot{p}_2$  and  $\dot{p}_3$  can be obtained by cyclic permutations of the above equation. The equations of motion are slightly different from the  $N = 1$  case now. However, using this set of equations and the properties of the functions  $g_i(p_1, p_2, p_3)$ , we can again rule out all the possibilities from the Table 4.1 except A1 by following an analysis analogous to the  $N = 1$  case given above. This yields the results on boundedness of the triads, the energy density, the Hubble rates, the expansion and shear scalars in all finite time evolution in this case as well even though the equations of motion differ slightly from the  $N = 1$  case. Thus changing the lapse changes the details of the dynamics slightly, but the results on boundedness behavior of quantities are unaffected.

In conclusion, we find that in contrast to results in previous subsection, when we include the inverse triad corrections in the ‘A’ quantization, then the energy density, the Hubble rates, and expansion and shear scalars all remain finite for all finite time evolution. However, we still need to consider the curvature invariants and the time derivative of the expansion scalar to analyze their divergence properties. We will consider them in section 4.5 and show that they can still diverge. But let us first discuss the ‘K’ quantization in the next section.

#### 4.4 Effective loop quantum cosmological dynamics: ‘K’ quantization

Inspired from our results on the relative ease of ‘K’ quantization over ‘A’ quantization in the previous chapter in the case of Bianchi-II model, we consider here the effective dynamics of the ‘K’ quantization in case of Bianchi-IX model, the effective Hamiltonian for which has already



been obtained in [176]. The effective Hamiltonian for lapse  $N = 1$  is given by:

$$\begin{aligned} \mathcal{H} = & -\frac{\sqrt{p_1 p_2 p_3}}{8\pi G \gamma^2} \left[ \frac{1}{\lambda^2} (\sin(\bar{\mu}_1 \gamma k_1) \sin(\bar{\mu}_2 \gamma k_2) + \sin(\bar{\mu}_2 \gamma k_2) \sin(\bar{\mu}_3 \gamma k_3) + \sin(\bar{\mu}_3 \gamma k_3) \sin(\bar{\mu}_1 \gamma k_1)) \right. \\ & \left. + \frac{l_o^2}{4p_1 p_2 p_3} \left( 2p_1^2 + 2p_2^2 + 2p_3^2 - \frac{p_1^2 p_2^2}{p_3^2} - \frac{p_2^2 p_3^2}{p_1^2} - \frac{p_3^2 p_1^2}{p_2^2} \right) \right] + \rho \sqrt{p_1 p_2 p_3} . \end{aligned} \quad (4.56)$$

Using eq. (4.21), the resulting Hamilton's equations for  $p_1$  and  $k_1$  are:

$$\begin{aligned} \dot{p}_1 &= -8\pi G \frac{\partial \mathcal{H}}{\partial k_1} = \frac{p_1}{\gamma \lambda} (\sin(\bar{\mu}_2 \gamma k_2) + \sin(\bar{\mu}_3 \gamma k_3)) \cos(\bar{\mu}_1 \gamma k_1), \\ \dot{k}_1 &= 8\pi G \frac{\partial \mathcal{H}}{\partial p_1} \\ &= -\frac{\lambda}{2\gamma^2} \frac{1}{\bar{\mu}_1} \left[ \frac{1}{\lambda^2} (\sin(\bar{\mu}_1 \gamma k_1) \sin(\bar{\mu}_2 \gamma k_2) + \sin(\bar{\mu}_2 \gamma k_2) \sin(\bar{\mu}_3 \gamma k_3) + \sin(\bar{\mu}_3 \gamma k_3) \sin(\bar{\mu}_1 \gamma k_1)) \right. \\ &\quad + \frac{l_o^2}{4p_1 p_2 p_3} \left( 6p_1^2 - 2p_2^2 - 2p_3^2 - 3\frac{p_1^2 p_2^2}{p_3^2} + 5\frac{p_2^2 p_3^2}{p_1^2} - 3\frac{p_3^2 p_1^2}{p_2^2} \right) - 8\pi G \gamma^2 (\rho + 2p_1 \frac{\partial \rho}{\partial p_1}) \\ &\quad + \frac{\gamma}{\lambda^2} \left( k_1 \bar{\mu}_1 \cos(\bar{\mu}_1 \gamma k_1) (\sin(\bar{\mu}_2 \gamma k_2) + \sin(\bar{\mu}_3 \gamma k_3)) \right. \\ &\quad \left. \left. - k_2 \bar{\mu}_2 \cos(\bar{\mu}_2 \gamma k_2) (\sin(\bar{\mu}_1 \gamma k_1) + \sin(\bar{\mu}_3 \gamma k_3)) - k_3 \bar{\mu}_3 \cos(\bar{\mu}_3 \gamma k_3) (\sin(\bar{\mu}_2 \gamma k_2) + \sin(\bar{\mu}_1 \gamma k_1)) \right) \right]. \end{aligned} \quad (4.58)$$

Equations for other phase variables can be found from above by cyclic permutations. Thus we see that the quantities  $\dot{p}_i/p_i$  are generically bounded which imply that the Hubble rates given by (4.13), the expansion scalar (4.14) and the shear scalar (4.16) are also generically bounded for all time. Following an analysis similar to the previous chapter, we can show that the triads remain non-zero and finite for any finite time evolution. Consider the equation for  $p_1$ . Let  $p_1^o$  be some initial non-zero and finite value. Then the integration of the corresponding equation of motion gives,

$$p_1(t) = p_1^o \exp \left\{ \frac{1}{\gamma \lambda} \int_{t_0}^t \left( (\sin(\bar{\mu}_2 \gamma k_2) + \sin(\bar{\mu}_3 \gamma k_3)) \cos(\bar{\mu}_1 \gamma k_1) \right) dt \right\}. \quad (4.59)$$

Since  $|(\sin(\bar{\mu}_2\gamma k_2) + \sin(\bar{\mu}_3\gamma k_3)) \cos(\bar{\mu}_1\gamma k_1)| \leq 2$ , the integral in the above equation is bounded over a finite time evolution, implying:

$$0 < p_1(t) < \infty. \quad (4.60)$$

Analogously, we can show bounds on both  $p_2$  and  $p_3$ . Hence, we conclude that for any finite time evolution:

$$0 < p_i(t) < \infty \quad \text{and} \quad 0 < \frac{1}{p_i(t)} < \infty. \quad (4.61)$$

This in turn ensures that the energy density, obtained from vanishing of the Hamiltonian constraint (4.56):

$$\begin{aligned} \rho = & \frac{1}{8\pi G\gamma^2} \left[ \frac{1}{\lambda^2} (\sin(\bar{\mu}_1\gamma k_1) \sin(\bar{\mu}_2\gamma k_2) + \sin(\bar{\mu}_2\gamma k_2) \sin(\bar{\mu}_3\gamma k_3) + \sin(\bar{\mu}_3\gamma k_3) \sin(\bar{\mu}_1\gamma k_1)) \right. \\ & \left. + \frac{l_o^2}{4p_1p_2p_3} \left( 2p_1^2 + 2p_2^2 + 2p_3^2 - \frac{p_1^2p_2^2}{p_3^2} - \frac{p_2^2p_3^2}{p_1^2} - \frac{p_3^2p_1^2}{p_2^2} \right) \right]. \end{aligned} \quad (4.62)$$

is also non-zero and finite for all finite time evolution due to equation (4.61). Thus, the ‘K’ quantization leads us on the path to singularity resolution without having to include inverse triad corrections. This is in contrast to the ‘A’ quantization where inverse triad modifications are needed. We proceed in the next section to show that some curvature invariants may still diverge, those that depend on  $\ddot{p}_i$  and higher time derivatives.

## 4.5 Possible divergences in curvature invariants

In previous sections we showed that the energy density, expansion and shear scalars and Hubble rates remain finite and the volume remains non-zero and finite in the effective dynamics of LQC in both the ‘A’ quantization with inverse triad corrections, and the ‘K’ quantization. However, just like the isotropic and Bianchi-II cases, we will find in this section that the curvature invariants can still diverge. We will show that the curvature invariants and  $\dot{\theta}$  depend on partial derivatives of the energy density with respect to the triad variables, which depend on the matter content. Since we are keeping the matter content arbitrary, these derivatives may diverge for

some choices of matter. And if they do, they can cause the curvature invariants to diverge. As we discussed in section 4.3 and 4.4, it can be shown that the ratios  $\dot{p}_i/p_i$  remain bounded and that the triads  $p_i$  remain positive definite and finite for all finite time evolution for both the ‘A’ quantization with inverse triad corrections, and for the ‘K’ quantization. But, we also need to consider the divergence properties of the second derivatives,  $\ddot{p}_i$ , as the curvature invariants and  $\dot{\theta}$  depend on them as well. It is clear from the expressions for  $\dot{p}_i$  as given in previous sections that the second derivatives  $\ddot{p}_i$  will contain first time derivatives of the connection variables,  $\dot{c}_i$  or  $\dot{k}_i$ . These can be obtained from Hamilton’s equations, e.g. :

$$\dot{c}_i = 8\pi G\gamma \frac{\partial \mathcal{H}}{\partial p_i}. \quad (4.63)$$

We see that  $\dot{c}_i$  will have terms of type  $\partial\rho/\partial p_i$ . Hence,  $\ddot{p}_i$  and eventually the curvature invariants depend on the partial derivatives of the energy density with respect to the triad variables  $\partial\rho/\partial p_i$ . If  $\partial\rho/\partial p_i$  diverge at finite values of volume, energy density, and expansion and shear scalar for some specific choice of matter, then the curvature invariants will diverge.

As an illustration, let us consider the ‘K’ quantization discussed in previous section. The second derivative of  $p_1$  is given by,

$$\begin{aligned} \frac{\ddot{p}_1}{p_1} = & \left( \frac{\dot{p}_1}{p_1} \right)^2 + \frac{\cos(\bar{\mu}_1\gamma k_1)}{\lambda} \left( \cos(\bar{\mu}_2\gamma k_2)(\dot{k}_2\bar{\mu}_2 + k_2\dot{\bar{\mu}}_2) + \cos(\bar{\mu}_3\gamma k_3)(\dot{k}_3\bar{\mu}_3 + k_3\dot{\bar{\mu}}_3) \right) \\ & - \frac{\sin(\bar{\mu}_1\gamma k_1)}{\lambda} (\sin(\bar{\mu}_2\gamma k_2) + \sin(\bar{\mu}_3\gamma k_3))(\dot{k}_1\bar{\mu}_1 + k_1\dot{\bar{\mu}}_1). \end{aligned} \quad (4.64)$$

We find that the terms which may lead to divergence are of the form  $(\dot{k}_1\bar{\mu}_1 + k_1\dot{\bar{\mu}}_1)$ , as all other terms and factors are well behaved for any finite time evolution from our conclusions in section 4.3.2 and section 4.4. Let us compute the term  $(\dot{k}_1\bar{\mu}_1 + k_1\dot{\bar{\mu}}_1)$  to analyze it in detail. It turns

out to be:

$$\begin{aligned}
\dot{k}_1\bar{\mu}_1 + k_1\dot{\bar{\mu}}_1 = & -\frac{\lambda}{2\gamma^2} \left[ \frac{1}{\lambda^2} (\sin(\bar{\mu}_1\gamma k_1) \sin(\bar{\mu}_2\gamma k_2) + \sin(\bar{\mu}_2\gamma k_2) \sin(\bar{\mu}_3\gamma k_3) + \sin(\bar{\mu}_3\gamma k_3) \sin(\bar{\mu}_1\gamma k_1)) \right. \\
& + \frac{l_o^2}{4p_1p_2p_3} \left( 6p_1^2 - 2p_2^2 - 2p_3^2 - 3\frac{p_1^2p_2^2}{p_3^2} + 5\frac{p_2^2p_3^2}{p_1^2} - 3\frac{p_3^2p_1^2}{p_2^2} \right) - 8\pi G\gamma^2 \left( \rho + 2p_1 \frac{\partial \rho}{\partial p_1} \right) \\
& + \frac{\gamma}{\lambda^2} \left( (k_1\bar{\mu}_1 - k_2\bar{\mu}_2) \cos(\bar{\mu}_2\gamma k_2) (\sin(\bar{\mu}_1\gamma k_1) + \sin(\bar{\mu}_3\gamma k_3)) \right. \\
& \left. \left. + (k_1\bar{\mu}_1 - k_3\bar{\mu}_3) \cos(\bar{\mu}_3\gamma k_3) (\sin(\bar{\mu}_2\gamma k_2) + \sin(\bar{\mu}_1\gamma k_1)) \right) \right]. \tag{4.65}
\end{aligned}$$

We see from the above equation that the divergence can arise only from  $\partial\rho/\partial p_1$  and quantities of type  $(k_1\bar{\mu}_1 - k_2\bar{\mu}_2)$ , since all the other quantities are either made of bounded sine and cosine functions or made of the triad variables which will be finite for finite time evolution as shown in section 4.4. We further note that,

$$k_1\bar{\mu}_1 - k_2\bar{\mu}_2 = \frac{\lambda}{V} (k_1p_1 - k_2p_2) \tag{4.66}$$

and that,

$$\frac{d}{dt}(k_1p_1 - k_2p_2) = \frac{l_o^2}{\gamma^2 V} \left( p_2^2 - p_1^2 + \frac{p_3^2p_1^2}{p_2^2} - \frac{p_2^2p_3^2}{p_1^2} \right) + 8\pi GV \left( p_1 \frac{\partial \rho}{\partial p_1} - p_2 \frac{\partial \rho}{\partial p_2} \right). \tag{4.67}$$

In the above equation, the first term is bounded. Hence, the quantity  $(k_1p_1 - k_2p_2)$  (and consequently  $k_1\bar{\mu}_1 - k_2\bar{\mu}_2$ ), which is the integration of the right hand side of (4.67), may only diverge if the partial derivatives of the energy density with respect to triads diverges.

Therefore, we conclude from our discussion of equations (4.64), (4.65) and (4.67), that the quantities of the form  $(\dot{k}_i\bar{\mu}_i - k_j\dot{\bar{\mu}}_j)$ , and consequently the second derivatives  $\ddot{p}_i/p_i$ , and hence the curvature invariants and  $\dot{\theta}$  will only diverge when the partial derivatives of the energy density with respect to triad variables diverge at a finite value of energy density. Such conditions require highly exotic equations of state of matter. Also note that in case of matter with vanishing anisotropic stress, the quantities  $\partial\rho/\partial p_i$  are proportional to the pressure. So we can call these divergences in the curvature invariants and  $\dot{\theta}$  as “pressure divergences”.

Above we focused on the ‘K’ quantization. However, one reaches the same conclusion by repeating this exercise for the second derivatives of triad variables in the ‘A’ quantization with inverse triad corrections. To summarize, we note that the curvature invariants or the time derivative of the expansion scalar may not be bounded in effective dynamics. Some quantities of interest may diverge both in ‘A’ and ‘K’ quantizations. However, as we will see in the next two sections, that geodesics do not break down at such events if such divergences occur at a finite time, and that these divergences do not amount to strong singularities. Therefore, such potential curvature divergences will turn out to be harmless events.

## 4.6 Geodesic completeness

Given a spacetime metric, the geodesic equations are given by:

$$(x^i)'' = \Gamma_{jk}^i (x^j)' (x^k)'. \quad (4.68)$$

where prime denotes derivative with respect to the affine parameter. These equations give us the accelerations along the geodesic curves in terms of the Christoffel symbols and the velocity four vector along the geodesic. We can integrate them to find out the expression for the velocities as follows,

$$(x^i)' = \int d\tau \left( \Gamma_{jk}^i (x^j)' (x^k)' \right). \quad (4.69)$$

Let us note that for comoving observers  $t$  itself is the affine parameter. The coefficients  $\Gamma_{jk}^i$  are obtained from first derivatives of the metric, hence cannot depend on the second time derivatives of the triads. They only depend on the triads and their first time derivatives and the angular variables in the Bianchi-IX metric. Using the relations between triads and scale factors, we can express them in terms of the scale factors and their first time derivatives. Using our results in previous sections, the triads and their first time derivatives (and hence the scale factors and their first time derivatives) remain finite for all finite values of time  $t$ , which is the affine parameter. Hence, the coefficients  $\Gamma_{jk}^i$  as functions of the affine parameter will be finite for any finite value of the affine parameter for both the ‘A’ quantization with inverse triad modifications, and ‘K’ quantization.

In the classical dynamics of Bianchi-IX spacetime, the cosmological singularity is encountered due to vanishing of one or more scale factors while the rest are either diverging or remain finite. There is an associated breakdown of geodesics as some of the terms in the expressions for the accelerations and velocities along the geodesics contain powers of the scale factors or their first derivatives as discussed above. To see this, we consider the Bianchi-IX metric in presence of local rotational symmetry which simplifies the Christoffel symbols considerably. The metric takes the following form:

$$ds^2 = -dt^2 + a_1^2 dx^2 + a_2^2 dy^2 + (a_2^2 \sin^2 y + a_1^2 \cos^2 y) dz^2 - 2a_1^2 (\cos y) dx dz. \quad (4.70)$$

For this metric, the geodesic equations can be simplified to the following form in this case:

$$x'' = -2\frac{a_1'}{a_1^3} - \frac{C}{a_2^2}(\cot y)y' - 2z' \cos y \left( \frac{a_2'}{a_2} + y' \cot y \right) - y' z' \sin y, \quad (4.71)$$

$$y'' = -2\frac{a_2'}{a_2} y' + z'^2 \cos y \sin y + \frac{C}{a_2^2} z' \sin y, \quad (4.72)$$

$$z'' = -2\frac{a_2'}{a_2} z' - 2y' z' \cot y - \frac{C}{a_2^2} y' \csc y, \quad (4.73)$$

where  $C$  is a constant. We see that these geodesics have the scale factors and their first derivatives as coefficients, and will break down at the classical cosmological singularity precisely because one or more of these coefficients diverge.

The geodesic evolution in effective dynamics of 'A' quantization with inverse triad effects, and 'K' quantization differs significantly from the classical theory in the evolution of the scale factors. In the effective dynamics in above cases, as we discussed in the previous paragraph, these scale factors and their first derivatives remain finite for any finite value of the affine parameter. The effective dynamics modifies the spacetime in such a way that as we approach the classical cosmological singularity, the scale factors, instead of vanishing or diverging, reach some finite limiting value and then bounce back. The singularity is replaced by a bounce such that the scale factors are well behaved. As a result, the classical cosmological singularity is absent in the effective spacetime.

We found in the previous section that some of the curvature invariants may diverge if the derivatives of the energy density with respect to triad variables diverge. However if such divergence in curvature invariants happens in a finite time evolution, then from the results of this section we know that the geodesics will not break down at such events as the Christoffel symbols remain finite for any finite time evolution, hence the velocities and accelerations along the geodesics will be well defined. This means that such divergences in curvature invariants, if they happen in a finite time, do not amount to the breakdown of geodesics.

In summary, for the case of ‘A’ quantization with inverse triad effects included, and the ‘K’ quantization, geodesics will be well-behaved in effective spacetime at all those events where they could break down classically due to divergences in scale factors and their first derivatives in finite time evolution. In this sense we can say that the Bianchi-IX spacetime is geodesically complete in the effective dynamics of LQC for the ‘A’ quantization with inverse triad effects and the ‘K’ quantization. In the case of ‘A’ quantization without the inclusion of inverse triad effects, scale factors can vanish and diverge in finite time and geodesic evolution will not be complete.

## 4.7 Lack of strong singularities

In the previous section we have shown that geodesics will go past the events where divergences occur in curvature invariants in finite time evolution for the ‘A’ quantization with inverse triad modifications and for the ‘K’ quantization. We now show that these divergences do not amount to a strong curvature singularity. The analysis in this section is similar to the analysis of strength of singularities in the Bianchi-II case carried out in previous chapter. The necessary condition for a strong singularity is that for a timelike or null geodesic running into the singularity, the integral given in equation (2.2), which is

$$K_j^i = \int_0^\tau d\tau' |R^i_{0j0}(\tau')| \quad (4.74)$$

must diverge as the singularity is approached. Otherwise the singularity is termed as a weak singularity.

We follow a strategy similar to the previous chapter. First we note that the affine parameter for geodesics of comoving observers is the coordinate time  $t$  itself. Next, the integral (4.74) involves one of the Riemann curvature tensor components. Let us investigate the behavior of Riemann curvature tensor to gain insight into this. The Riemann curvature tensor is obtained from second derivatives of the metric. The metric is a function of time through the triad variables, and is a function of other three angular variables in terms of their sines or cosines in the numerator. When we compute all possible second derivatives of the metric, all the derivatives with respect to the angle variables again result into sines and cosines of those variables in the numerator. Hence, the curvature tensors will be made of only the following three types of terms:

T1) Terms of type  $f(p_1, p_2, p_3)$ , obtained when both the derivatives were with respect to the angle variables. These terms may also contain sines and cosines of the angle variables in their numerators. These will be excluded from discussion as they are bounded in any finite time evolution.

T2) Terms of type  $\left(\frac{\dot{p}_1}{p_1}\right)^m \left(\frac{\dot{p}_2}{p_2}\right)^n \left(\frac{\dot{p}_3}{p_3}\right)^q f(p_1, p_2, p_3)$  where  $m, n, q$  are positive integers. These terms are obtained when either one or both of the derivatives is with respect to time.

T3) Terms of type  $\left(\frac{\ddot{p}_i}{p_i}\right) f(p_1, p_2, p_3)$ , where  $i$  can be 1, 2 or 3, obtained when both the derivatives are with respect to time.

The components of the curvature tensors are made of sums or differences of these three types of terms. Let us look at the behavior of each type of term under the integral (4.74).

Since we have shown that all the triad variables are bounded for any finite evolution, and we see from (4.57) that  $\dot{p}_i/p_i$  is a bounded function, terms of type (T1) and (T2) are finite for finite time evolution. Since they themselves are bounded, they give a finite quantity when integrated over a finite interval. On the other hand, terms of type T3 contain the quantities  $\ddot{p}_i/p_i$  which may lead to divergences. However, upon integration in (4.74), these second derivatives of the



triads are removed as follows:

$$\int_0^{t_o} \frac{\ddot{p}_i}{p_i} f(p_1, p_2, p_3) dt = \frac{\dot{p}_i}{p_i} f(p_1, p_2, p_3) \Big|_0^{t_o} - \int_0^{t_o} \dot{p}_i \left( \frac{d}{dt} f_1(p_1, p_2, p_3) \right) dt. \quad (4.75)$$

We see that both the terms on the RHS are finite, hence the terms of type (T3) also do not lead to divergence upon integration over a finite interval.

Since these terms (T1), (T2) and (T3) individually do not lead to divergence upon integration over a finite interval, we can conclude that the integral (4.74) will also remain finite because the integral of the absolute value of a sum of terms is less than equal to the sum of integrals of individual terms:

$$\int_a^b |T_1 + T_2 + \dots + T_n| dt \leq \int_a^b |T_1| dt + \int_a^b |T_2| dt + \dots + \int_a^b |T_n| dt. \quad (4.76)$$

We have hence shown that the necessary conditions for existence of strong singularities are not satisfied in the Bianchi-IX model in effective dynamics of LQC for the ‘A’ quantization with inverse triad corrections and for the ‘K’ quantization. This means that any singularities, if present, are of weak curvature type. We have already shown in the previous section that geodesics can be extended beyond such events. Hence, these singularities turn out to be harmless.

## 4.8 Conclusion

In this chapter, we have generalized the work on generic singularity resolution in the effective dynamics of the FLRW model [214, 266], the Bianchi-I model [217] and Bianchi-II model of the previous chapter to the Bianchi-IX spacetime in the effective dynamics of LQC. This is a very encouraging result for generic singularity resolution in LQC as the Bianchi-IX spacetime is one of the most general homogeneous and anisotropic spacetime which is an important candidate for the description of the very early universe and also models the dynamics of a general spacetime in the approach to a singularity as per the BKL conjecture. In particular, the chaotic oscillatory dynamics described by the BKL conjecture in the approach to a generic singularity in GR is analogous to the Mixmaster dynamics of the approach to a singularity in the Bianchi-IX model.

Thus the result on singularity resolution in the effective Bianchi-IX model in this chapter is a strong indication for generic singularity resolution in LQC.

Specifically, we showed in this chapter that in the effective dynamics of the ‘A’ quantization with inverse triad corrections, and of the ‘K’ quantization even without needing inverse triad corrections, all the triads remain finite and non-zero for all finite time evolution which leads to expansion and shear scalars and Hubble rates being finite for any finite time evolution. The energy density also remains finite consequently for all finite time evolution. Analogous to the Bianchi-II case, both, the ‘A’ quantization with inverse triad corrections and the ‘K’ quantization, do not prevent the curvature invariants in Bianchi-IX case from diverging. However, just like Bianchi-II case, we further showed that geodesics are well behaved when such divergences occur and that such curvature divergent events turn out to be weak curvature singularities beyond which geodesics can be extended.

The contrast in the ‘A’ and ‘K’ quantization in the ease of singularity resolution observed in the loop quantized Bianchi-II model in the previous chapter is heightened in the loop quantized Bianchi-IX model. While in the loop quantized Bianchi-II model it was still possible to ignore inverse triad corrections in the ‘A’ quantization and obtain singularity resolution with the help of externally imposed energy conditions (namely WEC), this strategy is not sufficient in the ‘A’ quantization of the Bianchi-IX model. In contrast, the ‘K’ quantization leads to singularity resolution without needing inverse triad corrections or WEC in both cases. As we discussed at the end of the previous chapter, this shows the ‘K’ quantization to be more powerful and apt for singularity resolution and provides a motivation for considering the extrinsic curvature as the basis of quantization even in the full theory. Further, the results of this chapter show that, unlike GR, energy conditions are likely to be irrelevant in obtaining generic singularity resolution in LQC.

The classical Mixmaster dynamics of the Bianchi-IX spacetime in the approach to the singularity is characterized by a series of epochs resembling the Bianchi-I model (called Kasner phases in this context) mediated by Kasner transitions which can be modeled as a bounce from a potential [125]. However, our result in this chapter shows that any such singularity which is ap-

proached in the Mixmaster dynamics is resolved in the effective spacetime. Further exploration is needed how the Mixmaster dynamics is affected by the LQC bounce in Bianchi-IX model. It may be that the bounce occurs at such high curvatures and densities well into Planck regime that it is far from the classical Mixmaster epoch and leaves it unaffected. However, in this case, it will be interesting to investigate whether the bounce is followed by another Mixmaster epoch as the size of the universe grows and curvature decreases. On the other hand, if the bounce occurs at relatively large volumes that it is close enough to the Mixmaster epoch, quantum effects may modify the Mixmaster dynamics, or even lead to a cessation of the chaotic oscillations caused by multiple Kasner transitions in the classical dynamics. These are interesting questions to be explored in further investigations and are essential for a detailed understanding of quantum dynamics near generic singularities.

# Chapter 5

## Singularity Avoidance in Effective Loop Quantized Kantowski–Sachs Cosmology

### 5.1 Introduction

We have considered the resolution of cosmological singularities of effective loop quantized Bianchi-II and Bianchi-IX spacetimes in the past two chapters in the context of the BKL conjecture, and have succeeded in showing singularity resolution in the effective models for these spacetimes. Together with the results on singularity resolution in effective loop quantized isotropic [214, 266] and Bianchi-I models [217], this body of results tackles the problem of the initial cosmological singularity in solutions of GR and is of relevance to the initial state of our own universe. However, another type of singularity that is prominent in GR is the black hole singularity supposed to be found in astrophysical settings due to collapse of massive stars at the end of their life cycle. As we have noted before, the interior of the static black hole solution of GR, called the Schwarzschild spacetime, is isomorphic to the anisotropic and homogeneous Kantowski–Sachs spacetime in vacuum. Thus Kantowski–Sachs spacetime can be studied to gain some insights into the resolution of the black hole singularity. To this end, we will study the loop quantized Kantowski–Sachs spacetime in this and the next chapter. We focus in this chapter on the singularity resolution in the effective loop quantized Kantowski–Sachs spacetime without restricting it to the vacuum case, and will specialize to the vacuum case in the next chapter to draw conclusions about the resolution of the black hole singularity.

In the presence of arbitrary matter, the Kantowski–Sachs model is a cosmological model with both anisotropy and spatial curvature which has an initial and a final singularity, and hence allows us to further explore the contrast between the ‘A’ and ‘K’ quantizations as well as the necessity of inverse triad corrections in singularity resolution. Due to presence of both anisotropy and spatial curvature in the Kantowski–Sachs model, similar problems as in Bianchi-II and

---

This chapter is adapted from the contents of S. Saini and P. Singh, *Classical and Quantum Gravity*, 33(24), (2016), 245019 [268] with the permission of IOP Publishing Ltd. See Appendix A for the copyright permission from the publishers.

Bianchi-IX case are faced in obtaining an algebra of almost periodic functions by evaluating the holonomies of the connection around closed loops [178], hence open edges have to be considered for holonomies. Recall that in the spatially curved and anisotropic Bianchi-II and Bianchi-IX models of the previous chapters, inverse triad corrections were seen to emerge as essential in singularity resolution in the ‘A’ quantization. On the other hand, singularity resolution could be obtained in both Bianchi-II and Bianchi-IX models without needing inverse triad corrections in the extrinsic curvature based ‘K’ quantization. For the Kantowski–Sachs model, the analogues of both the ‘A’ quantization [180] and the ‘K’ quantization [178] have been obtained. In this regard, it is important to mention here that the symmetries of the Kantowski–Sachs spacetimes are such that the holonomies of the Ashtekar connection and those of the extrinsic curvature (when treated as a connection here in symmetry reduced model) along the straight edges are identical and thus lead to qualitatively similar quantizations [178]. Thus the sharp contrast between the ‘A’ and ‘K’ quantizations seen in Bianchi-II and Bianchi-IX models is not seen in case of Kantowski–Sachs model. Subsequent work on the Schwarzschild singularity using the Kantowski–Sachs model has mainly focused on improving the extrinsic curvature based quantization of [178] by exploiting quantization ambiguities based on how the area of the holonomy loops is calculated (similar to the ambiguity in the standard LQC quantization of the FLRW model leading to the choices of  $\mu_o$  and  $\bar{\mu}$  schemes as discussed in chapter 2). Note that the quantum Hamiltonian constraint of [178] does not include inverse triad corrections, and as we will show in this chapter working with a variant of this quantization, that singularity resolution can be obtained in the effective theory without needing inverse triad corrections.

The original work of [178] was similar to the  $\mu_o$  scheme of isotropic and homogeneous models where the edge lengths of the loop were considered to be constant. The effective description of this model was studied in [181, 269], and leads to dependence on fiducial parameters in the physical predictions. To overcome these problems, other quantizations where the edge lengths are functions of phase space variables have been studied [182, 221, 270, 271, 218, 222, 272]. However, imposing the physical requirements that the physical predictions must be independent of fiducial structures can be used to rule out various of the proposed quantizations. We find that

the Boehmer–Vandersloot quantization of [182], and the Corichi–Singh quantization of [183], both do not have fiducial cell dependence in their final results. However, as we mentioned above, the Kantowski–Sachs cosmology has both an initial and a final singularity. This is where one has to be careful with the correspondence with the Schwarzschild black hole interior. The final singularity in the Kantowski–Sachs cosmological model in the vacuum case will correspond to the surface of event horizon if the correspondence with the Schwarzschild interior is established. The Boehmer–Vandersloot quantization leads to the resolution of both the initial and the final singularity. Thus, it cannot be used as a viable quantization for the black hole interior case, as the resolution of the final singularity means the existence of unwanted quantum gravity effects at the event horizon which can even be at very low curvatures in higher mass black holes. This problem is addressed in the Corichi–Singh quantization [183] which is specifically tailored to the vacuum Kantowski–Sachs model when it is seen as the interior of a Schwarzschild black hole. However, the Corichi–Singh quantization cannot be considered for the Kantowski–Sachs cosmology when matter may also be present as it does not resolve the final singularity. Thus, we will work with the Boehmer–Vandersloot quantization, which in the case of Kantowski–Sachs cosmology in presence of matter is a unique quantization that gives fiducial structure independent predictions [218]. In this chapter, our reference to loop quantized Kantowski–Sachs model will imply Boehmer–Vandersloot prescription. Interestingly, a loop quantization of this spacetime, in absence of matter and also in presence of cosmological constant, results in a singularity resolution with a pre-bounce spacetime which is a product of two constant curvature spaces with an almost Planckian curvature [222]. An important result pertinent to our investigations is that the expansion and shear scalars in this quantization turn out to be universally bounded in the effective dynamics [268].

Our analysis assumes the validity of the effective dynamics in LQC at all scales. We will see in this chapter that the effective Kantowski–Sachs spacetime in Boehmer–Vandersloot quantization can be shown to be free from strong singularities without including the inverse triad corrections. Both the initial and final singularities are removed by the quantum gravity effects which prevent the triads and the physical volume from vanishing. There can still be some

pressure divergences in some curvature invariants such as the Ricci scalar, the Kretschmann scalar and the time derivative of the expansion scalar, however such divergences are harmless as the geodesics remain well behaved at such events and they do not lead to strong curvature singularities.

This chapter is organized in the following way. We review the classical dynamics of the Kantowski–Sachs model in terms of symmetry reduced Ashtekar variables in section 5.2. In the next section, we describe the dynamics of the effective Kantowski–Sachs spacetime in Boehmer–Vandersloot quantization. Using the effective equations of motion we restate the results on boundedness of the Hubble rates, the expansion scalar and the shear scalar obtained in [218]. We go further than previous investigations in this section to show that the triad variables remain non-zero and finite for finite time evolution, hence the spatial volume and the energy density also remain well behaved. We further show that some curvature invariants can still diverge in the effective dynamics. In section 5.4 we compute the geodesics and analyze their behavior in effective dynamics. We find that the geodesics remain well defined in the effective spacetime. Further, in section 5.5, we show that the effective spacetime is free from any strong curvature singularities, hence the above mentioned divergences in some curvature invariants turn out to be harmless. We conclude this chapter in the final section.

## 5.2 Classical dynamics of Kantowski–Sachs spacetime

This section outlines the classical dynamics of the Kantowski–Sachs spacetime in terms of Ashtekar variables. The Kantowski–Sachs spacetime can be foliated by homogeneous spatial slices of topology  $\mathbb{R} \times \mathbb{S}^2$ . The homogeneity of the spatial slices can be used to obtain a simple form for the Ashtekar variables as follows [178]:

$$A_a^i \tau_i dx^a = \tilde{c} \tau_3 dx + \tilde{b} \tau_2 d\theta - \tilde{b} \tau_1 \sin \theta d\phi + \tau_3 \cos \theta d\phi , \quad (5.1)$$

$$\tilde{E}_i^a \tau_i \partial_a = \tilde{p}_c \tau_3 \sin \theta \partial_x + \tilde{p}_b \tau_2 \sin \theta \partial_\theta - \tilde{p}_b \tau_1 \partial_\phi . \quad (5.2)$$

The spacetime line element can be expressed in terms of the symmetry reduced triads  $\tilde{p}_b$  and  $\tilde{p}_c$  as follows:

$$ds^2 = -N^2 dt^2 + g_{xx} dx^2 + g_{\Omega\Omega} (d\theta^2 + \sin^2 \theta d\phi^2). \quad (5.3)$$

where

$$g_{xx} = \frac{\tilde{p}_b^2}{\tilde{p}_c}, \quad \text{and} \quad g_{\Omega\Omega} = |\tilde{p}_c|. \quad (5.4)$$

The modulus sign arises due to two orientations of the triad. Since the matter considered in this analysis is non-fermionic, we can work with only symmetric wave functions which are eigenfunctions of the parity operator without any loss of generality. Thus, we can fix one orientation for the triads as changing the orientation leaves the wave functions invariant. In the following, the orientation of the triads is chosen to be positive without any loss of generality. Since the spatial slices are non-compact in  $x$ -direction, we restrict integrations along  $x$ -direction to a fiducial length  $L_o$  in order to define the symplectic structure. The Poisson brackets are:

$$\{\tilde{b}, \tilde{p}_b\} = G\gamma/L_o, \quad \{\tilde{c}, \tilde{p}_c\} = 2G\gamma/L_o. \quad (5.5)$$

We rescale the triad and the connection to make the symplectic structure independent of the fiducial parameter  $L_o$ :

$$p_b = L_o \tilde{p}_b, \quad p_c = \tilde{p}_c, \quad b = \tilde{b}, \quad c = L_o \tilde{c}. \quad (5.6)$$

The non-vanishing Poisson brackets between these new variables are given by,

$$\{b, p_b\} = G\gamma, \quad \{c, p_c\} = 2G\gamma. \quad (5.7)$$

Using these phase space variables, the classical Hamiltonian constraint can be written as (choosing lapse  $N = 1$ ):

$$\mathcal{H}_{\text{cl}} = -\frac{1}{2G\gamma^2} \left[ 2bc\sqrt{p_c} + (b^2 + \gamma^2) \frac{p_b}{\sqrt{p_c}} \right] + 4\pi p_b \sqrt{p_c} \rho, \quad (5.8)$$



Here  $\rho = \mathcal{H}_m/V$  is the energy density, and  $V = 4\pi p_b \sqrt{p_c}$  is the physical volume of the fiducial cell. The energy density on the constraint surface is given by the vanishing of the Hamiltonian constraint as follows,

$$\rho = \frac{1}{\kappa} \left( \frac{2bc}{\gamma^2 p_b} + \frac{b^2}{\gamma^2 p_c} + \frac{1}{p_c} \right). \quad (5.9)$$

We can see that the energy density diverges if the triad variables vanish or the connection variables diverge. This can happen at the cosmological singularity in the classical dynamics when the volume of the hypersurfaces vanishes. The time evolution of phase space variables is given by the equations of motion:

$$\dot{p}_b = -G\gamma \frac{\partial \mathcal{H}_{\text{cl}}}{\partial b} = \frac{1}{\gamma} \left( c\sqrt{p_c} + \frac{bp_b}{\sqrt{p_c}} \right), \quad (5.10)$$

$$\dot{p}_c = -2G\gamma \frac{\partial \mathcal{H}_{\text{cl}}}{\partial c} = \frac{1}{\gamma} 2b\sqrt{p_c}, \quad (5.11)$$

$$\dot{b} = G\gamma \frac{\partial \mathcal{H}_{\text{cl}}}{\partial p_b} = \frac{-1}{2\gamma\sqrt{p_c}} (b^2 + \gamma^2) + 4\pi G\gamma\sqrt{p_c} \left( \rho + p_b \frac{\partial \rho}{\partial p_b} \right), \quad (5.12)$$

$$\dot{c} = 2G\gamma \frac{\partial \mathcal{H}_{\text{cl}}}{\partial p_c} = \frac{-1}{\gamma\sqrt{p_c}} \left( bc - (b^2 + \gamma^2) \frac{p_b}{2p_c} \right) + 4\pi G\gamma \frac{p_b}{\sqrt{p_c}} \left( \rho + 2p_c \frac{\partial \rho}{\partial p_c} \right). \quad (5.13)$$

Let us consider the expressions of some curvature invariants. The expansion scalar  $\theta$  is given by

$$\theta = \frac{\dot{V}}{V} = \frac{\dot{p}_b}{p_b} + \frac{\dot{p}_c}{2p_c}. \quad (5.14)$$

and the shear scalar  $\sigma^2$  expressed in terms of the directional Hubble rates  $H_i = \dot{\sqrt{g_{ii}}}/\sqrt{g_{ii}}$  is given by

$$\sigma^2 = \frac{1}{2} \sum_{i=1}^3 \left( H_i - \frac{1}{3}\theta \right)^2 = \frac{1}{3} \left( \frac{\dot{p}_c}{p_c} - \frac{\dot{p}_b}{p_b} \right)^2. \quad (5.15)$$

The Hubble rates, the expansion and the shear scalars depend only on the triads and their first time derivatives. The time derivative of the expansion scalar is given by,

$$\dot{\theta} = \frac{\ddot{p}_b}{p_b} + \frac{\ddot{p}_c}{2p_c} - \left( \frac{\dot{p}_b}{p_b} \right)^2 - \frac{1}{2} \left( \frac{\dot{p}_c}{p_c} \right)^2, \quad (5.16)$$

which also depends on the accelerations  $\ddot{p}_i$ . Similarly, the components of the Riemann tensor,

the Ricci scalar, the Kretschmann scalar and any other curvature invariant obtained from the second derivatives of the metric will also depend on the accelerations  $\ddot{p}_i$ . As an example, the Kretschmann scalar is given as follows:

$$\begin{aligned}
K = & 6 \left( \frac{\dot{p}_b \dot{p}_c}{p_b p_c} \right)^2 - 8 \frac{\dot{p}_b \dot{p}_c \ddot{p}_b}{p_b p_c p_b} + 4 \left( \frac{\ddot{p}_b}{p_b} \right)^2 + 6 \frac{\ddot{p}_b}{p_b} \left( \frac{\dot{p}_c}{p_c} \right)^2 - 4 \frac{\ddot{p}_b \ddot{p}_c}{p_b p_c} \\
& - 8 \frac{\dot{p}_b}{p_b} \left( \frac{\dot{p}_c}{p_c} \right)^3 + 4 \frac{\dot{p}_b \dot{p}_c \ddot{p}_c}{p_b p_c p_c} + \frac{7}{2} \left( \frac{\dot{p}_c}{p_c} \right)^4 + 2 \left( \frac{\dot{p}_c}{p_c} \right)^2 \frac{1}{p_c} \\
& - 5 \left( \frac{\dot{p}_c}{p_c} \right)^2 \frac{\ddot{p}_c}{p_c} + \frac{4}{p_c^2} + 3 \left( \frac{\ddot{p}_c}{p_c} \right)^2.
\end{aligned} \tag{5.17}$$

It is evident that these curvature invariants diverge at the classical cosmological singularity where the triads vanish and the ratios  $\dot{p}_b/p_b$  and  $\dot{p}_c/p_c$  diverge. Other type of divergences could occur even if the triads and their first derivatives are finite if the matter content is such that the terms  $\partial\rho/\partial p_b$  or  $\partial\rho/\partial p_c$  diverge, as these can cause divergences in the connection variables and the second time derivatives of the triads. We will see in section 5.5 that the second type of divergences turn out to be weak singularities. However the cosmological singularity is a strong singularity, which will be resolved in the effective dynamics. We study the effective dynamics of the Kantowski–Sachs model in the next section.

### 5.3 Effective dynamics of the Kantowski–Sachs spacetime

As we discussed in the introduction, various quantizations have been proposed for the Kantowski–Sachs spacetime in the literature, some of them specifically suited to the vacuum Kantowski–Sachs spacetime when it is seen as the black hole interior. However, we are considering the Kantowski–Sachs cosmology with arbitrary minimally coupled matter in this chapter and will be considering the Boehmer–Vandersloot quantization which is free from fiducial cell dependence. The effective Hamiltonian constraint in this case is given by [182]:

$$\mathcal{H} = -\frac{p_b \sqrt{p_c}}{2G\gamma^2 \Delta} \left[ 2 \sin(b\delta_b) \sin(c\delta_c) + \sin^2(b\delta_b) + \frac{\gamma^2 \Delta}{p_c} \right] + 4\pi p_b \sqrt{p_c} \rho \tag{5.18}$$

where

$$\delta_b = \sqrt{\frac{\Delta}{p_c}}, \quad \delta_c = \frac{\sqrt{\Delta p_c}}{p_b}. \quad (5.19)$$

Let us first look at the effective equations of motion obtained for the triad and the connection variables. Using the above Hamiltonian, we obtain the following equations:

$$\dot{p}_b = \frac{p_b \cos(b\delta_b)}{\gamma\sqrt{\Delta}} (\sin(c\delta_c) + \sin(b\delta_b)), \quad (5.20)$$

$$\dot{p}_c = \frac{2p_c}{\gamma\sqrt{\Delta}} \sin(b\delta_b) \cos(c\delta_c), \quad (5.21)$$

$$\begin{aligned} \dot{b} = & -\frac{\sqrt{p_c}}{2\gamma\Delta} \left[ 2 \sin(b\delta_b) \sin(c\delta_c) + \sin^2(b\delta_b) + \frac{\gamma^2\Delta}{p_c} \right] \\ & + \frac{cp_c}{\gamma\sqrt{\Delta}p_b} \sin(b\delta_b) \cos(c\delta_c) + \frac{\kappa\gamma}{2} \sqrt{p_c} \left( \rho + p_b \frac{\partial \rho}{\partial p_b} \right) \end{aligned} \quad (5.22)$$

and

$$\begin{aligned} \dot{c} = & -\frac{p_b}{2\gamma\Delta\sqrt{p_c}} \left[ 2 \sin(b\delta_b) \sin(c\delta_c) + \sin^2(b\delta_b) + \frac{\gamma^2\Delta}{p_c} \right] \\ & - \frac{c}{\gamma\sqrt{\Delta}} \sin(b\delta_b) \cos(c\delta_c) + \frac{bp_b}{\gamma\sqrt{\Delta}p_c} \cos(b\delta_b) (\sin(c\delta_c) + \sin(b\delta_b)) \\ & + \frac{\gamma p_b}{\sqrt{p_c}} + \frac{\kappa\gamma}{2} \frac{p_b}{\sqrt{p_c}} \left( \rho + 2p_c \frac{\partial \rho}{\partial p_c} \right). \end{aligned} \quad (5.23)$$

Note that the ratios of the first derivatives  $\dot{p}_c/p_c$  and  $\dot{p}_b/p_b$  are now bounded which means the Hubble rates are bounded. It had been noted in [218] that unlike the classical dynamics, this means the expansion and shear scalars turn out to be bounded in this case. The expansion scalar is given by

$$\theta = \frac{1}{\gamma\sqrt{\Delta}} (\sin(b\delta_b) \cos(c\delta_c) + \cos(b\delta_b) \sin(c\delta_c) + \sin(b\delta_b) \cos(b\delta_b)), \quad (5.24)$$

and the shear scalar is,

$$\sigma^2 = \frac{1}{3\gamma^2\Delta} (2 \sin(b\delta_b) \cos(c\delta_c) - \cos(b\delta_b) (\sin(c\delta_c) + \sin(b\delta_b)))^2, \quad (5.25)$$

both of which are universally bounded in the effective dynamics due to quantum geometry effects incorporated in the effective dynamics.

We follow the strategy pursued in chapters 3 and 4, and show that the triads remain finite and non-zero in all finite time evolution. Suppose  $p_b$  and  $p_c$  have some non-zero finite initial values  $p_b^0$  and  $p_c^0$  at some initial time  $t_o$ . Then from (5.20), we get

$$p_b(t) = p_b^0 \exp \left\{ \frac{1}{\gamma \sqrt{\Delta}} \int_{t_o}^t \cos(b\delta_b) \left( \sin(c\delta_c) + \sin(b\delta_b) \right) dt \right\} . \quad (5.26)$$

Since  $|\cos(b\delta_b)(\sin(c\delta_c) + \sin(b\delta_b))|$  is bounded, the argument of the exponential remains finite for a finite time integration. Hence, we have:

$$0 < p_b(t) < \infty \quad (5.27)$$

for any finite time evolution. Similarly, using (5.21), we can show that

$$0 < p_c(t) < \infty \quad (5.28)$$

for any given finite time evolution. Hence the triads  $p_b$ ,  $p_c$  and the volume  $V = 4\pi p_b \sqrt{p_c}$  remain finite and non-zero for any finite time evolution. We can use this to further show that the energy density does not diverge in any finite time evolution. The energy density on the constraint surface is given by the vanishing of the Hamiltonian constraint:

$$\rho = \frac{1}{\kappa \gamma^2 \Delta} \left[ 2 \sin(b\delta_b) \sin(c\delta_c) + \sin^2(b\delta_b) + \frac{\gamma^2 \Delta}{p_c} \right] . \quad (5.29)$$

Hence the energy density remains finite by virtue of (5.28) and (5.27) for any finite proper time.

Note that these results are obtained in the effective dynamics of Kantowski–Sachs spacetime without the need for inverse triad corrections or WEC. This is in contrast with what happened in the effective dynamics of the Bianchi-II and Bianchi-IX model in the ‘A’ quantization as noted in previous chapters. As mentioned above, the holonomies of the Ashtekar connection

and the extrinsic curvature along straight edges are identical in Kantowski–Sachs model due to symmetries of the spacetime [178]. Thus the ‘A’ quantization of the Kantowski–Sachs model is analogous to the ‘K’ quantization considered in this chapter. And the ‘K’ quantization, as borne out by our analysis of the previous two chapters, can produce singularity resolution without requiring inverse triad modifications. Thus the intuition about the necessity of inverse triad corrections in the ‘A’ quantization in the presence of anisotropy and spatial curvature seems to be contradicted by the Kantowski–Sachs model. However, this is only due to special symmetries of the Kantowski–Sachs model and we would expect, based on the trend of the last two chapters, that inverse triad corrections will be needed in generic spacetime in the ‘A’ quantization when both anisotropy and spatial curvature are present and special symmetries of Kantowski–Sachs model are not available.

Analogous to the Bianchi-II and Bianchi-IX cases considered above, some curvature invariants can still diverge in the effective dynamics of the Kantowski–Sachs spacetime. These divergences come from the second time derivatives of the triads, on which the components of the Riemann tensor depend. A straightforward calculation yields:

$$\begin{aligned}
\ddot{p}_b = & p_b \left[ \frac{\cos(b\delta_b) \cos(c\delta_c)}{p_c} + \frac{\cos^2(b\delta_b)}{\gamma^2 \Delta} (\sin(b\delta_b) + \sin(c\delta_c))^2 \right. \\
& - \frac{4\pi}{\gamma^2 \sqrt{\Delta}} \frac{(cp_c - bp_b)}{V} \cos(c\delta_c) \left( \sin(c\delta_c) + \sin^3(b\delta_b) \right) \\
& \left. + \frac{\kappa}{2} \left( 2p_c \frac{\partial \rho}{\partial p_c} \cos(b\delta_b) \cos(c\delta_c) - p_b \frac{\partial \rho}{\partial p_b} \sin(b\delta_b) \sin(c\delta_c) + p_b \frac{\partial \rho}{\partial p_b} \cos(2b\delta_b) \right) \right]
\end{aligned} \tag{5.30}$$

and

$$\begin{aligned}
\ddot{p}_c = & p_c \left[ -2 \frac{\sin(b\delta_b) \sin(c\delta_c)}{p_c} + \frac{4 \sin^2(b\delta_b) \cos^2(c\delta_c)}{\gamma^2 \Delta} \right. \\
& + \frac{4\pi}{\gamma^2 \sqrt{\Delta}} \frac{(cp_c - bp_b)}{V} \sin(2b\delta_b) \left( 1 + \sin(b\delta_b) \sin(c\delta_c) \right) \\
& \left. + \kappa \left( p_b \frac{\partial \rho}{\partial p_b} \cos(b\delta_b) \cos(c\delta_c) - 2p_c \frac{\partial \rho}{\partial p_c} \sin(b\delta_b) \sin(c\delta_c) \right) \right].
\end{aligned} \tag{5.31}$$

The divergences in expressions above could arise from the factors  $(cp_c - bp_b)$  if the connection variables diverge, and/or from terms with  $\partial\rho/\partial p_b$  and  $\partial\rho/\partial p_c$ . Let us first consider the term  $(cp_c - bp_b)$ . The time derivative of  $(cp_c - bp_b)$  is given by

$$\frac{d}{dt}(cp_c - bp_b) = \frac{\gamma p_b}{\sqrt{p_c}} + G\gamma V \left( 2p_c \frac{\partial\rho}{\partial p_c} - p_b \frac{\partial\rho}{\partial p_b} \right).$$

In eq. (5.32), first term on the R.H.S is finite due to (5.27) and (5.28). The second term depends on the matter content and vanishes for matter with vanishing anisotropic stress. Integrating the right hand side, we see that the quantity  $(cp_c - bp_b)$  may diverge if the derivatives of the energy density with respect to triads diverge. Otherwise  $(cp_c - bp_b)$  will be finite at any finite past or future time. Hence, we conclude that the some curvature invariants may still diverge in the effective dynamics. The divergences come from the terms  $\partial\rho/\partial p_b$  and  $\partial\rho/\partial p_c$ . Since energy density is always finite for any finite time, this will only happen if we have matter with an equation of state which has divergent triad derivatives of energy density while energy density is finite. We refer to these divergences as pressure divergences because in the case of matter with vanishing anisotropic stress, the energy density is a function of the volume only and we have

$$p_b \frac{\partial\rho}{\partial p_b} = 2p_c \frac{\partial\rho}{\partial p_c} = -\rho - P, \quad (5.32)$$

where  $P = -\frac{\partial\mathcal{H}_{\text{matt}}}{\partial V}$  is the pressure. As we will explore in the proceeding sections, these divergences in curvature invariants can only lead to weak curvature singularities and all strong curvature singularities are absent in the effective dynamics.

## 5.4 Geodesics

We noted in the previous section that the curvature invariants are generically bounded in effective dynamics except for very specific type of pressure singularities. This means that there may be potential singularities in the effective spacetime description of Kantowski–Sachs spacetime. In this section we analyze the behavior of geodesics at such potential singularities in the effective dynamics.

For the metric of the Kantowski–Sachs spacetime (5.3), the geodesic equations yields the following second order equations:

$$(g_{xx}x')' = 0, \quad (g_{\Omega\Omega} \sin^2(\theta)\phi')' = 0, \quad (5.33)$$

$$(g_{\Omega\Omega}\theta')' = g_{\Omega\Omega} \sin \theta \cos \theta \phi'^2, \quad (5.34)$$

and

$$-2t't'' = g'_{xx}x'^2 + g'_{\Omega\Omega}(\theta'^2 + \sin^2 \theta \phi'^2) . \quad (5.35)$$

Here prime denotes derivative with respect to the affine parameter. Recall that the functions  $g_{xx}$  and  $g_{\Omega\Omega}$  are related to the triads  $p_b$  and  $p_c$  via eq.(5.4).

To find the solutions, we notice that one can rotate angular coordinates in such a way that initially when affine parameter  $\tau = 0$ ,  $\theta(0) = \pi/2$  and  $\theta'(0) = 0$ . Then  $\theta(\tau) = \pi/2$  for all  $\tau$  is a solution of the above  $\theta$  geodesic equation with these initial conditions. Due to the uniqueness of solutions of second order differential equations with given initial conditions, this is the unique solution. Therefore, we will assume that  $\theta = \pi/2$  hereafter. Using this result, the solutions to the remaining geodesic equations in  $x$ ,  $\phi$  and  $t$  are:

$$x' = \frac{C_x}{g_{xx}}, \quad \phi' = \frac{C_\phi}{g_{\Omega\Omega}} , \quad (5.36)$$

and

$$t'^2 = \epsilon + \frac{C_x^2}{g_{xx}} + \frac{C_\phi^2}{g_{\Omega\Omega}} . \quad (5.37)$$

Here  $C_x$  and  $C_\phi$  are constants of integration, and  $\epsilon = 1$  for timelike geodesics and  $\epsilon = 0$  for null geodesics. If we are considering the timelike geodesics of comoving observers, then  $t$  itself is the affine parameter, and is called the proper time in this case.

In classical GR, the geodesic equations break down if either  $g_{xx}$  or  $g_{\Omega\Omega}$ , which depend on the triads through expressions (5.4), vanishes at a finite value of the affine parameter. This is certainly the case for the classical cosmological singularity in the Kantowski–Sachs spacetime

which results in geodesic incompleteness. However in effective dynamics, both  $g_{xx}$  and  $g_{\Omega\Omega}$  remain finite and non-zero for all finite time evolution due to the bounds on the values of  $p_b$  and  $p_c$  given in (5.27) and (5.28). Hence the equations (5.36) represent a system of first order linear ODEs with bounded coefficients, which means that their solutions are maximally extendable. This implies that the geodesic evolution never breaks down in effective dynamics in loop quantized Kantowski–Sachs model. For any finite time evolution, effective spacetime is geodesically complete. This is a strong indication that the above mentioned pressure divergences in curvature invariants are harmless. We solidify this intuition in the next section where we show that there are no strong singularities in the effective Kantowski–Sachs spacetime.

## 5.5 Lack of strong singularities

For the analysis of strength of singularities, we use the criterion described in chapter 2. Recall that a strong singularity is defined as one which crushes all infalling objects to zero volume irrespective of their properties. The precise formulation of this is given in chapter 2 based on the works of Ellis and Schmidt [224], Tipler [229], Clarke and Krolak [230]. The necessary conditions provided by Krolak for a singularity to be a strong curvature singularity require that the integral,

$$K_j^i = \int_0^\tau d\tilde{\tau} |R^i_{0j0}(\tilde{\tau})|, \quad (5.38)$$

of the Riemann tensor components does not converge as the singularity is approached along a non-spacelike geodesic. That is, if there is a strong curvature singularity in the region, then for a non-spacelike geodesic running into the singularity the following necessary condition is satisfied:

$$\lim_{\tau \rightarrow \tau_o} K_j^i \rightarrow \infty \quad (5.39)$$

where  $\tau_o$  is the value of the affine parameter at which the singularity is located.

We have argued above that the Riemann tensor is obtained from the second derivative of the metric, hence contains the second time derivatives of the triads at most. For example, the



Riemann tensor components for the metric (5.3) for comoving observers are given by:

$$\begin{aligned} R_{212}^1 &= g_{xx} R_{121}^2 \\ &= \left( \frac{p_b^2}{L_o^2 p_c} \right) \left[ -\frac{3}{4} \left( \frac{\dot{p}_c}{p_c} \right)^2 - \left( \frac{\ddot{p}_b}{p_b} \right) + \left( \frac{\dot{p}_b}{p_b} \right) \left( \frac{\dot{p}_c}{p_c} \right) + \frac{1}{2} \left( \frac{\ddot{p}_c}{p_c} \right) \right], \end{aligned} \quad (5.40)$$

$$\begin{aligned} R_{441}^1 &= \sin^2 \theta R_{331}^1 = p_c \sin^2 \theta R_{131}^3 = p_c \sin^2 \theta R_{141}^4 \\ &= p_c \sin^2 \theta \left[ \frac{1}{4} \left( \frac{\dot{p}_c}{p_c} \right)^2 - \frac{1}{2} \left( \frac{\ddot{p}_c}{p_c} \right) \right], \end{aligned} \quad (5.41)$$

$$\begin{aligned} R_{442}^2 &= \sin^2 \theta R_{332}^2 = -\frac{p_c}{g_{xx}} R_{232}^3 = -\frac{p_c}{g_{xx}} R_{242}^4 \\ &= -p_c \sin^2 \theta \left[ \frac{1}{2} \left( \frac{\dot{p}_b}{p_b} \right) \left( \frac{\dot{p}_c}{p_c} \right) - \frac{1}{4} \left( \frac{\dot{p}_c}{p_c} \right)^2 \right], \end{aligned} \quad (5.42)$$

$$R_{443}^3 = -\sin^2 \theta R_{343}^4 = -\sin^2 \theta \left[ 1 + \frac{p_c}{4} \left( \frac{\dot{p}_c}{p_c} \right)^2 \right]. \quad (5.43)$$

Note that the factors of  $\sin^2 \theta$  can be ignored in this analysis, as we can always choose  $\theta = \pi/2$  along our geodesics as discussed in the previous section. Considering the timelike geodesics of the comoving observers, note that the affine parameter for the comoving observers is the coordinate time  $t$ . Now we use the familiar reasoning used in previous two chapters here. The Riemann tensor components are made up of sum of terms of the following types:

T1) Terms of type  $\left( \frac{\dot{p}_i}{p_i} \right) \left( \frac{\dot{p}_j}{p_j} \right) f(p_b, p_c)$  where  $i, j \in \{b, c\}$ .

T2) Terms of type  $\left( \frac{\ddot{p}_i}{p_i} \right) f(p_b, p_c)$ , where  $i \in \{b, c\}$ .

First note that the integral in (5.38) involves an integral of the absolute value of Riemann tensor components, and in turn each Riemann tensor component is a sum of several terms. Since the integral of the absolute value of a sum is always less than or equal to the integral of the sum of the absolute value of each term, for our purposes it would suffice to look individually at the integrals of the absolute value of each term separately. So we consider the different types of terms present in the Riemann tensor components mentioned above one by one.

We note that all the factors in terms of type (T1) are bounded for finite time evolution in the effective dynamics. Hence the integral (5.38) for terms of type (T1) does not diverge if the said singularity is reached in a finite proper time.

Now consider the terms of type (T2). These contain the second derivatives of the triads  $\ddot{p}_i/p_i$  which were shown to diverge in the effective dynamics due to pressure divergences. These are the potentially problematic events. However, upon integration in (5.38), these second derivatives of the triads are removed as follows:

$$\int_0^{t_o} \frac{\ddot{p}_i}{p_i} f(p_b, p_c) dt = \frac{\dot{p}_i}{p_i} f(p_b, p_c) \Big|_0^{t_o} - \int_0^{t_o} \dot{p}_i \left( \frac{d}{dt} f_1(p_b, p_c) \right) dt. \quad (5.44)$$

The derivative  $\frac{d}{dt} f_1(p_b, p_c)$  gives a factor of type (T1). So we see that the above integral does not diverge in integration over a finite interval as both the terms on the RHS are finite. Since both types of terms (T1) and (T2) individually do not lead to divergence upon integration over a finite interval, we can conclude that the integral (5.38) will also remain finite. Hence the necessary conditions for the existence of strong singularities are not satisfied in the effective Kantowski–Sachs spacetime. There can still be pressure divergences in the curvature invariants in finite time evolution, but we showed above that these divergences are harmless as geodesics remain well defined at these events and they do not lead to strong curvature singularities. All strong curvature singularities including the cosmological singularity are resolved in the loop quantized effective continuum spacetime (in the Boehmer–Vandersloot quantization).

## 5.6 Conclusions

Our goal in this chapter was to probe the issue of singularity resolution in effective Kantowski–Sachs spacetime with minimally coupled matter in LQC using the Boehmer–Vandersloot prescription. The choice of Boehmer–Vandersloot quantization is explained above, as this is a unique quantization of the Kantowski–Sachs model in the presence of matter which gives predictions independent of fiducial structures and also resolve both the initial and future singularity which are present when matter is included. This is in contrast to the Corichi–Singh quantization which is also fiducial structure independent, but is specifically tuned to the Schwarzschild interior

case, and does not resolve the future singularity. We further note that the Boehmer–Vandersloot quantization is an improved dynamics (i.e.  $\bar{\mu}$  scheme) inspired version of the extrinsic curvature based quantization of the work [178]. Further, due to the symmetries of the Kantowski–Sachs spacetime, the ‘A’ quantization in this case is qualitatively similar to the ‘K’ quantization [178], thus the qualitative conclusions obtained in the ‘K’ quantization are valid for the ‘A’ quantization (obtained in [180]) of Kantowski–Sachs model as well.

Previous investigations in this direction had shown that the expansion and shear scalars are generically bounded in the effective dynamics [218] and the cosmological singularity is shown to be replaced by a bounce using numerical methods [222]. It was shown using numerical techniques in these investigations that dynamical bounds exist on energy density in loop quantized Kantowski–Sachs model. In this chapter, we have provided analytical proof that the energy density remains dynamically bounded for any finite time evolution due to bounds on the triad variables themselves in the effective dynamics. This approach was needed to prove generic resolution of strong singularities. We showed that the volume of the spatial slices never vanishes or diverges in finite time evolution.

Even though some curvature invariants were found to contain certain pressure divergences, it was shown that the effective spacetime is geodesically complete and the geodesics remain well behaved at the said pressure divergences if they occur in any finite time evolution. Further, the necessary conditions for the existence of strong singularities (such as the classical cosmological singularity) are not satisfied in the effective dynamics obtained from loop quantization. Thus we conclude that the effective Kantowski–Sachs cosmology with arbitrary matter is free from strong singularities in the Boehmer–Vandersloot quantization. This extends the results on singularity resolution in the effective spacetimes of the isotropic, Bianchi-I, Bianchi-II and Bianchi-IX models. We emphasize that these results are obtained in the extrinsic curvature based quantization of Kantowski–Sachs cosmology without considering the inverse triad corrections or imposing the WEC. Due to the equivalence of the holonomies of the Ashtekar connection and the extrinsic curvature in Kantowski–Sachs model, these conclusions also hold for the ‘A’ quantization of the Kantowski–Sachs model. Thus, special symmetries of the Kantowski–Sachs model allow us to

ignore the inverse triad corrections even in ‘A’ quantization contrary to the intuition from the last two chapters. However, since such a scenario may only occur in the presence of special symmetries, we expect that inverse triad corrections will be indispensable for singularity resolution in the ‘A’ quantization in generic spacetimes as indicated by the analysis of the previous two chapters.

In the next chapter, we will focus on the vacuum Kantowski–Sachs model as the Schwarzschild interior. As we have already mentioned, the future singularity in the Kantowski–Sachs model in this case corresponds to the surface of the event horizon of the corresponding black hole. Since the event horizon of a large black hole can be at very low curvatures, quantum gravity modifications are not expected in general at the horizon. Thus the Boehmer–Vandersloot quantization of the present chapter is not viable in that case. We will work with the Corichi–Singh quantization [183] that is tuned to the black hole interior case and does not yield modifications at the event horizon, and also yields results independent of the fiducial structures.

# Chapter 6

## Symmetric Bounce in Effective Loop Quantized Black Hole Spacetimes

### 6.1 Introduction

In this chapter, we study the static black hole solution and assume that for the physics of singularity resolution, it is sufficient to consider the Schwarzschild interior region containing the singularity trapped by the event horizon. As discussed previously, the Schwarzschild interior is isomorphic to the vacuum Kantowski–Sachs spacetime. As we have mentioned in the previous chapter, the quantizations of the Kantowski–Sachs model are based on the primary work [178] and differ mainly in the choice of the edge lengths (denoted  $\delta_b$  and  $\delta_c$  in the previous chapter) along which the holonomies of the connection (or the extrinsic curvature) are constructed. In works [178, 180], the edge lengths have been taken to be constants on the phase space, similar to the approach in the  $\mu_o$  quantization of the FLRW model [123], and the corresponding effective dynamics was studied in [181, 269]. Even though the singularity is replaced by a bounce in this scenario, recent studies [183, 223] showed that the physical predictions in this case are dependent on the fiducial structure and large quantum corrections are also predicted in low curvature regime near the black hole horizon. A slightly different approach than [178, 180] is employed in [190] which also uses a  $\mu_o$  type approach and hence suffers from the same shortcomings. Considering these shortcomings and taking inspiration from the  $\bar{\mu}$  type improved dynamics scheme of the FLRW model [80], quantizations of the Kantowski–Sachs model involving the edge lengths as functions of phase space variables were considered [182, 221, 270, 271, 218, 222, 268] in which, instead of being constants, the edge lengths evolved along the phase space trajectories. Some of these introduced matter and were focused on studying singularity resolution in the Kantowski–Sachs cosmology. Although these quantizations resolved the problem of fiducial structure dependence in physical predictions, when applied to the Schwarzschild interior, they

---

This chapter is adapted from the contents of J. Olmedo, S. Saini and P. Singh, *Classical and Quantum Gravity*, 34(22), (2017), 225011 [273] with the permission of IOP Publishing Ltd. See Appendix A for the copyright permission from the publishers.

still suffered from the drawback of large quantum corrections at the horizon. The central singularity is also resolved in this approach. As we explained in the previous chapter, when seen from the point of view of Kantowski–Sachs cosmology in the presence of matter, the position of the horizon corresponds to a future cosmological singularity where energy density, expansion and shear scalars and curvature invariants diverge in the classical description, and the resolution of this singularity is desirable from the point of view of Kantowski–Sachs cosmology. However, in the vacuum Kantowski–Sachs model seen as the Schwarzschild interior, the horizon only corresponds to a coordinate singularity where the curvature invariants are regular except expansion and shear scalars which are ill-defined at the horizon. The quantization of the previous chapter is tuned to the case where matter is present, and is not able to distinguish the coordinate singularity in the vacuum case from a real singularity and leads to large quantum gravity effects at the horizon in order to cure the singular behavior of the expansion and shear scalars. For large mass black holes, the horizon could be at a very low curvature, thus the above mentioned large quantum effects at the horizon are undesirable when a correspondence with the Schwarzschild interior is established. Due to this reason, the  $\bar{\mu}$  type quantizations of the Kantowski–Sachs model such as the one used in previous chapter are not suited to be applied to the Schwarzschild interior problem.

As hinted in the previous chapter, a third approach to the quantization of the vacuum Kantowski–Sachs model specifically suited to the Schwarzschild interior has been devised, which can be thought of as an intermediate between  $\mu_o$  and  $\bar{\mu}$  type quantizations, and was first considered in the CS (Corichi–Singh) quantization [183], then in the OSS (Olmedo–Saini–Singh) quantization prescription [273] (on which this chapter is based) and recently in the AOS (Ashtekar–Olmedo–Singh) quantization prescription [223]. In this approach, the edge lengths  $\delta_b$  and  $\delta_c$  are functions of phase space variables which remain constant along any phase space trajectory, but may vary from one trajectory to another. In other words, they are the so called Dirac observables, i.e. functions of the phase space variables which commute with the Hamiltonian constraint. So they are not necessarily constant on the whole phase space, but remain invariant along a given phase space trajectory (Note that  $\delta_b$  and  $\delta_c$  are also Dirac observables in the  $\mu_o$

inspired quantizations but they are trivial Dirac observables which remain constant on the whole phase space). Both the shortcomings of the fiducial structure dependence and large quantum effects at horizon are resolved in these quantizations, while the central singularity is resolved and replaced by a bounce. The von-Neumann analysis of the CS quantization also establishes the agreement with classical GR in the low curvature limit [274]. We will focus on the OSS quantization prescription in this chapter, which is a modification of the CS quantization, and compare it with the AOS quantization prescription wherever possible.

The analysis of the effective dynamics of the CS quantization shows that the central singularity is replaced by a quantum bounce connecting the Schwarzschild interior trapped by the black hole event horizon to an anti-trapped region on the other side called a Schwarzschild white hole [183]. However, the bounce in the CS quantization is highly asymmetric and the mass of the white hole in general turns out to have a quartic dependence on the black hole mass. This is hardly surprising as the asymmetric nature of the bounce in anisotropic models is borne out by the results in other anisotropic models such as Bianchi-I model where the bounce leads to a Kasner transition in general [247], or the Kantowski–Sachs cosmology with matter in the Boehmer–Vandersloot quantization where the bounce leads to a product of constant curvature spaces mimicking the charged Nariai spacetime [222]. However, various phenomenological studies of black hole singularity resolution assume a symmetric bounce in the Schwarzschild interior. For instance, a symmetric bounce is assumed in the quantum gravitational regime in various phenomenological models of gravitational collapse (see e.g. [275, 276, 277]) and on black hole to white hole transition (see e.g. [278, 279, 280, 281, 282]). Thus a pertinent question is whether a symmetric bounce is possible in the loop quantized Schwarzschild interior. The main objective of our analysis in this chapter is to investigate whether a symmetric bounce is possible in the CS quantization, or with a slight modification of this quantization. This chapter is based on the OSS quantization prescription [273], where a symmetric bounce condition was obtained for the black hole interior and various quantization prescriptions satisfying this condition were obtained by modifying the CS scheme. We note that problems with both CS and OSS quantization prescription were discovered later- namely in the behavior of the curvature at bounce [223]. In the

CS case, the curvature at bounce decreases as we consider larger mass black holes, leading to a bounce at low curvatures in large mass black holes. This problem is overcome in the OSS scheme, but the OSS scheme does not lead to universal bounds on the curvature at the bounce. The AOS quantization prescription, which borrowed ideas from both the CS scheme and OSS scheme, resolves these problems by fixing the edge lengths using loops at the transition surface between the black hole and white hole regions. Universal bounds are obtained on the curvature at the bounce. Although the bounce is not exactly symmetric in the AOS quantization prescription, it becomes almost symmetric for black hole masses larger than few hundred Planck masses, and is indistinguishable from an exactly symmetric bounce for astrophysical mass black holes.

In this chapter we focus on the OSS scheme, which forms an important stepping stone for the AOS quantization prescription. To begin with, we note that the present model, described within either GR or the effective dynamics of LQC considered here, is characterized by a dynamics admitting solutions in closed form. In other words, this model is integrable (or explicitly solvable). But let us here recall that in general totally constrained theories, unfortunately, we lack an external absolute time such that a global and well-defined evolution can be constructed. Instead, the evolution is not absolute but relational. This means that one must choose a phase space function as time variable (and/or spatial coordinates in presence of spatial diffeomorphism constraints). In previous chapters, we have chosen the proper time as the time coordinate and have not specified which function of phase space variables it is. In principle, it could be a complicated function of the phase space variables. However, in the present chapter, since we can easily identify Dirac observables of the system, it allows us to make our choice of time as a function of phase space variables much more transparent. This idea of physical clocks has been discussed in the sense of evolving constants of the motion by Rovelli [283, 284]. There, one defines the evolution by means of parametrized observables: uniparametric families of Dirac observables providing the notion of time evolution. These ideas are of special interest in the context of the quantization of totally constrained theories, given the role played by Dirac observables in order to construct the physical Hilbert space [285, 286], like GR. In this context, further develop-



ments have been carried out in order to identify classical (partial) Dirac observables [109, 110] and various applications have been studied [287, 115, 288, 289].

With this in mind, the strategy that we will adopt in our analysis, as starting point, is to identify (weak) Dirac observables (constants of the motion on shell) and their conjugate momenta. This serves two purposes. On the one hand, to identify a condition for symmetric bounce in terms of geometrical clocks, and, on the other hand, to lead us to a reduced phase space description of the model. Reduced phase space description gives the evolution on the constraint surface by a reduced Hamiltonian free from constraints. Quantizing this constraint free version of the model is relatively easier and can be used to provide an alternative quantization of the model. A primary step in our analysis is to carry out a canonical transformation from the old Ashtekar–Barbero variables to the Dirac observables. We then proceed with the study of the dynamics. For the latter one can either choose a lapse function and then solve the equations of motion or, equivalently, one can implement a suitable gauge-fixing condition in this gauge system and solve the dynamics of the reduced Hamiltonian. In general, the conjugate variables to the weak Dirac observables provide a natural internal geometrical clock (or physical time), since they are usually well behaved monotonic functions on the phase space. We can then obtain the dynamical equations for the triad and connection variables as a function of our choice of time.

The symmetric bounce condition turns out to be an equation that needs to be satisfied by the edge lengths  $\delta_b$  and  $\delta_c$  and we show that this condition is not satisfied by the choice of edge lengths of the CS quantization. However, it is possible to generalize the CS choice using two parameters  $\alpha$  and  $\beta$  in order to accommodate the symmetric bounce condition. It is important to note here that the CS quantization, the Hamiltonian constraint is quantized by fixing a value of the black hole mass and the corresponding difference equation and its effective dynamics is obtained. In contrast, our analysis in this chapter is at the effective level and relies on assuming the validity of the effective dynamics. We consider three different choice of the parameters  $\alpha$  and  $\beta$  in this chapter that satisfy the symmetric bounce condition and study their dynamics using numerical simulations. Even though symmetric bounce is obtained for all three choices,

the study of the dynamics reveal important differences between the choices and a comparison with the CS and the AOS schemes is drawn. We discover from studying the properties of the Kretschmann scalar at the bounce that in the choice 1, curvature at the bounce can be very low for large mass black holes leading to large quantum effects at low curvatures. This is also one of the shortcomings of the CS quantization as pointed out in [223]. In choices 2 and 3, we do not have the problem of large quantum effects at low curvatures as the curvature remains Planckian at the bounce. However, unlike the AOS quantization prescription and various other LQC models where universal bounds on curvature invariants are obtained in the quantum dynamics, the curvature at the bounce in choices 2 and 3 depends on the mass in the large mass limit and can grow unboundedly as the mass increases. Nevertheless, our analysis in this chapter provides a method for obtaining an exactly symmetric bounce which can be applied to other LQC models where an asymmetric bounce is obtained.

Further we note that our approach to the black hole singularity is based on considering the correspondence of the Schwarzschild interior spacetime with the vacuum Kantowski–Sachs spacetime which leads to homogeneous spatial slices where the already developed techniques of LQC can be used. However, the black hole singularity has also been studied using spherically symmetric midi-superspace approach [128, 252, 191, 290, 291, 196, 197, 292, 293]. Unlike homogeneous models, the algebra of constraints is not a true Lie algebra which poses problems similar to the full theory in implementing the quantization program. In the above mentioned works, this issue has been overcome for the Schwarzschild spacetime by suitably modifying the Hamiltonian constraint and singularity resolution is obtained in the resulting quantization. Further, unlike the static black hole scenario considered in our approach, quantizations of collapsing dust shells have also been studied in the midi-superspace approach as a first step towards studying a dynamical collapse in quantum gravity [294, 295]. Recently, there has been progress in obtaining the effective Hamiltonian for the Schwarzschild spacetime directly from the full theory by symmetry reduction at the quantum level using semi-classical states [296]. Thus our approach is a conservative one studying only the static black hole scenario by exploiting its correspondence

with the vacuum Kantowski–Sachs model to gain insights into potential phenomenological aspects of the resolution of the central singularity.

This chapter is organized as follows. In Sec. 6.2 we begin with an outline of the classical Hamiltonian constraint in terms of symmetry-reduced connection and triad variables and after identifying two (weak) Dirac observables we rewrite the Hamiltonian constraint in terms of the latter. Then we perform a gauge fixing which identifies an internal clock. In Sec. 6.3 this exercise is repeated for the effective Hamiltonian constraint of the loop quantization of the Schwarzschild interior based on the analysis of Ref. [183]. The Dirac observables and the internal clock identified in the effective spacetime description yield the ones in the classical theory when the quantum discreteness vanishes. In Sec. 6.4 we identify the condition to obtain the symmetric bounce in the black hole to white hole transition. We show that this condition can not be satisfied for any real mass for CS quantization, but can be satisfied if modifications are made to the assignment of the minimum area of the loop over which holonomies are considered. Three such choices of modifications are considered, along with choice 0 corresponding to CS construction. These choices are parameterized through two parameters  $\alpha$  and  $\beta$  whose values can be fixed given the initial black hole mass. We then discuss numerical results from various choices which provide insights on the properties of the symmetric bounce obtain from each choice and compare it to the CS quantization and the AOS quantization prescription. We summarize our findings in Sec. 6.5.

## 6.2 Classical setting

In order to describe the interior of a black hole in real Ashtekar–Barbero variables we adopt the symmetry reduction of [178], such that the spatial slices are compatible with the Kantowski–Sachs symmetry group  $G = \mathbb{R} \times SO(3)$ .<sup>1</sup> However, there is a subtle difference from the treatment of Kantowski–Sachs cosmology considered in the previous chapter. As pointed out in the CS quantization [183], while the fiducial metric on the 2-spheres is considered to be a unit sphere

---

<sup>1</sup>There, the invariant connection and triad lead to a vanishing diffeomorphism constraint, while the Gauss constraint remains nontrivial. However, we impose this constraint by first identifying suitable phase space functions that commute with it, and either carrying out a canonical transformation that splits the phase space between gauge invariant and pure gauge variables or by introducing a gauge fixing [178].

in the treatments of Kantowski–Sachs cosmology, in order to establish the correspondence with the Schwarzschild interior, the fiducial metric must contain a length scale provided by the area of the horizon of the black hole being considered. Thus the area of the fiducial sphere turns out to be equal to the area of the horizon. The fiducial metric is taken to be:

$$ds_o^2 := dx^2 + r_o^2(d\theta^2 + \sin^2 \theta d\phi^2), \quad (6.1)$$

where  $4\pi r_o^2$  is given by the area of the horizon. The connection and the densitized triad take the form [183]:

$$A_a^i \tau_i dx^a = \bar{c} \tau_3 dx + \bar{b} r_o \tau_2 d\theta - \bar{b} r_o \tau_1 \sin \theta d\phi + \tau_3 \cos \theta d\phi, \quad (6.2)$$

and

$$E_i^a \tau^i \frac{\partial}{\partial x^a} = \bar{p}_c r_o^2 \tau_3 \sin \theta \frac{\partial}{\partial x} + \bar{p}_b r_o \tau_2 \sin \theta \frac{\partial}{\partial \theta} - \bar{p}_b r_o \tau_1 \frac{\partial}{\partial \phi}, \quad (6.3)$$

where  $x \in [0, L_o]$ ,  $\theta$  and  $\phi$  are the typical angular coordinates of the two-sphere of unit radius. Finally,  $r_o = 2GM$  (Schwarzschild radius), and  $(\bar{b}, \bar{p}_b)$  and  $(\bar{c}, \bar{p}_c)$  are the coordinates of the reduced phase space of this system.

The spacetime metric in terms of the triads is given by

$$ds^2 = -N^2 dt^2 + \frac{\bar{p}_b^2}{|\bar{p}_c|} dx^2 + |\bar{p}_c| r_o^2 (d\theta^2 + \sin^2 \theta d\phi^2). \quad (6.4)$$

We then choose the triad components  $\bar{p}_b$  and  $\bar{p}_c$  to be dimensionless, and such that  $\bar{p}_c$  is equal to unity at the horizon. The canonical Poisson brackets, respectively, are

$$\{\bar{c}, \bar{p}_c\} = \frac{2G\gamma}{L_o r_o^2}, \quad \{\bar{b}, \bar{p}_b\} = \frac{G\gamma}{L_o r_o^2}, \quad (6.5)$$

Now, we introduce the new set of phase space variables

$$c = L_o \bar{c}, \quad p_c = r_o^2 \bar{p}_c, \quad b = r_o \bar{b}, \quad p_b = r_o L_o \bar{p}_b, \quad (6.6)$$

such that the new Poisson brackets

$$\{c, p_c\} = 2G\gamma, \quad \{b, p_b\} = G\gamma, \quad (6.7)$$

are independent of  $r_o$  or  $L_o$ . However, the phase space variables now depend on the fiducial structure. The quantities invariant under fiducial rescaling are  $b$ ,  $\frac{c}{L_o}$ ,  $\frac{p_b}{L_o}$  and  $p_c$ .

One can show that the total Hamiltonian of the system is

$$H_{\text{class}} = \frac{1}{16\pi G} N C_{\text{class}}, \quad (6.8)$$

where  $C_{\text{class}}$  is the Hamiltonian constraint

$$C_{\text{class}} = -\frac{8\pi \text{sgn}(p_c)}{\gamma^2} \left( (b^2 + \gamma^2) \frac{p_b}{\sqrt{|p_c|}} + 2bc|p_c|^{1/2} \right). \quad (6.9)$$

Note that the diffeomorphism constraint identically vanishes due to the symmetry reduction.

### 6.2.1 Canonical transformation: Dirac observables

In this particular model, it is possible to identify a couple of phase space variables that weakly commute with the Hamiltonian constraint (weakly commuting here means that the Poisson bracket may not be zero on the whole phase space, but is zero on the constraint surface). They correspond to

$$o_1 = \frac{2}{\gamma^2} \frac{(\gamma^2 + b^2)p_b}{bL_o}, \quad \text{and} \quad o_2 = \frac{4c|p_c|}{\gamma^2 L_o}. \quad (6.10)$$

Note that  $o_1$  and  $o_2$  are independent of fiducial rescaling. Let us mention that, on shell, they are not independent from each other. Therefore, on shell, only one of them will correspond to a weak Dirac observable. In addition, we can introduce two conjugate momenta to these variables, namely

$$p_1 = -\frac{\gamma L_o}{4G} \log \left( 1 + \frac{b^2}{\gamma^2} \right), \quad \text{and} \quad p_2 = -\frac{\gamma L_o}{8G} \log \left| \frac{o_2 c}{L_o} \right|, \quad (6.11)$$

respectively. We have chosen to divide by  $L_o$  in the logarithm in  $p_2$  so that  $p_2$  will have a simple linear dependence on the fiducial length since the ratio  $c/L_o$  is invariant under fiducial rescaling. In order to keep the argument of the logarithm dimensionless, we multiply by  $o_2$  which doesn't affect the Poisson brackets. One can see that  $o_1 \in (-\infty, \infty)$  and  $p_1 \in (-\infty, 0)$  if  $b \in (-\infty, \infty)$  and  $p_b \in (-\infty, \infty)$ . Besides,  $o_2 \in (-\infty, \infty)$  and  $p_2 \in (-\infty, \infty)$  for  $c \in (-\infty, \infty)$  and  $p_c \in (-\infty, \infty)$ .

These new variables satisfy the Poisson algebra

$$\{o_i, p_j\} = \delta_{ij}, \quad \{o_i, o_j\} = 0, \quad \{p_i, p_j\} = 0, \quad (6.12)$$

for  $i, j = 1, 2$ .

We can invert the previous relations and obtain the original phase space variables as functions of the new configuration and momenta as

$$c = \frac{L_o}{o_2} e^{-8Gp_2/(\gamma L_o)}, \quad p_c = \epsilon_c \frac{o_2^2 \gamma^2}{4} e^{8Gp_2/(\gamma L_o)}, \quad (6.13)$$

$$b = \epsilon_b \gamma e^{-2Gp_1/(\gamma L_o)} \sqrt{1 - e^{4Gp_1/(\gamma L_o)}}, \quad p_b = \epsilon_b \frac{\gamma L_o o_1}{2} e^{2Gp_1/(\gamma L_o)} \sqrt{1 - e^{4Gp_1/(\gamma L_o)}}. \quad (6.14)$$

Here,  $\epsilon_c$  and  $\epsilon_b$  are equal to  $\pm 1$ . In terms of these observables, the Hamiltonian constraint takes the following form

$$C_{\text{class}} = -8\pi\epsilon_c\epsilon_b\text{sgn}(o_2)L_o e^{-2G(p_1+2p_2)/(\gamma L_o)} \sqrt{1 - e^{4Gp_1/(\gamma L_o)}} \frac{1}{o_2} (o_1 + o_2). \quad (6.15)$$

### 6.2.2 Classical dynamics

The classical dynamics can be solved by means of the Hamilton equations of the system. They can be obtained after computing Poisson brackets of the basic phase space variables with the Hamiltonian. However, since the total Hamiltonian is a constraint (obtained after varying the action with respect to the lapse function), not only the initial data must be specified within the constraint surface but also there is no preferred choice of time in the system. In order to

integrate the equations of motion, one should specify (as a prescribed function) the lapse, which plays the role of a Lagrange multiplier.

However, we will adopt an equivalent treatment. Concretely, we will provide below an example where, instead of solving the equations of motion after specifying the lapse function, we will introduce a suitable gauge fixing condition for one of the conjugate momenta of the weak Dirac observables defined above. This gauge fixing selects one of the phase space variables as a physical (internal) clock. With respect to this clock, we can compute a reduced (or true) Hamiltonian ruling the dynamics of the reduced system, which can actually be easily solved.<sup>2</sup> Finally, using Eqs. (6.13) and (6.14), we can explicitly write the original phase space variables as functions of Dirac observables and time.

Let us start with the following gauge fixing condition  $\Phi = (2G/\gamma L_o)p_2 - \tau \approx 0$ , where  $\tau$  plays the role of time parameter. We will assume, a priori, that it can take any value in the real line. Preservation of this condition upon evolution, after evaluation on shell (i.e.  $C_{\text{class}} \approx 0$  and  $\Phi \approx 0$ ), determines the lapse function, namely

$$0 \approx \dot{\Phi} = \{p_2, H_{\text{class}}\} - 1. \quad (6.16)$$

In terms of the new variables the lapse takes the following form (on shell)

$$N \approx \frac{\gamma}{\epsilon_c \epsilon_b \text{sgn}(-o_1)} \frac{e^{2Gp_1/(\gamma L_o)}}{\sqrt{1 - e^{4Gp_1/(\gamma L_o)}}} e^{2\tau} o_1, \quad (6.17)$$

after employing the constraint defined in Eq. (6.15) and the gauge condition, namely  $o_2 \approx -o_1$  and  $(2G/\gamma L_o)p_2 \approx \tau$ . Note that the lapse obtained here is essentially the same as the choice of lapse in CS quantization, the major difference being that in equation (6.17) it is represented in terms of our new phase space variables  $o_1, o_2, p_1$  and  $p_2$ , instead of  $b, c, p_b$  and  $p_c$  used in the CS quantization. Equation (6.17) gives the lapse in our variables whereas the Eventually, the

---

<sup>2</sup>This procedure is in agreement with the evolving constants introduced by Rovelli [283, 284]. See Refs. [109, 110] for an extended discussion.

replacement of these conditions in the full action allows us to obtain the reduced action as

$$S_{\text{red}} = \int d\tau (p_1 \dot{o}_1 - h_{\text{red}}), \quad (6.18)$$

with  $h_{\text{red}} = -o_1(\gamma L_o/2G)$  as the reduced Hamiltonian. The dynamics can be easily solved. Here,  $o_1$  is a constant of the motion and  $(2G/\gamma L_o)p_1 = \tau + \tau_0$ , with  $\tau_0$  another constant of the motion. Now, let us notice that the definition of  $p_1$  given in Eq. (6.11) involves  $p_1 < 0$ , namely, the parameter  $\tau$  must fulfill  $\tau < -\tau_0$ .

Finally, let us understand the physical meaning of the observables  $(o_1, \tau_0)$ . In order to do so, it is convenient to recall that in the interior of the black hole we have a clear interpretation regarding the values that the triads and connections take at the horizon. Concretely, if the mass of the black hole is  $M$ , we choose the standard conditions (see for instance Ref. [183]) at the horizon  $p_b(\tau_{\text{hor}}) = 0 = b(\tau_{\text{hor}})$ ,  $p_c(\tau_{\text{hor}}) = (2GM)^2$  and  $c(\tau_{\text{hor}}) = \frac{\gamma L_o}{4GM}$ . Using these conditions we find that  $\tau_0 = -\tau_{\text{hor}} = 0$ . Now, if we express the original variables in terms of the new ones by means of Eqs. (6.13) and (6.14), we set  $o_2 \approx -o_1$ ,  $(2G/\gamma L_o)p_2 \approx \tau$  and  $(2G/\gamma L_o)p_1 = \tau + \tau_0$ , we obtain

$$c(\tau) = \frac{\gamma L_o}{4GM} e^{-4\tau}, \quad p_c(\tau) = (2GM)^2 e^{4\tau}, \quad (6.19)$$

$$b(\tau) = -\gamma e^{-\tau} \sqrt{1 - e^{2\tau}}, \quad p_b(\tau) = 2GML_o e^{\tau} \sqrt{1 - e^{2\tau}}. \quad (6.20)$$

One can easily see that

$$o_1 = -4GM/\gamma. \quad (6.21)$$

Therefore, the Dirac observables are functions completely determined by the mass of the black hole. Let us also comment that, here, we have restricted the solutions to the sector  $p_b(\tau) \geq 0$  and  $p_c(\tau) \geq 0$  for all  $\tau$ , which involve  $\epsilon_c = 1$  and  $\epsilon_b = -1$ . Besides, the physical time fulfills  $\tau \in (-\infty, 0]$ . Then, the singularity is reached at  $\tau \rightarrow -\infty$ .

Note that we could also choose to gauge fix the momentum  $p_1$  as the time variable. The analysis is completely analogous to the above and does not affect physical results.



### 6.3 Effective loop quantum cosmology

In LQC, the situation changes drastically from a physical point of view, with respect to the previous classical model. As we have mentioned above, the classical singularity is removed in various loop quantized models of the Schwarzschild interior, however the details of the bounce differ depending on the choices of expressions for the edge lengths  $\delta_b$  and  $\delta_c$  for evaluating holonomies. As we described above, choices of these edge lengths inspired from both  $\mu_o$  and  $\bar{\mu}$  type approaches lead to undesirable features such as fiducial structure dependence of physical predictions or large quantum corrections at the horizon. Thus a third approach has been devised by choosing the edge lengths to be non-trivial Dirac observables which remain invariant on any phase space trajectory but can change from one trajectory to another. This approach was first applied in the CS quantization [183]. However the bounce obtained was highly asymmetric in the CS quantization. Specifically, the mass of the white hole on the other side of the bounce turns out to be a quartic power of the parent black hole mass. Based on the OSS scheme [273], we apply this approach here to obtain a symmetric bounce.

As mentioned above, drawbacks relating to the curvature at bounce were discovered later in both CS and OSS schemes. The AOS scheme [223] overcomes these shortcomings, which also chooses the edge lengths to be non-trivial Dirac variables and builds on the intuition in CS and OSS case. As discussed above, the bounce in the AOS scheme is approximately symmetric.

Our focus in this chapter is the OSS scheme [273], where we will explore several available dynamical schemes within a family of choices closely related to the CS choice [183] with the purpose of reconciling the loop quantum effective dynamics of this model with exactly symmetric bounces. The effective Hamiltonian constraint has been obtained in [183] using the standard procedure of re-expressing the classical expressions using the holonomies of the connection around closed loops. As we discussed in previous chapter, we may not be able to form closed loops giving holonomies in terms of almost periodic functions in the Kantowski–Sachs spatial slices due to presence of both anisotropy and spatial curvature. These issues had led to the construction of ‘A’ and ‘K’ quantizations in the Bianchi-II, Bianchi-IX models by consid-

ering the holonomies of the Ashtekar connection and the extrinsic curvature respectively along open edges. As pointed out in the previous chapter, the ‘A’ and ‘K’ quantization are equivalent in the Kantowski–Sachs model due to special symmetries of the spacetime which renders the holonomies of the Ashtekar connection and the extrinsic curvature along these straight edges equal to each other. The problem of lack of closed loops leading to almost periodic functions is overcome in the CS quantization slightly differently. Here, arguments using the homogeneity of the spacetime are used to assign the area to the loop which cannot be closed. Concretely, loops of holonomies are considered in the  $x - \theta$ ,  $x - \phi$  and  $\theta - \phi$  planes. Edges of the holonomies along  $x$  have length  $\delta_c L_o$  while edges along longitudes and equator on the two-sphere have length  $\delta_b r_o$ . The loop in  $\theta - \phi$  plane is not a closed loop but given the homogeneity of space it can still be assigned an ‘effective’ area [183]. The effective Hamiltonian constraint then turns out to be

$$H_{\text{LQC}} = \frac{1}{16\pi G} N C_{\text{LQC}}, \quad (6.22)$$

where  $C_{\text{LQC}}$  is the effective Hamiltonian constraint in LQC and takes the form

$$C_{\text{LQC}} = -\frac{8\pi \text{sgn}(p_c)}{\gamma^2} \left[ \left( \frac{\sin^2(\delta_b b)}{\delta_b^2} + \gamma^2 \right) \frac{p_b}{\sqrt{|p_c|}} + 2 \frac{\sin(\delta_b b)}{\delta_b} \frac{\sin(\delta_c c)}{\delta_c} |p_c|^{1/2} \right]. \quad (6.23)$$

As mentioned above, we will focus in a set of dynamical schemes where  $\delta_b$  and  $\delta_c$  are Dirac observables which commute with the effective Hamiltonian but may depend on the phase space variables in general. Since they commute with the effective Hamiltonian, we do not need to specify  $\delta_b$  and  $\delta_c$  now in order to solve the dynamics. It turns out that the dynamical equations can be used to find a condition for a symmetric bounce, which we will use in section 6.4 to give precise expressions for  $\delta_b$  and  $\delta_c$ .

### 6.3.1 Canonical transformation: Dirac observables

As in the classical theory, it is possible to identify two phase space variables that (weakly) commute with the effective Hamiltonian constraint under Poisson brackets, namely

$$O_1 = \frac{2}{\gamma^2 L_o} \left( \frac{\sin(\delta_b b)}{\delta_b} + \frac{\gamma^2 \delta_b}{\sin(\delta_b b)} \right) p_b, \quad \text{and} \quad O_2 = 4 \frac{\sin(\delta_c c)}{\gamma^2 L_o \delta_c} |p_c|. \quad (6.24)$$

Note that  $O_1$  and  $O_2$  are independent of fiducial rescaling and reduce to the classical observables  $o_1$  and  $o_2$  in the low curvature limit. If the effective constraint (6.23) is imposed, these two phase space variables are not linearly independent. Hence, only one of them (or a combination of both) codifies the physical degree of freedom, i.e. only one Dirac observable. Two conjugate momenta to these variables are

$$P_1 = \frac{\gamma L_o}{4G b_o} \log \left( \frac{\gamma^2 \delta_b^2}{4} \cdot \frac{1 + \frac{\cos(\delta_b b)}{b_o}}{1 - \frac{\cos(\delta_b b)}{b_o}} \right), \quad \text{and} \quad P_2 = -\frac{\gamma L_o}{8G} \log \left| O_2 \frac{\tan\left(\frac{\delta_c c}{2}\right)}{L_o \delta_c} \right|, \quad (6.25)$$

respectively, where  $b_o = \sqrt{1 + \gamma^2 \delta_b^2}$ .  $P_1$  and  $P_2$  are chosen in such a way that they reduce to the classical expressions in the low curvature limit. One can see that  $O_1 \in (-\infty, \infty)$  and  $P_1 \in (-P_1^{\max}, P_1^{\max})$  if  $b \in (-\infty, \infty)$  and  $p_b \in (-\infty, \infty)$ , with

$$P_1^{\max} = \frac{\gamma L_o}{4G b_o} \log \left( \frac{\gamma^2 \delta_b^2}{4} \cdot \frac{1 + \frac{1}{b_o}}{1 - \frac{1}{b_o}} \right), \quad (6.26)$$

while,  $O_2 \in (-\infty, \infty)$  and  $P_2 \in (-\infty, \infty)$  for  $c \in (-\infty, \infty)$  and  $p_c \in (-\infty, \infty)$ .

Let us notice that the relations between  $O_i$  and  $(c, b)$  involve trigonometric functions. Therefore, there is some degeneracy that we fix by restricting the connections  $(c, b)$  to the interval  $[-\pi/\delta_c, \pi/\delta_c)$  and  $[-\pi/\delta_b, \pi/\delta_b)$ , respectively.

The Poisson algebra of these new variables is

$$\{O_i, P_j\} = \delta_{ij}, \quad \{O_i, O_j\} = 0, \quad \{P_i, P_j\} = 0. \quad (6.27)$$

The canonical transformation can be inverted to obtain symmetry reduced connection and triad components in terms of  $(O_1, P_1)$  and  $(O_2, P_2)$ :

$$c = \frac{2}{\delta_c} \arctan \left( e^{-8G(P_2 + \Delta_2)/(\gamma L_o)} \right), \quad p_c = \epsilon_c \frac{\gamma^2 L_o \delta_c}{4} O_2 \cosh(8G(P_2 + \Delta_2)/(\gamma L_o)), \quad (6.28)$$

$$b = \epsilon_b \frac{1}{\delta_b} \arccos [b_o \tanh(2Gb_o(P_1 + \Delta_1)/(\gamma L_o))],$$

$$p_b = \epsilon_b \frac{\gamma^2 L_o \delta_b O_1}{2b_o^2} \cosh^2(2Gb_o(P_1 + \Delta_1)/(\gamma L_o)) \sqrt{1 - b_o^2 \tanh^2[2Gb_o(P_1 + \Delta_1)/(\gamma L_o)]}, \quad (6.29)$$

where

$$\Delta_1 = -\frac{\gamma L_o}{4Gb_o} \log \left( \frac{\gamma^2 \delta_b^2}{4} \right), \quad \Delta_2 = -\frac{\gamma L_o}{8G} \log \left( \frac{L_o \delta_c}{2O_2} \right), \quad (6.30)$$

and  $\epsilon_b$  and  $\epsilon_c$  are equal to  $\pm 1$  as before.

Furthermore, the effective Hamiltonian constraint in terms of these new variables takes the form

$$C_{\text{LQC}} = -\epsilon_c \epsilon_b \text{sgn}(O_2) \frac{8\pi L_o}{\gamma \delta_b} \frac{\sqrt{1 - b_o^2 \tanh^2[2Gb_o(P_1 + \Delta_1)/(\gamma L_o)]}}{\sqrt{L_o \delta_c |O_2| \cosh(8G(P_2 + \Delta_2)/(\gamma L_o))}} (O_1 + O_2). \quad (6.31)$$

### 6.3.2 Effective dynamics

As in the classical theory, in order to solve the effective dynamics in LQC, we will adopt the gauge fixing  $\Psi_1 = (2G/\gamma L_o)P_2 - T \approx 0$ , where  $T$  is the time parameter for this gauge fixing and it can take any value in the real line. Preservation of this condition upon evolution, after evaluation on shell,

$$0 \approx \dot{\Psi} = (2G/\gamma L_o) \{P_2, H_{\text{LQC}}\} - 1, \quad (6.32)$$

fixes the lapse

$$N = -\epsilon_c \epsilon_b \text{sgn}(-O_1) \gamma^2 \delta_b \frac{\sqrt{L_o \delta_c |O_1| \cosh[4T + 8G\Delta_2/(\gamma L_o)]}}{\sqrt{1 - b_o^2 \tanh^2[2Gb_o(P_1 + \Delta_1)/(\gamma L_o)]}}. \quad (6.33)$$

This lapse reduces to the classical expression (6.17) in the low curvature limit. Besides, the new configuration variables, on shell, satisfy  $O_2 = -O_1$ . Eventually, one can easily see that the reduced action takes the form

$$S_{\text{red}} = \int dT \left( P_1 \dot{O}_1 - H_{\text{red}} \right), \quad (6.34)$$

with  $H_{\text{red}} = -(\gamma L_o/2G)O_1$  the reduced Hamiltonian. As a consequence, one easily realizes that  $O_1$  is actually a constant of the motion while  $(2G/\gamma L_o)P_1 = T + T_0$ , with  $T_0$  another constant of the motion. Besides,  $T$  must be constrained such that  $|P_1| \leq P_1^{\text{max}}$ , i.e.  $|T + T_0| \leq (\gamma L_o/2G)P_1^{\text{max}}$ .

Eventually, in order to connect the dynamics in classical GR with the effective dynamics of LQC, we first identify the value of the Dirac observable in both descriptions. This amounts to

$$O_1 = -4GM/\gamma. \quad (6.35)$$

As found in CS case [183], we have  $b(T_{\text{hor}}) = 0$  and  $c(T_{\text{hor}}) = (2/\delta_c) \arctan(\gamma L_o \delta_c / (8GM))$ . These conditions yield the time  $T_{\text{hor}}$  and the Dirac observable  $T_0$  as follows,

$$T_{\text{hor}} = 0, \quad T_0 = \frac{1}{b_o} \operatorname{arctanh} \left[ \frac{1}{b_o} \right] - (2G/\gamma L_o) \Delta_1. \quad (6.36)$$

Then, we can write the triads and connections as functions of  $T$  and the constants of the motion  $O_1$  and  $T_0$  using Eqs. (6.28). We obtain

$$c(T) = \frac{2}{\delta_c} \arctan \left( e^{-4(T + \tilde{\Delta}_2)} \right), \quad p_c(T) = -\epsilon_c \frac{\gamma^2 L_o \delta_c}{4} O_1 \cosh \left( 4(T + \tilde{\Delta}_2) \right), \quad (6.37a)$$

$$b(T) = \epsilon_b \frac{1}{\delta_b} \arccos \left[ b_o \tanh \left( b_o(T + T_0 + \tilde{\Delta}_1) \right) \right], \quad (6.37b)$$

$$p_b(T) = \epsilon_b \frac{\gamma^2 L_o \delta_b O_1}{2b_o^2} \cosh^2 \left( b_o(T + T_0 + \tilde{\Delta}_1) \right) \sqrt{1 - b_o^2 \tanh^2 \left[ b_o(T + T_0 + \tilde{\Delta}_1) \right]}, \quad (6.37c)$$

where

$$\tilde{\Delta}_1 = \frac{2G}{\gamma L_o} \Delta_1 = -\frac{1}{2b_o} \log \left( \frac{\gamma^2 \delta_b^2}{4} \right), \quad \tilde{\Delta}_2 = \frac{2G}{\gamma L_o} \Delta_2 = \frac{1}{4} \log \left( \frac{8GM}{\gamma L_o \delta_c} \right). \quad (6.38)$$

As noted above, we could also choose to gauge fix the momentum  $P_1$  as the time variable instead of  $P_2$ . A completely analogous analysis to above can be followed for this choice. The physical results of this chapter are not affected by this change.

## 6.4 Dynamical prescriptions for symmetric bounces

Now that the effective dynamics has been solved (for constant  $\delta_b$  and  $\delta_c$ ), we can come to the main objective of this manuscript. We will prove here that this effective model admits symmetric bounces, regardless of the initial conditions (and the mass of the black hole). This condition is fulfilled if and only if complete dynamical trajectories in the phase space plane  $p_b$ - $p_c$  enclose a zero area. By complete trajectory we mean that they start and end at the horizons. In other words, if we start the evolution in a collapsing branch, once the trajectory reaches the bounce it must retrace the same phase space points during the expanding branch (by continuity the area enclosed will be zero) reaching the same phase space point it started at. As an analogy, we can consider the example of the phenomena of hysteresis in magnetism. In some magnetic materials, once they are magnetized using an external magnetizing field, the magnetization does not retrace its path when the magnetizing field is reduced again. This happens because the magnetized material retains the magnetization induced even if the magnetizing field is removed. This situation leads to the phenomena of hysteresis, which is marked by the presence of loops enclosing a finite area in the graphs of the magnetization versus magnetizing field as the sample is taken through various cycles of magnetization and demagnetization. Hysteresis is absent when the area enclosed by the loop is zero. Similarly, if the triad  $p_b$  does not retrace its path as the triad  $p_c$  bounces, the phase space trajectory of the system will enclose a finite area, which will not be the case if the bounce is symmetric. As is clear from the above equations, this condition

is fulfilled if and only if  $T_0 + \tilde{\Delta}_1 = \tilde{\Delta}_2$ , i.e.

$$\frac{\operatorname{arctanh}\left[\frac{1}{\sqrt{1+\gamma^2\delta_b^2}}\right]}{\sqrt{1+\gamma^2\delta_b^2}} = \frac{1}{4} \log\left(\frac{8GM}{\gamma L_o \delta_c}\right). \quad (6.39)$$

If this conditions are satisfied, then the effective evolution equations for the phase space variables are symmetric about  $T_b = -\tilde{\Delta}_2$ , which is where the bounce occurs. Since the black hole horizon is at  $T_{\text{hor}} = 0$ , the white hole horizon is at  $T = -2\tilde{\Delta}_2$ .

The edge lengths  $\delta_b$  and  $\delta_c$  must satisfy the above condition for the bounce to be symmetric. This means that  $\delta_c$  and  $\delta_b$  will not be independent. Thus, a symmetric bounce is a physical requirement that eliminates some the freedom in the choices of  $\delta_c$  and  $\delta_b$ . Thus, apart from being Dirac observables,  $\delta_b$  and  $\delta_c$  are those functions of the phase space which also satisfy the symmetric bounce condition while are also not trivially constant on the phase space.

In the CS quantization, dimensional considerations and the requirement of fiducial structure independence led to the following choice for  $\delta_b$  and  $\delta_c$  as Dirac observables [183]

$$\delta_b^2 r_o^2 = \Delta, \quad \delta_b r_o \delta_c L_o = \Delta. \quad (6.40)$$

In the CS quantization, the goal was to carefully consider the length scales involved and the rescaling properties of various quantities to obtain the simplest choice suited to the Schwarzschild interior which does not have large quantum effects at the horizon and gives fiducial structure independent predictions. However, as mentioned above, the bounce is highly non-symmetric in the CS quantization for all values of the black hole mass. We generalize the above choice by introducing two constant parameters  $\alpha$  and  $\beta$  which will allow us to accommodate the symmetric bounce condition

$$\delta_b^2 r_o^2 = \alpha^2 \Delta, \quad \delta_b r_o \delta_c L_o = \alpha \beta \Delta. \quad (6.41)$$

It is clear that the CS quantization involves the choice  $\alpha = 1 = \beta$ . We expect that this choice does not satisfy the symmetric bounce condition as the bounce was found to be highly non-symmetric in the CS quantization. We will confirm this below. Notice that together with the

symmetric bounce condition (6.39), the above choice implies that the parameters  $\alpha$  and  $\beta$  will be independent of  $L_o$ , but they will depend on  $r_o$ , namely, they will depend on the mass of the black hole. Note that this kind of dependence on the mass has been already suggested in the CS quantization [183]. The difference here is that such dependence will now be more involved. In some situations it will not be possible to provide the relation in a closed form.

Below, we will analyze some possible choices for these parameters. Note that among the simplest choices, there is a natural parametrization corresponding to  $\beta = 1$ . It is due to the freedom in the choice of the open loop in the  $\theta - \phi$  plane. Nevertheless, we will consider other simple choices, for the sake of completeness, such as  $\alpha = 1$  and  $\alpha = 1/\beta$ . But before that, we first consider the choice  $\alpha = 1 = \beta$  which corresponds to the CS quantization where asymmetric bounces occur. In all the numerical computations that will be shown below, we set  $\Delta = 4\sqrt{3}\pi\gamma G\hbar$ ,  $\gamma = 0.2375$ ,  $L_o = 1$ ,  $G = 1$  and  $\hbar = 1$ .

#### 6.4.1 Choice 1: asymmetric bounce

In this case, we reproduce the results already shown in Ref. [183]. Namely, the polymer parameters  $\delta_b$  and  $\delta_c$  are fixed by Eq. (6.40). We then plug them in Eq. (6.37) and, for this choice, we summarize our study of the dynamics in Fig. 6.1, 6.2 and 6.3. In Fig. 6.1 we show the spatial volume  $V = 4\pi p_b \sqrt{p_c}$  as a function of time  $T$ , for several values of the mass of the black hole, from semiclassical to very quantum black holes, namely, from large to small masses w.r.t the Planck mass, respectively. We see that the volume goes to zero at the horizons, since  $p_b$  does. Besides, for large enough values of the mass, the volume at each side of the bounce (minimum value reached by the volume away from the horizons) is different. This is an indication that the bounce is not symmetric. However, if the masses are small enough, we see an opposite behavior: the volume at the ‘bounce’ is maximum and the ‘bounce’ turns out to be almost symmetric. Hence for very small masses, the bounce turns out to be a recollapse. This appears to be a universal feature of all the choices studied in this manuscript. Using the symmetric bounce condition it is straightforward to see that for the current choice of prescribing areas to the loops, there is no real allowed value of mass  $M$ . Thus, a symmetric bounce can be approached but never obtained in CS quantization [183].



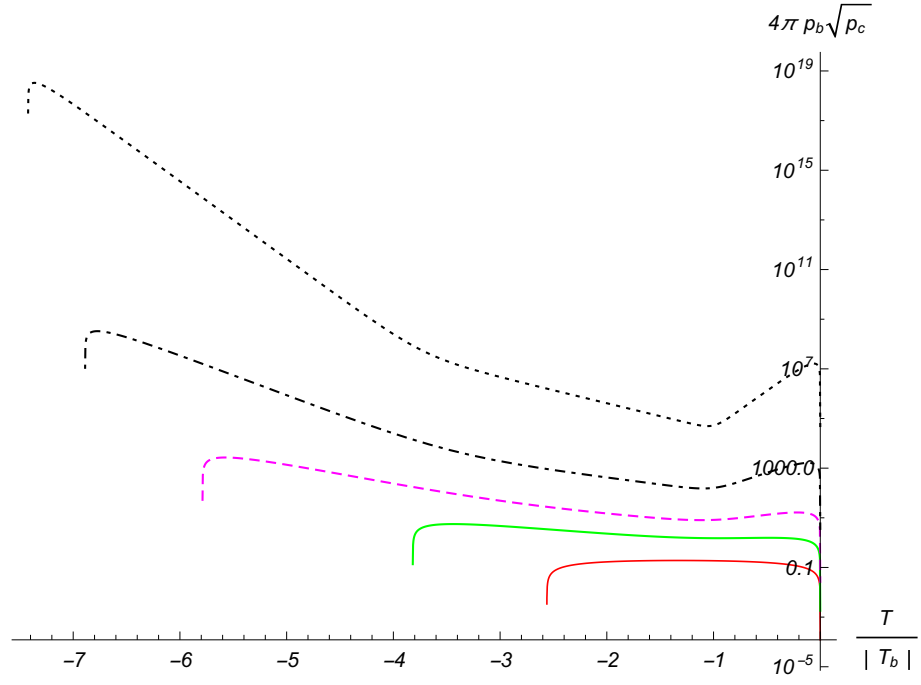


Figure 6.1: Choice 1: the evolution of the spatial volume as a function of the normalized time  $T/|T_b|$ . The curves ranging from thickest to the thinnest correspond to  $M = 0.1, 0.3, 1, 10, 1000$  (in Planck units), respectively.

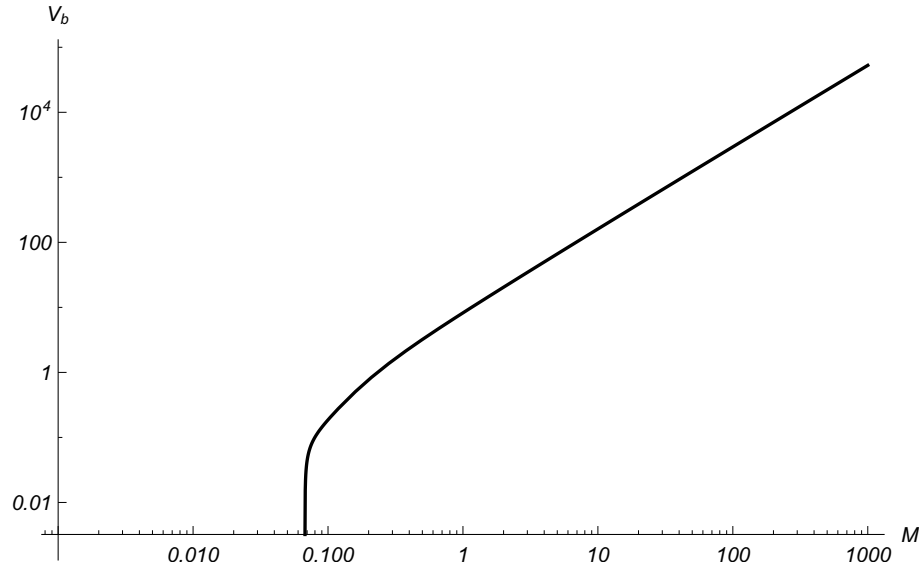


Figure 6.2: Choice 1: the volume at the bounce as a function of the mass.

In Fig. 6.2 we show the value of the volume at the bounce as a function of the mass. As we see, for a fixed value of the mass, the volume is finite. However, there is a threshold mass where it tends to zero. This is so because for masses equal to or smaller than this threshold mass, there is actually no black hole. Therefore, if one trusts the effective description provided here for very small values of the mass, one finds the existence of a minimum nonzero mass in this scenario. It should be emphasized that the existence of a minimum non-zero mass of the black hole and a recollapse replacing the bounce for tiny black holes are novel results noticed here for the first time in loop quantization of Schwarzschild interior.

However, as we noticed above, the bounce volume seems to increase linearly with the mass of the black hole. We further plot the Kretschmann scalar at bounce. Equation (5.17) gives the expression for the Kretschmann scalar as a function of proper time. However, the effective equations for the phase space evolution obtained in this chapter are in terms of the time  $T$ , which is not the proper time. Thus we replace the proper time derivatives  $\partial/\partial\tau$  in (5.17) by  $[N(T)]^{-1}\partial/\partial T$  and use the effective equations of motion (6.37) to evaluate the Kretschmann scalar as a function of time  $T$ . Here  $N(T)$  is the lapse given in equation (6.33). As shown in the plot of the Kretschmann scalar at bounce in Fig. 6.3, the curvature decreases as the mass of the black hole increases. This means that for very large black holes, the curvature at the bounce could be too small to have quantum effects leading to a bounce, thus implying the existence of large quantum effects in low curvature regimes in this choice. Indeed this has been verified to be the case for the CS quantization as pointed out in [223] by studying the value of the Kretschmann scalar at the bounce for large mass black holes. It was found in [223], that the value of the Kretschmann scalar  $1/M$  with the mass of the black hole. This means that the bounce can occur at very low curvatures in the CS quantization. Indeed, this is another drawback of the CS quantization which was earlier unknown, until it was pointed out in [223]. We will analyze below which one of the choices considered for symmetric bounce also remove this drawback.

As shown in fig. 6.1, the volume versus time curve starts becoming convex and approximately symmetric as we go to small enough masses. This corresponds to the kink in the plot for the

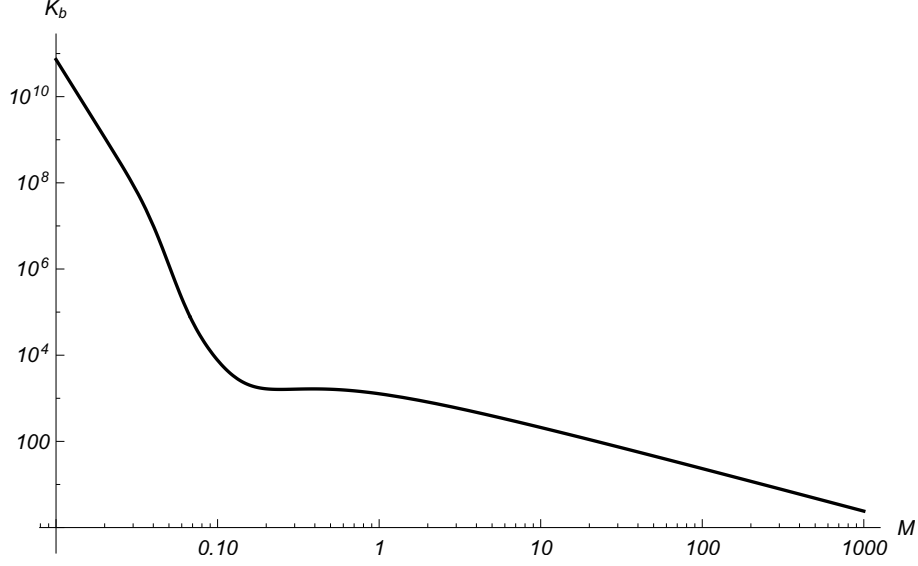


Figure 6.3: Choice 1: the value of the Kretschmann scalar at the bounce as a function of mass. Kretschmann scalar around 0.1 Planck mass, and the change in the nature of curve around 0.1 Planck mass in the bounce volume versus mass plot. Similar effects around 0.1 Planck mass are observed in all the other choices considered below as we approach small masses. This indicates that the effective dynamics predicts a bounce with qualitatively different features for small enough masses, namely, that the bounce becomes convex such that the volume is largest at the bounce and decreases on either side of the bounce. Such small mass black hole are extremely small in dimensions and are expected to behave in a completely quantum way with no classical analog. Thus the effective theory may not be a good approximation for the dynamics of such low mass black holes.

#### 6.4.2 Choice 2: $\beta = 1$

From now on, we will study the symmetric bounce scenarios, starting with the choice  $\beta = 1$  in Eq. (6.41). We obtain

$$\delta_b = \alpha \frac{\sqrt{\Delta}}{r_o}, \quad \delta_c = \frac{\sqrt{\Delta}}{L_o}. \quad (6.42)$$

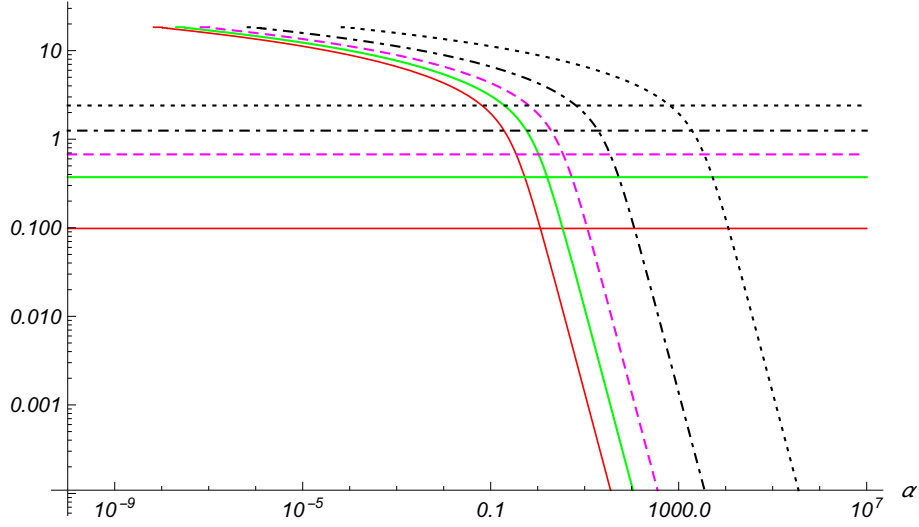


Figure 6.4: Choice 2: we plot the LHS and RHS of Eq. (6.43) as a function of  $\alpha$  for different values of the mass  $M$ . The horizontal lines correspond to the RHS of (6.43). The curves ranging from the thickest to the thinnest correspond to  $M = 0.1, 0.3, 1, 10, 1000$  in Planck units, respectively.

If we substitute these polymer parameters in the symmetric bounce condition given by Eq. (6.39), namely

$$\frac{1}{\left(\sqrt{1 + \alpha^2 \frac{\gamma^2 \Delta}{(2GM)^2}}\right)} \operatorname{arctanh} \left[ \frac{1}{\sqrt{1 + \alpha^2 \frac{\gamma^2 \Delta}{(2GM)^2}}} \right] = \frac{1}{4} \log \left[ \frac{8GM}{\gamma \sqrt{\Delta}} \right], \quad (6.43)$$

we can fix the parameter  $\alpha$  in order to fulfill this condition. In order to find the allowed values of  $\alpha$ , in Fig. 6.4 we plot the left and right hand sides of Eq. (6.43) separately, to find out the solutions given by their intersection points for different values of the mass. The right hand side, since it is independent of  $\alpha$ , is represented by the horizontal lines. As we see in Fig. 6.5,  $\alpha$  has a minimum around  $M = 0.1$  (in Planck units), increasing on either side of this point. Let us also notice that for higher masses,  $\alpha$  increases as a function of the mass following a power law.

We have also plotted the dynamical evolution of the triads in Fig. 6.6 and the spatial volume in Fig. 6.7. As we see in Fig. 6.6, the value of  $p_b$  goes to zero at the horizon. Regarding  $p_c$ , its value at the horizon is slightly higher than its classical value  $(2GM)^2$ . This is due to the small quantum corrections of the polymeric description. Besides, these curves enclose a vanishing area when ranging from horizon to horizon. This indicates that the bounce is symmetric. In Fig.

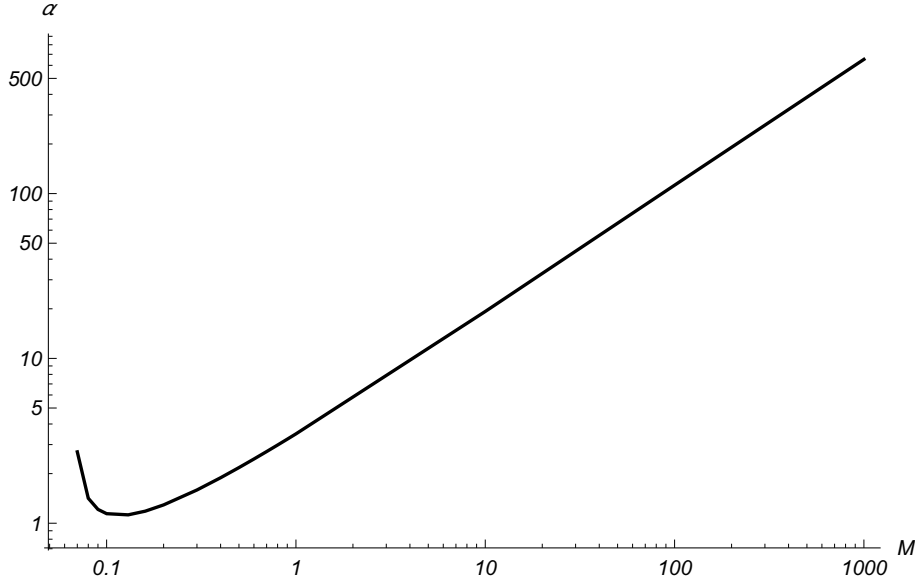


Figure 6.5: Choice 2:  $\alpha$  as a function of  $M$ .

6.7 we see that the spatial volume takes its absolute minimum value at the horizons (it vanishes there), as in the classical theory. For masses higher than 0.1 it has a local minimum at the bounce, however those local minima become local maxima at the bounce for smaller masses. The bounce turns out to be a quantum recollapse for such small black hole masses.

Besides, we plot the bounce volume versus the mass in Fig. 6.8. We see that it monotonically increases with the mass. We must notice that there is a change in the behavior around  $M = 0.1$ . This corresponds to the turn around in the value of  $\alpha$  as we go to lower masses, and for these masses the volume reaches local maxima at the bounce (instead of minima). The turn around in  $\alpha$  as a function of  $M$  does not lead to a turn around in the behavior of the volume at the bounce, but there is a change in the way the volume depends on the mass for these extremely low masses. We should note that for such a range of parameters we are essentially reaching the regime where effective spacetime description may not be well trusted, as the black holes for such low masses are of microscopic sizes and their behavior and dynamics may be of an essentially quantum nature without any correspondence with the classical world. We find that this peculiar behavior for masses below 0.1 is shared with all the other cases considered here.

Moreover, even though the bounce is now symmetric compared to the CS quantization, the drawback of the CS quantization is not removed by this choice. As pointed out above, the

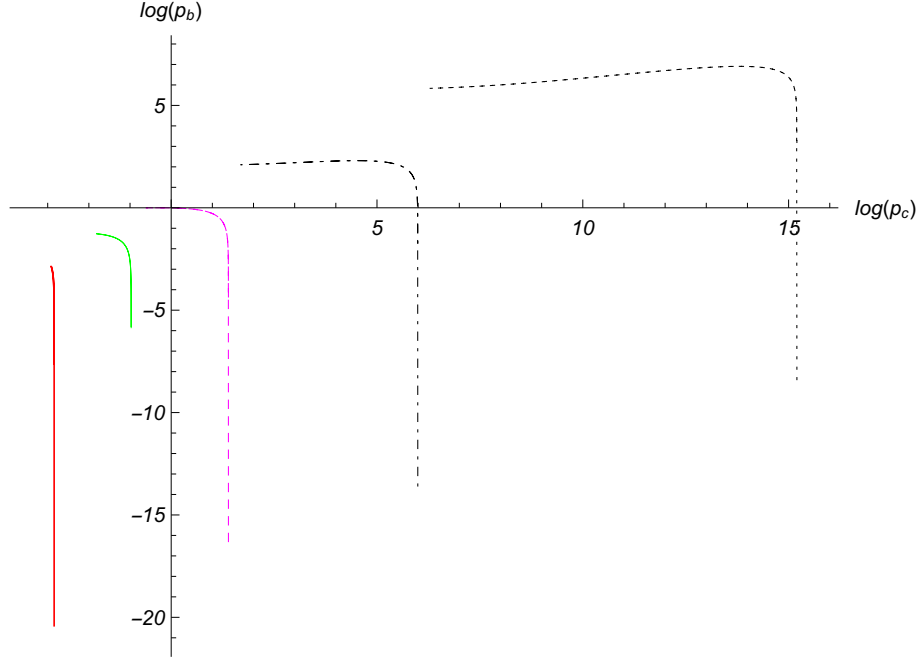


Figure 6.6: Choice 2: the logarithmic of  $p_b$  as a function of the logarithm of  $p_c$  for different values of the mass  $M$ . The curves ranging from the thickest to the thinnest correspond to  $M = 0.05, 0.1, 0.3, 1, 10, 1000$  in Planck units respectively.

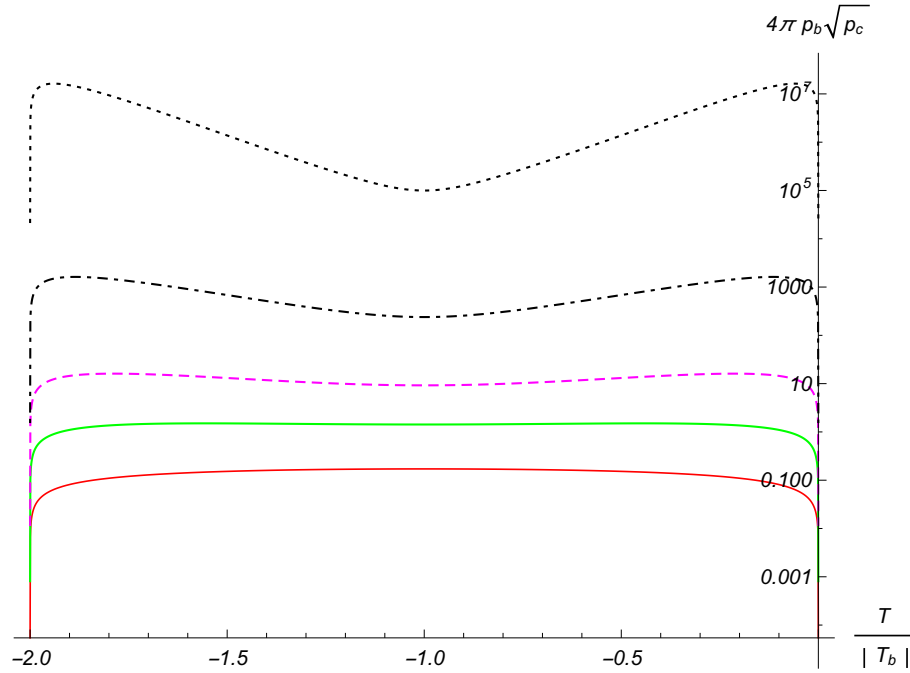


Figure 6.7: Choice 2: the evolution of the spatial volume as a function of the normalized time  $T/|T_b|$ . The curves ranging from the thickest to the thinnest correspond to  $M = 0.05, 0.1, 0.3, 1, 10, 1000$  in Planck units respectively.

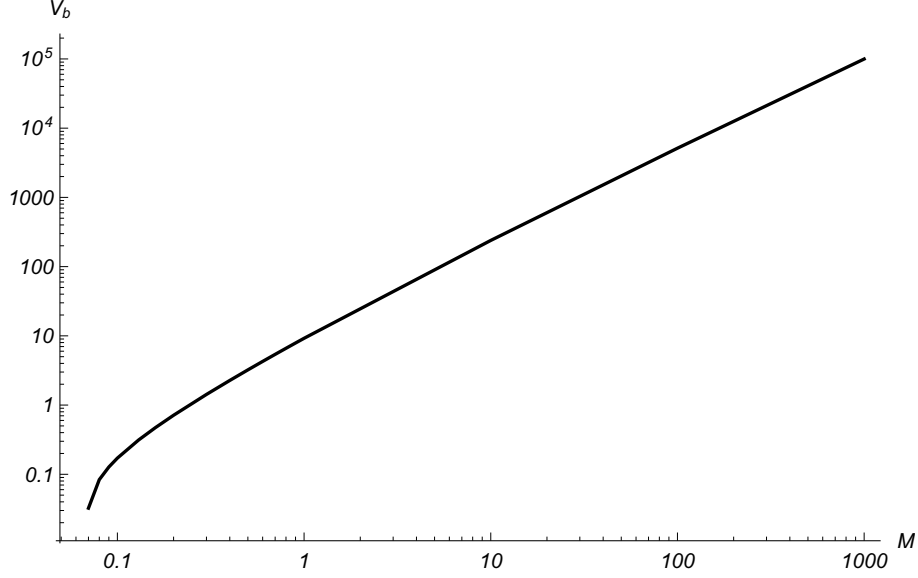


Figure 6.8: Choice 2: volume at the bounce as a function of mass.

bounce volume increases with the mass, and can be very large for large enough black hole mass. This may lead to very low curvatures at the bounce for large black holes. To investigate this, we look at the behavior of the Kretschmann scalar at the bounce. As plotted in Fig. 6.9, we find that the Kretschmann scalar at the bounce indeed decreases as the mass decreases, leading to low curvatures at the bounce for large mass black holes. Thus the choice 2 also suffers from the same drawback as the CS quantization, even though it achieves a symmetric bounce.

### 6.4.3 Choice 3: $\alpha = 1$

We now proceed with another possible choice for the polymer parameters which allows symmetric bounce. We fix the length of the open loop as  $\alpha = 1$ . Then, the polymer parameters take the form

$$\delta_b = \frac{\sqrt{\Delta}}{r_o}, \quad \delta_c = \beta \frac{\sqrt{\Delta}}{L_o}. \quad (6.44)$$

The loop with length determined by  $\beta$ , will be actually fixed by the symmetric bounce condition (6.39)

$$\frac{1}{\left(\sqrt{1 + \frac{\gamma^2 \Delta}{(2GM)^2}}\right)} \operatorname{arctanh} \left[ \frac{1}{\sqrt{1 + \frac{\gamma^2 \Delta}{(2GM)^2}}} \right] = \frac{1}{4} \log \left[ \frac{8GM}{\beta \gamma \sqrt{\Delta}} \right]. \quad (6.45)$$

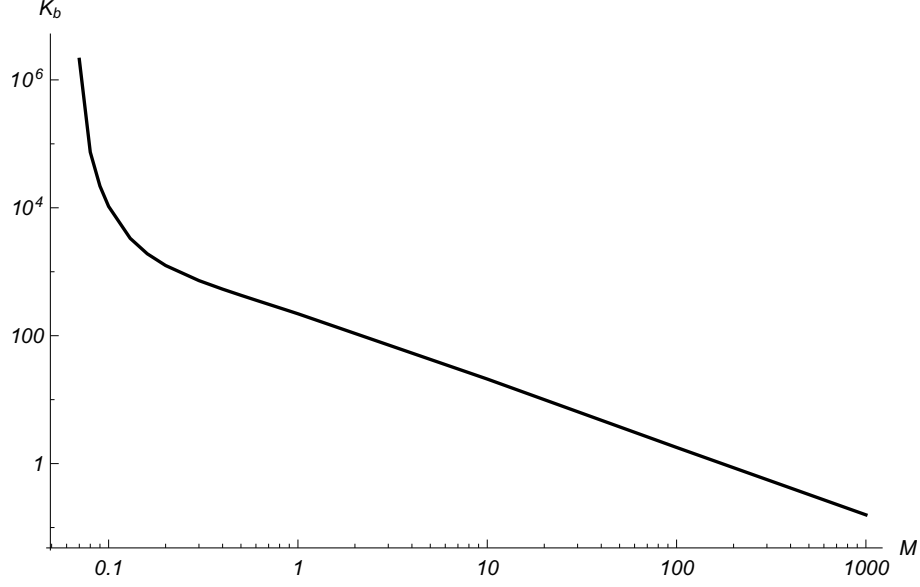


Figure 6.9: Choice 2: the value of the Kretschmann scalar at the bounce as a function of mass. Unlike the choice 2 for polymer parameters, this time this expression can be solved analytically for  $\beta$ , yielding

$$\beta = \frac{8GM}{\gamma\sqrt{\Delta}} \frac{(b_o - 1)^{2/b_o}}{(b_o + 1)^{2/b_o}}, \quad (6.46)$$

recalling that in this case

$$b_o = \sqrt{1 + \frac{\gamma^2 \Delta}{(2GM)^2}}. \quad (6.47)$$

It is useful to consider the asymptotic behavior of  $\beta$ :

$$\lim_{M \rightarrow \infty} \beta = \frac{\gamma^3 \Delta^{3/2}}{32G^3 M^3} + \mathcal{O}(M^{-5} \log[M]), \quad \lim_{M \rightarrow 0} \beta = \frac{8GM}{\gamma\sqrt{\Delta}} + \mathcal{O}(M^3). \quad (6.48)$$

In both cases (small and large black hole masses), the parameter  $\beta$  goes to zero. In Fig. 6.10 we plot  $\beta$  as a function of the mass  $M$ . We see that it goes to zero for sufficiently small and large values of the mass, and its maximum is around  $M = 0.2$  (in Planck units).

We plot the dynamical evolution of the triads in Fig. 6.11 and the spatial volume in Fig. 6.12. As we see in Fig. 6.11  $p_b$  goes to zero at the horizon and  $p_c$  is again slightly higher than its classical value  $(2GM)^2$ , as it is expected from the contribution of the small quantum corrections.



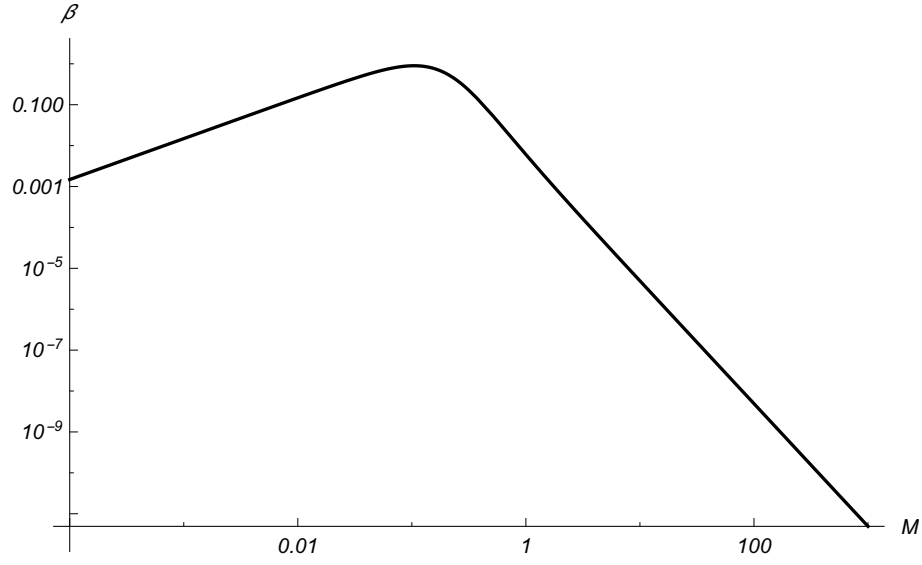


Figure 6.10: Choice 3 : the parameter  $\beta$  is plotted as a function of the mass  $M$ .

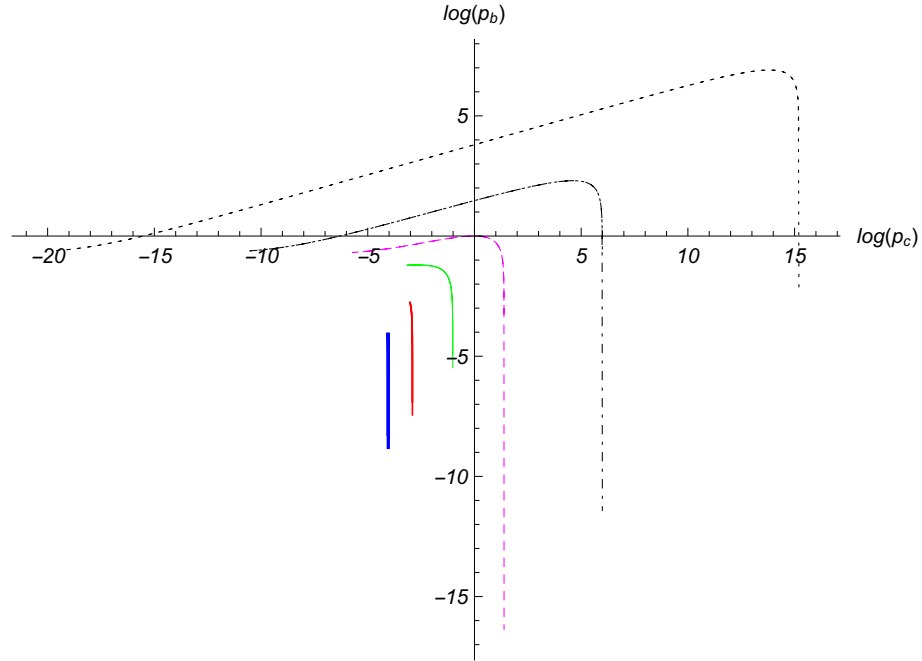


Figure 6.11: Choice 3: the logarithmic of  $p_b$  as a function of the logarithm of  $p_c$  for different values of the mass  $M$ . The curves ranging from the thickest to the thinnest correspond to  $M = 0.05, 0.1, 0.3, 1, 10, 1000$ , in Planck units, respectively.

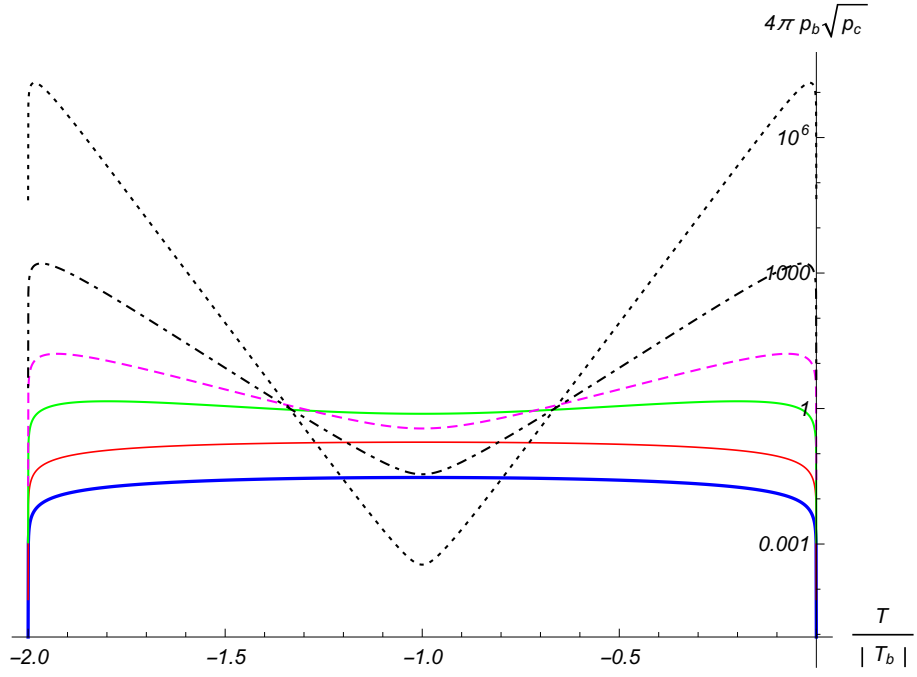


Figure 6.12: Choice 3: the evolution of the spatial volume as a function of the normalized time  $T/|T_b|$ . The curves ranging from the thickest to the thinnest correspond to  $M = 0.05, 0.1, 0.3, 1, 10, 1000$ , in Planck units, respectively.

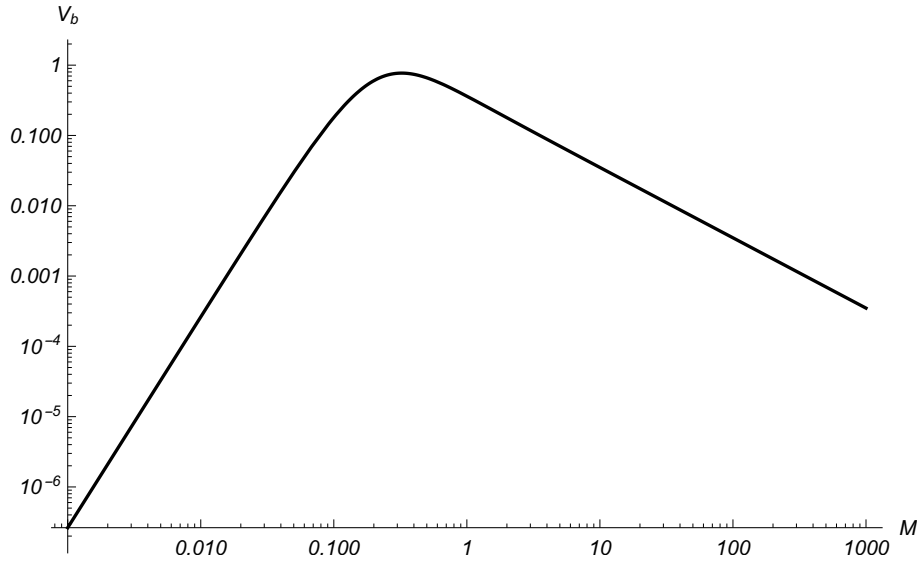


Figure 6.13: Choice 3: bounce volume as a function of mass.

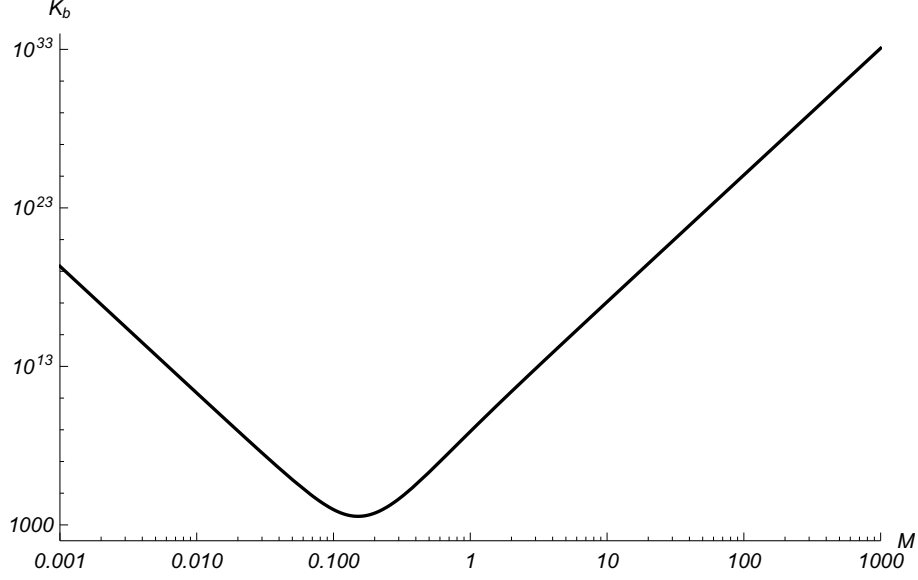


Figure 6.14: Choice 3: the value of the Kretschmann scalar at the bounce as a function of mass.

The triads  $p_c$  and  $p_b$  evaluated at the bounce take the form

$$p_c(T = -\tilde{\Delta}_2) = \gamma\sqrt{\Delta}GM\beta(M), \quad p_b(T = -\tilde{\Delta}_2) = \frac{L_o\gamma\sqrt{\Delta}}{1 + \frac{\gamma^2\Delta}{4G^2M^2}}. \quad (6.49)$$

Then, we see that, from Eq. (6.48), at large values of the mass  $M$ , the triad  $p_c$  at the bounce decreases quadratically (at leading order) as a function of the mass while  $p_b$  converges to the constant value  $L_o\gamma\sqrt{\Delta}$ . On the other hand, for very small mass  $M$ , both  $p_c$  and  $p_b$  at the bounce behave, at leading order, as quadratic functions of the mass. In Fig. 6.12 we show the behavior of the spatial volume. It takes its minimum absolute value at the horizons, since it vanishes there. Just like the previous cases, the volume reaches a local minimum at the bounce if the mass is higher than 0.1, but for smaller values of the mass the volume reaches a local maxima. However, unlike the previous case, the turn around in the value of  $\beta$  causes a turn around in the bounce volume as well. This is shown in Fig. 6.13 where we show the volume at the bounce versus the mass  $M$ . We see that it is no longer a monotonic function of the mass and remains low for all values of mass. This is analytically demonstrated above by the asymptotic behavior of  $\beta(M)$  in both low and high mass regimes. Thus we expect that the drawback of the CS quantization and the choice 2 above, which produce a bounce at low curvatures for large

mass black holes, to be absent in this case. This is indeed the case as shown by the plot 6.14 of the Kretschmann scalar at the bounce with respect to the mass shows.

#### 6.4.4 Choice 4: $\beta = 1/\alpha$

Now we will proceed with the most interesting choice among the ones considered here. The reason is that this choice allows us to work with a closed loop since, from Eq. (6.41) we get

$$\delta_b r_o \delta_c L_o = \Delta, \quad (6.50)$$

in partial agreement with Ref. [183]. The choice  $\beta = 1/\alpha$  amounts to

$$\delta_b = \alpha \frac{\sqrt{\Delta}}{r_o}, \quad \delta_c = \frac{\sqrt{\Delta}}{L_o \alpha}. \quad (6.51)$$

Together with the symmetric bounce condition (6.39)

$$\frac{1}{\sqrt{1 + \alpha^2 \frac{\gamma^2 \Delta}{(2GM)^2}}} \operatorname{arctanh} \left[ \frac{1}{\sqrt{1 + \alpha^2 \frac{\gamma^2 \Delta}{(2GM)^2}}} \right] = \frac{1}{4} \log \left[ \frac{8GM\alpha}{\gamma\sqrt{\Delta}} \right], \quad (6.52)$$

we can fix  $\alpha$  as in the previous sections. Unlike the case of choice 3, we do not have a closed form expression for  $\alpha$ . To find the allowed values of  $\alpha$ , in Fig. 6.15 we plot the left and right hand sides of Eq. (6.52) separately for different values of the mass  $M$ . The intersection points show that  $\alpha$  grows monotonically with the mass of the black hole  $M$ , just like for the case  $\beta = 1$ .

We note the striking similarity between the graphs obtained for the variation in  $\alpha$  with  $M$  in the present case with the case  $\beta = 1$ . First note that the left hand side of the symmetric bounce condition is identical in both cases and hence generate identical curves in Fig. 6.15. In the present case, even though the plots for the right hand side look quite different from the case  $\beta = 1$  (choice 2), the behavior of  $\alpha$  as a function of  $M$  has similarities with respect to the case  $\beta = 1$ , as shown in Fig. 6.16. We also find that the behavior of the triads and the spatial volume in the present case are similar to the case  $\beta = 1$ , as shown in Fig. 6.17 and 6.18 respectively. There, we have plotted the dynamical evolution of the triads and the spatial

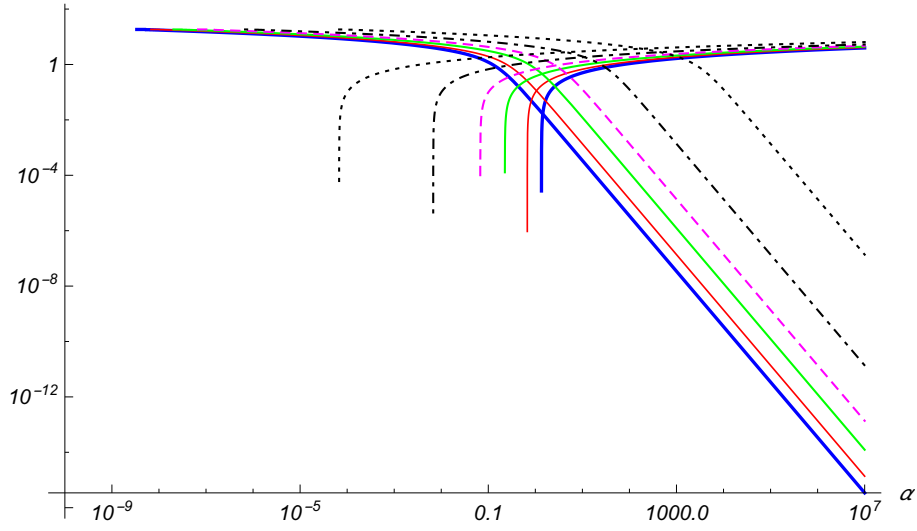


Figure 6.15: Choice 4: we plot the left and right hand side of Eq. (6.52) as a function of  $\alpha$  for several values of the mass  $M$ . The curves ranging from thickest to the thinnest correspond to  $M = 0.05, 0.1, 0.3, 1, 10, 1000$  (in Planck units), respectively. The curves converging on the left of the graph are of the left hand side of Eq. (6.52), and vice-versa.

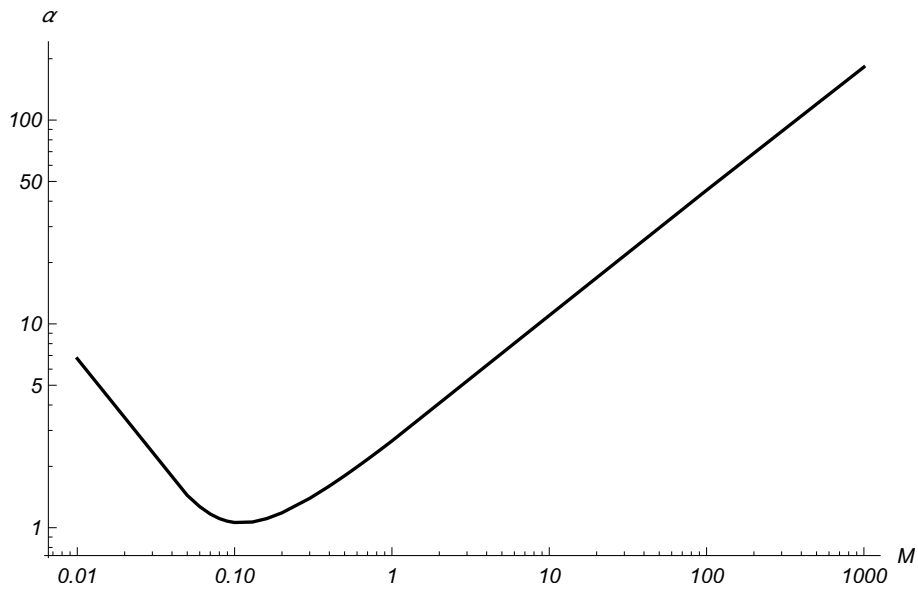


Figure 6.16: Choice 4:  $\alpha$  as a function of  $M$ .

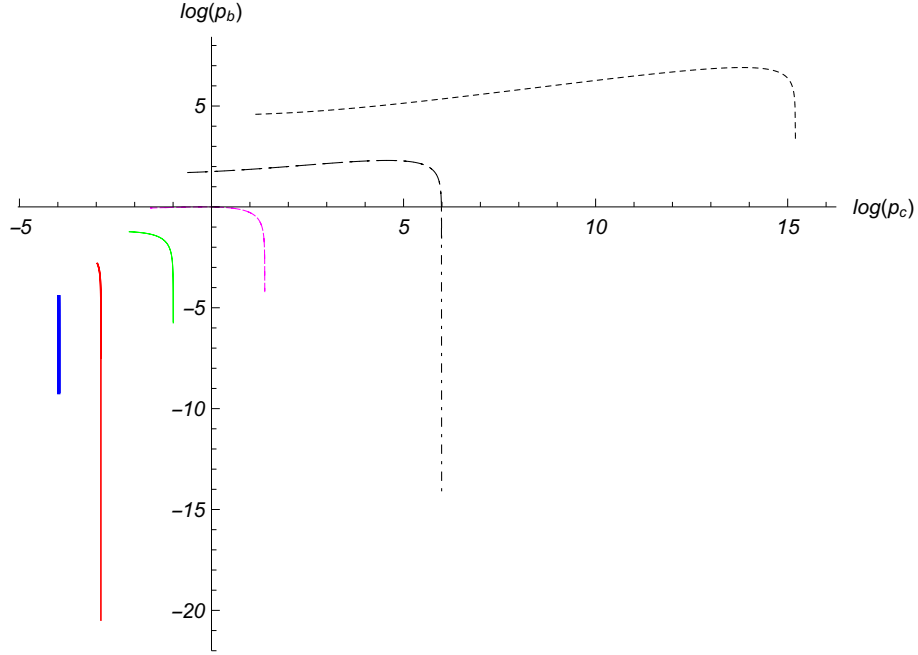


Figure 6.17: Choice 4: we plot the logarithmic of  $p_b$  as a function of the logarithm of  $p_c$  for different values of the mass  $M$ . The curves ranging from the thickest to the thinnest correspond to  $M = 0.05, 0.1, 0.3, 1, 10, 1000$ , in Planck units, respectively.

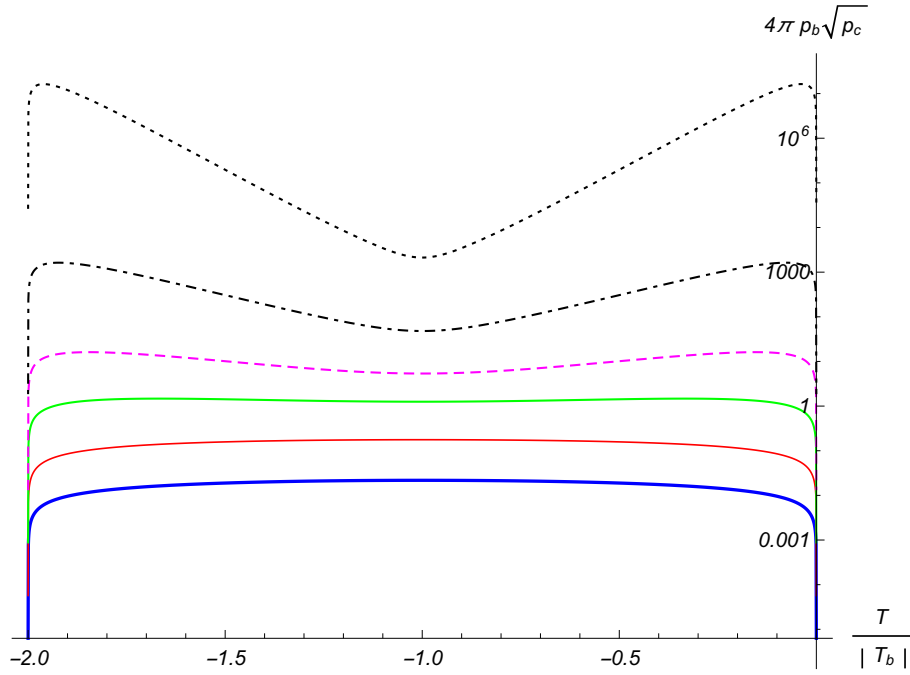


Figure 6.18: Choice 4: the evolution of the spatial volume as a function of the normalized time  $T/|T_b|$ . The curves ranging from the thickest to the thinnest correspond to  $M = 0.05, 0.1, 0.3, 1, 10, 1000$ , in Planck units, respectively.

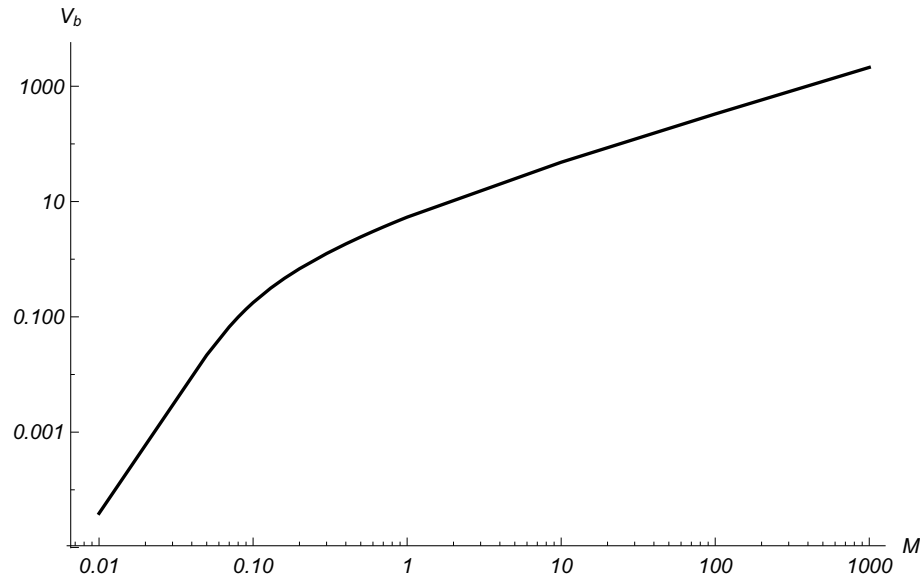


Figure 6.19: Choice 4: bounce volume as a function of mass.

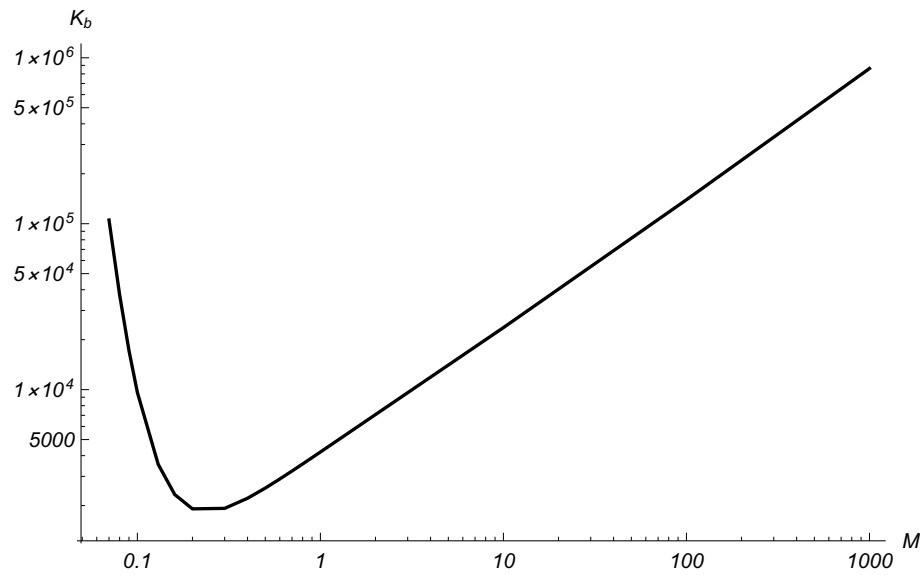


Figure 6.20: Choice 4: the value of the Kretschmann scalar at the bounce as a function of mass.

volume. As we see in Fig. 6.17, the value of  $p_b$  goes to zero at the horizon. Regarding  $p_c$ , due to quantum geometry corrections, its value at the horizon is slightly higher than its classical value  $(2GM)^2$ , as in the previous cases. The behavior of the spatial volume as a function of time and mass is very similar to the situation in choice 2. It shows the same peculiar behavior where the spatial volume for masses lower than a certain value is a convex function of time and reaches a global maximum (instead of a local minimum) at the bounce. This transition from normal to abnormal behavior is clearly indicated by the kink in the graph of bounce volume versus mass shown in Fig. 6.19, where we show the value of the spatial volume at the bounce as a function of the mass  $M$ . Furthermore, just like the asymmetric case and choice 2, the bounce volume turns out to be a monotonically growing function of the mass  $M$ . However, as shown in plot 6.20, the Kretschmann scalar at the bounce has a minimum and increases for both very low and very high mass black holes. Thus, even though the choice 4 seems quite similar to the choice 2, it surprisingly does not have the drawback of the CS quantization and choice 2 of producing bounce at low curvatures for large mass black holes.

Thus, we note that the choice 2 with  $\beta = 1$  leads to a symmetric bounce, but has the same drawback as the CS quantization of leading to low curvatures at the bounce for large mass black holes. Choice 2 and 3 on the other hand do not have this drawback while also lead to a symmetric bounce. However, for choices 3 and 4, the Kretschmann scalar increases unboundedly as the mass of the black hole increases. This is in contrast to results on universal bounds obtained in various LQC models of isotropic and homogeneous cosmologies on various quantities such as energy density, the expansion and shear scalars etc. From a conceptual point of view, it is desirable that a universal behavior is recovered in the deep Planck regime, which is indicated by the universal bounds on physical quantities obtained in other LQC models. Choices 2 and 3 suffer from this drawback where we do not have any universal bounds on the curvature at bounce for large masses.

It is interesting to compare these results with the AOS quantization prescription [223]. In the AOS quantization prescription, although the drawback of the CS quantization is removed, the bounce is only symmetric in large mass limit. In contrast, our choices 2, 3 and 4 lead an



exactly symmetric bounce for all values of the mass while also taking care of the drawback of the CS quantization. Furthermore, in choices 3 and 4, the Kretschmann scalar grows unboundedly for large masses. In contrast, the AOS quantization prescription leads to a mass independent value of the Kretschmann scalar at the bounce. In this regard, it is important to note that the values of  $\delta_b$  and  $\delta_c$  in the choices 3 and 4 here (and also the CS quantization) are the result of phenomenological considerations, while the AOS quantization prescription choices result from fundamental considerations by specifying the loops at the bounce surface.

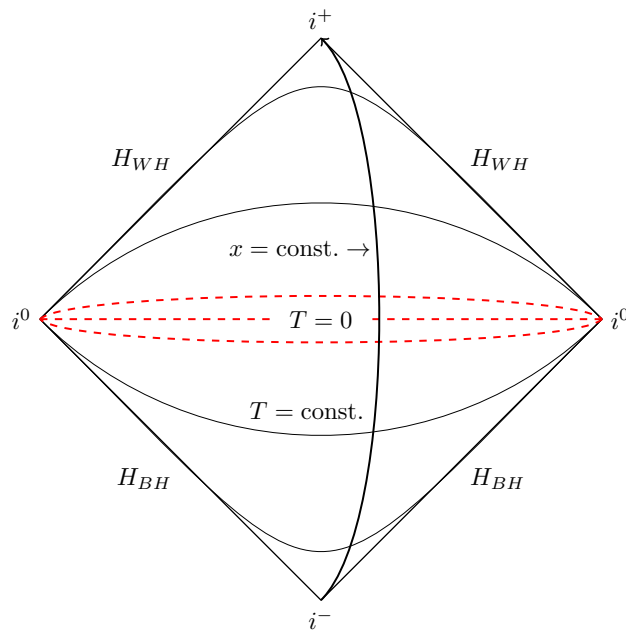


Figure 6.21: Penrose diagram for the interior of Schwarzschild spacetime undergoing symmetric bounce to white hole solution is shown.

Finally, for completeness, in Fig. 6.21 we include a Penrose diagram for the interior spacetime for these symmetric models. In the Penrose diagram, the black and white hole horizons are denoted by  $H_{BH}$  and  $H_{WH}$ , respectively. Horizontal curves represent Cauchy surfaces ( $T = \text{const.}$ ) while vertical curves denote  $x = \text{const.}$  observers. As usual,  $i^\pm$  represent  $T \rightarrow \pm T_{\text{hor}}$ , while  $i^0$  denotes  $x = 0$  and  $x = L_0$  (notice the symmetry of the diagram). A test observer which falls from the black hole horizon passes through the quantum gravitational regime, represented by red (shaded) dashed curves, and reaches the white hole horizon without encountering the classical singularity. Due to quantum geometric effects, the latter is removed from the effective spacetime. Due to the symmetric bounces in prescriptions I, II and III, the

$T = 0$  curve which represents the bounce time lies in the middle of the shaded regime. For the prescription in CS model, this region is not expected to be symmetric.

## 6.5 Conclusions

In this chapter, we have considered the black hole singularity of the Schwarzschild spacetime by considering the isomorphism between the Schwarzschild interior and the vacuum Kantowski–Sachs model. Various quantizations of the Schwarzschild model have been performed using this correspondence [178, 180, 190, 181, 269, 182, 221, 270, 271, 218, 222, 268], which showed that the singularity is resolved. However these earlier quantizations suffered from various drawbacks such as dependence of physical predictions such on fiducial structures and large quantum corrections at the horizon. To overcome these problems, quantizations of the vacuum Kantowski–Sachs spacetime by choosing the edge lengths  $\delta_b$  and  $\delta_c$  to be Dirac observables were obtained, namely the CS quantization [183], the OSS quantization prescription [273] studied here, and the most recent AOS quantization prescription [223]. The CS quantization led to a highly non-symmetric bounce where the white hole mass is a quartic power of the black hole mass, regardless of the mass of the black hole we start with. Moreover, the bounce can happen for the CS quantization at very low curvatures for large enough black holes as pointed out in [223]. Thus in this chapter (based on the OSS quantization prescription), we investigated whether the CS quantization can be modified to yield a symmetric bounce and also cure the drawback of the bounce at low curvature for large black holes. As we summarize below, we obtained exactly symmetric bounces in this chapter, but all our choices still suffered from undesirable behavior of the curvature at bounce in one way or another. These problems with the curvature at bounce were ameliorated eventually in the AOS quantization prescription [223], where the bounce is approximately symmetric.

We worked using the setting of Dirac observables to derive the equations of motion for the phase space variables of Kantowski–Sachs model when the edge lengths are assumed to be Dirac observables themselves. This way of approaching led to an easy identification of a symmetric bounce condition which needs to be satisfied by the edge lengths  $\delta_b$  and  $\delta_c$ . We considered a general ansatz for the choice of  $\delta_b$  and  $\delta_c$  which includes the CS quantization as a special case (however, our analysis is at the effective level and assumes the validity of the effective

dynamics, whereas the dynamics in the CS quantization is obtained from difference equations derived from the quantization of the Hamiltonian constraint). The assignment of the minimum area of the loops in our case, over which holonomies are considered, has some freedom which we parameterized using  $\alpha$  and  $\beta$ . Then given the mass of the black hole,  $\alpha$  and  $\beta$  can be fixed such that the symmetric bounce condition is satisfied and the child white hole mass turns out to be identical to the mother black hole mass. By considering three different choices of the edge lengths as well as the CS choice, we demonstrate that a symmetric bounce can indeed be obtained. We also show that the CS quantization does not satisfy the symmetric bounce condition and thus gives an asymmetric bounce.

It is notable that the features of the effective dynamics for very small masses (less than Planck mass) are essentially similar for all the choices considered in this chapter. In all of the choices the bounce volume is a non-linear function of the black hole mass, and a non-monotonic function in choice 3. There exists a smallest mass, approximately  $M \sim 0.1$ , below which effective dynamics does not permit a black hole solution. This is actually in good agreement with recent quantizations of the full spherically symmetric spacetime [196, 197]. On the other hand, for small masses such that the Schwarzschild radius is of the order or smaller than the discreteness scale, the bounce in the interior is replaced by a recollapse. The dynamics of such microscopic black holes could be purely quantum with no classical analog, thus we cannot trust the validity of the effective dynamics in this regime. The behavior of the volume at the bounce also shows a non-trivial behavior as function of the mass of the black hole. While it monotonically increases for choices 2 and 4, the bounce volume for choice 3 decreases in the limit of both small and large black hole masses. And further, plots of the Kretschmann scalar show that for two of the choices considered by us, namely choices 3 and 4, the curvature at the bounce does not decrease to low values for large enough black hole masses in contrast to the CS quantization, thus overcoming that limitation as well in addition to giving a symmetric bounce.

To compare our results with the AOS quantization prescription [223], first we note that in the AOS quantization prescription, the bounce is not exactly symmetric. Although it becomes almost symmetric for black hole masses larger than few hundred Planck masses for the AOS

quantization prescription. Whereas our choices give an exactly symmetric bounce for all masses. Two of our choices overcome the limitation of the CS quantization and also lead to a symmetric bounce. However, in these choices, the curvature at bounce can be made arbitrarily large by considering large enough black hole mass. On the other hand, in the AOS quantization prescription, the curvature has a well defined, mass independent value at the bounce surface. In this context, it should be noted that while the CS effective dynamics is obtained from a full quantization of the Schwarzschild interior spacetime, the OSS quantization prescription is phenomenologically inspired from considerations of a symmetric bounce. The AOS quantization, while also phenomenological, results from fundamental considerations of the bounce surface. Another major limitation of the quantization considered here is that it only covers the interior of the Schwarzschild spacetime. The effective spacetime of the AOS quantization prescription on the other hand has been successfully extended to the exterior Schwarzschild spacetime (however, there is a caveat to this extension, namely the exterior spacetime is quantized using  $SU(1,1)$  connections in contrast to the  $SU(2)$  connections usually used in LQG and LQC). Nevertheless, our approach provides a method for studying the phenomenological aspects of the symmetry or asymmetry of quantum bounces in LQC and can be applied to other spacetimes with asymmetric bounces such as loop quantized Bianchi-I models to understand the possibility of symmetric bounces there.

We conclude by pointing out that the CS quantization, the OSS scheme explored in this chapter, and the AOS scheme (and other studies based on Kantowski–Sachs model) study singularity resolution in the static black hole solution by exploiting the isomorphism with vacuum Kantowski–Sachs model. This involves a particular homogeneous foliation of the Schwarzschild spacetime which avoids certain problems with the constraint algebra faced in the full theory. However, as we have mentioned above, there are other approaches based on midi-superspace models obtained by reduction of the full LQG variables to the spherically symmetric case. In this case, one faces an obstruction in completing the quantization program which is inherited from the same problem in the full theory. Namely, the algebra of constraints involves structure functions instead of structure constants and hence does not form a true Lie algebra. This

prevents the full implementation of the quantization program. In contrast, in the studies using the Kantowski–Sachs spacetime as the Schwarzschild interior such as ours, a gauge-fixing allows identification with the spatially homogeneous foliation of the Kantowski–Sachs model where this problem of the full theory is absent. Nevertheless, by suitably re-expressing the Hamiltonian constraint in these spherically symmetric midi-superspace models, it has been possible to solve the constraint algebra and construct the physical Hilbert space to study the dynamics using Dirac variables, and it has been observed that the central singularity is replaced by a bounce [128, 252, 191, 290, 291, 196, 197, 292, 293]. Moreover, the whole Schwarzschild spacetime including the exterior and interior regions is covered by these quantizations. Phenomenological effects such as the Casimir effect [297] and Hawking radiation [298, 299] have been studied on these loop quantized spherically symmetric spacetimes. These studies have also been extended to charged black hole case [300]. Further work towards generalizing these models to a formulation closer to the full theory is also under way [301, 302].

Noting that astrophysical black holes are formed in nature by the collapse of massive stars, the spherically symmetric midi-superspace approach has also been used to study loop quantized models of collapsing dust shells [294, 295]. The study of statistical properties of black hole horizons has also been explored from the point of view of isolated horizons, and a quantum description of isolated horizons has been obtained [303, 304]. Further, the calculations of the black hole entropy in LQG using various different methods have been shown to yield the Bekenstein–Hawking formula in the large mass limit, which has been utilized to fix the value of the Barbero–Immirzi parameter [305, 306, 307, 308, 309, 310, 311, 312]. Recently, attempts have been made to obtain the effective Hamiltonian for black hole dynamics directly from the full theory by performing symmetry reduction at the quantum level using semiclassical states [296]. Thus the question of the black hole singularity is being pursued from various different points of view as the canonical quantization paradigm of LQG seems to be maturing to the stage where we can begin to address the question of the black hole singularity using a fundamentally quantum description and obtain phenomenological consequences.

## Chapter 7

### Conclusions

The primary motivation to study quantum cosmology comes from the realization that quantum cosmology is essential to answer some of the fundamental questions regarding the origins of our universe, and is also intimately tied with the problem of singularities as most of the cosmological models of interest in GR have an initial cosmological singularity. Thus, in cosmology, we face both of these challenges at once, which are linked to each other. And it is quite possible that solving the problem of singularities in cosmological models might shed some light on the origins (and the ultimate fate) of the universe as well. We have also entered the era of precise cosmological observations which may throw up new and interesting features of the early universe and can also help verify the predictions of our theoretical meditations. Thus, investigations in quantum cosmology, specially the problem of singularities, seems timely and is expected to be fruitful. Keeping this in mind, in this dissertation, we have applied the techniques of LQC to the problem of singularities in the cosmological and black hole models. In this endeavor, the problem of quantization ambiguities also appears to be of importance as it seems to have a non-trivial effect on both the question of resolution of singularities, the phenomenological details of the resulting model and hence the detailed predictions.

The field of LQC is the application of ideas and techniques of LQG to symmetry reduced cosmological models. LQG is a non-perturbative canonical quantization of GR using Ashtekar's triad and connection variables [45, 46, 48]. The holonomies of the connection provide a natural gauge invariant choice for the configuration variables for quantization and the fluxes of the triad variables across two dimensional surfaces turn out to be the conjugate variables. And the requirement of diffeomorphism invariance selects a unique representation of the quantum algebra based on these variables [313, 314]. Thus quantization proceeds by first reformulating GR in terms of these variables. While the work of completing the quantization for the full LQG is still in progress, application of these ideas to classically symmetry reduced cosmological models

has led to a great number of insights into the possible phenomenological effects and the fate of singularities in quantum gravity.

LQC of homogeneous and isotropic cosmologies has shown that the big bang cosmological singularity is replaced by a quantum bounce connecting the present expanding universe to a past contracting universe, and that there is an effective continuum description which approximates the effects of underlying discrete quantum geometry very well [257]. Similar results on singularity resolution and bounce have since been obtained in various homogeneous cosmological models and black hole spacetimes [315, 312]. Due to lack of a clear link with the full theory at the moment, symmetry reduction at the classical level and different choices during quantization lead to various quantization ambiguities in LQC models. Furthermore, these ambiguities have been found to lead to actual qualitative differences in the physical predictions. For example, in the homogeneous and isotropic FLRW models, the earlier  $\mu_o$  type quantization led to the fiducial structure dependent predictions and did not yield the correct infrared limit [316], which was later replaced by the  $\bar{\mu}$  type improved quantization to overcome these shortcomings. Further, the symmetric bounce in both these quantizations was replaced by a non-symmetric bounce when a more careful quantization of the FLRW models closer to the full theory was recently carried out [317, 318]. Thus, it is now well understood that the question of quantization ambiguities is intimately tied to the physics predicted by the quantization. Moreover, using the effective description, geodesic completeness and generic resolution of strong singularities has been shown in the isotropic [214, 266] and Bianchi-I models [217].

In this dissertation, we have focused on obtaining the generic resolution of singularities in the effective dynamics of important anisotropic and homogeneous cosmological models beyond the Bianchi-I model, such as the Bianchi-II, Bianchi-IX and Kantowski–Sachs models. Using the Kantowski–Sachs model, we also explore the possibility of a symmetric bounce in the resolution of black hole singularity as obtained in LQC. Recognizing the importance of understanding the effects of quantization ambiguities, we also explore the implications of various quantization ambiguities on the resolution of singularities in all these models. The importance of these anisotropic and homogeneous models is well accepted in understanding the generic features of

singularity resolution due to the BKL conjecture in GR [125], which states that in the vicinity of a generic singularity, the spatial derivatives in the Einstein's equations become negligible compared to the time derivatives such that the spacetime dynamics at each point can be well approximated by homogeneous cosmological models. Specifically, the approach to singularity is marked by phases resembling Bianchi-I model which are connected through Bianchi-II transitions. This kind of chaotic oscillatory approach to the singularity in the BKL scenario is also seen in the Mixmaster dynamics in the Bianchi-IX models [58]. These models are also potentially important in the description of the very early universe, thus an analysis of singularities in these models has important implications for the question of initial conditions for our universe. These models also allow us to study the important features of the loop quantization when both spatial curvature and anisotropy are present. In addition, the isomorphism between the Schwarzschild interior spacetime and the vacuum Kantowski–Sachs model can be exploited to study the resolution of the black hole singularity using the Kantowski–Sachs model.

We explored generic singularity resolution in the effective dynamics of the Bianchi-II model with minimally coupled matter in chapter 3. Unlike the isotropic and homogeneous FLRW model and the Bianchi-I model, the spatial slices in Bianchi-II model have both anisotropy and spatial curvature, which presents difficulties in performing the steps of quantization as followed in isotropic and Bianchi-I models. Specifically, the holonomies of the connection around closed loops does not yield an algebra of almost periodic functions which do not have a simple representation as operators on the kinematical Hilbert space of LQC. To overcome this, an operator corresponding to the connection itself is defined using holonomies of the Ashtekar connection along straight edges, and the homogeneity of the model is used to establish correspondence with the quantizations of the earlier models in suitable limits [231, 232, 174]. This leads to the so called ‘A’ quantization. Another approach to the quantization problem was inspired from a strategy employed in the quantization of isotropic models where problems were faced in going from spatially flat to spatially curved models. Unlike the full theory, due to symmetry reduction in LQC models, the extrinsic curvature can be treated as a connection, and we can use its holonomies (instead of the Ashtekar connection) to obtain the operator corresponding to the



Hamiltonian constraint [139, 250, 160, 251]. This quantization is called the ‘K’ quantization. In Bianchi-II model, both the ‘A’ and ‘K’ quantizations are viable, and we have considered the effective dynamics of both in chapter 3. While the effective Hamiltonian for the ‘A’ quantization of the Bianchi-II model was already available in the literature [174], we obtain the effective dynamics of the ‘K’ quantization for Bianchi-II model for our purposes. Using the effective dynamics, we were able to show geodesic completeness and generic resolution of singularities in both these quantizations. Building up on previous results showing boundedness of Hubble rates, expansion and shear scalars and energy density [215], we show that the triad variables (and hence the directional scale factors) remain finite for all finite time evolution. The volume remains non-zero and finite for all finite time evolution. Though some curvature invariants such as the Ricci scalar and the Kretschmann scalar may potentially diverge, we show that the geodesics will remain well-defined at such events. We also show that the geodesics remain regular at events where they break down classically due to the cosmological singularity, and show that the geodesics are maximally extendable. And using the necessary conditions for occurrence of strong curvature singularities provided by Clarke and Krolak [230], we show that the effective spacetime is free from all strong curvature singularities. (Recall that singularities which are not strong are harmless events beyond which geodesics can be shown to be extended). We are able to show all these results for the effective Bianchi-II model in both ‘A’ and ‘K’ quantizations, however, there were striking differences in the two cases. In the ‘A’ quantization, using holonomy corrections in the effective dynamics was not sufficient to obtain the results, and we needed to either include inverse triad corrections, or impose weak energy conditions (WEC) to achieve singularity resolution. In this context, it is important to remember that quantum gravity effects enter the effective description through two types of corrections- the holonomy corrections from expressing all the functions of the connection using holonomies, and the inverse triad corrections emerging from the discrete and non-singular spectrum of the inverse triad operators in LQG. In isotropic and Bianchi-I models, singularity resolution in the effective description could be obtained primarily due to the holonomy corrections and inverse triad corrections played a negligible role. Our results in the Bianchi-II model in the ‘A’ quantization are quite contrasting and

indicate that inverse triad corrections may play an indispensable role in singularity resolution in general spacetimes. We also find that energy conditions on the matter content, which have also been used in the singularity theorems of GR, may also play a role in a generic singularity resolution result in LQC. In contrast, the results on geodesic completeness and generic singularity resolution could be obtained in the ‘K’ quantization without needing the help of inverse triad corrections or weak energy conditions. Thus, the ‘K’ quantization seemed to be more adept at yielding singularity resolution. This extends the results on generic singularity resolution in the effective spacetimes of isotropic and Bianchi-I models to the Bianchi-II model.

The contrast in the ‘A’ and ‘K’ quantization gets further enhanced in the case of Bianchi-IX model for which both of these quantization are viable. Due to the presence of anisotropy and spatial curvature, the same problem as Bianchi-II model is faced in quantizing Bianchi-IX model on the lines of the procedure followed in isotropic and Bianchi-I models. Thus quantizations following the strategies of ‘A’ and ‘K’ quantizations have been performed for the Bianchi-IX model in the literature [175, 176]. However, similar to the effective Bianchi-II case, holonomy corrections alone are not able to ensure the boundedness of energy density, Hubble rates, expansion and shear scalars in the effective Bianchi-IX model in the ‘A’ quantization. Moreover, even imposing energy conditions on the matter content is not sufficient to obtain generic boundedness properties of these key physical quantities in this case. Thus, it had not been possible to make progress towards generic singularity resolution in the effective Bianchi-IX model in the ‘A’ quantization. In contrast, it had been shown using the effective dynamics of the ‘K’ quantization that the expansion and shear scalars, and the Hubble rates are generically bounded, while generic bounds on energy density could not be established [176]. In chapter 4, we include the effects of inverse triad modifications in the effective Hamiltonian of ‘A’ quantization to show that the triad variables, the energy density, the Hubble rates, the expansion and shear scalars remain finite, and the volume remains non-zero and finite, for all finite time evolution. Moreover, in the case of ‘K’ quantization, we obtain these results without having to include inverse triad corrections. We indicate that some curvature invariants such as the Ricci scalar and the Kretschmann scalar may still diverge, but show that the geodesics remain well-defined at such events. We

further show that the effective spacetime in both ‘A’ quantization with inverse triad corrections and the ‘K’ quantization is free from strong singularities. We conclude the chapter by noting that inverse triad corrections are likely to play an important role in singularity resolution in more general spacetimes if ‘A’ quantization is considered. In contrast, it remains unclear what role, if any, will energy conditions play in singularity resolution in more general spacetimes. The ‘K’ quantization again yields singularity resolution with relative ease without the input of inverse triad corrections, thus indicating that there might be some merit to considering extrinsic curvature based quantization of classical gravity.

In chapter 5, we move on to another homogeneous cosmological model which has both anisotropy and spatial curvature- the Kantowski–Sachs model. The Kantowski–Sachs model is also significant as, in vacuum, it is isomorphic to the Schwarzschild interior spacetime. Due to special symmetries of the Kantowski–Sachs model, the ‘A’ and ‘K’ quantizations turn out to be equivalent [178]. In chapter 5, we investigate the effective dynamics of the Kantowski–Sachs model in the presence of matter, in which case, there is both an initial cosmological singularity and a future cosmological singularity. This becomes the point of departure from the analysis of the vacuum Kantowski–Sachs spacetime as a model of the Schwarzschild interior, as in the absence of matter, the future singularity described above is no longer a singularity, instead corresponds to the black hole horizon where energy density and curvature remain regular. In chapter 5, we consider a quantization that suits the Kantowski–Sachs model with matter, and also gives fiducial structure independent physical predictions. It is called the Boehmer–Vandersloot quantization [182] and is based on the founding work [178] with a specific choice of the edge lengths  $\delta_b$  and  $\delta_c$  as functions of phase space variables. In this respect, it is similar to the  $\bar{\mu}$  type improved quantization of the isotropic cosmological models. Building on previous work [218], where the boundedness of the Hubble rates, the expansion and shear scalars was already established for the effective dynamics of the Boehmer–Vandersloot quantization, we show in chapter 5 that the triad variables and the energy density remain finite for all finite time evolution, and the spatial volume remains finite and non-zero for all finite time evolution. Further, it is shown that some curvature invariants may still diverge, but we point out that such

divergences are harmless and only amount to weak singularities. Specifically, we show that the effective Kantowski–Sachs model is geodesically complete and geodesics remain well-defined at such potential divergences. Moreover, we show that the effective Kantowski–Sachs spacetime in the Boehmer–Vandersloot quantization is free from strong singularities.

In chapter 6, our goal is to consider the Schwarzschild interior spacetime by using its correspondence with the vacuum Kantowski–Sachs model. As pointed out above, the  $\bar{\mu}$  type quantization, which is suited in the presence of matter, does not distinguish the coordinate singularity at the horizon in the Schwarzschild spacetime from a real singularity, and thus leads to large quantum gravity effects at the horizon. The horizon could be at very low curvatures for large enough black holes, implying that we would have large quantum effects at low curvatures. This is undesirable as classical GR is expected to describe the universe very well at low curvatures. Keeping this in mind, quantizations of the Kantowski–Sachs model based on considering the edge lengths as non-trivial Dirac observables, and carefully establishing correspondence with the length scales of the Schwarzschild spacetime have succeeded in overcoming the shortcoming of large quantum effects at the horizon while maintaining fiducial structure independence in physical predictions. These are the CS [183], the OSS [273] and AOS quantizations [223]. The black hole singularity is replaced in these quantizations by a quantum bounce connecting to a white hole on the other side. However, the bounce in the CS quantization was discovered to be highly asymmetric where the mass of the child white hole is a quartic power of the mass of the parent black hole. Moreover, the curvature at the bounce can be very low in the CS quantization. In chapter 6 based on the OSS quantization, we investigate whether it is possible to modify the CS quantization to accommodate a symmetric bounce and whether this modification alleviates the shortcomings of the CS quantization of leading to bounce at low curvatures for large mass black holes. We start with identifying the Dirac observables and their corresponding momenta, and use them as our new phase space variables. By gauge-fixing one of the momenta as the time variable, we find the corresponding lapse function and the equations of motion for the triad and connection variables as a function of this time. Getting the equations of motion in this form allows us to identify a symmetric bounce condition that needs to be satisfied by the edge lengths

$\delta_b$  and  $\delta_c$ . After showing that the symmetric bounce condition is not satisfied by the CS quantization, we add two parameters  $\alpha$  and  $\beta$  to the CS choice of edge lengths, which we determine using the symmetric bounce condition. We proceed to consider three different choices, (i)  $\beta = 1$ , (ii)  $\alpha = 1$  and (iii)  $\alpha = 1/\beta$ . Solving the symmetric bounce condition to obtain the remaining parameter, we obtain exactly symmetric bounces in all three choices. However, choice (i) has the same drawback of leading to bounces at low curvatures for large mass black holes. In choices (ii) and (iii), the curvature at the bounce is always Planckian, however, it grows unboundedly as the mass of the black hole grows in the large mass limit. In comparison, the recent AOS quantization leads to universal bounds in the curvature at bounce in the large mass limit, which is in line with earlier results on universal bounds in LQC of isotropic and homogeneous models. The AOS quantization also leads to an almost symmetric bounce for black hole masses larger than a few hundred Planck masses. Thus, none of the choices overcome all the shortcomings. Nevertheless, our analysis provides a way of obtaining symmetric bounces which can be applied to other spacetimes as well where the possibility of symmetric bounces can be explored. Also the reduced phase space description obtained using the Dirac observables can be used to obtain yet another quantization of the Kantowski–Sachs model.

Our work in this dissertation generalizes the results on generic singularity resolution in the effective LQC dynamics of the isotropic [214, 266] and Bianchi-I models [217] to Bianchi-II, Bianchi-IX and Kantowski–Sachs models with minimally coupled matter. We discussed the quantization ambiguities and the possible viable quantizations of these models and compared the results against those quantization ambiguities to obtain insights into the suitability of various different quantizations for singularity resolution. Further, for the black hole singularity in the Schwarzschild interior spacetime, building on the previous work [183], we were able to prescribe a symmetric bounce condition and obtain quantization prescriptions which yield an exactly symmetric bounce with fiducial structure independent predictions and no large scale quantum effects at the horizon, although the curvature at the bounce is not universally bounded in the choices considered by us. The work presented in this dissertation can be naturally extended in various directions. We describe some of them below.

A natural step will be to move forward towards more general spacetimes than considered in this thesis, in particular inhomogeneous spacetimes, and prove generic resolution of singularities. This will shed more light on the role of inhomogeneities near a generic quantum bounce. A simple class of inhomogeneous models called Gowdy models, which contain the Bianchi-I model as their homogeneous limit, have already been quantized using a hybrid quantization [186, 185] where the homogeneous sector represented by Bianchi-I models is loop quantized and the inhomogeneities which can be seen as propagating on this homogeneous background are Fock quantized. It is shown that such a quantization is self-consistent and preliminary investigations show that the effective spacetime obtained in this case is free from cosmological singularities. Further, the full loop quantization of the local rotationally symmetric Gowdy models has also been carried out recently [188]. Further work on analyzing various quantization ambiguities and proving generic singularity resolution in these models is needed, which will allow us to move towards more complex models and eventually to a general model independent non-singularity result in LQC.

The loop quantized Bianchi-IX model can be used to numerically probe generic singularity resolution and investigate the BKL phenomena in the loop quantized models. The numerical investigations on the Bianchi-I model show that the bounce in the loop quantized Bianchi-I model can be considered as a Kasner transition similar to Kasner transitions in the BKL scenario [247]. Using these results, recent analytical investigations [319, 320] in the loop quantized Bianchi-IX model based on heuristic arguments extend the Mixmaster dynamics observed in the classical Bianchi-IX model [127] beyond the Kasner transition like LQC bounce. Numerical investigations can be used to verify these results and provide more details of the dynamics. Moreover, if rigorous quantizations of the inhomogeneous cosmological models are obtained, then numerical investigations can be used to verify the BKL conjecture in LQC using the Hamiltonian formulation of the BKL conjecture provided in [321].

In chapter 6 on the Schwarzschild spacetime, we explored a few intuitive and simple choices for the edge lengths as Dirac observables which satisfied the symmetric bounce condition. However, the behavior of the curvature at bounce seems to be a limitation of these choices. While

it decreases to low curvatures for large black holes for one of the choices, it remains Planckian for the other two choices and increases unboundedly in the large mass limit. However, we have only considered a few choices. The space of solutions of the symmetric bounce condition can be further explored to investigate whether a symmetric bounce can be obtained while also giving universal bounds on the curvature. It will be fruitful even if a negative result could be proved to rule out the viability of an exactly symmetric bounce for the black hole singularity in LQC. Further, various phenomenological properties such as Hawking radiation and entropy bounds of these quantizations as well as CS and AOS quantizations of the black hole spacetime can be investigated.

Another interesting but challenging direction is to investigate the question of quantization ambiguities coming from the perspective of LQG. Our work in this dissertation substantiates the insight from earlier studies in LQC that quantization ambiguities lead to important qualitative differences in the predictions. We noted the contrast in the ‘A’ and ‘K’ quantization in the Bianchi-II and Bianchi-IX models. In the case of the Schwarzschild interior, we found that different choices of edge lengths led to phenomenological differences in predictions. One way to address the question of quantization ambiguities can be to obtain the effective Hamiltonian for a given cosmological model from the full theory by symmetry reduction at the quantum level. Studies using semi-classical states to obtain effective Hamiltonian for the spatially flat FLRW model from the Hamiltonian of LQG [318] have recently shown that some of the quantizations of the flat FLRW model are closer [317] to the full theory than others. Thus using such methods, the question of quantization ambiguities can be addressed more decisively.





# Appendix A

## Permissions from IOP Publishing Ltd.

11/7/2018

RightsLink Printable License

### IOP Publishing LICENSE TERMS AND CONDITIONS

Nov 07, 2018

This is a License Agreement between SAHIL SAINI ("You") and IOP Publishing ("IOP Publishing") provided by Copyright Clearance Center ("CCC"). The license consists of your order details, the terms and conditions provided by IOP Publishing, and the payment terms and conditions.

**All payments must be made in full to CCC. For payment instructions, please see information listed at the bottom of this form.**

License Number	4445430692059
License date	Sep 28, 2018
Licensed content publisher	IOP Publishing
Licensed content title	Classical and Quantum Gravity
Licensed content date	Jan 1, 1984
Type of Use	Thesis/Dissertation
Requestor type	Author of requested content
Format	Print, Electronic
Portion	chapter/article
The requesting person/organization is:	Sahil Saini
Title or numeric reference of the portion(s)	The whole article
Title of the article or chapter the portion is from	Resolution of strong singularities and geodesic completeness in loop quantum Bianchi-II spacetimes
Editor of portion(s)	N/A
Author of portion(s)	Sahil Saini and Parampreet Singh
Volume of serial or monograph.	34
Page range of the portion	
Publication date of portion	10 November 2017
Rights for	Main product
Duration of use	Life of current and all future editions
Creation of copies for the disabled	no
With minor editing privileges	yes
For distribution to	Worldwide
In the following language(s)	Original language of publication
With incidental promotional use	no
The lifetime unit quantity of new product	Up to 499
Title	SINGULARITY RESOLUTION IN ANISOTROPIC AND BLACK HOLE

## SPACETIMES IN LOOP QUANTUM COSMOLOGY

**Instructor name** Professor Parampreet Singh  
**Institution name** Louisiana State University, Baton Rouge, LA - 70803  
**Expected presentation date** Dec 2018  
**Billing Type** Invoice  
**Billing Address** SAHIL SAINI  
 202, Nicholson Hall

Baton Rouge, LA 70803  
 United States  
 Attn: SAHIL SAINI

**Total (may include CCC user fee)** 0.00 USD

**Terms and Conditions**

### TERMS AND CONDITIONS

#### The following terms are individual to this publisher:

These special terms and conditions are in addition to the standard terms and conditions for CCC's Reproduction Service and, together with those standard terms and conditions, govern the use of the Works.

As the "User" you will make all reasonable efforts to contact the author(s) of the article which the Work is to be reused from, to seek consent for your intended use. Contacting one author who is acting expressly as authorised agent for their co-author(s) is acceptable. User will reproduce the following wording prominently alongside the Work:

- the source of the Work, including author, article title, title of journal, volume number, issue number (if relevant), page range (or first page if this is the only information available) and date of first publication. This information can be contained in a footnote or reference note; and
- a link back to the article (via DOI); and
- if practicable, and IN ALL CASES for new works published under any of the Creative Commons licences, the words "© IOP Publishing. Reproduced with permission. All rights reserved"

Without the express permission of the author(s) and the Rightsholder of the article from which the Work is to be reused, User shall not use it in any way which, in the opinion of the Rightsholder, could: (i) distort or alter the author(s)' original intention(s) and meaning; (ii) be prejudicial to the honour or reputation of the author(s); and/or (iii) imply endorsement by the author(s) and/or the Rightsholder.

This licence does not apply to any article which is credited to another source and which does not have the copyright line '© IOP Publishing Ltd'. User must check the copyright line of the article from which the Work is to be reused to check that IOP Publishing Ltd has all the necessary rights to be able to grant permission. User is solely responsible for identifying and obtaining separate licences and permissions from the copyright owner for reuse of any such third party material/figures which the Rightsholder is not the copyright owner of. The Rightsholder shall not reimburse any fees which User pays for a republication license for such third party content.

This licence does not apply to any material/figure which is credited to another source in the Rightsholder's publication or has been obtained from a third party. User must check the Version of Record of the article from which the Work is to be reused, to check whether any of the material in the Work is third party material. Third party citations and/or copyright notices and/or permissions statements may not be included in any other version of the article from which the Work is to be reused and so cannot be relied upon by the User. User is solely

## IOP Publishing LICENSE TERMS AND CONDITIONS

Nov 07, 2018

This is a License Agreement between SAHIL SAINI ("You") and IOP Publishing ("IOP Publishing") provided by Copyright Clearance Center ("CCC"). The license consists of your order details, the terms and conditions provided by IOP Publishing, and the payment terms and conditions.

**All payments must be made in full to CCC. For payment instructions, please see information listed at the bottom of this form.**

License Number	4445430813669
License date	Sep 28, 2018
Licensed content publisher	IOP Publishing
Licensed content title	Classical and Quantum Gravity
Licensed content date	Jan 1, 1984
Type of Use	Thesis/Dissertation
Requestor type	Author of requested content
Format	Print, Electronic
Portion	chapter/article
The requesting person/organization is:	Sahil Saini
Title or numeric reference of the portion(s)	The whole article
Title of the article or chapter the portion is from	Generic absence of strong singularities in loop quantum Bianchi-IX spacetimes
Editor of portion(s)	N/A
Author of portion(s)	Sahil Saini and Parampreet Singh
Volume of serial or monograph.	35
Page range of the portion	
Publication date of portion	21 February 2018
Rights for	Main product
Duration of use	Life of current and all future editions
Creation of copies for the disabled	no
With minor editing privileges	yes
For distribution to	Worldwide
In the following language(s)	Original language of publication
With incidental promotional use	no
The lifetime unit quantity of new product	Up to 499
Title	SINGULARITY RESOLUTION IN ANISOTROPIC AND BLACK HOLE

## SPACETIMES IN LOOP QUANTUM COSMOLOGY

**Instructor name** Professor Parampreet Singh  
**Institution name** Louisiana State University, Baton Rouge, LA - 70803  
**Expected presentation date** Dec 2018  
**Billing Type** Invoice  
**Billing Address** SAHIL SAINI  
 202, Nicholson Hall

Baton Rouge, LA 70803  
 United States  
 Attn: SAHIL SAINI

**Total (may include CCC user fee)** 0.00 USD

**Terms and Conditions**

### TERMS AND CONDITIONS

#### The following terms are individual to this publisher:

These special terms and conditions are in addition to the standard terms and conditions for CCC's Reproduction Service and, together with those standard terms and conditions, govern the use of the Works.

As the "User" you will make all reasonable efforts to contact the author(s) of the article which the Work is to be reused from, to seek consent for your intended use. Contacting one author who is acting expressly as authorised agent for their co-author(s) is acceptable. User will reproduce the following wording prominently alongside the Work:

- the source of the Work, including author, article title, title of journal, volume number, issue number (if relevant), page range (or first page if this is the only information available) and date of first publication. This information can be contained in a footnote or reference note; and
- a link back to the article (via DOI); and
- if practicable, and IN ALL CASES for new works published under any of the Creative Commons licences, the words "© IOP Publishing. Reproduced with permission. All rights reserved"

Without the express permission of the author(s) and the Rightsholder of the article from which the Work is to be reused, User shall not use it in any way which, in the opinion of the Rightsholder, could: (i) distort or alter the author(s)' original intention(s) and meaning; (ii) be prejudicial to the honour or reputation of the author(s); and/or (iii) imply endorsement by the author(s) and/or the Rightsholder.

This licence does not apply to any article which is credited to another source and which does not have the copyright line '© IOP Publishing Ltd'. User must check the copyright line of the article from which the Work is to be reused to check that IOP Publishing Ltd has all the necessary rights to be able to grant permission. User is solely responsible for identifying and obtaining separate licences and permissions from the copyright owner for reuse of any such third party material/figures which the Rightsholder is not the copyright owner of. The Rightsholder shall not reimburse any fees which User pays for a republication license for such third party content.

This licence does not apply to any material/figure which is credited to another source in the Rightsholder's publication or has been obtained from a third party. User must check the Version of Record of the article from which the Work is to be reused, to check whether any of the material in the Work is third party material. Third party citations and/or copyright notices and/or permissions statements may not be included in any other version of the article from which the Work is to be reused and so cannot be relied upon by the User. User is solely

## IOP Publishing LICENSE TERMS AND CONDITIONS

Nov 07, 2018

This is a License Agreement between SAHIL SAINI ("You") and IOP Publishing ("IOP Publishing") provided by Copyright Clearance Center ("CCC"). The license consists of your order details, the terms and conditions provided by IOP Publishing, and the payment terms and conditions.

**All payments must be made in full to CCC. For payment instructions, please see information listed at the bottom of this form.**

License Number	4437661353387
License date	Sep 27, 2018
Licensed content publisher	IOP Publishing
Licensed content title	Classical and Quantum Gravity
Licensed content date	Jan 1, 1984
Type of Use	Thesis/Dissertation
Requestor type	Author of requested content
Format	Print, Electronic
Portion	chapter/article
The requesting person/organization is:	Sahil Saini
Title or numeric reference of the portion(s)	The whole article
Title of the article or chapter the portion is from	Geodesic completeness and the lack of strong singularities in effective loop quantum Kantowski-Sachs spacetime
Editor of portion(s)	N/A
Author of portion(s)	Sahil Saini and Parampreet Singh - jointly
Volume of serial or monograph.	N/A
Page range of the portion	
Publication date of portion	1 December 2016
Rights for	Main product
Duration of use	Life of current and all future editions
Creation of copies for the disabled	no
With minor editing privileges	yes
For distribution to	Worldwide
In the following language(s)	Original language of publication
With incidental promotional use	no
The lifetime unit quantity of new product	Up to 499
Title	SINGULARITY RESOLUTION IN ANISOTROPIC AND BLACK HOLE

## SPACETIMES IN LOOP QUANTUM COSMOLOGY

**Instructor name** Professor Parampreet Singh  
**Institution name** Louisiana State University, Baton Rouge, LA - 70803  
**Expected presentation date** Dec 2018  
**Billing Type** Invoice  
**Billing Address** SAHIL SAINI  
 202, Nicholson Hall

Baton Rouge, LA 70803  
 United States  
 Attn: SAHIL SAINI

**Total (may include CCC user fee)** 0.00 USD

**Terms and Conditions**

### TERMS AND CONDITIONS

#### The following terms are individual to this publisher:

These special terms and conditions are in addition to the standard terms and conditions for CCC's Reproduction Service and, together with those standard terms and conditions, govern the use of the Works.

As the "User" you will make all reasonable efforts to contact the author(s) of the article which the Work is to be reused from, to seek consent for your intended use. Contacting one author who is acting expressly as authorised agent for their co-author(s) is acceptable. User will reproduce the following wording prominently alongside the Work:

- the source of the Work, including author, article title, title of journal, volume number, issue number (if relevant), page range (or first page if this is the only information available) and date of first publication. This information can be contained in a footnote or reference note; and
- a link back to the article (via DOI); and
- if practicable, and IN ALL CASES for new works published under any of the Creative Commons licences, the words "© IOP Publishing. Reproduced with permission. All rights reserved"

Without the express permission of the author(s) and the Rightsholder of the article from which the Work is to be reused, User shall not use it in any way which, in the opinion of the Rightsholder, could: (i) distort or alter the author(s)' original intention(s) and meaning; (ii) be prejudicial to the honour or reputation of the author(s); and/or (iii) imply endorsement by the author(s) and/or the Rightsholder.

This licence does not apply to any article which is credited to another source and which does not have the copyright line '© IOP Publishing Ltd'. User must check the copyright line of the article from which the Work is to be reused to check that IOP Publishing Ltd has all the necessary rights to be able to grant permission. User is solely responsible for identifying and obtaining separate licences and permissions from the copyright owner for reuse of any such third party material/figures which the Rightsholder is not the copyright owner of. The Rightsholder shall not reimburse any fees which User pays for a republication license for such third party content.

This licence does not apply to any material/figure which is credited to another source in the Rightsholder's publication or has been obtained from a third party. User must check the Version of Record of the article from which the Work is to be reused, to check whether any of the material in the Work is third party material. Third party citations and/or copyright notices and/or permissions statements may not be included in any other version of the article from which the Work is to be reused and so cannot be relied upon by the User. User is solely

## IOP Publishing LICENSE TERMS AND CONDITIONS

Nov 07, 2018

This is a License Agreement between SAHIL SAINI ("You") and IOP Publishing ("IOP Publishing") provided by Copyright Clearance Center ("CCC"). The license consists of your order details, the terms and conditions provided by IOP Publishing, and the payment terms and conditions.

**All payments must be made in full to CCC. For payment instructions, please see information listed at the bottom of this form.**

License Number	4445430753030
License date	Sep 28, 2018
Licensed content publisher	IOP Publishing
Licensed content title	Classical and Quantum Gravity
Licensed content date	Jan 1, 1984
Type of Use	Thesis/Dissertation
Requestor type	Author of requested content
Format	Print, Electronic
Portion	chapter/article
The requesting person/organization is:	Sahil Saini
Title or numeric reference of the portion(s)	The whole article
Title of the article or chapter the portion is from	From black holes to white holes: a quantum gravitational, symmetric bounce
Editor of portion(s)	N/A
Author of portion(s)	Sahil Saini, Javier Olmedo and Parampreet Singh
Volume of serial or monograph.	34
Page range of the portion	
Publication date of portion	31 October 2017
Rights for	Main product
Duration of use	Life of current and all future editions
Creation of copies for the disabled	no
With minor editing privileges	yes
For distribution to	Worldwide
In the following language(s)	Original language of publication
With incidental promotional use	no
The lifetime unit quantity of new product	Up to 499
Title	SINGULARITY RESOLUTION IN ANISOTROPIC AND BLACK HOLE

## SPACETIMES IN LOOP QUANTUM COSMOLOGY

**Instructor name** Professor Parampreet Singh  
**Institution name** Louisiana State University, Baton Rouge, LA - 70803  
**Expected presentation date** Dec 2018  
**Billing Type** Invoice  
**Billing Address** SAHIL SAINI  
 202, Nicholson Hall

Baton Rouge, LA 70803  
 United States  
 Attn: SAHIL SAINI

**Total (may include CCC user fee)** 0.00 USD

**Terms and Conditions**

### TERMS AND CONDITIONS

#### The following terms are individual to this publisher:

These special terms and conditions are in addition to the standard terms and conditions for CCC's Reproduction Service and, together with those standard terms and conditions, govern the use of the Works.

As the "User" you will make all reasonable efforts to contact the author(s) of the article which the Work is to be reused from, to seek consent for your intended use. Contacting one author who is acting expressly as authorised agent for their co-author(s) is acceptable. User will reproduce the following wording prominently alongside the Work:

- the source of the Work, including author, article title, title of journal, volume number, issue number (if relevant), page range (or first page if this is the only information available) and date of first publication. This information can be contained in a footnote or reference note; and
- a link back to the article (via DOI); and
- if practicable, and IN ALL CASES for new works published under any of the Creative Commons licences, the words "© IOP Publishing. Reproduced with permission. All rights reserved"

Without the express permission of the author(s) and the Rightsholder of the article from which the Work is to be reused, User shall not use it in any way which, in the opinion of the Rightsholder, could: (i) distort or alter the author(s)' original intention(s) and meaning; (ii) be prejudicial to the honour or reputation of the author(s); and/or (iii) imply endorsement by the author(s) and/or the Rightsholder.

This licence does not apply to any article which is credited to another source and which does not have the copyright line '© IOP Publishing Ltd'. User must check the copyright line of the article from which the Work is to be reused to check that IOP Publishing Ltd has all the necessary rights to be able to grant permission. User is solely responsible for identifying and obtaining separate licences and permissions from the copyright owner for reuse of any such third party material/figures which the Rightsholder is not the copyright owner of. The Rightsholder shall not reimburse any fees which User pays for a republication license for such third party content.

This licence does not apply to any material/figure which is credited to another source in the Rightsholder's publication or has been obtained from a third party. User must check the Version of Record of the article from which the Work is to be reused, to check whether any of the material in the Work is third party material. Third party citations and/or copyright notices and/or permissions statements may not be included in any other version of the article from which the Work is to be reused and so cannot be relied upon by the User. User is solely



responsible for identifying and obtaining separate licences and permissions from the copyright owner for reuse of any such third party material/figures where the Rightsholder is not the copyright owner. The Rightsholder shall not reimburse any fees which User pays for a republication license for such third party content.

User and CCC acknowledge that the Rightsholder may, from time to time, make changes or additions to these special terms and conditions without express notification, provided that these shall not apply to permissions already secured and paid for by User prior to such change or addition.

User acknowledges that the Rightsholder (which includes companies within its group and third parties for whom it publishes its titles) may make use of personal data collected through the service in the course of their business.

If User is the author of the Work, User may automatically have the right to reuse it under the rights granted back when User transferred the copyright in the article to the Rightsholder. User should check the copyright form and the relevant author rights policy to check whether permission is required. If User is the author of the Work and does require permission for proposed reuse of the Work, User should select 'Author of requested content' as the Requestor Type. The Rightsholder shall not reimburse any fees which User pays for a republication license.

If User is the author of the article which User wishes to reuse in User's thesis or dissertation, the republication licence covers the right to include the Accepted Manuscript version (not the Version of Record) of the article. User must include citation details and, for online use, a link to the Version of Record of the article on the Rightsholder's website. User may need to obtain separate permission for any third party content included within the article. User must check this with the copyright owner of such third party content. User may not include the article in a thesis or dissertation which is published by ProQuest. Any other commercial use of User's thesis or dissertation containing the article would also need to be expressly notified in writing to the Rightsholder at the time of request and would require separate written permission from the Rightsholder.

User does not need to request permission for Work which has been published under a CC BY licence. User must check the Version of Record of the CC BY article from which the Work is to be reused, to check whether any of the material in the Work is third party material and so not published under the CC BY licence. User is solely responsible for identifying and obtaining separate licences and permissions from the copyright owner for reuse of any such third party material/figures. The Rightsholder shall not reimburse any fees which User pays for such licences and permissions.

As well as CCC, the Rightsholder shall have the right to bring any legal action that it deems necessary to enforce its rights should it consider that the Work infringes those rights in any way.

For STM Signatories ONLY (as agreed as part of the STM Guidelines)

Any licence granted for a particular edition of a Work will apply also to subsequent editions of it and for editions in other languages, provided such editions are for the Work as a whole in situ and do not involve the separate exploitation of the permitted illustrations or excerpts.

#### **Other Terms and Conditions:**

#### **STANDARD TERMS AND CONDITIONS**

1. Description of Service; Defined Terms. This Republication License enables the User to obtain licenses for republication of one or more copyrighted works as described in detail on the relevant Order Confirmation (the "Work(s)"). Copyright Clearance Center, Inc. ("CCC") grants licenses through the Service on behalf of the rightsholder identified on the Order Confirmation (the "Rightsholder"). "Republication", as used herein, generally means the inclusion of a Work, in whole or in part, in a new work or works, also as described on the Order Confirmation. "User", as used herein, means the person or entity making such republication.

2. The terms set forth in the relevant Order Confirmation, and any terms set by the Rightsholder with respect to a particular Work, govern the terms of use of Works in

connection with the Service. By using the Service, the person transacting for a republication license on behalf of the User represents and warrants that he/she/it (a) has been duly authorized by the User to accept, and hereby does accept, all such terms and conditions on behalf of User, and (b) shall inform User of all such terms and conditions. In the event such person is a “freelancer” or other third party independent of User and CCC, such party shall be deemed jointly a “User” for purposes of these terms and conditions. In any event, User shall be deemed to have accepted and agreed to all such terms and conditions if User republishes the Work in any fashion.

### **3. Scope of License; Limitations and Obligations.**

3.1 All Works and all rights therein, including copyright rights, remain the sole and exclusive property of the Rightsholder. The license created by the exchange of an Order Confirmation (and/or any invoice) and payment by User of the full amount set forth on that document includes only those rights expressly set forth in the Order Confirmation and in these terms and conditions, and conveys no other rights in the Work(s) to User. All rights not expressly granted are hereby reserved.

3.2 General Payment Terms: You may pay by credit card or through an account with us payable at the end of the month. If you and we agree that you may establish a standing account with CCC, then the following terms apply: Remit Payment to: Copyright Clearance Center, 29118 Network Place, Chicago, IL 60673-1291. Payments Due: Invoices are payable upon their delivery to you (or upon our notice to you that they are available to you for downloading). After 30 days, outstanding amounts will be subject to a service charge of 1-1/2% per month or, if less, the maximum rate allowed by applicable law. Unless otherwise specifically set forth in the Order Confirmation or in a separate written agreement signed by CCC, invoices are due and payable on “net 30” terms. While User may exercise the rights licensed immediately upon issuance of the Order Confirmation, the license is automatically revoked and is null and void, as if it had never been issued, if complete payment for the license is not received on a timely basis either from User directly or through a payment agent, such as a credit card company.

3.3 Unless otherwise provided in the Order Confirmation, any grant of rights to User (i) is “one-time” (including the editions and product family specified in the license), (ii) is non-exclusive and non-transferable and (iii) is subject to any and all limitations and restrictions (such as, but not limited to, limitations on duration of use or circulation) included in the Order Confirmation or invoice and/or in these terms and conditions. Upon completion of the licensed use, User shall either secure a new permission for further use of the Work(s) or immediately cease any new use of the Work(s) and shall render inaccessible (such as by deleting or by removing or severing links or other locators) any further copies of the Work (except for copies printed on paper in accordance with this license and still in User's stock at the end of such period).

3.4 In the event that the material for which a republication license is sought includes third party materials (such as photographs, illustrations, graphs, inserts and similar materials) which are identified in such material as having been used by permission, User is responsible for identifying, and seeking separate licenses (under this Service or otherwise) for, any of such third party materials; without a separate license, such third party materials may not be used.

3.5 Use of proper copyright notice for a Work is required as a condition of any license granted under the Service. Unless otherwise provided in the Order Confirmation, a proper copyright notice will read substantially as follows: “Republished with permission of [Rightsholder's name], from [Work's title, author, volume, edition number and year of copyright]; permission conveyed through Copyright Clearance Center, Inc.” Such notice must be provided in a reasonably legible font size and must be placed either immediately adjacent to the Work as used (for example, as part of a by-line or footnote but not as a separate electronic link) or in the place where substantially all other credits or notices for the new work containing the republished Work are located. Failure to include the required notice results in loss to the Rightsholder and CCC, and the User shall be liable to pay liquidated

damages for each such failure equal to twice the use fee specified in the Order Confirmation, in addition to the use fee itself and any other fees and charges specified.

3.6 User may only make alterations to the Work if and as expressly set forth in the Order Confirmation. No Work may be used in any way that is defamatory, violates the rights of third parties (including such third parties' rights of copyright, privacy, publicity, or other tangible or intangible property), or is otherwise illegal, sexually explicit or obscene. In addition, User may not conjoin a Work with any other material that may result in damage to the reputation of the Rightsholder. User agrees to inform CCC if it becomes aware of any infringement of any rights in a Work and to cooperate with any reasonable request of CCC or the Rightsholder in connection therewith.

4. Indemnity. User hereby indemnifies and agrees to defend the Rightsholder and CCC, and their respective employees and directors, against all claims, liability, damages, costs and expenses, including legal fees and expenses, arising out of any use of a Work beyond the scope of the rights granted herein, or any use of a Work which has been altered in any unauthorized way by User, including claims of defamation or infringement of rights of copyright, publicity, privacy or other tangible or intangible property.

5. Limitation of Liability. UNDER NO CIRCUMSTANCES WILL CCC OR THE RIGHTSHOLDER BE LIABLE FOR ANY DIRECT, INDIRECT, CONSEQUENTIAL OR INCIDENTAL DAMAGES (INCLUDING WITHOUT LIMITATION DAMAGES FOR LOSS OF BUSINESS PROFITS OR INFORMATION, OR FOR BUSINESS INTERRUPTION) ARISING OUT OF THE USE OR INABILITY TO USE A WORK, EVEN IF ONE OF THEM HAS BEEN ADVISED OF THE POSSIBILITY OF SUCH DAMAGES. In any event, the total liability of the Rightsholder and CCC (including their respective employees and directors) shall not exceed the total amount actually paid by User for this license. User assumes full liability for the actions and omissions of its principals, employees, agents, affiliates, successors and assigns.

6. Limited Warranties. THE WORK(S) AND RIGHT(S) ARE PROVIDED "AS IS". CCC HAS THE RIGHT TO GRANT TO USER THE RIGHTS GRANTED IN THE ORDER CONFIRMATION DOCUMENT. CCC AND THE RIGHTSHOLDER DISCLAIM ALL OTHER WARRANTIES RELATING TO THE WORK(S) AND RIGHT(S), EITHER EXPRESS OR IMPLIED, INCLUDING WITHOUT LIMITATION IMPLIED WARRANTIES OF MERCHANTABILITY OR FITNESS FOR A PARTICULAR PURPOSE. ADDITIONAL RIGHTS MAY BE REQUIRED TO USE ILLUSTRATIONS, GRAPHS, PHOTOGRAPHS, ABSTRACTS, INSERTS OR OTHER PORTIONS OF THE WORK (AS OPPOSED TO THE ENTIRE WORK) IN A MANNER CONTEMPLATED BY USER; USER UNDERSTANDS AND AGREES THAT NEITHER CCC NOR THE RIGHTSHOLDER MAY HAVE SUCH ADDITIONAL RIGHTS TO GRANT.

7. Effect of Breach. Any failure by User to pay any amount when due, or any use by User of a Work beyond the scope of the license set forth in the Order Confirmation and/or these terms and conditions, shall be a material breach of the license created by the Order Confirmation and these terms and conditions. Any breach not cured within 30 days of written notice thereof shall result in immediate termination of such license without further notice. Any unauthorized (but licensable) use of a Work that is terminated immediately upon notice thereof may be liquidated by payment of the Rightsholder's ordinary license price therefor; any unauthorized (and unlicensable) use that is not terminated immediately for any reason (including, for example, because materials containing the Work cannot reasonably be recalled) will be subject to all remedies available at law or in equity, but in no event to a payment of less than three times the Rightsholder's ordinary license price for the most closely analogous licensable use plus Rightsholder's and/or CCC's costs and expenses incurred in collecting such payment.

#### **8. Miscellaneous.**

8.1 User acknowledges that CCC may, from time to time, make changes or additions to the Service or to these terms and conditions, and CCC reserves the right to send notice to the User by electronic mail or otherwise for the purposes of notifying User of such changes or

additions; provided that any such changes or additions shall not apply to permissions already secured and paid for.

8.2 Use of User-related information collected through the Service is governed by CCC's privacy policy, available online here:

<http://www.copyright.com/content/cc3/en/tools/footer/privacypolicy.html>.

8.3 The licensing transaction described in the Order Confirmation is personal to User.

Therefore, User may not assign or transfer to any other person (whether a natural person or an organization of any kind) the license created by the Order Confirmation and these terms and conditions or any rights granted hereunder; provided, however, that User may assign such license in its entirety on written notice to CCC in the event of a transfer of all or substantially all of User's rights in the new material which includes the Work(s) licensed under this Service.

8.4 No amendment or waiver of any terms is binding unless set forth in writing and signed by the parties. The Rightsholder and CCC hereby object to any terms contained in any writing prepared by the User or its principals, employees, agents or affiliates and purporting to govern or otherwise relate to the licensing transaction described in the Order Confirmation, which terms are in any way inconsistent with any terms set forth in the Order Confirmation and/or in these terms and conditions or CCC's standard operating procedures, whether such writing is prepared prior to, simultaneously with or subsequent to the Order Confirmation, and whether such writing appears on a copy of the Order Confirmation or in a separate instrument.

8.5 The licensing transaction described in the Order Confirmation document shall be governed by and construed under the law of the State of New York, USA, without regard to the principles thereof of conflicts of law. Any case, controversy, suit, action, or proceeding arising out of, in connection with, or related to such licensing transaction shall be brought, at CCC's sole discretion, in any federal or state court located in the County of New York, State of New York, USA, or in any federal or state court whose geographical jurisdiction covers the location of the Rightsholder set forth in the Order Confirmation. The parties expressly submit to the personal jurisdiction and venue of each such federal or state court. If you have any comments or questions about the Service or Copyright Clearance Center, please contact us at 978-750-8400 or send an e-mail to [info@copyright.com](mailto:info@copyright.com).

v 1.1

**Questions? [customer@copyright.com](mailto:customer@copyright.com) or +1-855-239-3415 (toll free in the US) or +1-978-646-2777.**

## Vita

Sahil Saini was born in 1988 in Hisar, a city about a hundred miles northwest of Delhi in the state of Haryana. He earned his Bachelors in Science from Government Post Graduate College, Hisar in June 2008. He received his Masters in Physics at the Indian Institute of Technology Delhi in 2010. He then pursued teaching in various colleges in Delhi for some years and enrolled in a doctoral program in the Department of Physics and Astronomy in August 2015. His doctoral research has focused on loop quantum cosmology which he plans to continue further in his postdoctoral career.

## References

- [1] The LIGO Scientific Collaboration and the Virgo Collaboration, “Observation of gravitational waves from a binary black hole merger,” *Physical Review Letters*, vol. 116, pp. 061102, 2016.
- [2] C. L. Bennett *et. al.*, “Four-year COBE DMR Cosmic Microwave Background Observations: Maps and Basic Results,” *The Astrophysical Journal*, vol. 464, pp. L1, 1996.
- [3] C. L. Bennett *et. al.*, “Nine-year Wilkinson Microwave Anisotropy Probe (WMAP) observations: final maps and results,” *The Astrophysical Journal Supplement Series*, vol. 208, pp. 20, 2013.
- [4] G. Hinshaw *et. al.*, “Nine-year Wilkinson Microwave Anisotropy Probe (WMAP) observations: cosmological parameter results,” *The Astrophysical Journal Supplement Series*, vol. 208, pp. 19, 2013.
- [5] Planck Collaboration, “Planck 2015 results. I. Overview of products and scientific results,” *Astronomy & Astrophysics*, vol. 594, pp. A1, 2016.
- [6] Planck Collaboration, “Planck 2015 results. XIII. Cosmological parameters,” *Astronomy & Astrophysics*, vol. 594, pp. A13, 2016.
- [7] M. Davis *et. al.*, “Science objectives and early results of the DEEP2 redshift survey,” *Discoveries and Research Prospects from 6- to 10-Meter-Class Telescopes II* (P. Guhathakurta, ed.), SPIE, 2003.
- [8] M. Colless *et. al.*, “The 2df galaxy redshift survey: spectra and redshifts,” *Monthly Notices of the Royal Astronomical Society*, vol. 328, pp. 1039, 2001.
- [9] S. Cole *et. al.*, “The 2df galaxy redshift survey: power-spectrum analysis of the final data set and cosmological implications,” *Monthly Notices of the Royal Astronomical Society*, vol. 362, pp. 505, 2005.
- [10] B. Abolfathi *et al.*, “The Fourteenth Data Release of the Sloan Digital Sky Survey: First Spectroscopic Data from the Extended Baryon Oscillation Spectroscopic Survey and from the Second Phase of the Apache Point Observatory Galactic Evolution Experiment,” *Astrophys. J. Suppl.*, vol. 235, no. 2, pp. 42, 2018.
- [11] K. Schwarzschild, “Über das gravitationsfeld eines massenpunktes nach der einsteinischen theorie,” *Sitzungsberichte der Königlich Preußischen Akademie der Wissenschaften (Berlin)*, 1916, Seite 189-196, 1916.
- [12] J. Droste, “On the field of a single centre in einstein’s theory of gravitation,” *Koninklijke Nederlandse Akademie van Wetenschappen Proceedings Series B Physical Sciences*, vol. 17, pp. 998, 1915.
- [13] A. S. Eddington, “A comparison of whitehead’s and einstein’s formulae,” *Nature*, vol. 113, pp. 192, 1924.

- [14] G. Lemaitre, “L’univers en expansion,” *Annales de la Société Scientifique de Bruxelles*, vol. 53, 1933.
- [15] A. Einstein and N. Rosen, “The particle problem in the general theory of relativity,” *Physical Review*, vol. 48, pp. 73–77, 1935.
- [16] J. L. Synge, “The gravitational field of a particle,” in *Proceedings of the Royal Irish Academy. Section A: Mathematical and Physical Sciences*, pp. 83–114, JSTOR, 1950.
- [17] D. Finkelstein, “Past-future asymmetry of the gravitational field of a point particle,” *Physical Review*, vol. 110, pp. 965–967, 1958.
- [18] C. Fronsdal, “Completion and embedding of the schwarzschild solution,” *Physical Review*, vol. 116, pp. 778–781, 1959.
- [19] M. D. Kruskal, “Maximal extension of schwarzschild metric,” *Physical Review*, vol. 119, pp. 1743–1745, 1960.
- [20] G. Szekeres, “On the singularities of a riemannian manifold,” *Publicationes Mathematicae Debrecen* 7, 285 (1960), vol. 7, 1960.
- [21] I. D. Novikov, “On the evolution of a semiclosed world,” *Astronomicheskii Zhurnal*, vol. 40, pp. 772, 1963.
- [22] R. Penrose, “Gravitational collapse and space-time singularities,” *Physical Review Letters*, vol. 14, pp. 57–59, 1965.
- [23] H. Reissner, “Über die eigengravitation des elektrischen felde nach der einsteinschen theorie,” *Annalen der Physik*, vol. 355, no. 9, pp. 106–120, 1916.
- [24] H. Weyl, “Zur gravitationstheorie,” *Annalen der Physik*, vol. 359, no. 18, pp. 117–145, 1917.
- [25] G. Nordström, “On the energy of the gravitation field in einstein’s theory,” *Koninklijke Nederlandse Akademie van Wetenschappen Proceedings Series B Physical Sciences*, vol. 20, pp. 1238–1245, 1918.
- [26] G. B. Jeffery, “The field of an electron on einstein’s theory of gravitation,” *Proceedings of the Royal Society A: Mathematical, Physical and Engineering Sciences*, vol. 99, pp. 123–134, 1921.
- [27] R. P. Kerr, “Gravitational field of a spinning mass as an example of algebraically special metrics,” *Physical Review Letters*, vol. 11, pp. 237–238, 1963.
- [28] E. T. Newman, E. Couch, K. Chinnapared, A. Exton, A. Prakash, and R. Torrence, “Metric of a rotating, charged mass,” *Journal of Mathematical Physics*, vol. 6, pp. 918–919, 1965.
- [29] S. Chandrasekhar, “The maximum mass of ideal white dwarfs,” *Astrophysical Journal*, vol. 74, pp. 81, 1931.

- [30] L. D. Landau, “On the theory of stars,” *Phys. Z. Sowjetunion*, vol. 1, no. 285, pp. 152, 1932.
- [31] J. R. Oppenheimer and G. M. Volkoff, “On massive neutron cores,” *Physical Review*, vol. 55, pp. 374–381, 1939.
- [32] J. R. Oppenheimer and H. Snyder, “On continued gravitational contraction,” *Physical Review*, vol. 56, pp. 455–459, 1939.
- [33] A. G. Lematre, “A homogeneous universe of constant mass and increasing radius accounting for the radial velocity of extra-galactic nebulae,” *Monthly Notices of the Royal Astronomical Society*, vol. 91, pp. 483–490, mar 1931.
- [34] A. G. Lemaitre, “Contributions to a british association discussion on the evolution of the universe,” *Nature*, vol. 128, pp. 704–706, 1931.
- [35] R. A. Alpher, H. Bethe, and G. Gamow, “The origin of chemical elements,” *Physical Review*, vol. 73, pp. 803–804, 1948.
- [36] R. A. Alpher and R. Herman, “Evolution of the universe,” *Nature*, vol. 162, pp. 774–775, 1948.
- [37] E. Hubble, “A relation between distance and radial velocity among extra-galactic nebulae,” *Proceedings of the National Academy of Sciences*, vol. 15, pp. 168–173, 1929.
- [38] A. A. Penzias and R. W. Wilson, “A measurement of excess antenna temperature at 4080 mc/s.,” *The Astrophysical Journal*, vol. 142, pp. 419, 1965.
- [39] S. W. Hawking and G. Ellis, *The large scale structure of space-time*. Cambridge University Press, 1973.
- [40] A. Borde, A. H. Guth, and A. Vilenkin, “Inflationary spacetimes are not past-complete,” *Physical Review Letters*, vol. 90, pp. 151301, 2003.
- [41] M. Green, J. Schwarz, and E. Witten, *Superstring Theory*, vols. I and II, Cambridge University Press, 1987.
- [42] J. Polchinski, *String Theory*, vol. 1, 2, Cambridge University Press, vol. 402, 1998.
- [43] B. Zwiebach, *A first course in string theory*. Cambridge university press, 2004.
- [44] A. Ashtekar and J. Lewandowski, “Background independent quantum gravity: a status report,” *Classical and Quantum Gravity*, vol. 21, pp. R53–R152, 2004.
- [45] C. Rovelli, *Quantum gravity (Cambridge Monographs on Mathematical Physics)*. Cambridge University Press, 2004.
- [46] T. Thiemann, *Modern Canonical Quantum General Relativity (Cambridge Monographs on Mathematical Physics)*. Cambridge University Press, 2010.
- [47] R. Gambini and J. Pullin, *A first course in loop quantum gravity*. OUP Oxford, 2011.



- [48] A. Ashtekar and J. Pullin, *Loop Quantum Gravity: The First 30 Years*, vol. 4. World Scientific, 2017.
- [49] R. Loll, “Discrete lorentzian quantum gravity,” *Nuclear Physics B - Proceedings Supplements*, vol. 94, pp. 96–107, 2001.
- [50] J. Ambjorn and R. Loll, “Causal dynamical triangulations and the quest for quantum gravity,” *Foundations of Space and Time: Reflections on Quantum Gravity*, pp. 321, 2012.
- [51] J. Ambjørn, A. Görlich, J. Jurkiewicz, and R. Loll, “Nonperturbative quantum gravity,” *Physics Reports*, vol. 519, pp. 127–210, 2012.
- [52] L. Bombelli, J. Lee, D. Meyer, and R. D. Sorkin, “Space-time as a causal set,” *Physical Review Letters*, vol. 59, pp. 521–524, aug 1987.
- [53] R. D. Sorkin, “Causal sets: Discrete gravity,” *Lectures on Quantum Gravity*, pp. 305–327, Springer-Verlag.
- [54] J. Henson, “The causal set approach to quantum gravity,” *Approaches to quantum gravity: towards a new understanding of space, time and matter*, vol. 393, 2009.
- [55] S. Surya, “Directions in causal set quantum gravity,” *arXiv preprint arXiv:1103.6272*, 2011.
- [56] R. Penrose and M. MacCallum, “Twistor theory: An approach to the quantisation of fields and space-time,” *Physics Reports*, vol. 6, pp. 241–315, 1973.
- [57] R. Penrose and W. Rindler, *Spinors and Space-Time*. Cambridge University Press, 1986.
- [58] R. M. Wald, *General Relativity*. Chicago University Press, 1984.
- [59] P. A. M. Dirac, “Quantum theory of localizable dynamical systems,” *Physical Review*, vol. 73, pp. 1092–1103, 1948.
- [60] P. A. M. Dirac, “Forms of relativistic dynamics,” *Reviews of Modern Physics*, vol. 21, pp. 392–399, 1949.
- [61] P. A. M. Dirac, “Generalized hamiltonian dynamics,” *Proceedings of the Royal Society A: Mathematical, Physical and Engineering Sciences*, vol. 246, pp. 326–332, 1958.
- [62] P. A. M. Dirac, “The theory of gravitation in hamiltonian form,” *Proceedings of the Royal Society A: Mathematical, Physical and Engineering Sciences*, vol. 246, pp. 333–343, 1958.
- [63] P. A. M. Dirac, *Lectures on quantum mechanics*, vol. 2. Courier Corporation, 2001.
- [64] J. L. Anderson and P. G. Bergmann, “Constraints in covariant field theories,” *Physical Review*, vol. 83, pp. 1018–1025, 1951.
- [65] P. G. Bergmann and I. Goldberg, “Dirac bracket transformations in phase space,” *Physical Review*, vol. 98, pp. 531–538, 1955.

- [66] A. Komar, “Covariant conservation laws in general relativity,” *Physical Review*, vol. 113, pp. 934–936, 1959.
- [67] P. G. Bergmann and A. B. Komar, “Poisson brackets between locally defined observables in general relativity,” *Physical Review Letters*, vol. 4, pp. 432–433, 1960.
- [68] R. L. Arnowitt, S. Deser, and C. W. Misner, “Canonical variables for general relativity,” *Phys. Rev.*, vol. 117, pp. 1595–1602, 1960.
- [69] J. A. Wheeler, *Geometrodynamics*, Academic Press, 1962.
- [70] B. S. DeWitt, “Quantum theory of gravity. I. The canonical theory,” *Physical Review*, vol. 160, pp. 1113–1148, 1967.
- [71] B. S. DeWitt, “Quantum theory of gravity. II. The manifestly covariant theory,” *Physical Review*, vol. 162, pp. 1195–1239, 1967.
- [72] B. S. DeWitt, “Quantum theory of gravity. III. Applications of the covariant theory,” *Physical Review*, vol. 162, pp. 1239–1256, 1967.
- [73] J. B. Hartle and S. W. Hawking, “Wave function of the universe,” *Physical Review D*, vol. 28, pp. 2960–2975, 1983.
- [74] A. Vilenkin, “Boundary conditions in quantum cosmology,” *Physical Review D*, vol. 33, pp. 3560–3569, 1986.
- [75] D. N. Page, “Symmetric-bounce quantum state of the universe,” *Journal of Cosmology and Astroparticle Physics*, vol. 2009, pp. 026–026, 2009.
- [76] T. Padmanabhan and J. V. Narlikar, “Quantum conformal fluctuations in a singular space-time,” *Nature*, vol. 295, pp. 677–678, 1982.
- [77] A. Y. Kamenshchik, C. Kiefer, and B. Sandhofer, “Quantum cosmology with a big-brake singularity,” *Physical Review D*, vol. 76, no. 6, pp. 064032, 2007.
- [78] C. Kiefer, *Quantum Gravity*. Oxford University Press, 2007.
- [79] J. B. Hartle, S. W. Hawking, and T. Hertog, “Classical universes of the no-boundary quantum state,” *Physical Review D*, vol. 77, pp. 123537, 2008.
- [80] A. Ashtekar, T. Pawłowski, and P. Singh, “Quantum Nature of the Big Bang: Improved dynamics,” *Phys. Rev.*, vol. D74, pp. 084003, 2006.
- [81] A. Ashtekar, A. Corichi, and P. Singh, “Robustness of key features of loop quantum cosmology,” *Physical Review*, vol. D77, pp. 024046, 2008.
- [82] D. A. Craig and P. Singh, “Consistent Probabilities in Wheeler-DeWitt Quantum Cosmology,” *Physical Review*, vol. D82, pp. 123526, 2010.
- [83] A. Ashtekar, “New hamiltonian formulation of general relativity,” *Physical Review D*, vol. 36, no. 6, pp. 1587, 1987.

- [84] A. Sen, “Gravity as a spin system,” *Physics Letters B*, vol. 119, pp. 89–91, 1982.
- [85] A. Sen, “Quantum theory of spin-3/2 field in einstein spaces,” *International Journal of Theoretical Physics*, vol. 21, pp. 1–35, 1982.
- [86] J. F. B. G., “Real ashtekar variables for lorentzian signature space-times,” *Physical Review D*, vol. 51, pp. 5507–5510, 1995.
- [87] K. G. Wilson, “Confinement of quarks,” *Physical Review D*, vol. 10, pp. 2445–2459, 1974.
- [88] J. Kogut and L. Susskind, “Hamiltonian formulation of wilson’s lattice gauge theories,” *Physical Review D*, vol. 11, pp. 395–408, 1975.
- [89] R. Gambini and A. Trias, “Geometrical origin of gauge theories,” *Physical Review D*, vol. 23, pp. 553–555, 1981.
- [90] R. Giles, “Reconstruction of gauge potentials from wilson loops,” *Physical Review D*, vol. 24, pp. 2160–2168, 1981.
- [91] A. Ashtekar and C. J. Isham, “Representations of the holonomy algebras of gravity and nonAbelian gauge theories,” *Classical and Quantum Gravity*, vol. 9, pp. 1433–1467, 1992.
- [92] A. Ashtekar and J. Lewandowski, “Quantum theory of gravity I: Area operators,” *Classical and Quantum Gravity*, vol. 14, pp. A55, 1997.
- [93] C. Rovelli and L. Smolin, “Discreteness of area and volume in quantum gravity,” *Nuclear Physics*, vol. B442, pp. 593, 1995.
- [94] A. Ashtekar and J. Lewandowski, “Quantum theory of geometry II: Volume operators,” *Advances in Theoretical and Mathematical Physics*, vol. 1, pp. 388, 1998.
- [95] C. Rovelli, “Black hole entropy from loop quantum gravity,” *Physical Review Letters*, vol. 77, pp. 3288, 1996.
- [96] A. Ashtekar and B. Krishnan, “Isolated and dynamical horizons and their applications,” *Living Reviews in Relativity*, vol. 7, pp. 10, 2004.
- [97] A. Ashtekar, J. Baez, A. Corichi, and K. Krasnov, “Quantum geometry and black hole entropy,” *Physical Review Letters*, vol. 80, pp. 904, 1998.
- [98] A. Ashtekar, J. Baez, and K. Krasnov, “Quantum geometry of isolated horizons and black hole entropy,” *Advances in Theoretical and Mathematical Physics*, vol. 4, pp. 1, 2000.
- [99] A. Ghosh and A. Perez, “Black hole entropy and isolated horizons thermodynamics,” *Physical Review Letters*, vol. 108, pp. 169901, 2012.
- [100] A. Ghosh and A. Perez, “The scaling of black hole entropy in loop quantum gravity,” *arXiv preprint arXiv:1210.2252*.
- [101] T. Thiemann, “The phoenix project: master constraint programme for loop quantum gravity,” *Classical and Quantum Gravity*, vol. 23, pp. 2211–2247, 2006.

- [102] C. Rovelli, “What is observable in classical and quantum gravity?,” *Classical and Quantum Gravity*, vol. 8, pp. 297–316, 1991.
- [103] C. Rovelli, “Partial observables,” *Physical Review D*, vol. 65, 2002.
- [104] D. N. Page and W. K. Wootters, “Evolution without evolution: Dynamics described by stationary observables,” *Physical Review D*, vol. 27, pp. 2885–2892, 1983.
- [105] K. Kuchar, “Time and interpretations of quantum gravity,” in The 4th canadian conference on general relativity and relativistic astrophysics, eds. G. Kunstatter, D. Vincent and J. Williams, *World Scientific*, Singapore, 1992. 1992.
- [106] K. Kuchař, “The problem of time in quantum geometrodynamics,” *The arguments of time*, 1999.
- [107] J. M. Pons and D. C. Salisbury, “Issue of time in generally covariant theories and the komar-bergmann approach to observables in general relativity,” *Physical Review D*, vol. 71, 2005.
- [108] J. M. Pons, D. C. Salisbury, and K. A. Sundermeyer, “Observables in classical canonical gravity: Folklore demystified,” *Journal of Physics: Conference Series*, vol. 222, pp. 012018, 2010.
- [109] B. Dittrich, “Partial and complete observables for canonical general relativity,” *Classical and Quantum Gravity*, vol. 23, pp. 6155–6184, 2006.
- [110] B. Dittrich, “Partial and complete observables for hamiltonian constrained systems,” *General Relativity and Gravitation*, vol. 39, pp. 1891–1927, 2007.
- [111] B. Dittrich and J. Tambornino, “A perturbative approach to dirac observables and their spacetime algebra,” *Classical and Quantum Gravity*, vol. 24, pp. 757–783, 2007.
- [112] T. Thiemann, “Reduced phase space quantization and dirac observables,” *Classical and Quantum Gravity*, vol. 23, pp. 1163–1180, 2006.
- [113] T. Thiemann, “Solving the problem of time in general relativity and cosmology with phantoms and k-essence,” *arXiv preprint astro-ph/0607380*, 2006.
- [114] K. Giesel, S. Hofmann, T. Thiemann, and O. Winkler, “Manifestly gauge-invariant general relativistic perturbation theory: I. foundations,” *Classical and Quantum Gravity*, vol. 27, pp. 055005, 2010.
- [115] J. Tambornino, “Relational observables in gravity: a review,” *Symmetry, Integrability and Geometry: Methods and Applications*, 2012.
- [116] K. Giesel and A. Oelmann, “Comparison between dirac and reduced quantization in LQG-models with klein–gordon scalar fields,” *Acta Physica Polonica B Proceedings Supplement*, vol. 10, no. 2, pp. 339, 2017.
- [117] K. Giesel, A. Herzog, and P. Singh, “Gauge invariant variables for cosmological perturbation theory using geometrical clocks,” *Classical and Quantum Gravity*, vol. 35, pp. 155012, 2018.

- [118] R. Gambini, R. A. Porto, and J. Pullin, “A relational solution to the problem of time in quantum mechanics and quantum gravity: a fundamental mechanism for quantum decoherence,” *New Journal of Physics*, vol. 6, pp. 45–45, 2004.
- [119] R. Gambini, R. A. Porto, and J. Pullin, “Fundamental decoherence from quantum gravity: a pedagogical review,” *General Relativity and Gravitation*, vol. 39, pp. 1143–1156, 2007.
- [120] R. Gambini, R. A. Porto, and J. Pullin, “Fundamental spatio-temporal decoherence: A key to solving the conceptual problems of black holes, cosmology and quantum mechanics,” *International Journal of Modern Physics D*, vol. 15, no. 12, pp. 2181–2185, 2006.
- [121] R. Gambini, R. A. Porto, and J. Pullin, “Loss of entanglement in quantum mechanics due to the use of realistic measuring rods,” *Physics Letters A*, vol. 372, pp. 1213–1218, 2008.
- [122] R. Gambini, R. A. Porto, J. Pullin, and S. Torterolo, “Conditional probabilities with dirac observables and the problem of time in quantum gravity,” *Physical Review D*, vol. 79, 2009.
- [123] A. Ashtekar, T. Pawłowski, and P. Singh, “Quantum nature of the big bang,” *Physical Review Letters*, vol. 96, pp. 141301, 2006.
- [124] A. Ashtekar, T. Pawłowski, and P. Singh, “Quantum Nature of the Big Bang: An Analytical and Numerical Investigation. I,” *Physical Review D*, vol. 73, p. 124038, 2006.
- [125] K. Belinskii, Lifshitz, “Oscillatory approach to the singular point in relativistic cosmology,” *Soviet Physics Uspekhi*, vol. 13, no. 6, p. 745, 1971.
- [126] L. Bianchi, “Sugli spazi a tre dimensioni che ammettono un gruppo continuo di movimenti,” *Memorie della Societa Italiana delle Scienze. detta dei XL.(3)*, vol. 11, pp. 267–352, 1897.
- [127] C. W. Misner, “Mixmaster universe,” *Physical Review Letters*, vol. 22, no. 20, pp. 1071, 1969.
- [128] M. Bojowald, “Spherically symmetric quantum geometry: states and basic operators,” *Classical and Quantum Gravity*, vol. 21, no. 15, pp. 3733, 2004.
- [129] J. Engle, “Relating loop quantum cosmology to loop quantum gravity: symmetric sectors and embeddings,” *Classical and Quantum Gravity*, vol. 24, pp. 5777–5802, 2007.
- [130] T. A. Koslowski, “A cosmological sector in loop quantum gravity,” *arXiv preprint arXiv:0711.1098*, 2007.
- [131] N. Bodendorfer, “Quantum reduction to Bianchi-I models in loop quantum gravity,” *Physical Review D*, vol. 91, 2015.
- [132] C. Beetle, J. S. Engle, M. E. Hogan, and P. Mendonça, “Diffeomorphism invariant cosmological sector in loop quantum gravity,” *Classical and Quantum Gravity*, vol. 34, pp. 225009, 2017.
- [133] C. Fleischhack, “Loop quantization and symmetry: Configuration spaces,” *Communications in Mathematical Physics*, vol. 360, pp. 481–521, 2018.

- [134] M. Bojowald, “Absence of a singularity in loop quantum cosmology,” *Physical Review Letters*, vol. 86, no. 23, pp. 5227, 2001.
- [135] M. Bojowald, “Isotropic loop quantum cosmology,” *Classical and Quantum Gravity*, vol. 19, no. 10, pp. 2717, 2002.
- [136] M. Bojowald and F. Hinterleitner, “Isotropic loop quantum cosmology with matter,” *Physical Review D*, vol. 66, no. 10, pp. 104003, 2002.
- [137] M. Bojowald, “Inverse scale factor in isotropic quantum geometry,” *Physical Review D*, vol. 64, 2001.
- [138] M. Bojowald, “Inflation from quantum geometry,” *Physical Review Letters*, vol. 89, 2002.
- [139] M. Bojowald and K. Vandersloot, “Loop quantum cosmology, boundary proposals, and inflation,” *Physical Review D*, vol. 67, no. 12, pp. 124023, 2003.
- [140] M. Bojowald, “Homogeneous loop quantum cosmology,” *Classical and Quantum Gravity*, vol. 20, pp. 2595–2615, 2003.
- [141] G. Date and G. M. Hossain, “Genericness of a big bounce in isotropic loop quantum cosmology,” *Physical Review Letters*, vol. 94, 2005.
- [142] G. Date and G. M. Hossain, “Genericness of inflation in isotropic loop quantum cosmology,” *Physical Review Letters*, vol. 94, 2005.
- [143] A. Ashtekar, M. Bojowald, J. Lewandowski, *et al.*, “Mathematical structure of loop quantum cosmology,” *Advances in Theoretical and Mathematical Physics*, vol. 7, no. 2, pp. 233–268, 2003.
- [144] J. Brunnemann and T. Thiemann, “On (cosmological) singularity avoidance in loop quantum gravity,” *Classical and Quantum Gravity*, vol. 23, pp. 1395–1427, feb 2006.
- [145] D. A. Craig and P. Singh, “Consistent probabilities in loop quantum cosmology,” *Classical and Quantum Gravity*, vol. 30, pp. 205008, 2013.
- [146] A. Corichi and P. Singh, “Quantum bounce and cosmic recall,” *Physical Review Letters*, vol. 100, pp. 161302, 2008.
- [147] A. Corichi and E. Montoya, “On the Semiclassical Limit of Loop Quantum Cosmology,” *International Journal of Modern Physics D*, vol. 21, pp. 1250076, 2012.
- [148] A. Corichi and E. Montoya, “Coherent semiclassical states for loop quantum cosmology,” *Physical Review*, vol. D84, pp. 044021, 2011.
- [149] W. Kaminski and T. Pawłowski, “Cosmic recall and the scattering picture of Loop Quantum Cosmology,” *Physical Review*, vol. D81, pp. 084027, 2010.
- [150] A. Corichi and P. Singh, “Is loop quantization in cosmology unique?,” *Physical Review*, vol. D78, pp. 024034, 2008.

- [151] A. Corichi and P. Singh, “A Geometric perspective on singularity resolution and uniqueness in loop quantum cosmology,” *Physical Review*, vol. D80, p. 044024, 2009.
- [152] W. Kaminski, J. Lewandowski, and L. Szulc, “The status of quantum geometry in the dynamical sector of loop quantum cosmology,” *Classical and Quantum Gravity*, vol. 25, pp. 055003, 2008.
- [153] W. Kaminski and J. Lewandowski, “The flat FRW model in LQC: self-adjointness,” *Classical and Quantum Gravity*, vol. 25, pp. 035001, 2008.
- [154] W. Kaminski, J. Lewandowski, and T. Pawłowski, “Physical time and other conceptual issues of quantum gravity on the example of loop quantum cosmology,” *Classical and Quantum Gravity*, vol. 26, pp. 035012, 2009.
- [155] W. Kaminski, J. Lewandowski, and T. Pawłowski, “Quantum constraints, dirac observables and evolution: group averaging versus the schrödinger picture in LQC,” *Classical and Quantum Gravity*, vol. 26, pp. 245016, 2009.
- [156] P. Diener, B. Gupt, and P. Singh, “Chimera: A hybrid approach to numerical loop quantum cosmology,” *Classical and Quantum Gravity*, vol. 31, pp. 025013, 2014.
- [157] P. Diener, B. Gupt, and P. Singh, “Numerical simulations of a loop quantum cosmos: robustness of the quantum bounce and the validity of effective dynamics,” *Classical and Quantum Gravity*, vol. 31, pp. 105015, 2014.
- [158] P. Diener, B. Gupt, M. Megevand, and P. Singh, “Numerical evolution of squeezed and non-Gaussian states in loop quantum cosmology,” *Classical and Quantum Gravity*, vol. 31, pp. 165006, 2014.
- [159] A. Ashtekar, T. Pawłowski, P. Singh, and K. Vandersloot, “Loop quantum cosmology of  $k=1$  FRW models,” *Physical Review*, vol. D75, pp. 024035, 2007.
- [160] K. Vandersloot, “Loop quantum cosmology and the  $k = -1$  RW model,” *Phys. Rev.*, vol. D75, pp. 023523, 2007.
- [161] L. Szulc, “An open frw model in loop quantum cosmology,” *Classical and Quantum Gravity*, vol. 24, no. 24, pp. 6191, 2007.
- [162] L. Szulc, W. Kaminski, and J. Lewandowski, “Closed FRW model in Loop Quantum Cosmology,” *Classical and Quantum Gravity*, vol. 24, pp. 2621–2636, 2007.
- [163] A. Corichi and A. Karami, “Loop quantum cosmology of  $k=1$  FRW: A tale of two bounces,” *Physical Review*, vol. D84, pp. 044003, 2011.
- [164] A. Corichi and A. Karami, “Loop quantum cosmology of  $k = 1$  FLRW: Effects of inverse volume corrections,” *Classical and Quantum Gravity*, vol. 31, pp. 035008, 2014.
- [165] E. Bentivegna and T. Pawłowski, “Anti-deSitter universe dynamics in LQC,” *Physical Review*, vol. D77, pp. 124025, 2008.

- [166] W. Kaminski and T. Pawłowski, “The LQC evolution operator of FRW universe with positive cosmological constant,” *Physical Review*, vol. D81, p. 024014, 2010.
- [167] T. Pawłowski and A. Ashtekar, “Positive cosmological constant in loop quantum cosmology,” *Physical Review*, vol. D85, pp. 064001, 2012.
- [168] T. Pawłowski, R. Pierini, and E. Wilson-Ewing, “Loop quantum cosmology of a radiation-dominated flat FLRW universe,” *Physical Review*, vol. D90, no. 12, pp. 123538, 2014.
- [169] V. Husain and T. Pawłowski, “Dust reference frame in quantum cosmology,” *Classical and Quantum Gravity*, vol. 28, pp. 225014, 2011.
- [170] D.-W. Chiou, “Loop Quantum Cosmology in Bianchi Type I Models: Analytical Investigation,” *Physical Review*, vol. D75, pp. 024029, 2007.
- [171] M. Martin-Benito, G. A. Mena Marugan, and T. Pawłowski, “Loop Quantization of Vacuum Bianchi I Cosmology,” *Physical Review*, vol. D78, pp. 064008, 2008.
- [172] M. Martin-Benito, G. A. M. Marugan, and T. Pawłowski, “Physical evolution in Loop Quantum Cosmology: The Example of vacuum Bianchi I,” *Physical Review*, vol. D80, pp. 084038, 2009.
- [173] A. Ashtekar and E. Wilson-Ewing, “Loop quantum cosmology of Bianchi I models,” *Physical Review*, vol. D79, pp. 083535, 2009.
- [174] A. Ashtekar and E. Wilson-Ewing, “Loop quantum cosmology of Bianchi type II models,” *Physical Review*, vol. D80, pp. 123532, 2009.
- [175] E. Wilson-Ewing, “Loop quantum cosmology of Bianchi type IX models,” *Physical Review*, vol. D82, pp. 043508, 2010.
- [176] P. Singh and E. Wilson-Ewing, “Quantization ambiguities and bounds on geometric scalars in anisotropic loop quantum cosmology,” *Classical and Quantum Gravity*, vol. 31, pp. 035010, 2014.
- [177] A. Corichi and A. Karami, “Loop quantum cosmology of Bianchi IX: Inclusion of inverse triad corrections,” *International Journal of Modern Physics D*, vol. 25, no. 08, p. 1642011, 2016.
- [178] A. Ashtekar and M. Bojowald, “Quantum geometry and the schwarzschild singularity,” *Classical and Quantum Gravity*, vol. 23, pp. 391–411, 2005.
- [179] L. Modesto, “The kantowski-sachs space-time in loop quantum gravity,” *International Journal of Theoretical Physics*, vol. 45, pp. 2235–2246, 2006.
- [180] L. Modesto, “Loop quantum black hole,” *Classical and Quantum Gravity*, vol. 23, pp. 5587, 2006.
- [181] L. Modesto, “Black hole interior from loop quantum gravity,” *Advances in High Energy Physics*, vol. 2008, pp. 1–12, 2008.



- [182] C. G. Boehmer and K. Vandersloot, “Loop Quantum Dynamics of the Schwarzschild Interior,” *Physical Review*, vol. D76, pp. 104030, 2007.
- [183] A. Corichi and P. Singh, “Loop quantization of the Schwarzschild interior revisited,” *Classical and Quantum Gravity*, vol. 33, no. 5, pp. 055006, 2016.
- [184] M. Martin-Benito, L. J. Garay, and G. A. M. Marugan, “Hybrid quantum gowdy cosmology: Combining loop and fock quantizations,” *Physical Review D*, vol. 78, 2008.
- [185] M. Martín-Benito, G. A. M. Marugán, and E. Wilson-Ewing, “Hybrid quantization: from Bianchi I to the gowdy model,” *Physical Review D*, vol. 82, no. 8, pp. 084012, 2010.
- [186] L. J. Garay, M. Martín-Benito, and G. M. Marugán, “Inhomogeneous loop quantum cosmology: hybrid quantization of the gowdy model,” *Physical review D*, vol. 82, no. 4, pp. 044048, 2010.
- [187] M. Martin-Benito, D. M. de Blas, and G. A. M. Marugan, “Matter in inhomogeneous loop quantum cosmology: The Gowdy T3 model,” *Physical Review D*, vol. 83, 2011.
- [188] D. M. de Blas, J. Olmedo, and T. Pawłowski, “Loop quantization of the gowdy model with local rotational symmetry,” *Physical Review*, vol. D96, no. 10, p. 106016, 2017.
- [189] V. Husain and O. Winkler, “Quantum resolution of black hole singularities,” *Classical and Quantum Gravity*, vol. 22, pp. L127–L133, 2005.
- [190] M. Campiglia, R. Gambini, and J. Pullin, “Loop quantization of spherically symmetric midi-superspaces : the interior problem,” *AIP Conference Proceedings*, Vol. 977, 2008.
- [191] M. Campiglia, R. Gambini, and J. Pullin, “Loop quantization of spherically symmetric midi-superspaces,” *Classical and Quantum Gravity*, vol. 24, pp. 3649, 2007.
- [192] J. Ziprick and G. Kunstatter, “Dynamical singularity resolution in spherically symmetric black hole formation,” *Physical Review D*, vol. 80, jul 2009.
- [193] B. K. Tippet and V. Husain, “Gravitational collapse of quantum matter,” *Physical Review D*, vol. 84, 2011.
- [194] A. Kreienbuehl, V. Husain, and S. S. Seahra, “Model for gravitational collapse in effective quantum gravity,” *arXiv preprint arXiv:1109.3158* , 2011.
- [195] D.-W. Chiou, W.-T. Ni, and A. Tang, “Loop quantization of spherically symmetric midisuperspaces and loop quantum geometry of the maximally extended schwarzschild space-time,” *arXiv preprint arXiv:1212.1265*, 2012.
- [196] R. Gambini and J. Pullin, “Loop quantization of the schwarzschild black hole,” *Physical Review Letters*, vol. 110, pp. 211301, 2013.
- [197] R. Gambini, J. Olmedo, and J. Pullin, “Quantum black holes in loop quantum gravity,” *Classical and Quantum Gravity*, vol. 31, pp. 095009, 2014.
- [198] J. Ziprick, J. Gegenberg, and G. Kunstatter, “Polymer quantization of a self-gravitating thin shell,” *Physical Review D*, vol. 94, 2016.

- [199] A. Ashtekar and T. A. Schilling, “Geometrical formulation of quantum mechanics,” in *On Einstein’s Path*, pp. 23–65, Springer, 1999.
- [200] V. Taveras, “Corrections to the Friedmann Equations from LQG for a Universe with a Free Scalar Field,” *Physical Review*, vol. D78, pp. 064072, 2008.
- [201] V. I. Arnold, V. V. Kozlov, and A. I. Neishtadt, *Mathematical Aspects of Classical and Celestial Mechanics*. 2013.
- [202] A. Heslot, “Quantum mechanics as a classical theory,” *Physical Review D*, vol. 31, pp. 1341–1348, mar 1985.
- [203] J. Anandan and Y. Aharonov, “Geometry of quantum evolution,” *Physical Review Letters*, vol. 65, pp. 1697–1700, 1990.
- [204] G. Gibbons, “Typical states and density matrices,” *Journal of Geometry and Physics*, vol. 8, pp. 147–162, mar 1992.
- [205] T. W. B. Kibble, “Geometrization of quantum mechanics,” *Communications in Mathematical Physics*, vol. 65, pp. 189–201, 1979.
- [206] L. Hughston, “Geometric aspects of quantum mechanics,” in *Twistor theory*, pp. 59–80, Routledge, 2017.
- [207] R. Cirelli, A. Mania, and L. Pizzocchero, “Quantum mechanics as an infinite-dimensional hamiltonian system with uncertainty structure: Part I,” *Journal of Mathematical Physics*, vol. 31, no. 12, pp. 2891–2897, 1990.
- [208] R. Cirelli, A. Mania, and L. Pizzocchero, “Quantum mechanics as an infinite-dimensional hamiltonian system with uncertainty structure: Part II,” *Journal of Mathematical Physics*, vol. 31, no. 12, pp. 2898–2903, 1990.
- [209] T. A. Schilling, *Geometry of quantum mechanics*. PhD thesis, Pennsylvania State University, 1996.
- [210] M. Bojowald and A. Skirzewski, “Effective theory for the cosmological generation of structure,” *Advanced Science Letters*, vol. 1, pp. 92–98, 2008.
- [211] M. Bojowald, B. Sandhofer, A. Skirzewski, and A. Tsobanjan, “Effective constraints for quantum systems,” *Reviews in Mathematical Physics*, vol. 21, no. 01, pp. 111–154, 2009.
- [212] J. L. Willis, “On the low-energy ramifications and a mathematical extension of loop quantum gravity,” *PhD Thesis*, Pennsylvania State University, 2004.
- [213] P. Diener, A. Joe, M. Megevand, and P. Singh, “Numerical simulations of loop quantum Bianchi-I spacetimes,” *Classical and Quantum Gravity*, vol. 34, no. 9, p. 094004, 2017.
- [214] P. Singh, “Are loop quantum cosmos never singular?,” *Classical and Quantum Gravity*, vol. 26, pp. 125005, 2009.
- [215] B. Gupt and P. Singh, “Contrasting features of anisotropic loop quantum cosmologies: The Role of spatial curvature,” *Physical Review*, vol. D85, p. 044011, 2012.

- [216] P. Singh, “Bianchi-I spacetimes in loop quantum cosmology: Physics of singularity resolution,” *Journal of Physics: Conference Series*, vol. 360, pp. 012008, 2012.
- [217] P. Singh, “Curvature invariants, geodesics and the strength of singularities in Bianchi-I loop quantum cosmology,” *Physical Review*, vol. D85, p. 104011, 2012.
- [218] A. Joe and P. Singh, “Kantowski-Sachs spacetime in loop quantum cosmology: bounds on expansion and shear scalars and the viability of quantization prescriptions,” *Classical and Quantum Gravity*, vol. 32, no. 1, pp. 015009, 2015.
- [219] D.-W. Chiou and K. Vandersloot, “The Behavior of non-linear anisotropies in bouncing Bianchi I models of loop quantum cosmology,” *Physical Review*, vol. D76, pp. 084015, 2007.
- [220] D. Brizuela, G. A. M. Marugan, and T. Pawłowski, “Big bounce and inhomogeneities,” *Classical and Quantum Gravity*, vol. 27, pp. 052001, 2010.
- [221] D.-W. Chiou, “Phenomenological loop quantum geometry of the schwarzschild black hole,” *Physical Review D*, vol. 78, 2008.
- [222] N. Dadhich, A. Joe, and P. Singh, “Emergence of the product of constant curvature spaces in loop quantum cosmology,” *Classical and Quantum Gravity*, vol. 32, no. 18, pp. 185006, 2015.
- [223] A. Ashtekar, J. Olmedo, and P. Singh, “Quantum extension of the kruskal space-time,” *Physical Review D*, vol. 98, pp. 126003, 2018.
- [224] G. F. Ellis and B. G. Schmidt, “Singular space-times,” *General Relativity and Gravitation*, vol. 8, no. 11, pp. 915–953, 1977.
- [225] D. A. Konkowski and T. M. Helliwell, “Singularities in colliding gravitational plane-wave spacetimes,” *Classical and Quantum Gravity*, vol. 6, pp. 1847–1854, 1989.
- [226] R. A. Sussman, “On spherically symmetric shear-free perfect fluid configurations (neutral and charged). II. equation of state and singularities,” *Journal of Mathematical Physics*, vol. 29, pp. 945–970, 1988.
- [227] J. O. Weatherall, “What is a singularity in geometrized newtonian gravitation?,”
- [228] C. J. S. Clarke, *The analysis of space-time singularities*. Cambridge University Press, 1993.
- [229] F. J. Tipler, “Singularities in conformally flat spacetimes,” *Physics Letters A*, vol. 64, no. 1, pp. 8–10, 1977.
- [230] C. Clarke and A. Królak, “Conditions for the occurrence of strong curvature singularities,” *Journal of Geometry and Physics*, vol. 2, no. 2, pp. 127–143, 1985.
- [231] T. Thiemann, “Anomaly-free formulation of non-perturbative, four-dimensional lorentzian quantum gravity,” *Physics Letters B*, vol. 380, pp. 257–264, 1996.

- [232] T. Thiemann, “Quantum spin dynamics (QSD),” *Classical and Quantum Gravity*, vol. 15, pp. 839–873, 1998.
- [233] B. K. Berger, D. Garfinkle, J. Isenberg, V. Moncrief, and M. Weaver, “The singularity in generic gravitational collapse is spacelike, local and oscillatory,” *Modern Physics Letters A*, vol. 13, no. 19, pp. 1565–1573, 1998.
- [234] B. K. Berger, “On the nature of the generic big bang,” *Frontiers of Fundamental Physics*, pp. 113, 1999.
- [235] D. Garfinkle, “Numerical simulations of generic singularities,” *Physical review letters*, vol. 93, no. 16, pp. 161101, 2004.
- [236] D. Garfinkle, “The nature of gravitational singularities,” *International Journal of Modern Physics D*, vol. 13, no. 10, pp. 2261–2265, 2004.
- [237] J. Curtis and D. Garfinkle, “Numerical simulations of stiff fluid gravitational singularities,” *Physical Review D*, vol. 72, no. 6, p. 064003, 2005.
- [238] D. Garfinkle, “Numerical simulations of general gravitational singularities,” *arXiv preprint arXiv:0808.0160*, 2008.
- [239] M. Reiterer and E. Trubowitz, “The bkl conjectures for spatially homogeneous space-times,” *arXiv preprint arXiv:1005.4908*, 2010.
- [240] M. P. Ryan and L. C. Shepley, *Homogeneous Relativistic Cosmologies*. Princeton University Press ( Princeton Series In Physics), 1975.
- [241] D. A. Craig and P. Singh, “A consistent histories formulation of Wheeler-DeWitt quantum cosmology,” *AIP Conference Proceedings*, vol. 1232, pp. 275–282, 2010.
- [242] S. Saini and P. Singh, “Resolution of strong singularities and geodesic completeness in loop quantum Bianchi-II spacetimes,” *Classical and Quantum Gravity*, vol. 34, no. 23, pp. 235006, 2017.
- [243] M. Martin-Benito, L. Garay, G. M. Marugán, and E. Wilson-Ewing, “Loop quantum cosmology of the Bianchi I model: complete quantization,” in *Journal of Physics: Conference Series*, vol. 360, pp. 012031, IOP Publishing, 2012.
- [244] D.-W. Chiou, “Effective dynamics for the cosmological bounces in Bianchi type I loop quantum cosmology,” 2007.
- [245] D.-W. Chiou, “Effective dynamics, big bounces and scaling symmetry in Bianchi type I loop quantum cosmology,” *Physical Review*, vol. D76, pp. 124037, 2007.
- [246] R. Maartens and K. Vandersloot, “Magnetic Bianchi I Universe in Loop Quantum Cosmology,” 2008.
- [247] B. Gupt and P. Singh, “Quantum gravitational Kasner transitions in Bianchi-I spacetime,” *Physical Review*, vol. D86, pp. 024034, 2012.

- [248] P. Singh, “Is classical flat Kasner spacetime flat in quantum gravity?,” *International Journal of Modern Physics D*, vol. 25, no. 08, pp. 1642001, 2016.
- [249] P. Tarrío, M. F. Méndez, and G. A. M. Marugán, “Singularity avoidance in the hybrid quantization of the Gowdy model,” *Physical Review*, vol. D88, p. 084050, 2013.
- [250] M. Bojowald, G. Date, and K. Vandersloot, “Homogeneous loop quantum cosmology: The Role of the spin connection,” *Classical and Quantum Gravity*, vol. 21, pp. 1253–1278, 2004.
- [251] K. Vandersloot, *Loop Quantum Cosmology*. PhD thesis, Penn State University, 2006.
- [252] M. Bojowald and R. Swiderski, “Spherically symmetric quantum geometry: Hamiltonian constraint,” *Classical and Quantum Gravity*, vol. 23, pp. 2129–2154, 2006.
- [253] M. Bojowald, “Loop quantum cosmology and inhomogeneities,” *General Relativity and Gravitation*, vol. 38, pp. 1771–1795, 2006.
- [254] J. L. Dupuy and P. Singh, “Implications of quantum ambiguities in  $k=1$  loop quantum cosmology: distinct quantum turnarounds and the super-Planckian regime,” *Physical Review D*, vol. 95, pp. 023510, 2017.
- [255] P. Singh and A. Toporensky, “Big crunch avoidance in  $K=1$  semiclassical loop quantum cosmology,” *Physical Review*, vol. D69, pp. 104008, 2004.
- [256] M. Bojowald, J. D. Reyes, and R. Tibrewala, “Nonmarginal lemaître-tolman-bondi-like models with inverse triad corrections from loop quantum gravity,” *Physical Review D*, vol. 80, 2009.
- [257] A. Ashtekar and P. Singh, “Loop Quantum Cosmology: A Status Report,” *Class. Quant. Grav.*, vol. 28, pp. 213001, 2011.
- [258] M. Bojowald, G. Calcagni, and S. Tsujikawa, “Observational test of inflation in loop quantum cosmology,” *Journal of Cosmology and Astroparticle Physics*, vol. 2011, pp. 046–046, 2011.
- [259] I. I. Vrabie, *Differential equations: an introduction to basic concepts, results and applications*. World Scientific Publishing Co Inc, 2016.
- [260] J. D. Barrow, “Sudden future singularities,” *Classical and Quantum Gravity*, vol. 21, no. 11, pp. L79, 2004.
- [261] L. Fernandez-Jambrina and R. Lazkoz, “Geodesic behavior of sudden future singularities,” *Physical Review D*, vol. 70, 2004.
- [262] L. Fernandez-Jambrina and R. Lazkoz, “Classification of cosmological milestones,” *Physical Review D*, vol. 74, no. 6, pp. 064030, 2006.
- [263] L. Fernández-Jambrina and R. Lazkoz, “Geodesic behaviour around cosmological milestones,” *Journal of Physics: Conference Series*, vol. 66, pp. 012015, 2007.
- [264] J. D. Barrow, S. Cotsakis, and A. Tsokaros, “A general sudden cosmological singularity,” *Classical and Quantum Gravity*, vol. 27, pp. 165017, 2010.

- [265] J. D. Barrow and S. Cotsakis, “Geodesics at sudden singularities,” *Physical Review D*, vol. 88, 2013.
- [266] P. Singh and F. Vidotto, “Exotic singularities and spatially curved Loop Quantum Cosmology,” *Physical Review*, vol. D83, pp. 064027, 2011.
- [267] S. Saini and P. Singh, “Generic absence of strong singularities in loop quantum Bianchi-IX spacetimes,” *Classical and Quantum Gravity*, vol. 35, no. 6, p. 065014, 2018.
- [268] S. Saini and P. Singh, “Geodesic completeness and the lack of strong singularities in loop quantum Kantowski-Sachs spacetime,” 2016.
- [269] L. Modesto, “Semiclassical loop quantum black hole,” *International Journal of Theoretical Physics*, vol. 49, pp. 1649–1683, 2010.
- [270] D.-W. Chiou, “Phenomenological dynamics of loop quantum cosmology in kantowski-sachs spacetime,” *Physical Review D*, vol. 78, 2008.
- [271] J. Brannlund, S. Kloster, and A. DeBenedictis, “Evolution of  $\Lambda$  black holes in the minisuperspace approximation of loop quantum gravity,” *Physical Review D*, vol. 79, pp. 084023, 2009.
- [272] J. Cortez, W. Cuervo, H. A. Morales-Técotl, and J. C. Ruelas, “Effective loop quantum geometry of schwarzschild interior,” *Physical Review D*, vol. 95, 2017.
- [273] J. Olmedo, S. Saini, and P. Singh, “From black holes to white holes: a quantum gravitational, symmetric bounce,” *Classical and Quantum Gravity*, vol. 34, pp. 225011, 2017.
- [274] A. Yonika, G. Khanna, and P. Singh, “von-neumann stability and singularity resolution in loop quantized schwarzschild black hole,” *Classical and Quantum Gravity*, vol. 35, pp. 045007, 2018.
- [275] M. Bojowald, R. Goswami, R. Maartens, and P. Singh, “Black hole mass threshold from nonsingular quantum gravitational collapse,” *Physical Review Letters*, vol. 95, 2005.
- [276] R. Goswami, P. S. Joshi, and P. Singh, “Quantum evaporation of a naked singularity,” *Physical Review Letters*, vol. 96, 2006.
- [277] Y. Tavakoli, J. Marto, and A. Dapor, “Semiclassical dynamics of horizons in spherically symmetric collapse,” *International Journal of Modern Physics D*, vol. 23, pp. 1450061, 2014.
- [278] C. Barceló, L. J. Garay, and G. Jannes, “Quantum non-gravity and stellar collapse,” *Foundations of Physics*, vol. 41, pp. 1532–1541, 2011.
- [279] C. Barcelo, R. Carballo-Rubio, L. J. Garay, and G. Jannes, “The lifetime problem of evaporating black holes: mutiny or resignation,” *Classical and Quantum Gravity*, vol. 32, pp. 035012, 2015.
- [280] C. Barcelo, R. Carballo-Rubio, and L. J. Garay, “Black holes turn white fast, otherwise stay black: no half measures,” *Journal of High Energy Physics*, vol. 2016, 2016.

- [281] H. M. Haggard and C. Rovelli, “Quantum-gravity effects outside the horizon spark black to white hole tunneling,” *Physical Review D*, vol. 92, 2015.
- [282] A. Barrau, B. Bolliet, F. Vidotto, and C. Weimer, “Phenomenology of bouncing black holes in quantum gravity: a closer look,” *Journal of Cosmology and Astroparticle Physics*, vol. 2016, pp. 022–022, 2016.
- [283] C. Rovelli, “Quantum mechanics without time: A model,” *Physical Review D*, vol. 42, pp. 2638–2646, 1990.
- [284] C. Rovelli, “Time in quantum gravity: An hypothesis,” *Physical Review D*, vol. 43, pp. 442–456, 1991.
- [285] A. D. Rendall, “Unique determination of an inner product by adjointness relations in the algebra of quantum observables,” *Classical and Quantum Gravity*, vol. 10, pp. 2261–2269, 1993.
- [286] A. D. Rendall, “Adjointness relations as a criterion for choosing an inner product,” in *Canonical Gravity: From Classical to Quantum*, pp. 319–326, Springer Berlin Heidelberg.
- [287] K. Giesel, J. Tambornino, and T. Thiemann, “LTB spacetimes in terms of dirac observables,” *Classical and Quantum Gravity*, vol. 27, pp. 105013, 2010.
- [288] V. Husain and T. Pawłowski, “Time and a physical hamiltonian for quantum gravity,” *Physical Review Letters*, vol. 108, 2012.
- [289] K. Giesel and T. Thiemann, “Scalar material reference systems and loop quantum gravity,” *Classical and Quantum Gravity*, vol. 32, pp. 135015, 2015.
- [290] R. Gambini and J. Pullin, “Black holes in loop quantum gravity: The complete space-time,” *Physical Review Letters*, vol. 101, 2008.
- [291] D.-W. Chiou, W.-T. Ni, and A. Tang, “Loop quantization of spherically symmetric midisuperspaces and loop quantum geometry of the maximally extended schwarzschild space-time,” *arXiv preprint arXiv:1212.1265*, 2012.
- [292] R. Gambini, J. Olmedo, and J. Pullin, “Schrodinger-like quantum dynamics in loop quantized black holes,” *International Journal of Modern Physics D*, vol. 25, no. 08, pp. 1642006, 2016.
- [293] J. Olmedo, “Brief review on black hole loop quantization,” *Universe*, vol. 2, pp. 12, 2016.
- [294] R. Gambini and J. Pullin, “Quantum shells in a quantum space-time,” *Classical and Quantum Gravity*, vol. 32, pp. 035003, 2015.
- [295] M. Campiglia, R. Gambini, J. Olmedo, and J. Pullin, “Quantum self-gravitating collapsing matter in a quantum geometry,” *Classical and Quantum Gravity*, vol. 33, pp. 18LT01, 2016.
- [296] E. Alesci, S. Bahrami, and D. Pranzetti, “Quantum evolution of black hole initial data sets: Foundations,” *Physical Review D*, vol. 98, 2018.

- [297] R. Gambini, J. Olmedo, and J. Pullin, “Casimir effect in a quantum space–time,” *Classical and Quantum Gravity*, vol. 32, p. 115002, 2015.
- [298] R. Gambini and J. Pullin, “Hawking radiation from a spherical loop quantum gravity black hole,” *Classical and Quantum Gravity*, vol. 31, p. 115003, 2014.
- [299] J. Pullin and R. Gambini, “A scenario for black hole evaporation on a quantum geometry,” in *Proceedings of Frontiers of Fundamental Physics 14 — PoS(FFP14)*, Sissa Medialab, 2016.
- [300] R. Gambini, E. M. Capurro, and J. Pullin, “Quantum spacetime of a charged black hole,” *Physical Review D*, vol. 91, 2015.
- [301] N. Bodendorfer, J. Lewandowski, and J. Świeżewski, “A quantum reduction to spherical symmetry in loop quantum gravity,” *Physics Letters B*, vol. 747, pp. 18–21, 2015.
- [302] N. Bodendorfer and A. Zipfel, “On the relation between reduced quantisation and quantum reduction for spherical symmetry in loop quantum gravity,” *Classical and Quantum Gravity*, vol. 33, pp. 155014, 2016.
- [303] A. Ashtekar, C. Beetle, O. Dreyer, S. Fairhurst, B. Krishnan, J. Lewandowski, and J. Wiśniewski, “Generic isolated horizons and their applications,” *Physical Review Letters*, vol. 85, pp. 3564–3567, 2000.
- [304] A. Ashtekar, J. C. Baez, and K. Krasnov, “Quantum geometry of isolated horizons and black hole entropy,” *Advances in Theoretical and Mathematical Physics*, vol. 4, no. 1, pp. 1–94, 2000.
- [305] M. Domagala and J. Lewandowski, “Black-hole entropy from quantum geometry,” *Classical and Quantum Gravity*, vol. 21, pp. 5233–5243, 2004.
- [306] K. A. Meissner, “Black-hole entropy in loop quantum gravity,” *Classical and Quantum Gravity*, vol. 21, pp. 5245–5251, 2004.
- [307] A. Ghosh and P. Mitra, “Counting black hole microscopic states in loop quantum gravity,” *Physical Review D*, vol. 74, 2006.
- [308] H. Sahlmann, “Toward explaining black hole entropy quantization in loop quantum gravity,” *Physical Review D*, vol. 76, 2007.
- [309] I. Agulló, E. F. Borja, and J. Díaz-Polo, “Computing black hole entropy in loop quantum gravity from a conformal field theory perspective,” *Journal of Cosmology and Astroparticle Physics*, vol. 2009, pp. 016–016, 2009.
- [310] I. Agullo, J. F. B. G., E. F. Borja, J. Diaz-Polo, and E. J. S. Villaseñor, “Detailed black hole state counting in loop quantum gravity,” *Physical Review D*, vol. 82, 2010.
- [311] J. Engle, K. Noui, A. Perez, and D. Pranzetti, “The  $SU(2)$  black hole entropy revisited,” *Journal of High Energy Physics*, vol. 2011, 2011.



- [312] A. Perez, “Black holes in loop quantum gravity,” *Reports on Progress in Physics*, vol. 80, pp. 126901, 2017.
- [313] J. Lewandowski, A. Okołów, H. Sahlmann, and T. Thiemann, “Uniqueness of diffeomorphism invariant states on holonomy–flux algebras,” *Communications in Mathematical Physics*, vol. 267, pp. 703–733, 2006.
- [314] C. Fleischhack, “Representations of the weyl algebra in quantum geometry,” *Communications in Mathematical Physics*, vol. 285, pp. 67–140, 2008.
- [315] I. Agullo and P. Singh, “Loop Quantum Cosmology: A brief review,” in *The First 30 Years ed A Ashtekar and J Pullin*, 2017.
- [316] P. Singh, “Numerical loop quantum cosmology: an overview,” *Classical and Quantum Gravity*, vol. 29, pp. 244002, 2012.
- [317] J. Yang, Y. Ding, and Y. Ma, “Alternative quantization of the hamiltonian in loop quantum cosmology,” *Physics Letters B*, vol. 682, no. 1, pp. 1–7, 2009.
- [318] A. Dapor and K. Liegener, “Cosmological effective hamiltonian from full loop quantum gravity dynamics,” *Physics Letters B*, vol. 785, pp. 506, 2017.
- [319] E. Wilson-Ewing, “The loop quantum cosmology bounce as a kasner transition,” *Classical and Quantum Gravity*, vol. 35, pp. 065005, 2018.
- [320] E. Wilson-Ewing, “A quantum gravity extension to the mixmaster dynamics,” *arXiv preprint arXiv:1809.09659*, 2018.
- [321] A. Ashtekar, A. Henderson, and D. Sloan, “Hamiltonian formulation of the belinskii-khalatnikov-lifshitz conjecture,” *Physical Review D*, vol. 83, 2011.